ISTANBUL TECHNICAL UNIVERSITY ★ INSTITUTE OF SCIENCE AND TECHNOLOGY

EFFECTS OF POZZOLANIC MATERIALS ON MECHANICAL PROPERTIES AND CHLORIDE DIFFUSIVITY OF CONCRETE

Ph.D. Thesis by

Özkan ŞENGÜL, M.Sc.

Department : Civil Engineering

Programme: Structural Engineering

MAY 2006

İSTANBUL TECHNICAL UNIVERSITY ★ INSTITUTE OF SCIENCE AND TECHNOLOGY

EFFECTS OF POZZOLANIC MATERIALS ON MECHANICAL PROPERTIES AND CHLORIDE DIFFUSIVITY OF CONCRETE

Ph.D. Thesis by

Özkan ŞENGÜL, M.Sc.

(501002110)

Date of submission : 21 December 2005

Date of defence examination: 3 May 2006

Supervisors (Chairman) : Prof.Dr. Mehmet Ali TAŞDEMİR

Prof.Dr.Techn. Odd E. GJØRV (NTNU.)

Members of the Examining Committee : Prof.Dr. Saim AKYÜZ

Prof.Dr. Hulusi ÖZKUL

Prof.Dr. Turan ÖZTURAN (BÜ.)

Prof.Dr. Halit Yaşa ERSOY (MSÜ.)

Assoc. Prof.Dr. Yılmaz AKKAYA

MAY 2006

CONTENTS

EFFECTS OF POZZOLANIC MATERIALS ON MECHANICAL PROPERTIES AND CHLORIDE DIFFUSIVITY OF CONCRETE

SUMMARY

The main objective of this work was to study the effects of pozzolanic materials on the mechanical properties and durability of concrete. Fly ash, granulated blast furnace slag and silica fume were used in the study. Mixtures were prepared using binary, ternary and quaternary blends of cements and pozzolans.

Mechanical properties of concretes were obtained at different ages. The resistance of concretes against chloride ion penetration was an important part of the study. In addition, electrical resistivities of the mixtures were monitored with two different methods. An extensive study on the factors affecting the resistivity obtained by the wenner electrode method was also included.

In addition; chloride binding, temperature measurements and capillary water absorption tests were conducted. To investigate the effects of the pozzolans on the aggregate - cement paste interface, a new indentation technique was included in the study. Studies on existing structures also formed an important part of the experimental program.

In general, depending on the replacement ratio, mechanical properties of the concretes containing pozzolans had lower early strength when compared to portland cement concretes. Partially replacing portland cement by slag or fly ash was more effective in low water/binder ratios for obtaining better concrete strength properties. Concretes containing pozzolanic materials had substantially higher resistance to chloride penetration. Test results proved that in order to decrease diffusivity, partially replacing portland cement by pozzolanic materials was more effective than reducing the water/cement ratio of portland cement concrete.

Ternary (three-part) or quaternary (four-part) blended concretes had higher electrical resistivity than the binary blended concretes. Test results confirmed the strong relationship between electrical resistivity and chloride diffusivity. Using such a relationship, the diffusivity can be estimated by testing the resistivity.

Field studies proved that, depending on the test location and micro-climate, chloride penetration into concrete can vary considerably even for the same structure. Results showed that for the structures produced with portland cement and exposed to chlorides for 10 to 20 years, at the depth of steel reinforcements, the chloride concentrations were high enough to initiate corrosion.

Durability analyses were carried out using a probability based design method and chloride diffusivities obtained from the testing of different concrete mixtures were used as input. The results confirmed that reinforcing steel embedded in a structural member produced with ordinary portland cement could start corroding in within 10 to 20 years. However, the risk for corrosion reduced substantially for the concretes containing pozzolanic materials.

1. INTRODUCTION

1.1. Background

Poor durability; and as a result uncontrolled and short service life, is a major concern for structures and can lead to great economical losses. Chloride induced corrosion of the embedded steel in concrete is one of the most severe durability problems of reinforced concrete structures. The source of chloride may be de-icing salts, seawater or chloride containing constituent materials. Embedded steel in concrete is normally well protected against the corrosion due to the high alkalinity of concrete. However, the pH of concrete can decrease by the effect of chloride ions and as a result; the passivation layer protecting the embedded steel can be lost and with the presence of oxygen and water, corrosion of the reinforcement takes place.

Today's codes and practice for obtaining durable structures are based on prescriptive requirements. However, field studies reveal that most of these structures confirming the code requirements have severe durability problems within the 10 to 20 years after the completion.

In order to prevent corrosion of steel in concrete and increase the service life of structures, different approaches such as; modifying element geometry (for example increasing cover depth), changing concrete composition, or additional measures like cathodic protection or surface protections, can be used. Some of these approaches, however, may sometimes be ineffective and very costly.

Extensive research has been carried out for modelling the corrosion of steel in concrete and different modelling methods are being developed. Concrete structures usually have a high scatter of material properties, cover depths and environmental conditions; all of which must be taken into account for the design. Probability based durability design methods are based on not only the mean values but also the scatter of these variables.

Chloride diffusion coefficient is an important input parameter for the probability based durability design of concrete structures and reducing chloride diffusivity has a

big impact on the service life of structures. Concrete composition is the main factor affecting the chloride diffusivity of concrete.

One of the effective ways of minimizing the chloride diffusivity of concrete is to substitute portland cement by pozzolanic materials which are finely divided materials and can react with calcium hydroxide at ordinary temperatures to form calcium silicate hydrates. The most widely used pozzolanic materials are fly ash, granulated blast furnace slag and silica fume, all of which are industrial by-products. Natural mineral admixtures are also available. There are two major reasons to use these pozzolans in concrete: i) decreasing portland cement consumption by replacing a part of cement with these supplementary cementing materials, thus saving energy, ii) improving fresh and hardened concrete properties. Pozzolanic materials affect the microstructure of the cement paste in concrete. Pore structure and aggregate – cement paste interface may be improved by using these materials which affects the mechanical and durability properties of the concrete. Substitution of portland cement by these materials also helps to minimize the impact on the environment.

By using pozzolans in concrete with higher amounts, it is possible to obtain better properties than normal concrete. Replacing high amounts of portland cement by pozzolans, however, may have some drawbacks such as low early strength or high early permeability. In order to overcome the disadvantages of using pozzolans in high amounts, pozzolan quality can be increased (for example with increasing its reactivity by increasing the fineness) or using different pozzolans in combination.

1.2. Objective and Scope

The primary objective of the present work is to study the effects of pozzolans on the mechanical and durability properties of concrete.

Fly ash, granulated blast furnace slag and silica fume were used in the study. In order to utilize the potential of these materials and obtain better concrete performance, pozzolans with smaller particle sizes were used, which were obtained by grinding. Substitutions of cements by pozzolans varied from low to high amounts, and in order to compensate some of the disadvantages caused by using high replacement ratios, ternary (three part) and quaternary (four part) blended mixtures were also prepared in addition to binary blends.

In the study, some mechanical properties such as compressive strength and brittleness index were obtained at different ages. The study has focused on the resistance to chloride ion penetration in order to characterize the durability of concretes. Electrical resistivity and capillarity of some of the mixtures were also obtained. For some of the series, chloride binding and temperature measurements were also included in the experimental program. In addition, a new indentation technique was carried out on paste specimens in order to characterize the aggregate - cement paste interface.

Based on the test results, two different optimization techniques; one based on only one response and the other; a multi-objective optimization based on several responses, were performed on some of the mixtures.

Condition assessment of five different structures exposed to sea water, formed a part of the experimental program. Results obtained from chloride penetration tests and data obtained from field studies were used as input in a probability based durability design of a typical structure in a marine environment.

Electrical resistivity is an important characteristic of the concrete quality, which can be used as a quality control parameter. Some of the factors affecting the resistivity obtained by wenner electrode method were also investigated in this study.

1.3. Organization of the Thesis

The thesis starts with an introductory chapter, where the background for the study is described briefly. Objective and scope of the study is also given in the chapter.

A literature review is given in Chapter 2 where characteristics of fly ash, ground granulated blast furnace slag and silica fume and the effects of these materials on some concrete properties are summarized based on previous studies. Background and calculation steps of the indentation test are also included in this chapter.

Details of the experimental program are given in Chapter 3 where all the material characteristics, mixture proportions and test method are presented.

Chapter 4 provides the results and discussion on the effects of the pozzolanic materials on the mechanical properties of the concrete. A calculation method for the

assessment of the pozzolanic activity of fly ashes is included in the chapter. Results of the indentation tests are also discussed in this chapter.

Results of the chloride penetration tests are discussed in Chapter 5. Electrical resistivities of the concretes are also presented and relationship between chloride diffusivity and resistivity is included in the chapter. Temperature development in concrete may not be considered as a durability parameter but because it can affect cracking in concrete, the results of temperature measurements are presented in this chapter. Chloride binding test results are also given in Chapter 6.

Chapter 6 first presents the optimization carried out based on only one response, the compressive strength. Multi-criteria optimization based on several responses is the second method presented in the chapter.

Chapter 7 starts with the transport mechanisms in concrete, then deterioration processes of concrete structures are summarized. Chloride induced corrosion of the embedded steel is given in more detail. Current codes and practice for obtaining durable structures are discussed in the chapter. A probability based durability design method is presented which is the basis of the durability analysis given in Chapter 8.

Condition assessments of five different structures are presented in Chapter 8. Some of the chloride diffusivities given in Chapter 5 are also summarized in Chapter 8 for an easier comparison. These values were used as input for a durability design of a structure and as a result; effects of pozzolanic materials on the durability of a structure in a marine environment are demonstrated.

Chapter 9 first focuses on the chloride diffusivity – electrical resistivity relationship. Based on this relation, quality control of the diffusivity using electrical resistivity is discussed. Test results on the factors affecting the resistivity obtained by wenner electrode method are presented in this chapter.

Chapter 10 summarizes the test results and provides overall conclusions.

2. LITERATURE REVIEW

2.1. General

The following literature review focuses on fly ash, blast furnace slag and silica fume which are the most widely used pozzolans. Brief information about the structure, formation and properties of these pozzolanic materials are presented in this chapter. The effects of these supplementary cementing materials on the microstructure, mechanical behaviour and resistance to chloride penetration of concretes are summarized based on previous studies.

2.2. Pozzolanic Materials

2.2.1. Fly Ash

Fly ash is a by-product of the combustion of coal in thermal power plants for electricity production. It is also known as pulverized fuel ash. It is removed by the dust collection system as a fine particulate residue from the combustion gases before discharging into atmosphere. Fly ash includes meta-stable alumino-silicates that react with calcium ions, in the presence of moisture to form silica hydrates.

Coal used in thermal power plants is pulverized before use. The fine coal particles are transported in an air stream to the boiler where they are burned, and the heat produced is used to generate steam in the steam-generating unit. During the combustion process, the volatile matter is vaporized and carbon is burned off. As the particles enter the burning zone, temperatures increase rapidly and typically reach values around 1000 – 1500° C. Mineral components present in the coal gangue, the inorganic part of the coal, such as clays and feldspars melt and form fused droplets that on rapid cooling solidify as spherical glassy particles that comprise the coal ash. Some mineral components also remain in the crystalline phase. The coarser ash collects at the bottom of the furnace, and is known as bottom ash. The finer ash is carried in the flue gases are collected by precipitators. It is this ash that is termed fly ash (Luke, 1999).

Fly ash is the most common artificial pozzolan worldwide. The use of fly ash in concrete technology dates back to late 1930s. It is estimated that about 450 million tons of fly ash is produced worldwide annually, but only about 6 percent of the total available fly ash is used as a pozzolan in blended cements or in concrete mixtures (Mehta, 2000). There are twelve active coal-burning power plants in Turkey (Bayat, 1998). The annual fly ash production in the country is about 15 million tons (Tokyay, 1998). Fly ash can be utilized as a blending component in blended cement or can be added separately during the concrete production.

According to ASTM C 618 (2000), fly ash can be divided into two categories: Class F and Class C. The Class F fly ash generally contains analytical CaO less than 10 %, whereas Class C fly ash typically contains it 15 % to 35 %. On the other hand, the Class F fly ash, produced from combustion of anthracite and bituminuous coals, is a low lime fly ash and mainly classified as a pozzolan. The Class C fly ash, however, is produced from combustion of either lignite or subbituminous coal. Due to the high calcium content Class C ashes possess substantial cementious properties besides pozzolanic properties (Naik et al., 1992). Fly ash particles, as shown in Figure 2.1, have mostly spherical, glassy particle shapes with different sizes varying from a few μm to 100μm (ACI Committee 232, 1996).

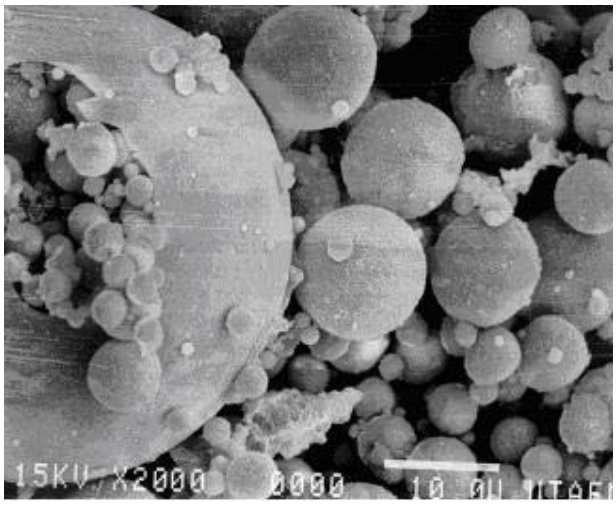

Figure 2.1: Fly ash particles

2.2.2. Ground Granulated Blast-Furnace Slag

Ground granulated blast-furnace slag is a by-product of iron production. The iron ore is a mixture of oxides of iron, silica and alumina, and the chemical reactions within

the blast-furnace reduce iron ore to iron. The iron ore is fed into the furnace with coke and limestone. The slag is formed at a temperature of 1300 – 1600^{o}C as a liquid layer floating on the top of liquid iron. It is then collected and cooled (Lee, 1974). The method of cooling affects the properties of the slag. When cooled rapidly, the slag has a non-crystalline, glassy structure. If water is used for cooling, sand sized particles of slag is obtained. An alternative treatment, pelletization, can also be used for granulation. The granular slag is then dried and finally ground to cement fineness or finer.

During the iron production process about 300 kg of slag is produced for each ton of pig iron (Neville, 2004). In production plants with older technology, however, the amount of slag obtained is usually higher. The use of blast furnace slag as a cementitious material dates back to the second half of 19th century. About 100 million tons of slag is produced annually worldwide but only a very small fraction is utilized. Today slag is widely used in Europe as a component in blended cements but the degree of usage varies significantly between different countries. Netherlands, for example, utilizes about 90 % of its slag production (Regourd, 2004) and slag cement has a market share of about 60 % in the country (Bijen, 1996a). According to the American Slag Cement Association, in US 3.1 million tons of slag cement was shipped for use in concrete and construction applications in 2003. Besides used as a blending component in cement, slag can also be added to concrete during production.

Although many pozzolanic by-products are being used as blending materials, blast furnace slag is the nearest to portland cement in chemical composition. The chemical composition of the slag depends on the materials used for iron production and the procedure for cooling. The CaO content of slags are mostly between 40% and 50%, and the SiO_2 is between 30% and 40%. ASTM C 989 (1999) classifies blast furnace slag into three grades; 80, 100 and 120 where this classification is based on the strength of the mortar containing 50 % slag by mass. Particle size of the blast furnace slag depends on its grinding process. Blast furnace slag particles have mostly rough, sharp edged shapes as shown in Figure 2.2.

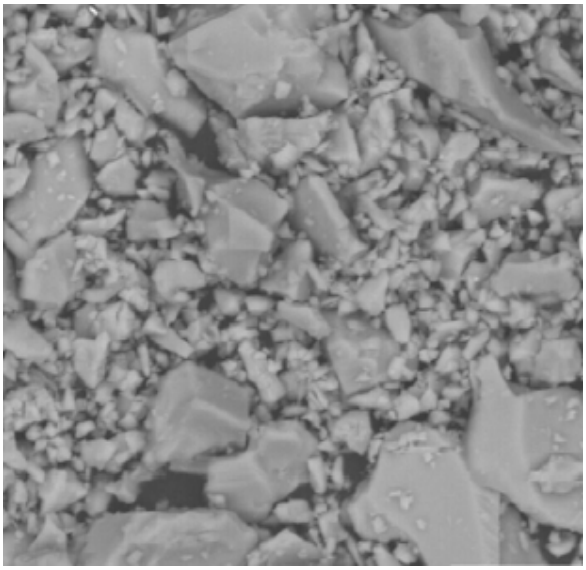

Figure 2.2: Ground granulated blast furnace slag particles

2.2.3. Silica Fume

Silica Fume is a by-product of silicon and ferrosilicon industries. It is also known as condensed silica fume or microsilica. Quartz is reduced to silicon in electric arc furnaces at temperatures up to 2000^{o}C. During this process, some SiO lost as gas oxidizes and condensates into spherical particles with very high amounts of amorphous SiO_2. It is filtered from the exhaust gases before discharging into atmosphere (Malhotra et.al, 1987). The raw materials used for producing silicon and also the type and design of the furnace affects the properties of the silica fume.

The usa of silica fume in concrete technology is relatively new when compared to fly ash or slag. The studies at the Norwegian Institute of Technology in Trondheim during the late 1970s and 1980s formed a basis for utilizing silica fume in concrete technology (Khayat and Aitcin, 1993; Fidjestøl and Lewis, 2004). Silica fume production is very low when compared to those of fly ash or slag. The annual production of silica fume is about half a million ton worldwide and Norway is the biggest producer of silica fume with about 140 thousand tons (Chandra and Berntsson, 1997). Silica fume is commercially available in various forms; undensified, densified (compacted), micro-pelletized and slurry form. Some synthetic forms of silica are also available on the market such as colloidal silica, silica gel, fumed and fused silica (Chandra and Berntsson, 1997).

Silica fume has spherical particles with average particle sizes of about 0.1 – 0.2 μm, which is more than 100 times smaller than the particle size of ordinary portland cement. Figure 2.3 illustrates the particle size of silica fume compared to those of cement (Aitcin, 1998). The SiO_2 content of silica fume is usually more than 85 % and in many national standards the minimum SiO_2 content of silica fume is also specified as 85 % (ASTM C 1240, 2000; NS 3045, 1992). Figure 2.4 gives a comparison of different pozzolans and cements based on their chemical compositions. Because of its extreme fineness and high silicon dioxide content, silica fume is very reactive when compared to fly ash or slag (Roy, 1989).

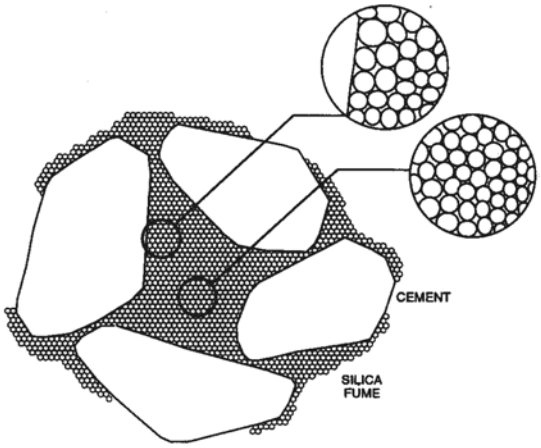

Figure 2.3: Comparison of silica fume and cement particles

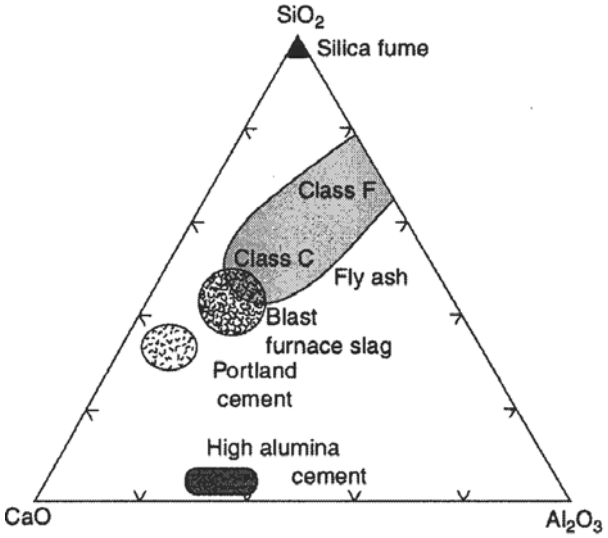

Figure 2.4: Compositions of cements and some pozzolanic materials; simplified representations of components as CaO-Al_2O_3-SiO_2

2.3. Hydration Mechanisms

2.3.1. Hydration of Portland Cement

Limestone and clay is burned up to 1450^{o}C for producing portland cement clinker. This material is then ground with gypsum and portland cement is obtained. The main constituents of portland cement are CaO, SiO_2, Al_2O_3 , which form the major phases; C_3S, C_2S, C_3A and C_4AF, where C: CaO, S: SiO_2, A: Al_2O_3 and F: Fe_2O_3. These phases have different characteristics and affect the properties of the cement.

The hydration of calcium silicates forms the calcium silicate hydrate (CSH) which is the main constituent of solids in cement paste. The reactions of the C_3S and C_2S may be expressed as:

$$2\ C_3S + 6\ H \longrightarrow C_3S_2H_3 + 3\ CH \qquad \textbf{(2.1)}$$

$$2\ C_2S + 4\ H \longrightarrow C_3S_2H_3 + \ CH \qquad \textbf{(2.2)}$$

where H and CH represents H_2O and $Ca(OH)_2$, respectively. The reaction of the aluminate phase is very fast and can cause rapid setting of cement. In order to control the rate of the reaction, about 5 % gypsum (calcium sulfate) is added to portland cement during grinding. The hydration reaction of C_3A with gypsum and water is given as:

$$C_3A + 3\ C\overline{S}\ H_2 + 26H \longrightarrow C_3A.3C\overline{S}\ .32H \qquad \textbf{(2.3)}$$

in which $\overline{S}$ represents SO_3. The product of this reaction, ettringite, is formed on the surfaces of C_3A as prismatic crystals. The ettringite then reacts with C_3A and transforms into calcium monosulfate that has lower sulfate content. The hydration of C_4AF is similar to C_3A but with a slower rate.

The studies on of these pure phases helps to understand the hydration process but the hydration of portland cement is more complex due to the interaction of the phases and minor constituents. (Taylor, 1992).

Many different techniques such as NMR, XRD, neutron activation analysis, atomic absorption spectroscopy, IR/UV spectroscopy, electron microscopy, surface area techniques, pore characterization, zeta potential, viscometry, differential thermal analysis (DTA), thermo-gravimetric analysis (TG), differential scanning calorimetry

(DSC), and conduction calorimetric methods have been used for investigating the hydration and microstructure of concrete.

The hydration reactions start right after mixing cement with water. The rates of the reactions are very fast during the first days. Calcium hydroxide content, chemically bound water and heat of development are the most commonly investigated properties during the hydration. As the hydration continues, the amount of CH and bound water increase as a result of the chemical reactions. The morphology of the CSH also changes with hydration. Figure 2.5 show the change of hydration products with the degree of hydration (Neville, 2004).

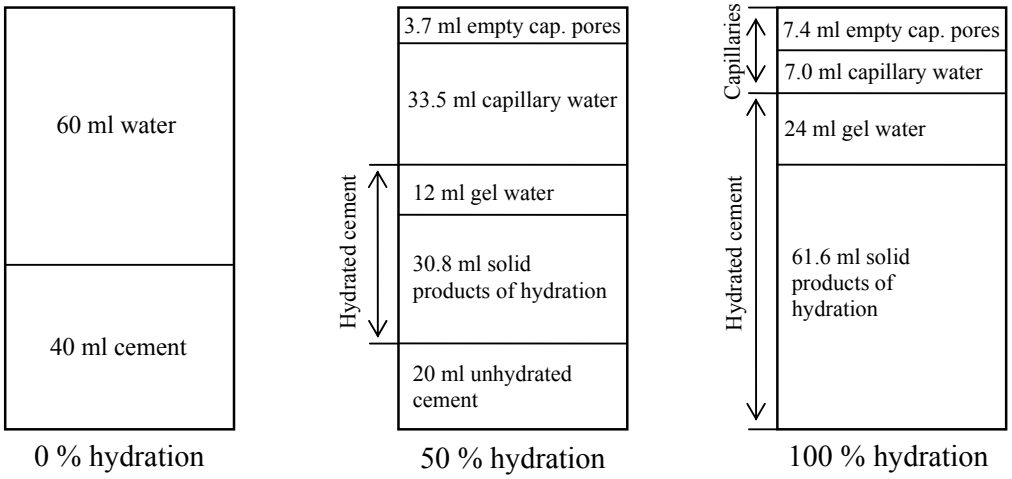

Figure 2.5: Diagrammatic representations of the volumetric proportions of cement paste at different stages of hydration

2.3.2. Hydration of Portland Cement with Fly Ash

The high calcium fly ashes have self hardening characteristics but low calcium fly ashes have very little or no cementing property. The pozzolanic reaction takes place between the CH and the fly ash. The CH, however, is produced from the hydration of cement. The CH reacts with the SiO_2 in the fly ash and CSH is formed as a result. These reactions are slower when compared to cement hydration and the rate of the reaction affects the characteristics of concrete.

The reaction of fly ash depends on the breakdown and dissolution of the glass phase which occurs when the pH of pore solution is higher than 13 (Fraay, 1989). The increase of the alkalinity of the pore water is because of the hydration of portland cement. The amount of CH formed during the first days is not enough for the

dissolution of the glass phase of fly ash and because of this, the fly ash is usually considered inert during the early days of hydration.

The amount of CH formed in the fly ash – cement system is initially lower than pure portland cement system. As a result of the pozzolanic reaction, the CH amount decreases and CH is consumed to form CSH. The change in the CH content is an indication of the pozzolanic activity. Figure 2.6 shows the change in CH content for different fly ash replacement levels (Taylor, 1992).

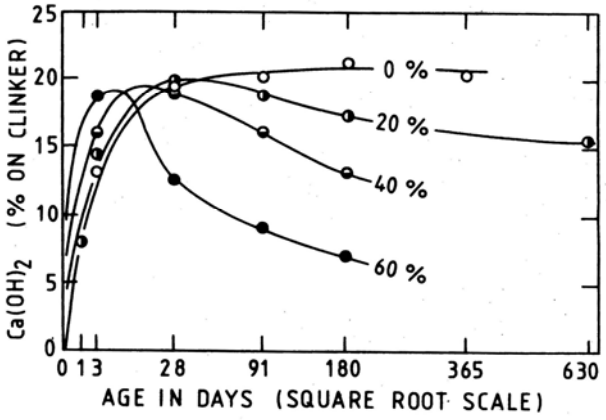

Figure 2.6: CH contents of pastes with different amounts of fly ash

2.3.3. Hydration of Portland Cement with Blast Furnace Slag

Granulated blast furnace slag reacts with the CH produced from the hydration of portland cement. CH serve as an activator for the dissolution of ions containing Si and Al by breaking the Si-O, Al-O, Al-O-Si covalent bonds (Roy and Malek, 1993). After slag cement is mixed with water, a pH level of about 12 is obtained in concrete within a short period, which is the reason the reaction of slag is more rapid when compared to fly ash.

Studies have shown that the principal hydration products of portland blast furnace slag cements are similar to those formed in pure portland cements (Taylor, 1992; Chandra, 2002). Some early slag hydration also takes place and the surface of slag is modified as soon as it contacts with water and a layer of CSH is formed on the surface of slag (Regourd et.al., 1983). A schematic representation of the blast furnace slag hydration products are shown in Figure 2.7 (Glasser, 1991). The gold coated surface in the figure shows the original slag surface before the hydration.

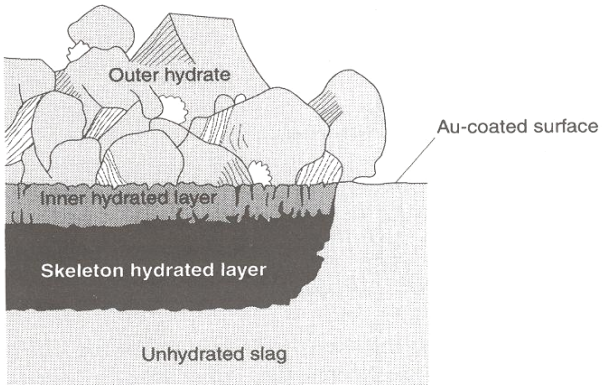

Figure 2.7: A schematic representation of the blast furnace slag products

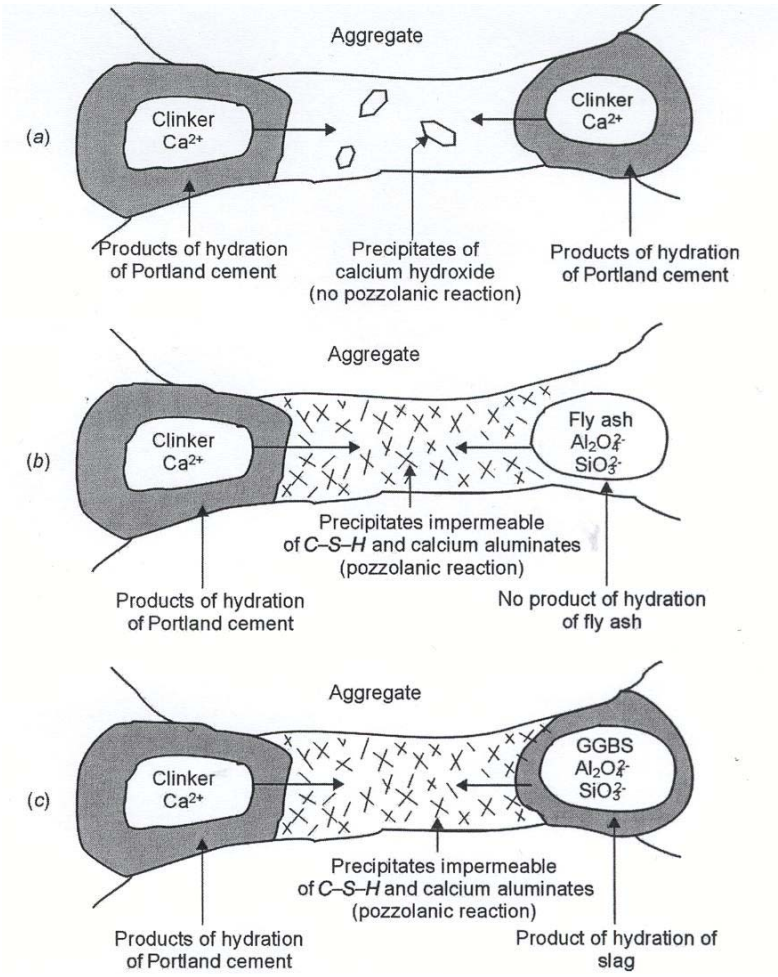

Figure 2.8: Hydration of (a) portland cement, (b) cement – fly ash blend, (c) cement – slag blend

Figure 2.8 shows the hydration of (a) portland cement, (b) cement – fly ash blend, (c) cement – slag blend (Bertolini et al., 2004). As seen in the figure, addition of fly ash

or slag leads to formation of very fine products of hydration that lead to refinement of pores.

2.3.4. Hydration of Portland Cement with Silica Fume

The hydration of a silica fume – portland cement is very rapid when compared to other pozzolans like fly ash or slag. Silica fume dissolves in a saturated CH solution within few minutes. When enough CH is produced as a result of cement hydration, CSH starts to form on the silica fume particles (Chandra, 2002). It was reported that half of silica fume can react in 1 day and two-thirds during the first 3 days (Neville, 2004). The characteristics of CSH, however, are different than those of produced by pure cement hydration. A schematic representation of CSH produced in silica fume pastes is shown in Figure 2.9 (Justnes, 2002).

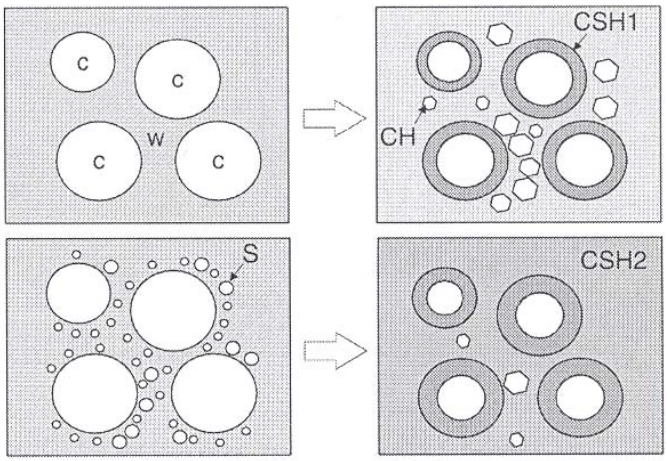

Figure 2.9: A schematic representation of the formation of two different CSH gels

In Figure 2.9; C, W, CH and S represent cement, water, calcium hydroxide, and silica fume, respectively. CSH-1 and CSH-2 are the CSHs by pure portland cement and silica fume, respectively. The general differences between these two gels are that CSH-2 produced in silica fume paste has longer linear polysilicate anions and has lower Ca/Si ratio. This ratio can be as low as 1 (Neville, 2004; Chandra, 2002). Ca/Si ratio decreases as the silica fume content increases (Taylor, 1992).

2.4. Microstructure

2.4.1. Microstructure of Portland Cement Concrete

Mechanical properties and durability of concrete is controlled by the microstructure (Mindess, 1985). On micro scale, concrete has a high degree of heterogeneity, consisting of different hydration products, aggregates, pores of different sizes and interfaces between these different phases. Figure 2.10 shows a schematic representation of the microstructure of a well hydrated portland cement paste (Mehta and Monteiro, 1996). In this figure A represents CSH particles, H shows hexagonal particles such as CH and C describes the capillary pores.

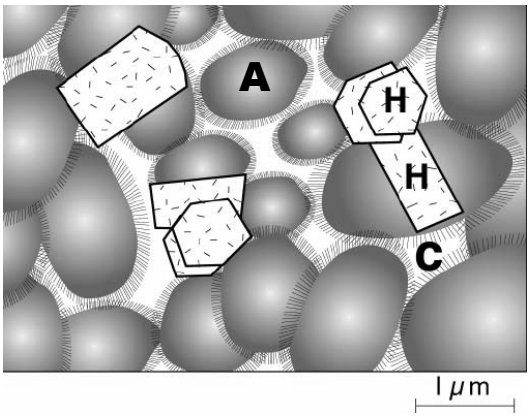

Figure 2.10: Model of a well hydrated portland cement paste

The amount of these different phases changes with the degree of hydration (see Figure 2.5); i.e. the volume of the CSH increases as the hydration proceeds but the amount of capillary pores decreases. The amount of gel pores in the cement paste also increases with the CSH amount. The CSH forms about 50 to 60 % of the volume of the solids in a completely hydrated cement paste and it is the main constituent responsible for the strength of the cement paste. Different types of CSHs are formed during the hydration process (Taylor, 1993). About 20 to 25 of the volume of solids in the cement paste is calcium hydroxide (CH) which are large hexagonal shaped crystals. Calcium sulfoaluminate hydrates form about 15 to 20 % of the volume of the solids. Besides these solid hydration products, the pores in the cement paste also have an important role on the properties of concrete.

A hardened cement paste is a porous material with an interconnected continuous pore system and depending on their sizes the pores can be divided as gel pores, capillary

pores and macro pores. Gel pores are interlayer spaces between the gel particles and have dimensions ranging from a few fractions of a nm to several nm (Neville, 2004). Because of their small sizes, gel pores do not affect the durability of concrete. Capillary pores, however, have much larger sizes ranging from 10 nm to several microns and interconnected capillary pores are one of the main factors affecting the permeability of cement paste. Macro pores such as entrained or entrapped air, are also present in the hardened cement paste with the dimensions sometimes up to a few mm.

Water/cement ratio is one of the main factors affecting the pore structure of hardened cement paste. Figure 2.11 shows the change of pore size distribution of cement paste due to change in water/cement ratio (Mehta and Monteiro, 1996).

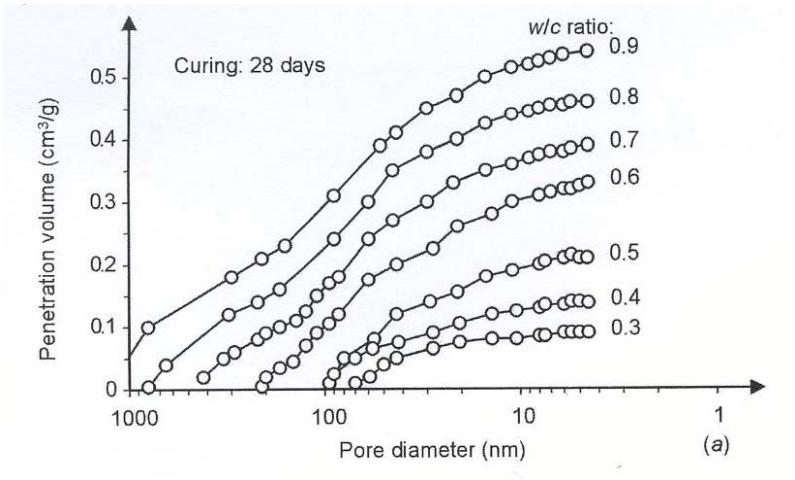

Figure 2.11: Effect of water/cement ratio on the pore size distribution of cement paste

The microstructure of cement paste at the immediate vicinity of the aggregate is different from that of the bulk paste. Figure 2.12 gives a schematic representation of this aggregate – cement paste interfacial zone (Mehta and Monteiro, 1996). Another representation of this zone is shown in Figure 2.13 (Chandra, 2002).

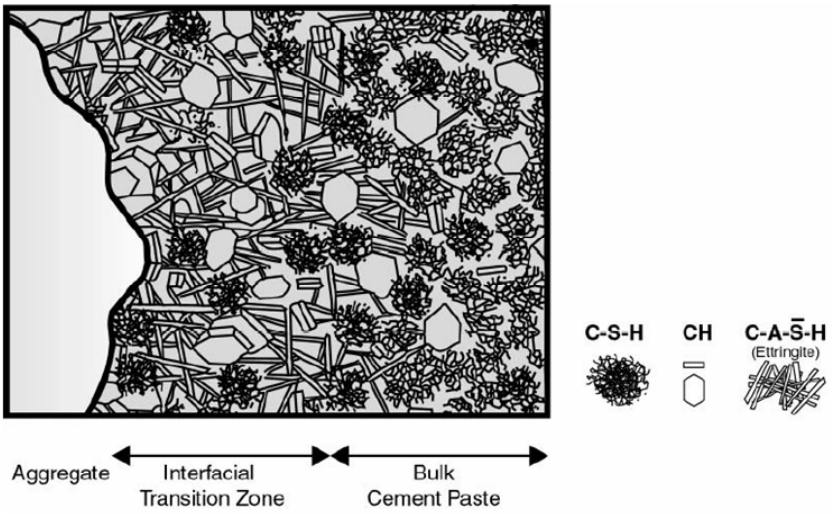

Figure 2.12: Aggregate – cement paste interfacial zone (Mehta and Monteiro, 1996)

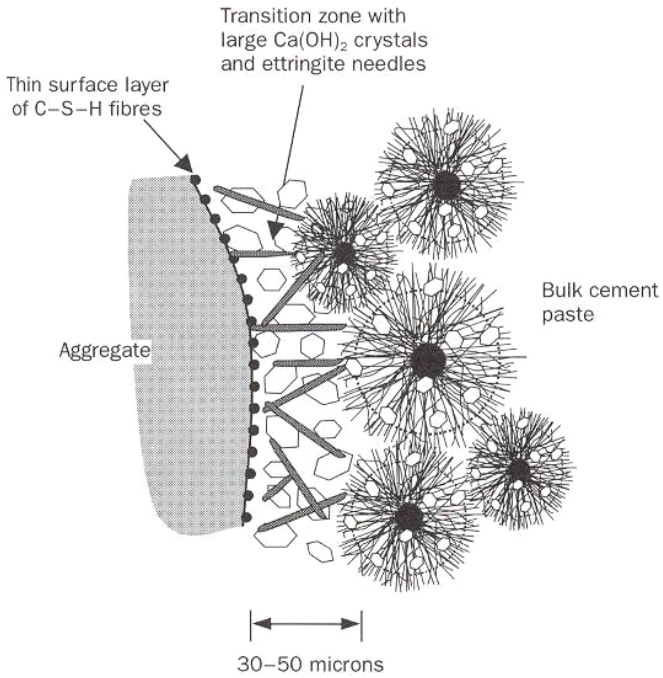

Figure 2.13: Aggregate – cement paste interface (Chandra, 2002)

Studies show that the amount of CH at the aggregate – cement paste interface is higher and the CH crystals are oriented perpendicular to the aggregate surface (Monteiro et al., 1985). A procedure for studying the orientation of CH crystals at the interface was developed in which the interface at the cement matrix side is successively removed by abrasion and X – ray diffraction analyses are carried out at each step. The diffraction intensities of CH crystals after the abrasions are then used for calculating an orientation index. The method is based on the fact that in the bulk

paste matrix the CH crystals are randomly oriented and the orientation index for random orientation equals to 1.0 (Monteiro et.al., 1985). Figure 2.14 shows the change of orientation index at the paste – aggregate interface (Massaza and Costa, 1986).

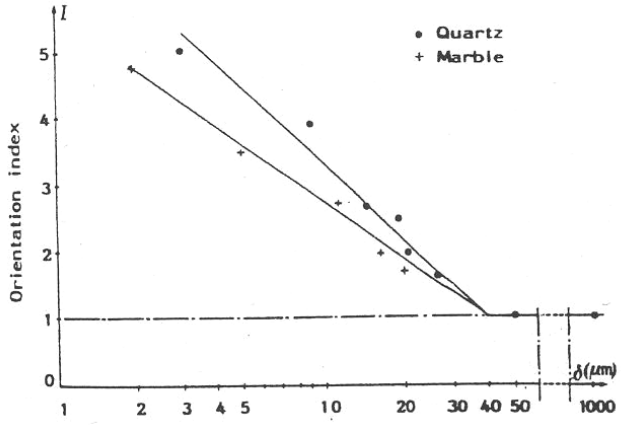

Figure 2.14: CH orientation index at the paste – aggregate interface

The porosity of the aggregate – cement interface is much higher and the strength is lower at this region. Figure 2.15 presents the variation in porosity of hydrated cement paste with distance from the surface of an aggregate particle (Neville, 2004).

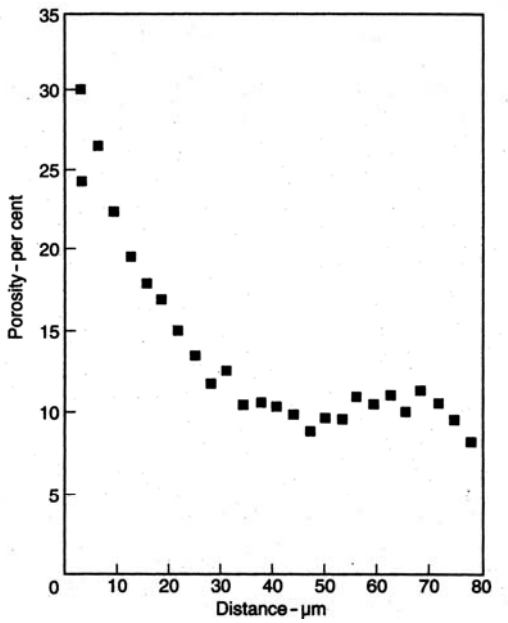

Figure 2.15: Porosity of the cement paste at the aggregate – cement interface

The formation of this interfacial zone with different properties may be due to combination different mechanisms. The cement grains pack poorly against a large

aggregate and as a result; there is less cement in this region to hydrate and to fill the voids. During the mixing of concrete, a water film forms around aggregate particles which causes a higher water/cement ratio at the aggregate surface. These effects may be the reasons behind the interface having different properties than the bulk paste.

The interface is the weakest link in concrete and has a big impact on the properties of concrete. Because of the higher porosity and lower strength, the interface can contain microcracks caused by shrinkage or thermal movements and these microcracks have an important effect on the stress – strain relationship of concrete. As a result of the higher porosity, the interface may also have an effect on the permeability of concrete.

2.4.2. Microstructure of Concrete Containing Fly Ash

Incorporation of fly ash into portland cement has an important influence on the microstructural properties of concrete such as refined pore size distribution or improved aggregate – cement paste interface.

Figure 2.16 shows the pore size distribution of a portland cement paste with and without fly ash (Fraay, 1989). As shown in the figure, the pore size distribution of cement paste with fly ash is initially coarser than the one without fly ash. At later ages, however, the pore size distribution of the paste containing fly ash is finer.

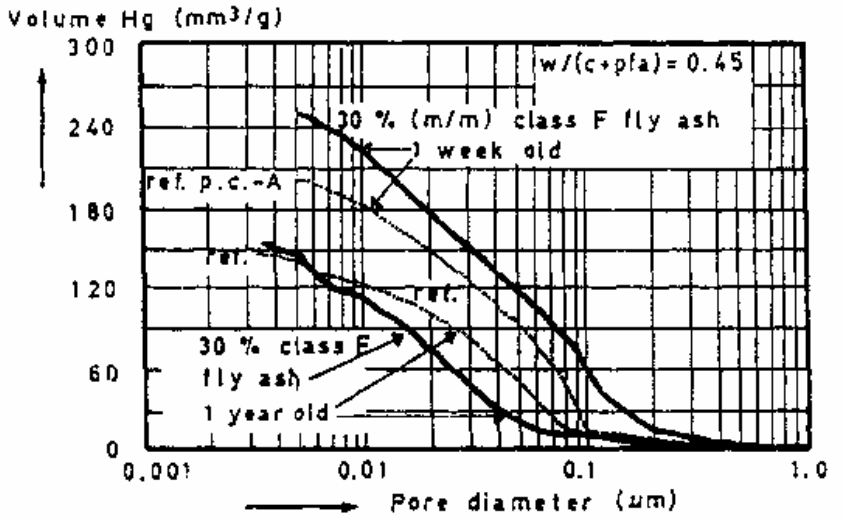

Figure 2.16: Pore size distribution of portland cement paste with and without fly ash

Fly ash has a significant effect on the aggregate – cement paste interface. Figure 2.17 shows the CH orientation index obtained for portland cement with and without fly ashes and quartz flour at 28 days age (Larbi, 1991). As seen in the figure, partially

replacing portland cement by fly ash reduced the orientation index in the immediate vicinity of the aggregate interface which indicates the decrease in the amount of CH at the interface. The thickness of the aggregate – cement paste interface can be defined as the region where properties are different than that of the bulk cement paste and as seen in Figure 2.17, the reduction in the CH orientation index indicates that the thickness of interface decreases with the use of fly ash. Since CH crystals have the planes of cleavage, the reduction of the orientation index values suggest that the resistance of the interface against the propagation of cracks increases with the use of fly ash (Saito and Kawamura, 1989). Pozzolanic reaction between the fly ash and CH is one of the reasons for the refinement of concrete microstructure. Better particle packing with the inclusion of fly ash also plays an important role for the improvement of the paste – aggregate interface.

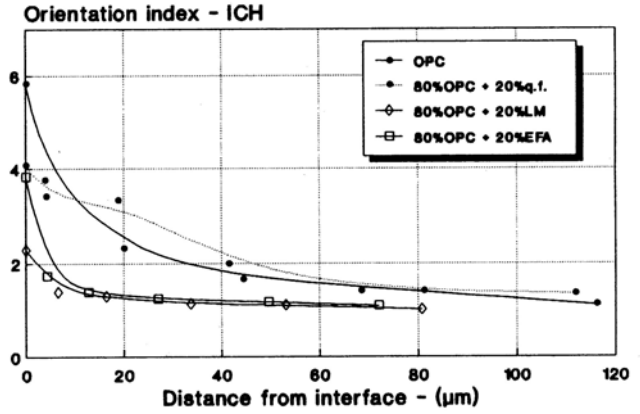

Figure 2.17: Effect of fly ash on the CH orientation index

2.4.3. Microstructure of Concrete Containing Blast Furnace Slag

Similar to the effects of fly ash, incorporation of granulated ground blast furnace slag also modifies the microstructure of concrete. CSH gel content of slag cement paste is significantly higher than that of portland cement as a result of less free lime generated (Bijen, 1996a). The CSH generated in concretes containing slag is compact, well crystallized and dense. Cement paste containing blast furnace slag has differences in total porosity and pore size distribution when compared to those of portland cement paste. At early ages slag, cement exhibits the same porosity as that of portland cement. However, at later ages, because the slag reaction continues for a long period, the volume of fine pores increases and the volume of capillary pores become lower. Although gel porosity increases and capillary porosity decreases by

the incorporation of slag, the total porosity is not affected significantly (Regourd, 2004). The amount used is also important for the effect of slag and Figure 2.18 schematically illustrates the change in the gel and capillary porosities based on the slag content (Lang, 2004). As seen in the figure, although the total porosity of the cement paste remains constant, capillary porosity decreases with slag amount.

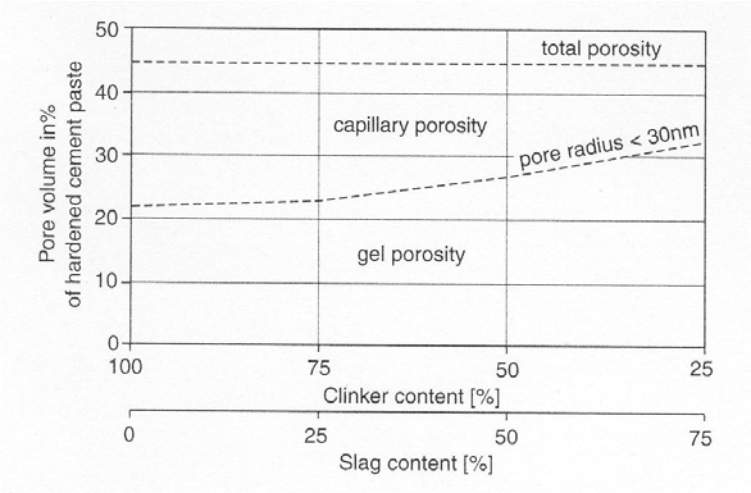

Figure 2.18: Pore size distributions of pastes based on the slag content

The additions of slag have a major effect on the transition zone between aggregate and cement paste. Figure 2.19 compares the degree of orientation of CH at the paste – aggregate interface in portland cement and blast furnace slag cement, for the age of 7 days (Larbi, 1991). As seen in the figure, the orientation index of slag paste is significantly lower even at 7 days.

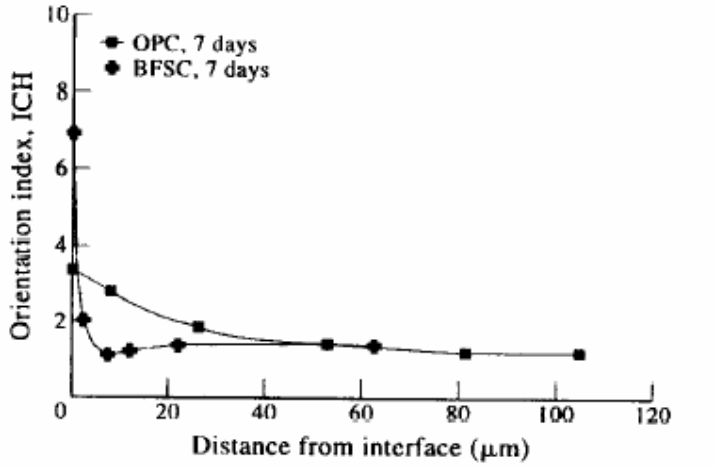

Fig. 2.19: Effect of slag on the orientation index at 7 days

2.4.4. Microstructure of Concrete Containing Silica Fume

Due to its high reactivity and extreme fineness, silica fume has a substantial effect on the concrete microstructure. Studies show that the pore structure of cement paste can be improved by the addition of silica fume. It was reported that refinement of pore size distribution of pastes takes place in a way that the content of larger pores reduces for decreasing water/cement ratios (Zhang and Gjørv, 1991). Figure 2.20 shows the effect of silica fume on the pore size distribution of low porosity cement pastes.

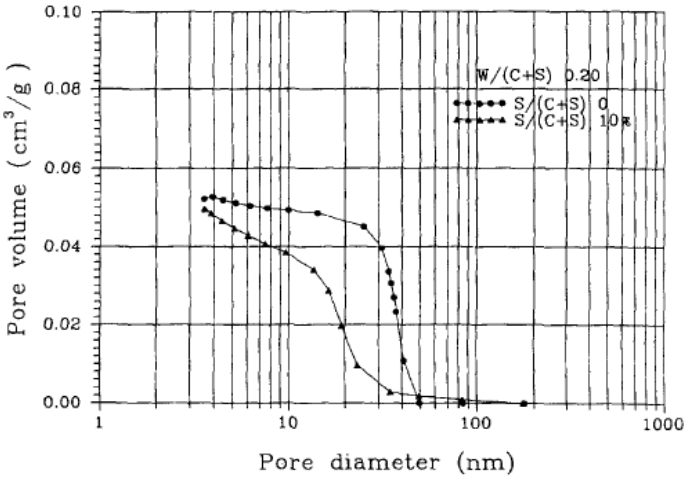

Figure 2.20: Effect of silica fume on the pore size distribution of paste

In addition to the refinement in pore size distribution of cement paste, silica fume also has an important effect in strengthening the aggregate – cement paste interfacial zone. This strengthening is attributed to the pozzolanic and the filler effects. For some researchers, however, the filler effect is more important than the pozzolanic effect. The filler effect depends on the fineness of the material which affects particle packing (Chengzhi et al., 1996).

In a previous study (Goldman and Bentur, 1994), strength of silica fume concrete was compared with that of a concrete containing an inert filler of similar fineness (carbon black). On the basis of microstructural studies and compressive strength tests, it was concluded that the primary effect of silica fume was generated by its physical (microfiller) properties, since the strengthening provided by reactive silica fume was similar to that obtained with nonreactive carbon black of similar size and shape. This effect was more significant from the point of view of the concrete strength enhancement than the chemical (pozzolanic) activity of the silica fume.

In the presence of silica fume or carbon black, densification of the transition zone occurred and significant refinement of pore structure was observed in both types of paste matrices (containing silica fume or carbon black). However, this refinement led to a relatively small influence on the paste strength. On the other hand, concretes containing reactive silica fume or an inert carbon black microfiller behaved as a composite material, unlike normal concrete. Figure 2.21 shows the results obtained in the study which indicates that microfiller effect has a higher importance than pozzolanic effect in strength enhancement of concrete (Goldman and Bentur, 1993).

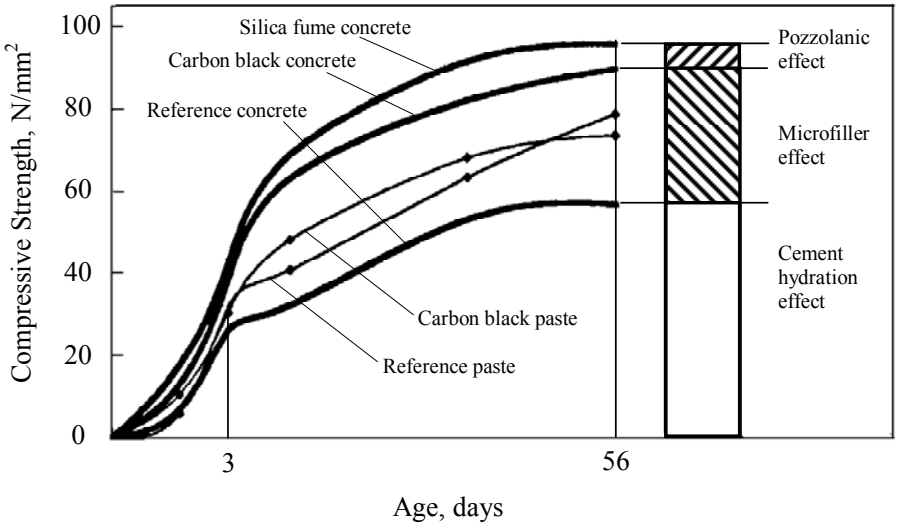

Figure 2.21: Strength of concretes containing silica fume and carbon black, and the contribution of pozzolanic and microfiller effects

It was also reported that, in the presence of silica fume, the orientation of CH crystals at the aggregate surface is affected during the first seven days of hydration, and at 28 days the CH is almost non-existent at the interface (Larbi and Bijen, 1990). Figure 2.22 schematically illustrates the aggregate – cement paste interface in the presence of silica fume (Larbi and Bijen, 1990).

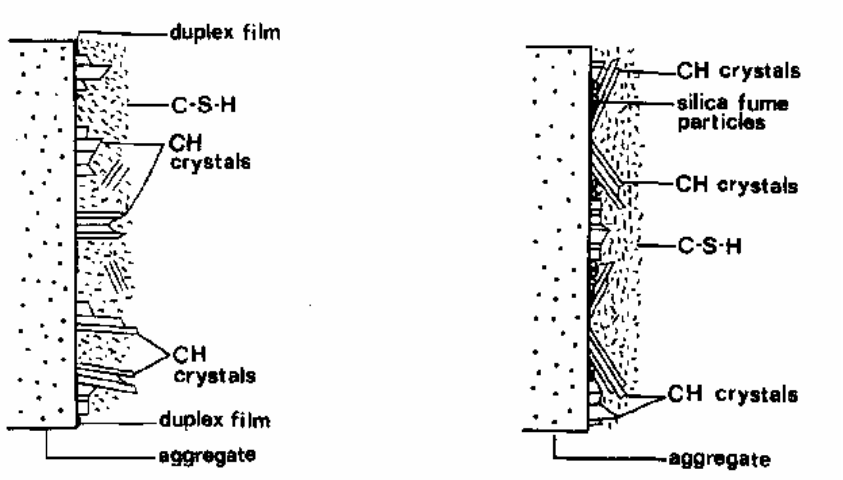

Figure 2.22: Schematic representation of the aggregate – cement paste interface (a) without silica fume, (b) with silica fume

2.5. Mechanical Properties of Concretes with Pozzolans

2.5.1. Concretes Containing Fly Ash

Due to the slow pozzolanic reaction of fly ash, fly ash concretes generally have a lower early strength. This strength reduction depends on the content and properties of the fly ash (Mehta, 1985). At later ages, however, with proper curing fly ash concretes can have a higher strength than the portland cement concrete. Figure 2.23 illustrates the effect of fly ash content on the strength of concrete (Neville, 2004).

Pozzolanic reaction takes place on the surface of the particles, thus, increasing the surface area of fly ash has an important effect on pozzolanic activity. The fineness of the fly ash is very important for the modification of cement paste-aggregate interfacial zone, which is the weakest link in concrete.

In a recent study (Demir et al., 2002), in order to study the influence of fly ash fineness on the strength development of concrete and the effect of grinding on the physical properties fly ash, a coarse F type fly ash with a Blaine surface area of 222 m^2/kg was ground to four different finenesses such as 337, 450, 538 and 604 m^2/kg. The corresponding retained values on a 45 μm sieve were 50%, 29.9%, 10.1%, 5.2%, and 3.7%, respectively. In grinding of the fly ash, a ball mill type of grinder has been used. Results showed that there is substantial effect of fly ash fineness on the strength development of concrete especially for long curing times; as the fineness of fly ash increases, the compressive strength of concrete increases significantly, and

more noticeable results are obtained for low cement/binder ratio. Results confirmed that the performance of concrete with fly ash depend not only on the mineralogical and chemical composition of fly ash, but also on its physical properties such as fineness and particle shape, and also on the water-binder ratio of the mix.

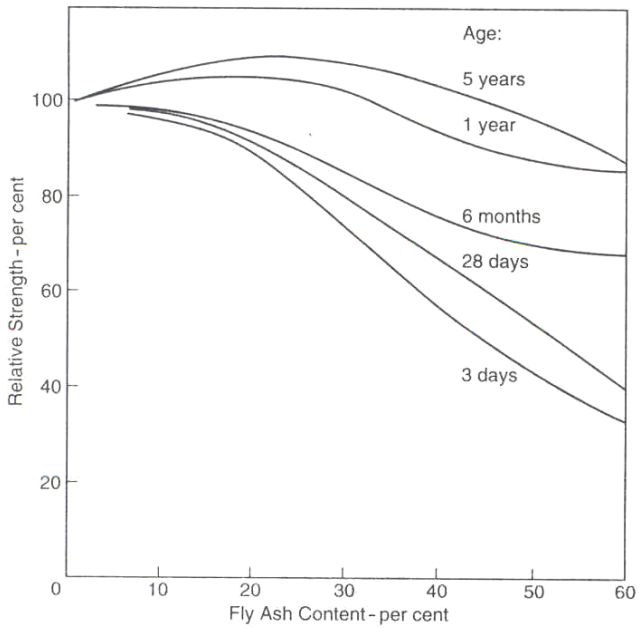

Figure 2.23: Effect of fly ash content on the strength development of concrete

The effect of fly ash fineness on the compressive strength is illustrated in Figure 2.24. In order to obtain higher strength with coarse fly ash, it was recommended to reduce water content or increase the binder content (McCarthy and Dhir, 1999).

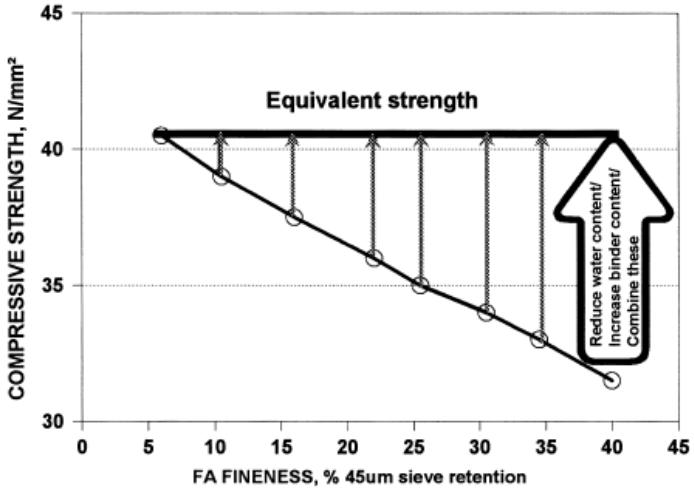

Figure 2.24: Effect of fly ash fineness on compressive strength

2.5.2. Concretes Containing Blast Furnace Slag

Strength of slag concretes are generally lower at early ages but slag concrete can outperform portland cement concrete at later ages. The replacement amount and properties of slag and curing conditions are important factors affecting the strength development of the slag concretes. The early age strengths of slag concretes are inversely proportional to the amount of slag (ACI Committee 233, 1995) and the replacement amount of slag is usually higher than fly ash (i.e. 50–70%). Separate grinding of slag and clinker, and blending them according to specific needs is a more optimized process (Oner, 2000). Figure 2.25 shows the effect of slag content on the strength development mortars (ACI Committee 233, 1995). As illustrated in the figure, at later ages the strength of mixtures containing slag are significantly higher than that of the portland cement mixture.

The particle size is also an important factor for the pozzolanic activity of the granulated blast furnace slag. Similar to the fly ash, the strength of slag concretes also increases with increasing slag fineness (Tasdemir et al. 1997). By using finely ground blast furnace slag, the aggregate – cement paste interface which is the weakest link in concrete can be improved and the thickness of this zone can be reduced. Better particle packing due to finer materials and the pozzolanic reaction of the slag are the reasons for this enhancement. By the densification of the aggregate – cement paste transition zone, concrete becomes more homogeneous and higher strengths can be obtained. This improvement may be more effective at lower water/binder ratios which can cause a better performance of the pozzolanic material. Figure 2.26 shows the effect of slag fineness on the compressive strength of mortars containing 75% slag (Hooton, 1987). As illustrated in the figure, the mortar strength increased about 30 % when the fineness of the slag was changed from 300 m^2/kg to 450 m^2/kg.

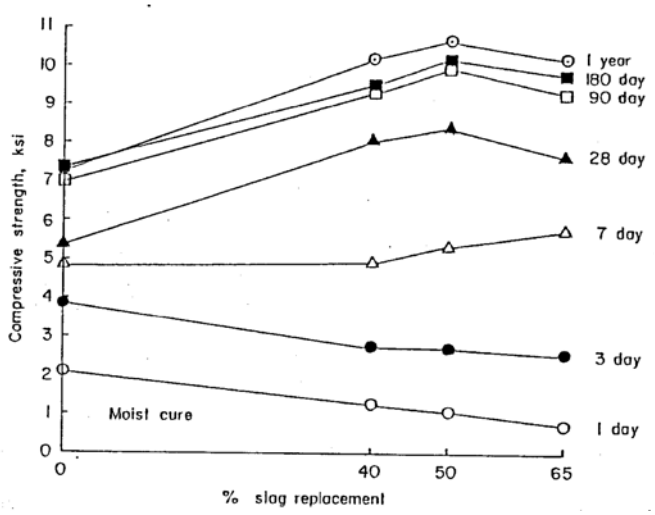

Figure 2.25: Effect of slag replacement amount on the strength development of mortars

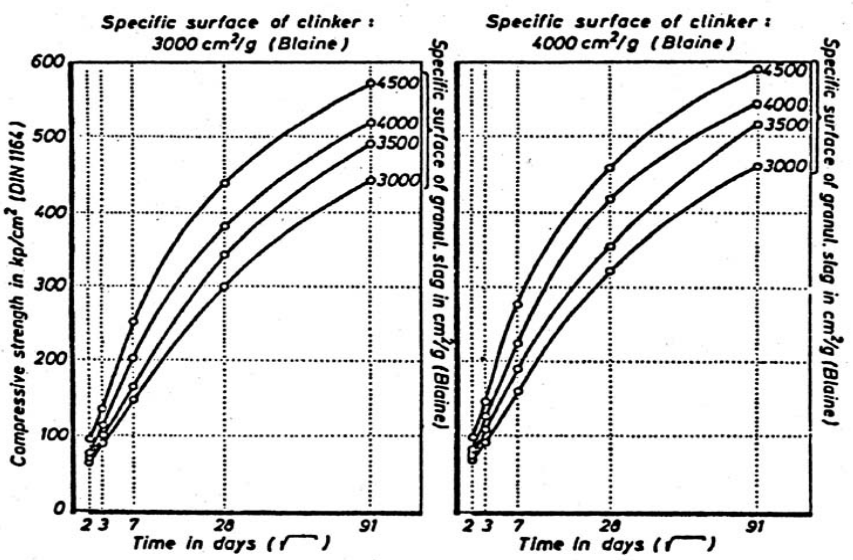

Figure 2.26: Effect of slag fineness on the strength development of mortars

2.5.3. Concretes Containing Silica Fume

Silica fume has an important impact on the aggregate – cement paste interface. The enhanced interfaces in silica fume concretes have been reported in numerous papers. As a result of strengthening the interfacial zone, mechanical properties of concrete is affected substantially. Unlike the other pozzolans (fly ash or slag), the silica fume takes effect at early ages and its contribution to the strength is important also in these ages. The effect of silica fume on the microstructure and strength of concrete was already discussed in previous chapters and strength development of silica fume

concrete was presented in Figure 2.21. Figure 2.27 illustrates the effect of silica fume replacement ratio on the compressive strength of concrete (ACI Committee 234, 1996). Although the figure shows the result for replacement up to 30%, the amounts used in practice are less than 15%.

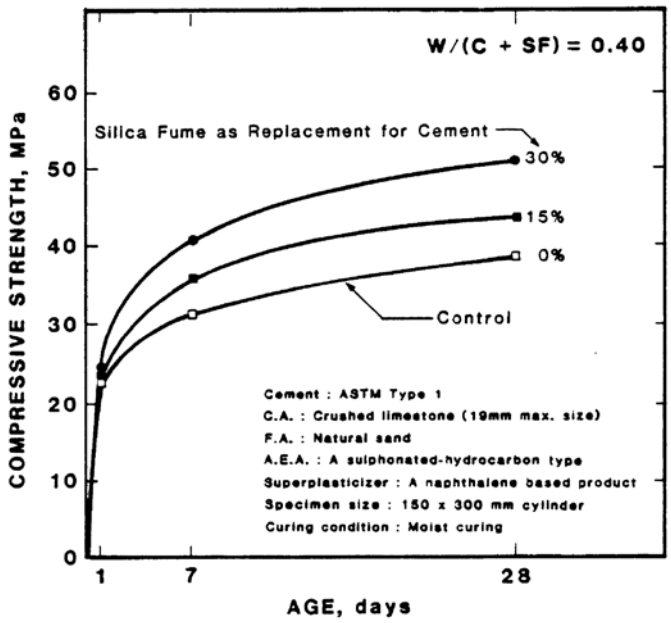

Figure 2.27: Effect of silica fume replacement ratio on the strength of concrete

Some of the disadvantages of using fly ash or slag concretes can be overcomed by the use of silica fume. Ternary (three part) and quaternary (four part) binders can be optimized with a synergistic effect in order to compensate for shortcomings of the component ingredients (Nehdi, 2001). By incorporating fly ash or slag with a highly reactive material such as silica fume, it is possible to obtain concretes with enhanced early age and also late age characteristics. For example, the low early age strength of high volume fly ash or slag concretes which can cause problems in winter concreting or in removal of formwork, can be improved with use of silica fume; or the heat development of silica fume concretes can be controlled by the use of fly ash or slag. Optimized particle packing and hydration characteristics are the main factors of the better performance of ternary and quaternary binder systems. The strength and density of interfacial zones in concrete are governed by the packing of materials at these zones. By using mineral admixtures of various sizes, the particle size distribution of the binder can be widened and a better particle packing can be obtained.

In addition to the filler effect, the synergic action in the multi blended binder systems continues for a long term. The early hydration of portland cement produces CH which is consumed by the early hydration of the highly reactive pozzolan (silica fume). The CH produced by the later hydration of the portland cement is consumed by the less reactive component in the blend such as fly ash or blast furnace slag, to provide further refinement of porosity and improvement of microstructure. This sequence of hydration reactions has a big impact in decreasing the permeability and a result in improving the durability of the concrete (Nehdi, 2001).

2.6. Chloride Resistance of Concretes Containing Pozzolans

2.6.1. Concretes Containing Fly Ash

Deterioration of concrete depends on the penetration of aggressive substances into concrete via microcracks and interconnected pore system. Permeability of fly ash concretes at early ages can be significantly higher when compared to that of portland cement concrete. At later ages, however, fly ash concretes can have much lower permeability depending on the replacement ratio and characteristics of the fly ash. Proper curing is especially important for fly ash concretes in order to achieve lower permeability (Tasdemir, 2003). As briefly discussed in previous chapters, the incorporation of fly ash modifies the microstructure of concrete and a much finer pore system can be obtained which affects the durability of concrete. Clogging of pores and increase in tortuosity of pore channel are responsible for the improved permeability properties (Li and Roy, 1986). The substantial effect of fly ash on the pore structure is not reflected so much in the permeability, but rather in the diffusivity of ions (Bijen, 1996b).

Figure 2.28 shows the effect of fly ash replacement ratio on the chloride diffusivity and chloride binding ratio, which were obtained on specimens 28 days old (Dhir et al., 1997). As seen in the figure, chloride diffusion coefficient is reduced with the fly ash replacement amount. The figure also shows that as the PFA content increases the chloride binding capacity increased up to a level of 50%. At 50% PFA content and a chloride exposure concentration of 5 mole/liter, the chloride binding capacity increases by a factor of 4 compared with the control. These results indicate that chloride binding would appear to be at least as important as improving the physical aspects of concrete and in the case of FA concrete may even be the dominant factor

in improving the resistance of concrete to chloride attack. The combined effect of improved permeability properties and chloride binding further improves the resistance of fly ash concrete against chloride penetration. Long – term sea water exposure tests confirm the better performance of fly ash concretes. Results obtained from reinforced concretes in a marine environment show that, concretes containing 30 % or more fly ash provides much improved protection to steel reinforcement compared with portland cement of equal strength grade, equal binder content or equal water/binder ratio (Thomas, 1991; Thomas and Matthews, 2004). A report on the resistance of the concrete to chloride ion penetration measured according to ASTM C 1202 on 10 year old concretes also indicate the long term performance of concretes with pozzolans (Malhotra, 2000). The charge passed through the concrete mixtures investigated in the study was less than 1000 coulombs at 10 years indicating very low chloride-ion penetrability. For the high-volume fly ash concrete, the charge passed was 0, giving a chloride-ion penetrability rating of this concrete as negligible. It is extremely rare to achieve values as low as this in portland cement concrete; one can obtain such a low value only for polymer or polymer impregnated concrete because of the extremely low porosity of the system (Malhotra, 2000).

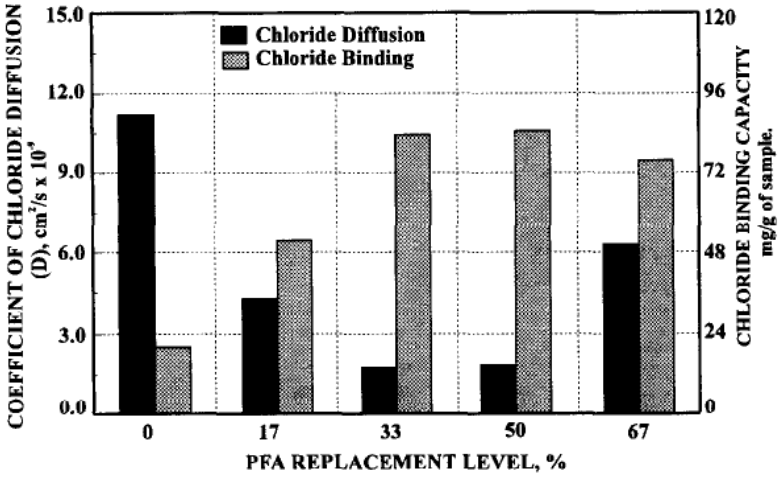

Figure 2.28: Effect of fly ash replacement ratio on the chloride diffusivity and chloride binding

Fineness of fly ash is one of the important factors influencing the chloride diffusivity of the fly ash concrete. Figure 2.29 compares the chloride diffusivity of a normal concrete with two fly ash concretes; one containing a normal (unprocessed) fly ash and the other with a ground fly ash (Dhir and Jones, 1999). In the study, a coarse fly

ash was processed until all particles were finer than 10 μm. This fine ash was used to directly replace portland cement by up to 30 % by weight to produce concrete samples with cube strength of 40 MPa. The accelerated chloride diffusion test was then used to determine the coefficient of chloride diffusion, as shown in the figure. As illustrated in Figure 2.29 the addition of unprocessed fly ash decreased the diffusivity more than 60 %. When the ground fly ash was used, the diffusivity was 88% lower than that of the portland cement concrete. If only the concretes containing fly ash are compared, the ones produced with ground fly ash had about 70 % lower diffusivity than the one produced with the unprocessed fly ash. The improved chloride resistance of concretes containing fine fly ash has been reported also in other studies (Dhir, et al., 1991; Schiessl and Wiens, 1995).

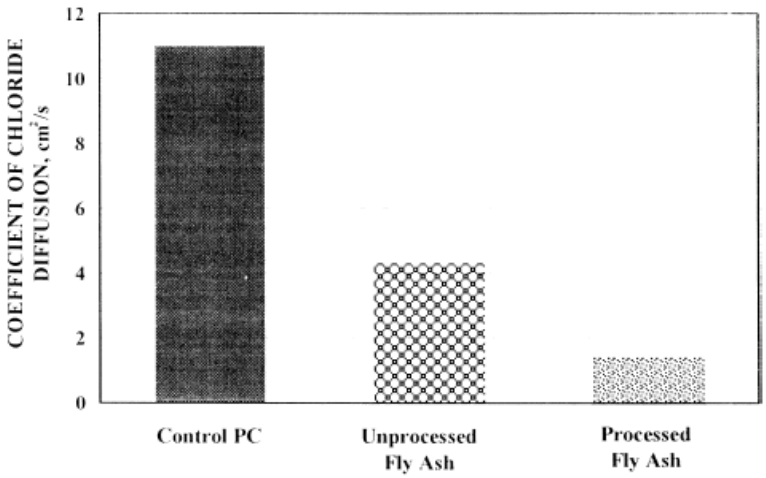

Figure 2.29: Effect of fly ash fineness on the chloride diffusivity of concrete

2.6.2. Concretes Containing Blast Furnace Slag

Studies have shown that concretes containing blast furnace slag provides significant protection against chloride induced corrosion of embedded steel. The rate of chloride is greatly reduced due to the improved pore structure of concrete. Depending on the amount and characteristics of the slag, the chloride diffusivity of concrete can be decreased by a factor 150 (Bijen, 1996). The resistance of concretes to chloride ion penetration increases with an increase in the slag content (Sivasundaram and Malhotra, 1992; Gjrøv and Vennesland, 1979; Pal, et al., 2002). Figure 2.30 illustrates the effect of slag replacement amount on the resistance of concrete against chloride penetration (Lang, 2004). Results given in the figure were obtained on concrete cubes stored in NaCl solution for one year. The chloride content had been

analyzed in a layer 20 – 40 mm under the concrete surface. As seen in the figure, the effect of slag is insignificant up to 20 % replacements, but beyond this ratio a substantial decrease in the chloride content was observed. Very similar results for the effect of slag content on the chloride diffusivity were also reported (Bijen, 1996a and 1996b). Field studies carried out on concrete structures along the sea coast confirm the better performance of slag concretes in marine environment (Bijen, 1996a; Osborne, 1999).

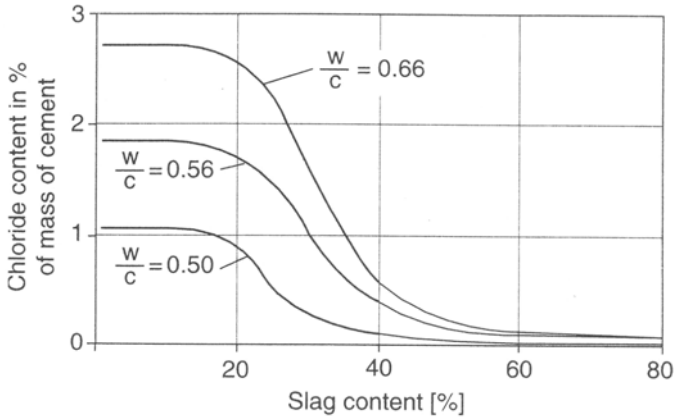

Figure 2.30: Effect of slag replacement amount on resistance of concrete against chloride penetration

The electrical resistivity of concrete is an important component of reinforcing steel corrosion cells, as high resistivity of the concrete reduce corrosion currents and slow the rate of corrosion (Whiting and Nagi, 2003). The electrical resistivities of concretes containing slag are significantly higher which extends the initiation and propagation period of corrosion of the embedded steel (Hou et al., 2004). As seen in Figure 2.31 the electrical resistivity of concrete increases with the slag amount (Geiseler et al., 1995).

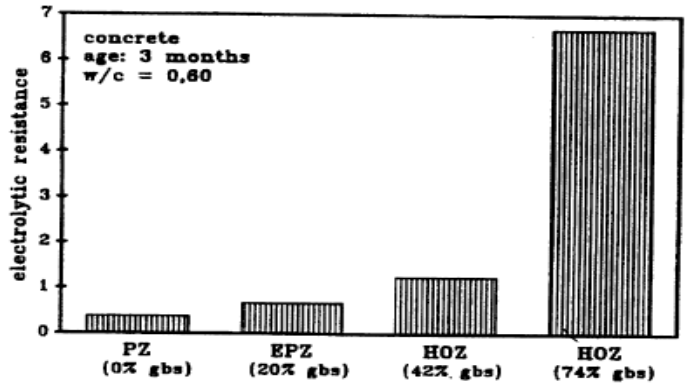

Figure 2.31: Effect of slag amount on the electrical resistivity of concrete

2.6.3. Concretes Containing Silica Fume

Silica fume is very effective in controlling chloride penetration into concrete and paste (Bentz et al., 2000). Improved cement paste pore system and densification of the porous aggregate – cement paste interface are the causes of better performance of the concretes containing silica fume. The replacement ratio has an important effect on the resistance against chloride penetration. It has been reported that inclusion of 7% silica fume can cause 80 % decrease in the diffusivity of portland cement concrete and this reduction can be about 90 % when 12 % silica fume is used (Hooton, et al, 1997). Silica fume is more efficient for reducing diffusivity of mixtures with lower water/cement ratios (Bentz, 2000).

In chloride containing environments, multi-blended binder systems containing silica fume perform better than the binary blends (Bleszynski et al., 2002) In a recent study, it was concluded that regardless of the type of fly ash, water/binder ratio or the fly ash and silica fume contents, the concrete made with the ternary blend of fly ash and silica fume outperforms the concrete made with portland cement alone as well as the concrete made with the binary system (Bouzoubaa et al., 2004).

The better durability characteristics of multi-blended binder systems are the results of decreased permeability properties. Porosity and microstructure are improved by the pozzolanic effects (of silica fume and fly ash or slag) and filler effect (of silica fume) that affect particle packing (Mangat et al., 1994). Interface porosity is reduced significantly by the incorporation of silica fume together with another pozzolan (Poon et al., 1999). The synergic action in the multi-blended binder systems continues for a long period and as a result very high resistance against the penetration of chlorides can be obtained (Hisada et al., 1999; Malhotra et al., 2000). Thus, substantial increase in the service life of the structures can be obtained.

2.7. Environmental and Economical Aspects of Concrete Production

2.7.1. Human Impacts on the Planet

During the last 100 years, world population has increased from 1.5 billion to more than 6 million. This increase was dramatic in the last 50 years in which the population has doubled. The increase from 5 billions to 6 billions has taken only 12

years (Swamy, 2001). It is estimated that the population will increase about 50 % in the next 50 years (US Census Bureau, 2004).

The lifestyle of people also changed noticeably in the last century; about 50 % of population now lives in and around cities rather than rural areas. As a result of the rapid growth in population and industrialization, the demand and consumption of natural resources of the planet is increasing and this consumption is unrestricted. Current economic models and technology choices are promoting wasteful consumption of materials. It is estimated that only 6 % of global flow of materials, some 500 million tons a year, actually ends up in the desired products while most of the virgin materials are returned to the environment as harmful solid, liquid and gaseous wastes (Mehta, 2001). The uncontrolled and wasteful consumption of resources is one of the main causes of the environmental damage.

The demand for energy is constantly increasing in today's world. During the past 100 years, the energy production from burning of the fossil fuels has increased 16 fold (Mehta, 2002) and fossil fuels are the primary source of energy today. Combustion of fossil fuels is a direct cause of the green house gas CO_2 release into the atmosphere. Thus, any approach to decrease fossil fuel consumption has a beneficial effect in reducing CO_2 emissions. In the past 100 years, the release of large volumes of CO_2 has increased atmospheric concentration of this gas from 260 to 370 ppm which is the highest level in 400000 years. The consequence of the emission of greenhouse gas is the global warming which causes serious disruptions to environment and also lives.

2.7.2. Ecological Impact of Concrete

Concrete is the world's most important and widely used construction material (Aitcin, 1995). According to CEMBUREAU, in 1998, the total world production of cement was about 1.6 billion tons and if it is assumed that about 250 kg of cement are used to produce 1 m^3 of concrete, about 6.5 billion m^3 of concrete was used in 1998. The cement production in the world is expected to exceed 2.5 billion tons in the year 2050. Being the largest user of natural resources, concrete production has a serious effect on environment (Mehta, 1999). Every year, concrete industry is consuming 10 billions tons of sand and rock, 1 billion tons of mixing water and even larger amounts for wash water and curing.

After aluminium and steel, the manufacture of portland cement is the most energy intensive material production process. Producing a ton of portland cement requires about 4 GJ energy and this manufacture releases about 1 ton of CO_2 greenhouse gas into the atmosphere. Minor amounts of other gases are also released. Cement production releases about 1.4 billion tons of CO_2 every year which is about 7 % of the CO_2 production worldwide (Malhotra, 2000). About half of the CO_2 emissions are due to the calcinations of limestone and the other half are due to the combustion of fossil fuels. The mining, processing and transport of the large quantities of aggregates also consume considerable amounts of energy and affect ecology.

Uncontrolled and short service life of concrete structures is another source of the environmental impact of concrete. Considerable amounts of concrete are being used for repair and strengthening of existing structures. In UK, for example, 50 % of the construction industry output is spent on repair, strengthening and maintenance. It is estimated that the structural damage repair in Europe costs 1.4 billion Euros annually (Swamy, 2001).

2.7.3. Environmental and Economical Effects of Using Pozzolans in Concrete

The long term approach to decrease environmental impact of any material is to reduce its rate of consumption, but reducing concrete consumption cannot be done in the next few decades. Increasing the effective use of the materials and portland cement, production of low energy intensive cements, increasing the service life of the structures and infrastructure, and recycling are some of the measures to reduce the environmental impact of concrete (Aïtcin, 2000).

First step in decreasing the energy consumption and greenhouse emissions caused by the concrete production can be reducing the portland cement use by incorporating pozzolanic materials in concrete (Malhotra, 1999). The pressure of ecological constraints and environmental regulations are bound to increase in the coming years which will lead to greater use of supplementary cementitious materials such as fly ash, blast furnace slag or silica fume (Bentur, 2002). As summarized in previous chapters, by replacing part of cement with the pozzolanic materials, it possible to obtain improved fresh and hardened concrete properties. Replacing more than 50% of cement by pozzolanic materials lead to the definition of “green concrete” (Glavind and Petersen, 2002). This term represents environmentally friendly concrete, which

contains high volumes of pozzolans, generally has low water/cement ratio and high durability properties.

Because most of the pozzolans are readily available for utilization and no need for production is needed, the cost of incorporating them into concrete includes mostly the transporting and storage costs. In some cases there can be a need for processing the pozzolan to obtain better performance. The cost of processing the pozzolan, however, is significantly lower than producing portland cement. Fly ash and silica fume normally do not need additional energy input before use, and with the use of fly ash for replacement of cement, energy saving in direct proportion to the amount of pozzolan can be obtained. Blast furnace slags, however, need to be dried and ground before use and it is estimated that the total energy requirement for this purpose is about 20% of that required for portland cement (Lohtia and Joshi, 1995).

Energy requirements for the production of pozzolan blended cements depend on the properties and the amounts of the pozzolan used in cement (Frigione, 1996). Figure 2.33 illustrates the effect of slag replacement amount on the energy consumption of cement (Lang, 2004). As seen in the figure, the energy consumption decreases with the slag replacement amount. For the 30 % slag replacement, the energy requirement decreased 24 %. The energy required for the production of cement with 75 % slag replacement is 38 % of the energy needed for portland cement.

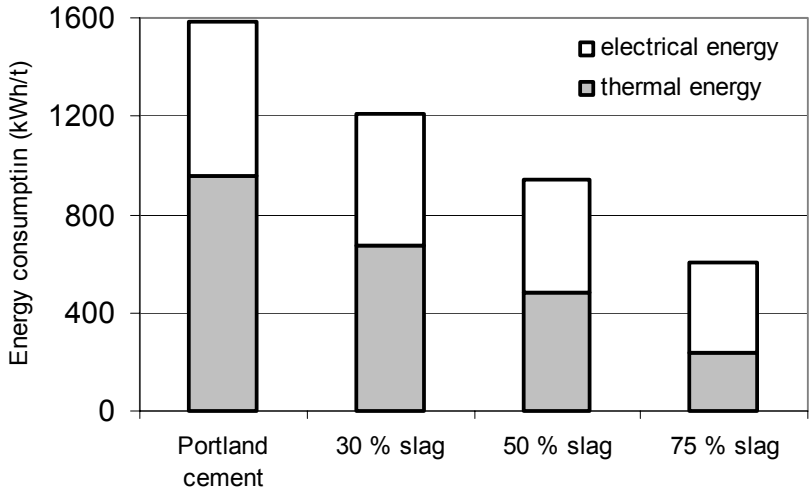

Figure 2.33: Effect of slag replacement on energy consumption

Among several methods, use of large amounts of pozzolanic materials in concrete appears to be the most effective method for reducing the emissions of CO_2 caused by the portland cement manufacture (Gartner, 2004). By incorporating pozzolans into cement, CO_2 emissions can be decreased substantially. For example, for the cement with 30%, 50% and 75% slag replacements, the emissions are 72%, 51% and 29.7% of the portland cement, respectively (Lang, 2004).

The most available pozzolan worldwide is fly ash. It is estimated that about 600 million tons of fly ash was available in 2000 but only 6% of it was used in cement or concrete industry. The annual slag production is about 100 million tons worldwide but again, only a very small fraction is utilized. These pozzolans are by-products and storage of these huge amounts is a major challenge. When they are stockpiled on land, they cause air pollution and during rainfall or snow melt season, the migration of ions from the dumped wastes can cause pollution of subsoil and ground water. In additon, toxic metals which are usually present as trace elements, can be released and pollute lakes or streams. By increased utilization in concrete and cement, some of the problems and costs associated with the environmentally safe storage or disposal of these materials can also be reduced. Besides using in concrete as supplementary cementing materials, pozzolans can be utilized in other applications in construction industry. Fly ash, for example, can be used in road construction for sub bases, in landfill applications or to produce aggregate for concrete (Sear, 2002).

2.8. Micro Indentation Testing of Cementitious Materials

2.8.1. Introduction

Concrete is an extremely complex system of solid phases, pores and water, with a high degree of heterogeneity. The properties of concrete are determined by the characteristics of constituent materials and the interfaces between cement paste and aggregate. Since about 75 percent of the concrete volume is occupied by aggregate, interfacial region between aggregate and cement paste matrix forms an important proportion of cement paste and this region greatly affect the durability and the structural performance of concrete. As described in Chapter 2.4, the microstructure of the hydrated cement paste in the immediate vicinity of coarse aggregate particles is different from that of the bulk cement paste. The thickness of the interfacial zone varies from 20 μm to 100 μm which depends on the materials used and the properties

of the concrete (Monterio et al., 1985; Zimbelman, 1985). The interfacial zone is porous and contains large crystals of $Ca(OH)_2$ perpendicular to the aggregate surface. There are two major reasons for the formation of this interfacial zone: i) wall effect: inefficient packing of the cement particles at the aggregate interface, ii) high water/cement ratio at the aggregate surface. It was well established that the paste-aggregate interface is the weakest link and therefore the mechanical properties of concrete are significantly affected by the properties of this interfacial zone. When the aggregate and cement paste are individually subjected to uni-axial compression, they exhibit an almost linear stress-strain relation. Concrete, however, shows inelastic behaviour due to the presence of interfaces between the cement paste and the aggregate (Neville, 1997). To determine the influence of the interfacial zone on the mechanical properties of concrete, the material can be considered as a three phase composite model consisting of mortar matrix (or cement paste), aggregate and interfacial zone between cement paste and aggregate (Tasdemir et al., 1998).

There are various techniques for determining the porosity, orientation of crystals or the chemical composition of the cement-paste aggregate interface, but measurement of the mechanical properties of such a small zone is difficult. Hardness measurements have been used successfully for many years and it is a useful technique for characterizing the properties of materials like metals, ceramics or rocks (Van Vlack, 1994). Hardness can be defined as the resistance of a material to penetration. An indenter is pushed into a smooth material surface under controlled load and the size of residual impression is measured to calculate the hardness (ASTM E 384a, 2005). The geometry of indenter tip may differ and hardness type is named after it (i.e. vickers, brinell, knopp hardness).

Hardness measurement is also used in characterizing the properties of cement-based materials and because of using very small loads; it is often termed as microhardness (Igarashi, et al., 1996). Microstructural properties of interfacial transition zone between cement paste and aggregate, and bulk paste can be evaluated by microhardness tests. It is a non-destructive technique by which the transition zone can be easily mapped.

In recent years there have been great developments in testing techniques. With the developments in “thin film” industry, measuring the mechanical properties at such a small scale became important and this need lead to a new testing method known as

depth sensing indentation. In this form of indentation testing; displacement of the indenter tip and load are recorded continuously under computer control and load – displacement curve is obtained during loading and unloading cycle. Elastic, plastic and time – dependent deformation properties of the material such as hardness, modulus of elasticity, fracture toughness or creep can be obtained with such loading (Trtik and Bartos, 1999). The interfacial zone between concrete and reinforcement and elastic modulus of cement phases can be studied by nano – indentation (Velez et al., 2001). Sub – micrometer indentations are possible and this technique is often referred as ultra – low load or nano – indentation. It is routinely used to characterize the properties of thin films, very soft coatings and materials like polymers, magnetic storage systems, micro-electromechanical system devices and in medical research (Li and Bhushan, 2002).

Nanotechnology based techniques like scanning and transmission electron microscopy, atomic force microscopy or mercury intrusion porosimetry have been used for characterizing cementitious materials, but up to recent years there were no nano – technology based mechanical testing methods. With the development in depth sensing nano – indentation testing techniques, it is now possible to evaluate the micromechanical properties of cement – based materials. There is very little information in the literature about mechanical testing of the aggregate – cement paste interface by nanotechnology based testing techniques.

Mechanical and physical properties of cementitious materials depend on the microstructure and the development of microstructure is a nanoscale process which is not fully understood. Establishing a realistic model of aggregate – cement paste is not possible without the mechanical properties of the interfacial zone.

2.8.2. Depth Sensing Nano Indentation Technique

In conventional indentation testing, a specified load is pressed onto a surface and hardness is obtained by;

$$H = \frac{P}{A} \tag{2.4}$$

where H is hardness of the material, P is the maximum load, and A is the projected area of permanent impression measured after the indentation.

A typical hysteresis curve, obtained during loading – unloading indentation cycle by a new – generation depth sensing microhardness tester, is given in Figure 2.34.

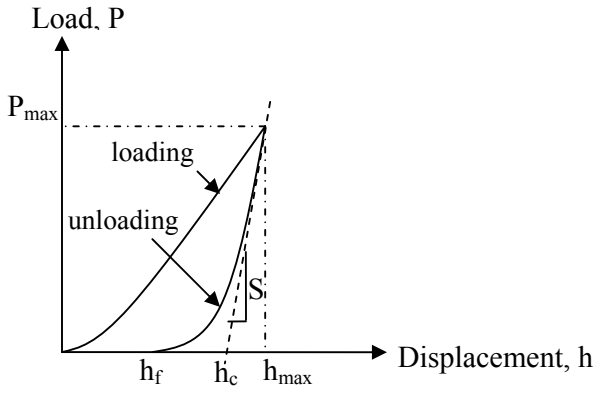

Figure 2.34: A typical load-deformation indentation curve

In Figure 2.34, h_{max} is the displacement at peak load P_{max}, h_f is the final displacement after complete unloading, hc is the plastic contact depth of indentation, and S is the initial unloading contact.

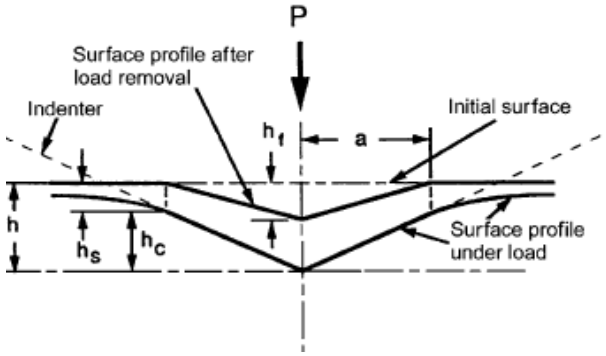

Figure 2.35: Deformations of a material during and after indentation

As seen in Figure 2.35, when indenter is pressed into the sample during loading both elastic and plastic deformations occur. During indenter withdrawal, however, only the elastic deformation is recovered and modulus of elasticity of the material can be obtained by analyzing this unloading curve. The load – displacement curves produced by depth sensing indentations may be analyzed based on Oliver – Pharr method (1992).

Initial unloading contact stiffness shown in Figure 2.34 is given as;

$$S = \frac{dP}{dh} \qquad \textbf{(2.5)}$$

which is equal to;

$$S = \frac{2\beta}{\sqrt{\pi}} E_r \sqrt{A} \tag{2.6}$$

where; A is the projected area of contact, β is a constant depending on indenter geometry, and E_r is the reduced modulus of elasticity which accounts for deformation of both sample and the indenter. E_r is given by

$$\frac{1}{E_r} = \frac{(1-\nu^2)}{E} + \frac{(1-\nu_i^2)}{E_i} \tag{2.7}$$

where E and ν are the elastic modulus and Poisson's ratio for the sample and E_i and ν_i are those of indenter. For diamond indenter E_i=1141 GPa and ν_i=0.07.

From Equations (2.6) and (2.7) the modulus of elasticity of the material can be calculated. The projected area of contact for an indenter with known geometry can be obtained as a function of depth. There is no need to measure the permanent impression using this type of new generation indentation testing machines as in conventional testing. The contact depth hc is given as

$$h_c = h_{\max} - \varepsilon \frac{P_{\max}}{S} \tag{2.8}$$

where ε depends on the geometry of indenter.

The deformation of the testing system must be calibrated and taken into account for the calculation of S, otherwise the measured displacement will be the displacement of the loading system and the obtained stiffness will be total system stiffness. The displacement of the load-frame is removed from the measured displacement and only the displacement of the indenter tip into the sample is obtained which is used to calculate the modulus of elasticity of the sample.

3. EXPERIMENTAL PROGRAM

3.1. General

The experimental program is described in this chapter. Materials, mixture compositions and test methods are presented in details. Concrete, mortar and paste mixtures were produced in the study. The experimental work consists of several parts; in some of the mixtures mechanical tests were carried out, but in some, the resistance to chloride penetration was the only focus.

Some of the experiments were conducted at I.T.U., Istanbul and some at N.T.N.U., Trondheim, Norway.

3.2. Materials

Six different cements, two different granulated blast furnace slags, a silica fume, a coarse unprocessed fly ash and a finely ground fly ash were used in the mixtures produced. Details regarding the materials are presented below.

3.2.1. Cements

Commercially available different cements; two ordinary portland cements (OPC), two slag cements, a high performance portland cement (HPC) and a fly ash cement (FAC), were used in this study. Only an ordinary portland cement (OPC 1) was used in the concrete mixtures produced at ITU and the other five cements in mixtures cast at NTNU. The amount of fly ash in the fly ash cement was 20 %. The slag contents are 53% for the slag cement 1 (CEM III/A 52.5) and 70 % for the slag cement 2 (CEM III/B 42.5 LH HS). Chemical compositions and some characteristics of the cements are shown in Table 3.1. However, the chemical compositions of the some of the cements are not available.

3.2.2. Mineral Admixtures

3.2.2.1. Ground Fly Ash

The fly ash used in this study to investigate the effects of grinding, was brought from Catalagzi power plant, which is located in the west coast region of Black Sea in Turkey. Chemical composition of fly ash is shown in Table 3.2. The average particle size of the fly ash used is relatively fine and characterized by a high density. Some physical properties of the ground fly ash are shown in Table 3.3. In this experimental study, only the ground fly ash indicated in Table 3.3 was used.

Table 3.1: Chemical compositions of cements

Oxide Composition (%)	Ordinary Portland Cement 1	Ordinary Portland Cement 2	High Performance Portland Cement	Fly Ash Cement	Slag Cement 1 (53.5%)	Slag Cement 2 (70%)
	CEM I 42.5 R	CEM I 42.5 R	CEM I 52.5 LA	CEM II A/V 42.5 R	CEM III/A 52.5	CEM III/B 42.5 LH HS
SiO_2	20.0	19.9	22.7	-	-	-
Fe_2O_3	3.6	3.4	3.2	-	-	-
Al_2O_3	5.1	4.7	4.3	-	-	-
CaO	63.2	62.4	65.6	-	-	-
MgO	1.1	2.1	-	-	-	-
SO_3	2.8	3.2	3.0	3.0	-	-
K_2O	0.8	0.9	-	-	-	-
Na_2O	0.3	0.3	0.5	0.9	-	-
Cl^-	0.03	0.04	<0.07	<0.07	-	-
Loss on ignition	2.8	2.5	2.5	1.5	-	-
Blaine fineness, m^2/kg	355	377	400	420	615	435
Specific weight, kg/dm^3	3.10	3.10	2.95	2.95	3.00	2.95
Compressive strength						
at 7 days	40.3	43.3	46.0	41.2	-	35.3
at 28 days	54.6	53.2	60.1	54.3	75.0	56.4

Table 3.2: Chemical compositions of the mineral admixtures

Oxide Composition (%)	Ground Fly Ash	GGBS 1	GGBS 2	Silica Fume
SiO_2	60.2	40.5	33.5	> 90
Fe_2O_3	6.7	1.2	0.3	-
Al_2O_3	21.8	10.3	12.0	-
CaO	2.5	32.2	31.5	-
MgO	1.6	11.3	16.8	-
SO_3	0.5	1.3	3.5	-
K_2O	4.9	1.1	0.6	-
Na_2O	0.5	0.35	0.6	-
Cl^-	0.006	0.0105	0.01	-
Loss on ignition	0.3	1.9	1.4	< 3
Blaine fineness, m^2/kg	604	600	500	-
Specific weight, kg/dm^3	2.51	2.86	2.92	-

The physical properties such as density and fineness change as the fly ash is ground. The physical changes due to grinding are: i) the fineness of fly ash increases, ii) there is a remarkable increase in density by reducing the porosity of the fly ash particles, iii) the spherical fly ash particles transform into the mostly irregular shapes; some small fly ash particles keep their original shapes.

Pozzolanic activity is the most critical property of the fly ash. There are different methods for the determination of the pozzolanic activity index of fly ashes. For the fly ash used in this study, the pozzolanic activity test with lime was done according to ASTM C 311-85 [1985]. An increase in the fineness of the fly ash leads to a substantial increase in its activity index at 7 days. As seen in Table 3.3, increasing the Blaine surface area from 222 m^2/kg to 604 m^2/kg has resulted in an increase of approximately 80 % in corresponding compressive strengths at 7 days.

Table 3.3: Some physical properties of fly ash before and after grinding

Property	Fly Ash	
	Before grinding	After grinding
Density	2.00	2.51
Blaine surface area, m^2/kg	222	604
Retained on 200 μm sieve, %	12.0	0.0
Retained on 90 μm sieve, %	33.0	0.7
Retained on 45 μm sieve, %	50.0	3.7

Table 3.4: Results of pozzolanic activity index test of the ground fly ash

Compressive strength at 7 days, MPa	Fly ash	
	Before grinding, Blaine S.A.: $222 m^2/kg$	After grinding, Blaine S.A.: $604 m^2/kg$
Experiment	7.9	14.2
Class F in ASTM C618-85, min.	5.5	5.5

3.2.2.2.Granulated Blast Furnace Slag

Two ground blast furnace slags (GGBS) with high finenesses were used in the mixtures. Throughout this study, ground granulated blast furnace slag will simply be referred as slag. GGBS 1 used at ITU was obtained from Karabük and was finely ground by Akcansa Cement Industry Co. GGBS 2 used at NTNU is a commercially available slag in Sweden with the brand Merox 5000. Some of the physical properties and chemical compositions of the slags are given in Table 3.2.

3.2.2.3. Silica Fume

The silica fume (SF), a production of Elkem Materials, was used in powder form. It is in the undensified form and available on the market as Microsilica 940 U. Chemical composition of silica fume is given in Table 3.2.

3.2.3. Aggregates

Bazalt aggregates from Corlu were used in the mixtures produced at ITU. Previous studies (Sengül, 2002) proved that this aggregate, especially for high strength concretes, performs better than the other aggregates available in the Istanbul area. In

order to ensure a good aggregate – cement paste bond, all the aggregates were washed and used in air dry condition.

Granite aggregates from Ardal, were used for the concrete productions at NTNU. Studies on concrete quality showed that the Ardal aggregate is of high quality and well suited for use in high strength concrete.

3.2.4. Superplasticizers

In low water/binder ratio concretes, superplasticizers were used to obtain enough workability. Glenium 51, an admixture based on modified polycarboxylic ether, was used in the mixtures produced at ITU and Scancem SP 40, a superplasticizer based on sulpho-melamin condensate, in mixtures cast at NTNU.

3.3. Concrete Mixture Compositions

Several series of concrete mixtures were prepared, most of which had a water/binder ratio between 0.35 and 0.42. Different concrete series have been given a serial number, and each concrete mix was designated with a mixture code. As explained in the following chapters, the serial numbers were given based on the pozzolan content in the mixture.

For a particular concrete series, the aggregate grading, water-binder ratio, and the maximum particle size of aggregate were kept constant in all mixtures. Except one concrete series, the grading curves of concrete aggregate were between ISO A16-B16 and closer to B16. All the partial replacements of cements by mineral admixtures were on one to one weight basis in all the mixtures.

All mixes were prepared in a laboratory mixer with vertical rotation axis. Specimens were demolded after 24 hours, and stored in water tank saturated with lime at 20^{o}C until the testing day.

3.3.1. Fly Ash Concretes

3.3.1.1. Concretes Produced with OPC and Ground Fly Ash

As pointed out in Chapter 2, use of fly ash in high amounts can have some disadvantages such as lower early strength. A possible way for overcoming these shortfalls is to improve the quality of the fly ash, which, for example, can be obtained by increasing the fineness of the fly ash by grinding. In order to study the

effects of finely ground fly ash (i.e. 604 m^2/kg) on the mechanical behaviour and resistance to chloride ion penetration of high strength concretes, a series of concretes were produced at ITU; in which eight concrete mixtures were prepared using the same ordinary portland cement (OPC 1) and the same type of low-lime ground fly ash (Class F in ASTM C 618). The partial replacement of cement by the fly ash was varied from 0 % (OPC concrete) to 70 %, in steps of 10 %. All the concrete mixtures had a water-binder ratio of 0.35. Glenyum 51 superplasticizer was used to maintain approximately the same slump of 100 ± 20 mm.

The concrete mixtures were designated with the following codes: NC, FAC 10, FAC 20, FAC 30, FAC 40, FAC 50, FAC 60, and FAC 70. Concretes without and with fly ash were named NC and FAC, respectively. The number following FAC shows the partial replacement of cement by fly ash, which varies from 0 % (NC) to 70 % (FAC 70). Mix proportions of concretes are presented in Table 3.5.

Table 3.5: Mixture proportions of concrete containing ground fly ash

Mix Code	NC	FC 10	FC 20	FC 30	FC 40	FC 50	FC 60	FC 70
Ordinary Portland cement (C), kg/m^3	472	424	375	330	283	237	189	142
Fly Ash (FA), kg/m^3	0	47	94	141	189	237	284	330
Water (W), kg/m^3	166	165	164	165	165	165	165	165
W/(C+FA)	0.35	0.35	0.35	0.35	0.35	0.35	0.35	0.35
Superplasticizer, kg/m^3	2.6	2.1	2.3	2.4	2.5	2.5	2.5	2.5
Sand (0-2 mm), kg/m^3	260	259	256	256	255	254	252	249
Basalt fines, kg/m^3	475	472	467	466	465	463	460	456
Crushed basalt No. I, kg/m^3	1121	1114	1101	1100	1096	1092	1084	1074
Air, %	2.2	2.2	2.8	2.3	2.1	1.8	1.9	2.2
Slump, mm	110	90	105	105	110	100	95	110
Unit weight, kg/m^3	2496	2483	2459	2460	2455	2450	2436	2418

3.3.1.2. Concretes Produced with HPC, Silica Fume and Coarse Fly Ash

Previous chapter presents the concretes produced with finely ground fly ash. However, grinding of fly ash is a time consuming process which can also affect the cost of the concrete. It must also be remembered that plants for grinding fly ash or cement are not available for most of the construction projects or ready mixed concrete companies. In today's practice, the use of fly ash as received from the thermal power plant is much more common. The main objective of producing this series of concretes is to investigate the effect of unprocessed fly ash on the resistance of concrete agains chloride penetration. It has been known that fly ash can have a beneficial effect on the chloride resistance of concrete. To obtain concretes with better performance against chloride penetration silica fume was also used in combination with the fly ash. A high performance portland cement was used in the mixtures. Table 3.6 gives the mixture compositions of these concretes containing ternary blend of HPC, fly ash and silica fume. Because these concrete mixtures were produced at NTNU, they are not directly comparable to the ones produced with the ground fly ash at ITU. The mixtures were designated as 00F, 20F, 40F, 60F and 33F, where the two digits denote the fly ash replacement ratio.

Table 3.6: Mixture proportions of concrete containing coarse fly ash and silica fume

Mix Code	00 F	20 F	40 F	60 F	33 F
High Performance Portland Cement (C), kg/m^3	388	314	235	159	261
Fly Ash (FA), kg/m^3	0	79	157	239	129
Silica Fume (SF), kg/m^3	31	31	31	32	31
(C+FA+SF)	419	424	423	430	421
Water (W), kg/m^3	175	177	177	179	176
W/(C+FA+SF)	0.42	0.42	0.42	0.42	0.42
Superplasticizer, kg/m^3	6.2	7.4	6.3	1.2	7.4
Aggregate I, (0-8 mm), kg/m^3	918	930	926	940	930
Aggregate II, (8-16 mm), kg/m^3	821	831	828	840	831
Slump, mm	50	190	170	165	190
Unit weight, kg/m^3	2340	2370	2360	2390	2370

3.3.2. Blast – Furnace Slag Concretes

3.3.2.1. Concretes Produced with OPC and Slag

For investigating the effects of the ground granulated blast furnace slag on the properties of concrete, four mixtures were prepared using the same ordinary portland cement (OPC 2) and the same type of finely ground blast furnace slag. Portland cement was substituted with GGBS 2 at 40%, 60 % and 80 % replacement levels.

The concrete mixes were designated with the following codes: N00, G40, G60, and G80. The N shows the normal concrete without GGBS and G shows concretes containing GGBS. The number following G shows the amount of partial replacement of cement by GGBS 2, which vary from 40 % (G40) to 80 % (G80). Concrete mixture proportions are given in Table 3.7. Compressive strength, chloride diffusivity and capillary water suction tests were carried out. Temperature developments in these concretes were also measured.

Table 3.7: Mixture proportions of concretes containing slag

Mix Code	N00	G40	G60	G80
Ordinary portland cement (C), kg/m^3	425	255	169	85
Slag (GGBS), kg/m^3	0	170	254	339
(Cement+GGBS)	425	425	423	424
Water (W), kg/m^3	170	170	169	169
W/(C+GGBS)	0.40	0.40	0.40	0.40
Superplasticizer, kg/m^3	5.8	5.1	4.84	4.03
Sand (0-8 mm), kg/m^3	918	910	905	903
Crushed stone I, (8-11 mm), kg/m^3	313	311	309	308
Crushed stone II, (11-16 mm) kg/m^3	606	601	597	596
Air, %	0.24	0.43	0.69	0.70
Slump, mm	165	175	145	165
Unit weight, kg/m^3	2437	2421	2409	2404

3.3.2.2. Concretes Produced with HPC, Silica Fume and Slag

The previous chapter presented the mixtures in which ordinary portland cement was partially replaced by slag. However, in some construction projects where concrete is exposed to marine environments, high performance portland cements (HPC) are preferred. In order to investigate the effects of slag on the concretes containing this cement, new concrete mixtures were prepared. The high performance portland cement was partially replaced by slag with the replacement ratios of 20%, 40% and 60%. To obtain better concrete performance, 7 % of silica fume was also added to these concretes. The mixture proportions of concretes containing slag and silica fume are given in Table 3.8. The codes A, 2A, 4A and 6A show the concrete with only HPC and the concretes with 20%, 40% and 60% slag replacements, respectively.

In addition, two concrete mixtures were produced using blast furnace slag cements. The code 4 represents the mixture containing the cement CEM III/B 42.5 LH HS (slag content: 70 % slag) and the code 5 shows the concrete cast with the cement CEM III/A 52.5 (slag content: 53 % slag).

Table 3.8: Mixture proportions of concretes containing HPC, slag and silica fume

Mix Code	A	2 A	4 A	6 A	*4*	*5*
High Performance Portland Cement (C), kg/m^3	388	308	236	153	0	0
Slag cement (C)	0	0	0	0	395	395
Slag (GGBS), kg/m^3	0	77	157	230	(70%)	(53%)
Silica Fume (SF), kg/m^3	31	31	31	30	31	31
(C+GGBS+SF)	419	416	424	413	426	436
Water (W), kg/m^3	175	174	178	173	178	178
W/(C+GGBS+SF)	0.42	0.42	0.42	0.42	0.42	0.42
Superplasticizer, kg/m^3	3.2	3.2	3.2	3.1	3.2	3.2
Aggregate I, (0-8 mm), kg/m^3	918	912	932	908	936	934
Aggregate II, (8-16 mm), kg/m^3	821	815	833	812	836	835
Slump, mm	50	160	180	165	210	90
Unit weight, kg/m^3	2340	2319	2370	2310	2380	2376

3.3.2.3. Concretes Produced with FAC, SF and Slag

The fly ash mixtures presented in Chapter 3.3.1 contain fly ash as separate additions. However, fly ash cement, produced by inter-grinding of clinker and fly ash, is more widely used in construction projects. In order to investigate the effect of fly ash cement and slag on the chloride resistance of concretes, the mixtures cast with the high performance portland cement presented in Chapter 3.3.2.2 were also produced using fly ash cement. The mixture proportions of these concretes with fly ash cement are shown in Table 3.9. The concretes without slag were designated as 0F and the ones with slag replacements as 2 F, 4 F, 6 F which indicate 20%, 40% and 60% replacement ratios, respectively. All these concretes contain the same amount of silica fume. Resistance to chloride penetration was monitored on the concretes.

Table 3.9: Mixture proportions of the concretes produced with fly ash cement, slag and silica fume

Mix Code	0 F	2 F	4 F	6 F
Fly Ash Cement (C), kg/m^3	405	317	238	157
Slag (GGBS), kg/m^3	0	79	159	236
Silica Fume (SF), kg/m^3	32	31	32	31
(C+GGBS+SF)	437	427	429	424
Water (W), kg/m^3	183	179	179	177
W/(C+GGBS+SF)	0.42	0.42	0.42	0.42
Superplasticizer, kg/m^3	3.3	4.1	3.3	3.2
Aggregate I, (0-8 mm), kg/m^3	959	938	940	930
Aggregate II, (8-16 mm), kg/m^3	857	838	840	831
Slump, mm	40	150	120	160
Unit weight, kg/m^3	2440	2385	2390	2366

3.3.3. Silica Fume Concretes

3.3.3.1. Concretes Produced with OPC, Slag and SF

Results obtained from the concretes containing different amounts of slag (Chapter 3.3.2.1) show that the chloride diffusivities decrease by increasing the slag contents, however, the differences between these diffusivities were not significant. In order to

obtain lower chloride diffusivity values, a new series of concretes were produced by using silica fume. The ordinary portland cement concrete and the 60 % slag concrete presented in Chapter 3.3.2.1 were taken as basis and were produced by 5 % and 10 % silica fume replacements. The mixture proportions are given in Table 3.10. In addition to the strength and diffusivity tests, temperature measurements on these concretes were also carried out. The specimens were designated as S5, S10, S5-G55 and S10-G50, where SF indicates silica fume and the number following SF (5 or 10) shows the silica fume replacement ratio. Similarly S represents slag and the numbers (50 or 55) are the slag replacement ratios.

Table 3.10: Mixture compositions of concretes produced with OPC, Slag and SF

Mix Code	SF5	SF5-S55	SF10	SF10-S50
Ordinary Portland cement (C), kg/m^3	405	170	383	170
GGBS, kg/m^3	0	234	0	213
Silica Fume (SF), kg/m^3	21	21	43	43
Water (W), kg/m^3	170	170	170	170
W/(C+GGBS+SF)	0.40	0.40	0.40	0.40
Superplasticizer, kg/m^3	5.3	5.1	7.1	6.0
Sand (0-8 mm), kg/m^3	917	909	916	908
Crushed stone I, (8-11 mm), kg/m^3	313	310	313	310
Crushed stone II, (11-16 mm) kg/m^3	605	600	605	600
Unit weight, kg/m^3	2438	2419	2436	2420
Air, %	0.20	0.31	0.14	0.22
Slump, mm	140	165	145	160

3.3.3.2. Concretes produced with FAC, Slag and SF

This series has the same mixture compositions of the concretes presented in Chapter 3.3.3.1 but instead of ordinary portland cement, the fly ash cement was used. A concrete without any pozzolans, containing only fly ash cement as binder, was also produced as a control mixture. Mixture proportions of the concretes are presented in Table 3.11. Temperature measurements were carried out on the concrete produced only by the fly ash cement.

Table 3.11: Mixture composition of concretes produced with FAC, slag and SF

Mix Code	FAC 0	SF5	SF10	SF5-G55	SF10-G50
Fly Ash Cement (C), kg/m^3	425	404	383	170	170
GGBS, kg/m^3	0	0	0	234	213
Silica Fume (SF), kg/m^3	0	21	43	21	43
Water (W), kg/m^3	170	170	170	170	170
W/(C+GGBS+SF)	0.40	0.40	0.40	0.40	0.40
Superplasticizer, kg/m^3	6.7	6.7	8.2	5.9	6.8
Sand (0-8 mm), kg/m^3	907	907	905	904	604
Crushed stone I, (8-11 mm), kg/m^3	310	310	309	309	308
Crushed stone II, (11-16 mm) kg/m^3	599	599	597	597	597
Unit weight, kg/m^3	2417	2417	2415	2411	2412
Air, %	0.22	0.24	0.23	0.26	0.19
Slump, mm	160	150	175	180	150

3.3.4. Slag and Fly Ash Concretes

3.3.4.1. Concretes Produced at Two Different Water/Binder Ratios and High Volume Ground Fly Ash or Slag

The main objective of producing this series of concretes is to investigate the combined effects of finely ground blast furnace slag and ground fly ash on the compressive strength and rapid chloride permeability.

Two series of concrete with water/binder ratios of 0.60 and 0.38 were produced at ITU. Ordinary portland cement (OPC1) was partially replaced by finely ground fly ash, finely ground granulated blast furnace (GGBS 1). For both water/binder ratios cement was replaced by i) 50% fine fly ash, ii) 50% finely ground granulated blast furnace, iii) 25%fly ash +25% finely ground granulated blast furnace. The concrete compositions are shown in Table 3.12.

The concrete mixtures were designated as follows: 50S-60, 50F-60, 25FS-60, 100PC-38, 50S-38, 50F-38, and 25FS-38. The first two digits show the partial replacement amount of cement by fly ash or slag. The letters after the digits represent the binder type, where S shows the blast furnace slag and F indicates the fly ash. The

last two digits indicate the water/binder ratio. For example 25FS-38 represents the concrete with a water/binder ratio of 0.38 and containing 25% fly ash + 25 % blast furnace slag. On the other hand, the mixtures 100PC-60 and 100PC-38 show Portland cement concretes with water-cement ratios of 0.60 and 0.38, respectively.

Table 3.12: Mixture proportions of concrete containing ground fly ash and slag

kg/m^3	100 PC	50 S	50 F	25 S+ 25 F	100 PC	50 S	50 F	25 S+ 25 F
Ordinary portland cement	348	175	176	176	450	222	221	222
GGBS	0	175	0	88	0	222	0	111
Ground Fly Ash	0	0	176	88	0	0	221	111
Water	209	210	211	211	167	168	167	168
Water/Binder	0.60	0.60	0.60	0.60	0.38	0.38	0.38	0.38
Superplasticizer	0	0	0	0	4,4	4,5	3,4	4,7
Sand	503	503	497	502	500	499	487	493
Basalt fines	380	380	375	379	377	377	368	372
Crushed basalt No. I	951	952	940	951	946	945	921	933
Unit weight	2389	2394	2375	2396	2436	2438	2389	2415
Slump, mm	90	130	140	140	80	150	110	160
Air, %	2.2	1.6	1.1	0.9	3.3	2.7	3.1	2.8

3.3.4.2. Ternary Blends of Ordinary Portland Cement, Slag and Ground Fly Ash

In order to investigate the combined effects of fly ash and slag on the properties of concrete, obtain more data and perform a multi objective optimization process, a more comprehensive series of concretes were produced.

16 concrete mixtures were prepared in this series. Ordinary portland cement (OPC1) was replaced by the ground fly ash and slag (GGBS1) 2 up to 60 % with the steps of 10%. Water/binder ratio was 0.35 in all concretes. Concretes were coded as follows; OPC shows the concrete with ordinary portland cement, SXYFWZ defines the concretes with pozzolan replacements where; S shows slag and F: the fly ash. XY and WZ represent the replacement amounts for slag and fly ash respectively. For

example 40S20F represents the concrete with 40% slag and 20% fly ash. The mixture proportions are shown in Table 3.13.

Table 3.13: Compositions of the concretes containing ground fly ash and slag

Mixtures	Cement, kg/m^3	Slag, kg/m^3	Ground Fly Ash, kg/m^3	Water, kg/m^3	S.plasticizer, kg/m^3	Aggregates, kg/m^3	Unit weight, kg/m^3	Slump, cm
100 PC	472	0	0	165	5.2	1816	2459	19
20S	379	95	0	166	5.3	1816	2462	23
10S10F	377	47	47	165	4.8	1792	2442	21
20F	377	0	94	165	5.2	1793	2435	19
40S	286	190	0	166	5.2	1820	2467	20
30S10F	282	141	47	164	4.8	1792	2431	21
20S20F	282	94	94	164	5.2	1785	2424	20
10S30F	283	47	142	165	5.2	1781	2423	22
40F	283	0	189	165	5.4	1773	2415	21
60S	190	285	0	166	5.1	1808	2456	21
50S10F	189	236	47	165	5.0	1790	2432	19
40S20F	190	190	95	166	5.0	1798	2446	22
30S30F	188	141	141	164	4.9	1765	2402	21
20S40F	188	94	188	164	4.3	1761	2401	20
10S50F	187	47	234	163	5.2	1746	2383	21
60F	188	0	282	165	5.4	1750	2391	22

3.4. Mortar Mixture Composition

Mortar phase of the concretes cast with ground fly ash (Chapter 3.3.1.1), were also produced. In the preparation of these mixtures; water, cement, fly ash, sand, and basalt fines were in the mortar phase. Table 3.14 shows mixture compositions and some properties of fresh mortars. The mortar mixtures were designated with the following codes: NM.00, FM.10, FM.20, FM.30, FM.40, FM.50, FM.60, and FM.70. Mortars without and with fly ash were named NM and FM, respectively; the two digits following FM shows the partial replacement of cement by fly ash, which varies from 0 % (NM.00) to 70 % (FM.70).

Table 3.14: Mixture compositions and some properties of fresh mortars

Mix Code	NM00	FM10	FM20	FM30	FM40	FM50	FM60	FM70
Ordinary Portland Cement (C), kg/m^3	804	722	639	557	477	395	314	234
Ground Fly Ash (FA), kg/m^3	0	79	160	238	317	395	470	545
Water (W), kg/m^3	281	280	280	278	278	271	274	273
Sand, (0-2 mm), kg/m^3	444	441	436	432	428	423	417	411
Basalt fines, (0-4mm), kg/m^3	809	803	796	787	781	772	762	753
W/(C+FA)	0.35	0.35	0.35	0.35	0.35	0.34	0.35	0.35
Air, %	0.9	0.7	0.5	0.6	0.4	1.0	0.9	1.0
Spread, %	72	62	68	60	62	65	54	47
Unit weight, kg/m^3	2337	2325	2311	2293	2280	2256	2237	2216

3.5. Cement Paste – Aggregate Model Specimens for Micro Indentation

Composite specimens consisting of model aggregate and cement matrix were produced. Ordinary portland cement (OPC 1) was used to produce two types of cement paste mixtures with water/binder ratios of 0.22. 10% silica fume in the form of slurry was incorporated in one of the mixtures. A water-reducing admixture was also used in mixtures to increase the workability of the mixtures. The model aggregates were 30x60 mm drilled cores taken from limestone rock.

Cylinder moulds of 150 mm in diameter and 60 mm in height were used to produce the composite specimens. The model aggregates were placed inside the moulds, at the centre and fixed by screws attached to the top of the moulds. Cement pastes were then placed in these moulds.

Three cylinders, 100 mm in diameter and 200 mm in height, were also prepared for the determining the modulus of elasticity of the cement pastes. All the specimens were kept in their moulds for 24 hours. After demolding, they were stored in a water tank saturated with lime at 20^{o}C until 28 days.

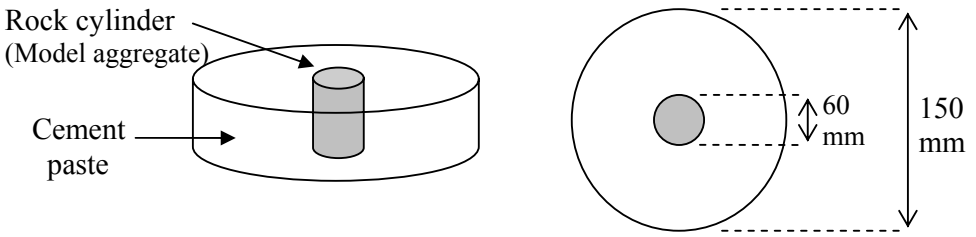

Figure 3.1: Specimens used for the indentation tests

3.6. Test Methods

3.6.1. Mechanical Tests

Compressive tests were conducted on some of the mixtures. These tests were made on 100 mm or 150 mm cubes. The loading rate was constant and same for all concretes. Strength tests of mortars, however, were done in accordance with the RILEM-Cembureau Method. The beams prepared for the standard RILEM-Cembureau tests were 160 mm in length and 40 mm x 40 mm in cross-section. After the bending tests, the compressive tests were performed on the half beams using 40 mm x 40 mm cross-section.

Splitting strengths of some mixtures were determined. Six cylinders of 150 mm diameter and 60 mm height were used for the splitting tests.

Modulus of elasticity tests were made on cylinders of ø100x200 mm or ø150x300 mm. The elastic moduli were calculated from the stress-strain curve for stresses below approximately 30 percent of the ultimate strength.

In order to obtain the complete stress – strain curve of the slag concretes presented in Chapter 3.3.2.1, these concretes were tested in uniaxial compression in a close-loop test machine. 100x200 mm cylinders were used and both ends of the specimens were ground before testing in order to obtain smooth surfaces.

The Brittleness Index B, obtained from the loading-unloading curve, is defined as the ratio of the elastic deformation energy to the irreversible deformation energy corresponding to the pre-peak point of the stress-strain curve. As shown in Figure 3.2, Brittleness Index B may be expressed as the ratio of area S_{II} to area S_I, where S_I is the irreversible deformation energy due to damage and S_{II} is the elastic (reversible) deformation energy. When the ratio of S_{II}/S_I approaches zero, all energies become

irreversible; when it tends to infinity, all energies become reversible. Thus, an increase in B indicates increased brittleness (Brandt, 1995).

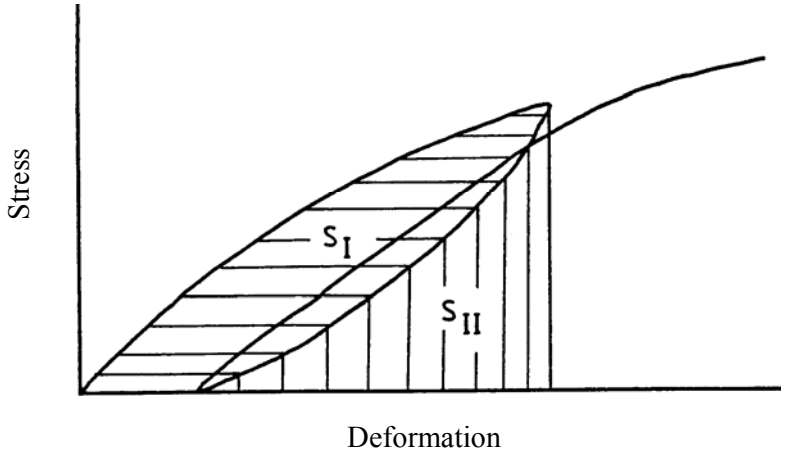

Figure 3.2: Reversible and irreversible energies

3.6.2. Capillary Water Absorption

Capillary water absorption test was made according to Norwegian test method NT 368 (1991). Six concrete discs of 100 mm diameter and 25 mm height were used in the test. Specimens were first dried at 105^{o}C to constant weight and preconditioned before exposure to water absorption. The specimens were exposed to one side and the changes in weights were recorded for four days. The rate of water absorptions were estimated based on the weight gain, and the square root of time vs. the capillarity water absorption graphs were obtained. A schematic time – water suction graphic is given in Figure 3.3.

Linear lines are fitted to the test data by regression analysis as shown in Figure 3.3. The intersection of these two lines represents the time (t_{cap}) when the capillary pores are filled and the waterfront reaches the top. The capillary number (k) is the slope of the line in the first stage of water absorption and calculated as follows:

$$k = \frac{Q_{cap}}{\sqrt{t_{cap}}} \qquad \textbf{(3.1)}$$

where Q_{cap} is the amount of water absorbed in a period of time t_{cap} after which a distinct change in the rate of water absorption occurs.

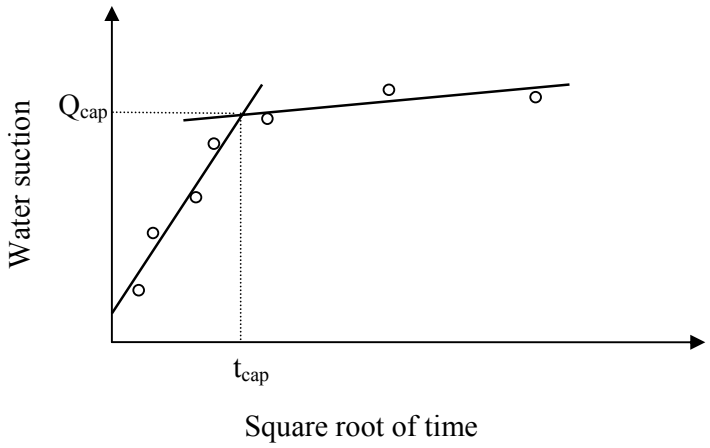

Figure 3.3: Schematic representation of water suction by time

A capillary resistance number (m) describes the relative time that the water front reaches the top of the specimen and is given by:

$$m = \frac{t_{cap}}{l^2} \quad \textbf{(3.2)}$$

where l is the thickness of the specimen.

3.6.3. Porosity

The specimens used for the capillary water absorption test are also used for the calculation of the concrete porosity. After the capillarity test, the specimens are immersed into water for 3 days to ensure complete saturation. Then the specimens are further saturated under a pressure of 5 MPa. After the pressure saturation, the weight of the specimen in water is measured. Finally, the dry weight is obtained after drying at 105°C. The following porosity parameters can then be calculated:

Total porosity: $\varepsilon_{tot} = \frac{W_3 - W_1}{W_3 - W_4} \, x\,100$ **(3.3)**

Suction porosity: $\varepsilon_{suc} = \frac{W_2 - W_1}{W_3 - W_4} \, x\,100$ **(3.4)**

Air porosity: $\varepsilon_{tot} = \frac{W_3 - W_2}{W_3 - W_4} \, x\,100$ **(3.5)**

Frost protection number: $PF = \frac{\varepsilon_{air}}{\varepsilon_{tot}}$ **(3.6)**

where; W_1 = weight of oven dry specimen

W_2 = weight of specimen after three days immersion in water

W_3 = weight of specimen after pressure saturation

W_4 = weight of specimen in water after pressure saturation

3.6.4. Test Methods for Evaluating Chloride Penetration

ASTM C1202, NT 492 and NT 433 test methods were used in this study for the evaluation of resistance of concrete to chloride penetration.

ASTM C1202 (1997) Rapid Chloride Permeability Test is based on the electrical conductivity of the concrete. Concrete discs of 100 mm in diameter and 50 mm in height were used for the test. The curved surface of the specimen is coated with epoxy first. Before the test, a standardized vacuum saturation procedure was applied to the specimens. Specimens were put between test cells, one of which containing NaCl solution and the other NaOH solution. The concrete sample was then subjected to a potential difference of 60 V and the total charge passing through during the first 6 hours was measured and expressed in terms of Coulombs as a basis for the evaluation of the concrete chloride permeability.

NT 492 (1999) is based on a non-steady state migration of chloride ions into the specimen. Same type of specimens and same vacuum treatment for ASTM C1202 test are used for the test. After preconditioning, the samples were assembled in a water sleeve and tightened with steel clamps. The specimens were then placed in a container filled with NaCl solution. The rooms of the sleeve above the specimens were filled with a solution of NaOH. An external potential was then applied axially across the specimen to force chloride ions migrate into the specimen. The level of potential depends on the concrete quality. At the end of a certain test duration, the specimens were axially split into two pieces and silver nitrate solution was sprayed onto the fresh split surface. The chloride penetration depth was then measured from the visible white silver chloride precipitation. By using this depth, the chloride migration coefficient was calculated based on the Nerst-Planck equation.

NT 443 (1995) test, also called “bulk diffusion test”, is based on the immersion of sample into a chloride solution. A concrete cylinder was epoxy coated first and then cut into half perpendicular to the axis of the cylinder for leaving a surface for exposure to the salt solution. The specimen was then immersed in a solution of 3 N

NaCl. After a certain period of exposure, powder samples were obtained at every 1 mm depth by grinding off concrete in parallel to exposed surface. The profile of the chloride penetration was then determined by chemical analysis on the powder samples. A spectrophotometric method was used for the determination of the chloride content. Based on the chloride profile obtained, the effective chloride diffusion coefficient was calculated according to Fick's law of diffusion.

3.6.5. Test Methods for Measuring Electrical Resistivity

Two type of resistivity measurements were performed on some of the concrete mixtures; two electrode method and wenner electrode method.

The test setup for the two electrode method is shown in schematically in Figure 3.4. A resistance meter with an alternating current at the frequency of 1 kHz was used. The resistivity of concrete was calculated as follows:

$$\rho_{concrete} = R_{measured} \frac{A}{L} \quad \textbf{(3.7)}$$

where $\rho_{concrete}$: resistivity of concrete,

$R_{measured}$: resistance of concrete,

A : surface area of concrete,

L : length of the specimen.

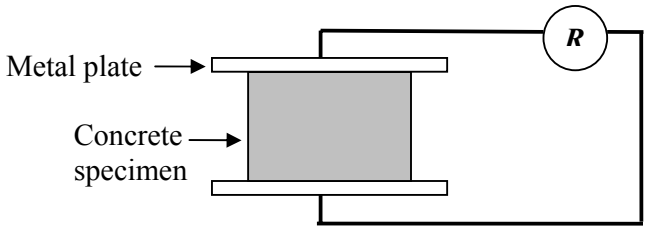

Figure 3.4: Resistivity testing of a concrete using two external electrodes

Four point wenner technique was also used for measuring the resistivity of concrete. Schematic representation of wenner electrode method and the flow lines are shown in Figure 3.5. CNS Farnell RM MKII wenner electrode was used for the tests. Probe spacing of 25 mm was chosen for the cubes and ø100x50 mm disc specimens and 50 mm spacing for the cylinders. Specimens were tested in saturated – surface dry condition. The wenner electrode used has wooden probe tips and the tips were in

water saturated condition. To ensure a good electrolytic contact with the concrete surface, before testing the wooden tips were also wetted enough to saturate the wood without depositing the water on the concrete.

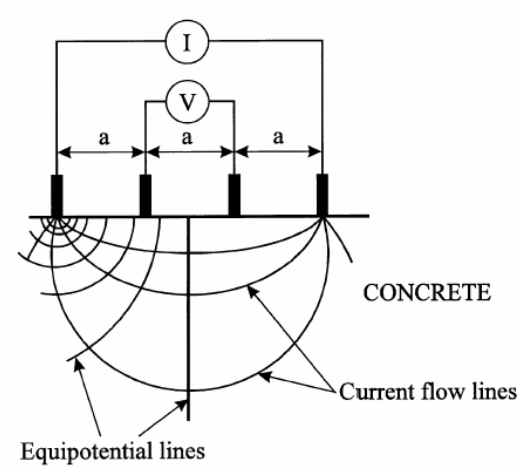

Figure 3.5: Schematic representation of wenner electrode method

3.6.6. Temperature Development in Concrete

Temperature developments in concretes during the first few days after casting were monitored by using an insulated container. About 5 minutes after mixing the water, 20 liters of concrete was placed in the container, thermocouples were inserted into the fresh concrete and by using a data logger the temperature at the center of the concrete sample was recorded at every 15 minutes over a period of 170 hours. Tests were carried out in a room with temperature of 21±1^{o}C and the ambient temperature was also recorded at every 15 minutes.

Seven different concretes with the same water/binder ratio and same binder content were produced for investigating the effect of binder system on the temperature development in concrete. A concrete with ordinary portland cement was selected as the reference concrete. Concretes containing 40%, 60% and 80% slag were cast to study the effect of slag replacement. Temperature measurements on the concretes with partial replacements of 5% and 10 % silica fume was also carried out. In addition, the reference concrete was also cast with fly ash cement to investigate the effect of the fly ash cement. Compositions of these concretes are given in Table 3.15.

Table 3.15: Compositions of the concretes used for measuring heat development

	Ordinary portland cement	60 % OPC + 40% GGBS	40 % OPC + 60% GGBS	20 % OPC + 80% GGBS	95 % OPC +5% silica fume	90% OPC + 10 % silica fume	Fly ash cement
Cement (C)	425	255	169	85	405	383	425
GGBS	0	170	254	339	0	0	0
Silica Fume (SF)	0	0	0	0	21	43	0
Water (W)	170	170	169	169	170	170	170
W/(C+GGBS+SF)	0.40	0.40	0.40	0.40	0.40	0.40	0.40
Aggregates	1837	1822	1811	1807	1835	1834	1816
Unit weight	2437	2421	2409	2404	2438	2436	2417

3.6.7. Chloride Binding

In order to study the effect of slag replacement on chloride binding of pastes, tests based on a SINTEF procedure (Justnes, 1998), were carried out on paste specimens produced with a water/binder ratios of 0.40. Portland cement was partially replaced by blast furnace slag on one to one weight basis with the replacement ratios of 40%, 60% and 80%. Tests were conducted at 7, 14 and 28 days and the specimens were kept in water until the testing day. The paste specimens were crushed to obtain fine dust samples between 0 mm - 0.5 mm particle size. In order stop the hydration, the dust samples were placed in ethanol for 2 hours. The samples were then dried at 110^{o}C for 3 hours and free water content was determined. Afterwards the dry samples were mixed with 3.5 % NaCl solution with a ratio of 1 to 1 by weight. At the end of 20 hours, the solution was filtered. The solution was then analyzed by spectrophotometer for determining the chloride amount. The bound water content of the dust samples were also determined by heating them up to 1000^{o}C. The chloride content was corrected based on the free and bound water contents.

Because the chloride content of the NaCl solution was determined after a certain period, decrease in the chloride content indicates increased chloride binding by the cement paste powder.

3.6.8. Micro Indentation

The composite specimens shown in Chapter 3.5, were cut by diamond saw and small prisms with dimensions of 25x15x15mm containing both model aggregate and

cement paste matrix were obtained. These prisms were then placed in small moulds with the surface to be tested facing the bottom mould surface. A resin was filled in these moulds afterwards and as a result; a disc with parallel surfaces was obtained. The surface of the resin disc containing the test surface was ground first with a relatively coarse silicon carbide paper, then with finer papers up to No. 1200 paper mounted on a rotating wheel. After necessary calibrations of the micro-indentation test set-up, the sample was placed on the indentation testing system and the tests were started.

The indentation tests were carried out using a Fischer HP 100 XY-PROG ultra-microhardness tester in Metallurgical and Materials Engineering Department, Surface Technology Laboratories at Istanbul Technical University. The indentation procedure consisted of 60 steps, with a waiting period between consecutive steps of 1 second, and a constant load of 100 mN was applied with constant loading and unloading rate. The indentations were performed at different points starting from the aggregate – cement interface and moving away from the interface with steps of 25 μm. At each testing distance, 5 to 8 indentations were made. Test locations were selected not close to each other in order to assure enough distance between individual measuring points and avoid affecting from previous testing. The unloading data were fit to a function and the fitting parameters were used to calculate the unloading stiffness S which was used to calculate the contact depth h_c. Vickers indenter was used in the test and area function of this indenter is given as $A=24.5\ h_c^2$. The modulus of elasticity of the specimens were then calculated using A and S in Equations 2.6 and 2.7.

Compressive strength and modulus of elasticity of the cement pastes were also found on cylindrical specimens of 100 mm diameter and 200 mm height, and the elastic moduli were calculated from the stress-strain curve below approximately 30 percent of the ultimate strength.

4. RESULTS AND DISCUSSION ON MECHANICAL PROPERTIES

4.1. General

In this chapter, the results of the mechanical tests are given and possible reasons for these behaviours are discussed. For the assessment of the effect of the ground fly ash on strength development, calculation pozzolanic effectiveness ratios are also presented in this chapter.

4.2. Effects of Water/Binder Ratio and High Volume Slag or Fly Ash

The mixture compositions of the slag and fly ash concretes are given in chapter 3.3.4.1. Compressive strengths of these concretes are given in Table 4.1 and illustrated in Figure 4.1 and 4.2. As seen in the table and Figure 4.1, for the water/binder ratio of 0.60, the compressive strength of the concrete with 50 % slag replacement is slightly lower than the portland cement concrete both for 28 and 90 days. The compressive strength of the concrete with 50% fly replacement, however, is significantly lower. For the 0.60 water/binder ratio, at 28 days the strength of the fly ash concrete is 59 % of the portland cement concrete. At 90 days, however, this ratio is 75 %, which shows the significant strength development rate of the fly ash concrete between 28 and 90 days. Despite the significant strength decrease when compared to portland cement concrete, at 0.60 water/binder ratio and 28 days age, the compressive strength of the concrete with 50 % fly ash is still over 34 MPa and this concrete can be classified as a structural concrete.

The pozzolanic reaction of fly ash in concrete depends on the break-down and dissolution of the glass phase which occurs when the pH of pore solution is higher than 13 (Fraay et al., 1989). The pozzolanic reaction takes place between the fly ash and the CH produced from the hydration of portland cement. This pozzolanic reaction is a slow process and is responsible for the low early strength of the high volume fly ash concrete.

At the 0.60 water/binder ratio, the compressive strength increase between 28 and 90 days is about 3 % for the portland cement concrete, 27 % for the fly ash concrete, 8 % for the slag concrete and 19 % for the concrete with the ternary binder. This important strength increase of fly ash concrete indicates that the pozzolanic reaction of the fly ash continues at a higher rate for a longer period.

Table 4.1: Compressive strengths of slag and fly ash concretes

Water/binder	Mixture Code	Cube compressive strength of concrete (MPa)	
		28 days	90 days
0.60	100PC-60	55.7	57.5
	50S-60	51.3	55.3
	50F-60	34.2	43.3
	25FS-60	42.9	51.2
0.38	100PC-38	86.1	92.2
	50S-38	89.9	91.5
	50F-38	72.8	78.2
	25FS-38	83.1	86.6

The pozzolanic reaction of the blast furnace slag is more rapid when compared to that of the fly ash (Bijen, 1996a). For the dissolution of the glass phase of blast furnace slag, pore water pH of about 12 is enough and this alkalinity level occurs in a short period after mixing the slag – portland cement blend with water. This rapid reaction is one of the factors causing a higher early strength of slag concretes.

As shown in Figure 4.1, for the water/binder ratio of 0.60, the compressive strength of the concrete with ternary blend binder is between those of the slag concrete and fly ash concrete. The ternary binder containing 25 % fly ash and 25 % slag also has a significant strength increase between 28 and 90 days.

The compressive strength of the concretes at 0.38 water/binder ratios are shown in Figure 4.2. As seen in the figure, the strength of the slag concrete is higher than that of the portland cement concrete at 28 days and almost equal at 90 days. The compressive strength of the concrete with 50 % fly ash is 72.8 MPa at 28 days and

78.2 MPa at 90 days and this high volume fly ash concrete can be classified as a high strength concrete.

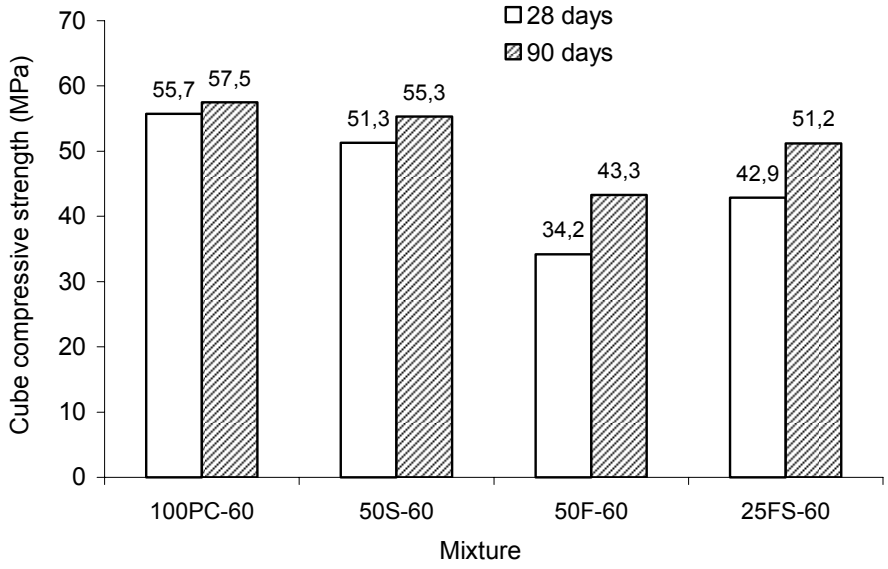

Figure 4.1: Compressive strengths of concretes with water/binder ratio of 0.60

For the 0.38 water/binder concretes, the strength of the fly ash concrete is about 85 % of the portland cement at both ages. For normal strength concretes, however, this strength ratio is 59 % at 28 days and 75% at 90 days. When the results for the 0.38 and 0.60 water/binder ratios are compared, it can be concluded that the fly ash is much more effective for the strength of concrete at the low water/binder ratio. The better performance of fly ash at lower water/binder ratios was also reported in other studies (Demir et al, 2002; Poon et al, 2000; Lam et al., 2000; McCharty, 1999). Similar conclusions can also be drawn for the slag concrete and the concrete with the ternary binder. For the high water/binder ratio, the ratio of the compressive strength of slag concrete to that of portland cement is 92 % at 28 days and 96 % at 90 days, but this strength ratio increases to 105 % at 28 days and 99 % at 90 days for 0.38 water/binder ratio.

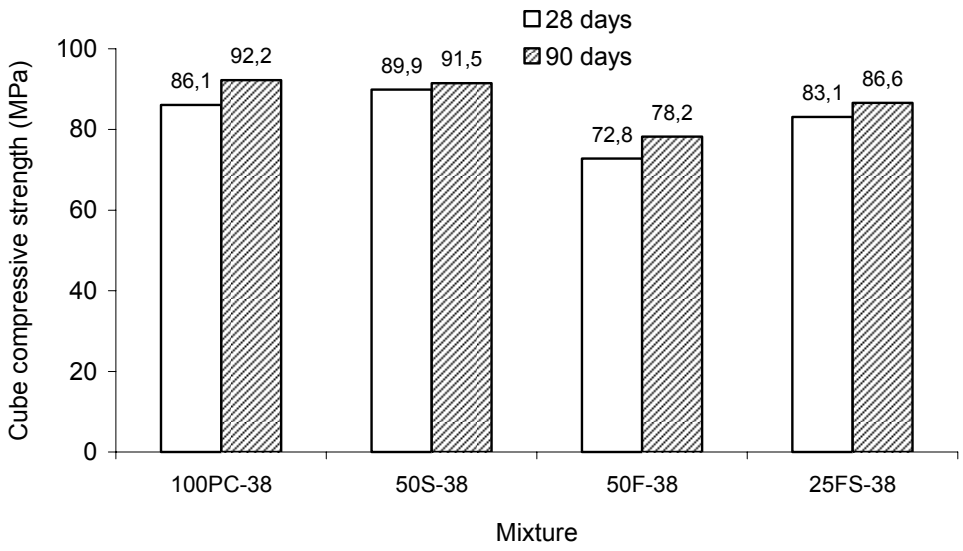

Figure 4.2: Compressive strengths of concretes with water/binder ratio of 0.38

Mineral admixtures have two effects in concrete: pozzolanic effect and filler effect. A finer pore size distribution and less capillary pores can be obtained by using fine mineral admixtures in concrete. Fine pozzolanic materials have an important effect also on the aggregate – cement paste interface which is the weakest link in concrete and the thickness of this transition zone can be reduced by using pozzolans (Bijen, 1996b). Better particle packing due to finer materials and the pozzolanic reaction may be the reasons for this enhancement. By the densification of the aggregate – cement paste transition zone, concrete becomes more homogeneous and higher strengths can be obtained. This improvement may be more effective at lower water/binder ratios which can cause a better performance of the pozzolan.

For the low water/binder ratio concretes, superplasticizers are used to obtain enough workability. These chemical admixtures causes better dispersion of cement particles and higher early compressive strengths can be achieved due to the greater hydration rate in a well dispersed system (Mehta and Monterio, 1996). The enhanced hydration in a well dispersed binder system also depends on the size of the mineral admixture. The superplasticizer used in the 0.38 water/binder ratio concretes may have helped for a better dispersion of the pozzolans which may have caused a less strength decrease when compared to the 0.60 water/binder ratio concretes. The particle sizes of the fly ash and slag used in this study are relatively fine and have Blaine finenesses of 600 m^2/kg. The fine particle size of the pozzolans may have contributed to the better performance of concretes at the low water/binder ratio.

4.3. Effect of Ground Fly Ash

The mixture compositions of the concretes with the ground fly ash are presented at Chapter 3.3.1.1.

4.3.1. Compressive Strength

The mechanical properties of the fly ash concretes are given in Table 4.2 and the development of compressive strength with age is illustrated in Figure 4.3.

Table 4.2: Mechanical properties of the concretes containing ground fly ash

Mix Code	Cube compressive strength of concrete (MPa)				Modulus of elasticity at 56 days (GPa)	Brittleness index at 56 days
	28 days	56 days	120 days	365 days		
NC 00	82.8	92.1	93.8	116.2	47.3	3.60
FC 10	70.2	87.5	92.9	127.8	47.4	3.47
FC 20	60.2	90.9	94.0	125.2	49.3	3.26
FC 30	66.0	93.0	93.3	125.1	47.8	3.63
FC 40	66.1	84.7	87.0	115.4	47.5	3.32
FC 50	58.5	74.6	76.7	107.8	46.2	2.90
FC 60	43.4	64.3	66.8	94.6	44.6	2.27
FC 70	34.1	49.3	51.4	80.0	40.1	1.75

As seen in the figure and table, in general, compressive strengths increase with the age of concrete and decrease with the amount of fly ash. The compressive strengths obtained in this study were in excess of 34 MPa at 28 days even at 70 % replacement of cement by a ground fly ash; such a fly ash concrete can be considered as a structural concrete. For concretes up to 70 % cement replacement by fly ash and 28-day age, the fly ash concretes show slightly lower strengths compared to no fly ash concrete. At later ages compressive strength becomes stable up to 40 % ground fly ash replacement. The compressive strength of concretes containing 40% fly ash is almost the same with that of the no fly ash concrete. Beyond this level, since the amount of fly ash used is relatively high, it has insufficient binding value and causes reduction compressive strengths. At one year, however, even the compressive strength of the concrete containing 70 % fly ash is 80 MPa and this concrete can be

classified as a high strength concrete. The results obtained shows that the rate of strength gain in concretes with fly ash is significant between 28 and 56 days. It can be concluded that high strength concrete could be made with 40 % cement replacement by finely ground fly ash (Sengül et al., 2005).

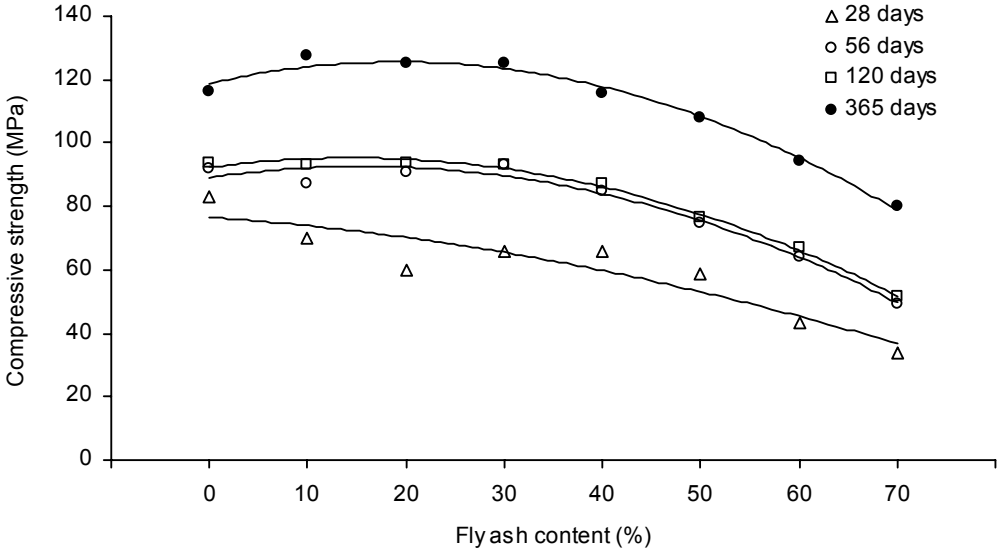

Figure 4.3: Compressive strengths of the concretes with ground fly ash

4.3.2. Brittleness Index and Modulus of Elasticity

The Brittleness index of the fly ash concretes are given in Table 4.2 and Figure 4.4 shows the brittleness index versus compressive strength plot in concretes with and without fly ash at 56 days. The circles indicated in the figure show individual test results obtained from the brittleness index test, but the data given in the last column of Table 4.2 shows the average values. As seen in this figure, substantial increase in the brittleness index is typical for high strength concretes. At HSCs, the interface becomes more homogeneous and dense; as a result bond strength increases. The stress-strain relation in these concretes is almost linear up to a stress as high as 90 % of the ultimate strength and the loop obtained becomes narrower. Thus, in these concretes the irreversible deformation energy decreases and the material becomes more brittle. Similar results were obtained in some previous works [Keru and Jianhua, 1988; Tasdemir, 1995; Tasdemir et al., 1995; Tasdemir et al., 1997; Sengül et al., 2002).

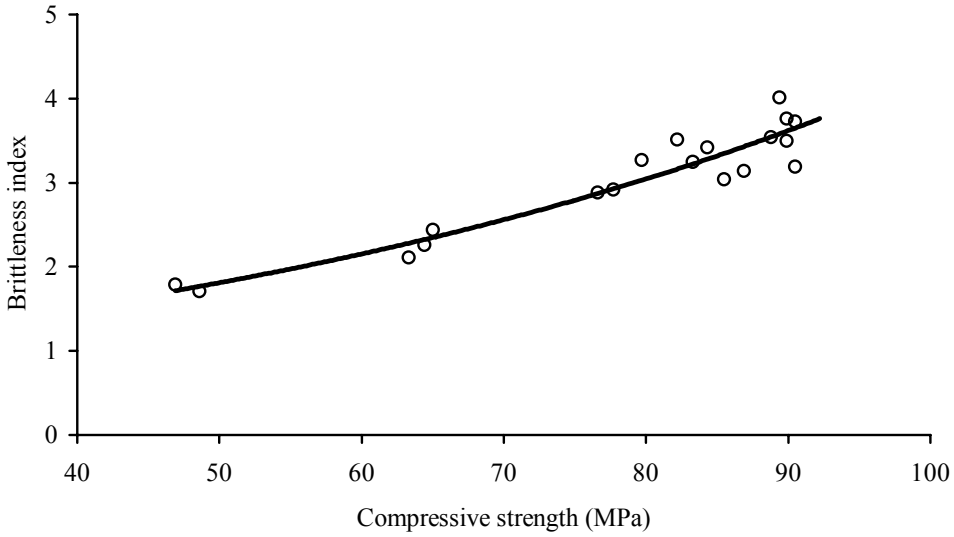

Figure 4.4: Brittleness index versus compressive strengths at 56 days

As seen in Table 4.2 the modulus of elasticity values at 56 days are almost the same up to 40 % fly ash replacement. Beyond this percentage the elasticity values decreases slightly with increasing replacement amount. Up to 50% replacement the modulus of elasticity of fly ash concretes are not different from portland cement concrete.

4.3.3. Effect of Ground Fly Ash on Mortar Compressive Strength

The mixture compositions of the mortars containing ground fly ash are given in Chapter 3.4. As seen in Table 4.3 and Figure 4.5, as the dosage of fly ash increases, the 2, 7, and 28-day compressive strengths decrease. As seen in the figure, at 56 days the compressive strength of mortar phase of concrete, up to 40 % cement replacement by ground fly ash becomes stable and almost the same. It can be concluded that mortar made with low cement content and high volumes of ground low lime calcium fly ash exhibits relatively low strengths at early ages, but higher strengths at later ages. As in the concretes, the compressive strength of mortars containing 40 % fly ash is almost identical to the portland cement mortar.

Table 4.3: Compressive strengths of fly ash mortars

Mix Code	Compressive strength of mortar, MPa					
	2 days	7 days	28 days	56 days	120 days	365 days
NM 00	48.3	80.8	97.3	103.8	105.3	126.1
FM 10	43.3	75.3	97.1	105.6	105.3	132.3
FM 20	38.0	67.1	91.7	103.1	110.0	130.1
FM 30	33.3	58.5	92.1	102.8	111.5	138.3
FM 40	25.9	51.0	85.2	101.6	104.3	128.1
FM 50	18.3	43.3	74.4	92.7	95.6	110.9
FM 60	14.0	34.3	64.8	75.4	79.8	97.1
FM 70	7.3	21.9	46.1	56.9	61.5	88.7

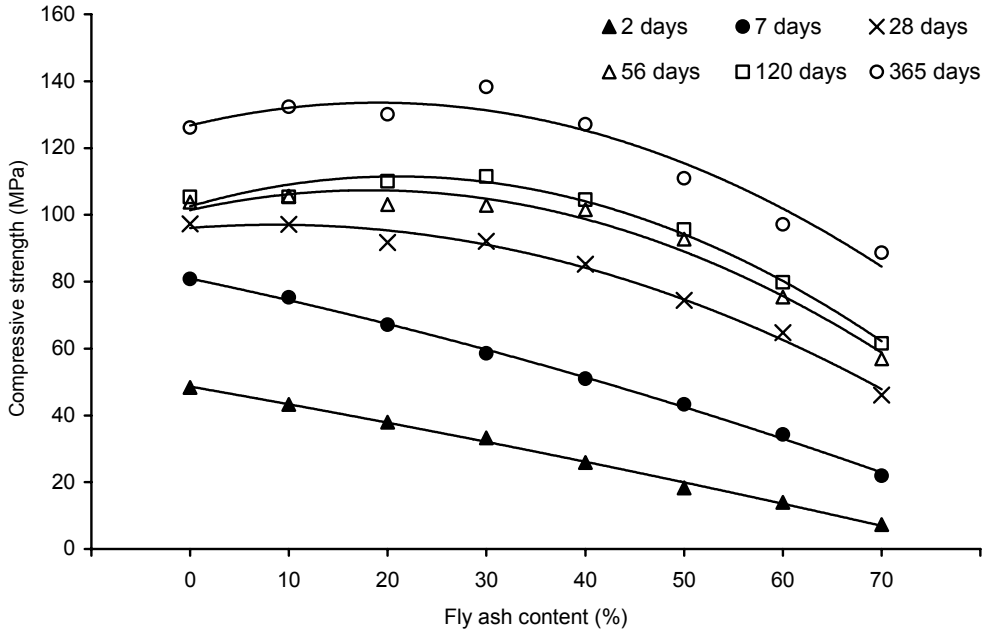

Figure 4.5: Compressive strengths of mortar phases

4.4. Pozzolanic Effectiveness Ratio of Mixtures Produced with Ground Fly Ash

For evaluation of the pozzolanic behaviour of the fly ash, pozzolanic effectiveness ratio can be calculated (Paya et al., 1997; Berry, 1980; Berry et al., 1989). This ratio depends on the experimental strength and the theoretical strength of the fly ash concrete and it is based on the Feret's equation (Lea, 1970);

$$f = K\left[\frac{c}{c+w+a}\right]^2 \quad \textbf{(4.1)}$$

where; f shows compressive strength of concrete, K is a constant, c, w, and a show the absolute volumes of cement, water and air, respectively. If the air contents of all the concretes are considered almost to be the same, the volume of air can be ignored and Equation 4.1 becomes;

$$f = K\left[\frac{c}{c+w}\right]^2 \quad \textbf{(4.2)}$$

Based on Equation 4.2, estimated compressive strength of OPC concrete (f_o), and that of fly ash concrete (f_i) can be obtained;

$$f_o = K\left[\frac{c_o}{c_o+w_o}\right]^2 \quad \textbf{(4.3)}$$

$$f_i = K^I\left[\frac{c_i}{c_i+w_i}\right]^2 \quad \textbf{(4.4)}$$

If it is assumed that fly ash is an inert constituent and do not contribute to the cementing action in the concrete, the value of K in Equation 4.3 for OPC concrete can be considered equal to the K^I value in Equation 4.4 for fly ash concrete (Berry et.al., 1989). Based on Equations 4.3 and 4.4, a theoretical strength ratio between the OPC and fly ash concrete can be given as;

$$F = \frac{f_i}{f_o} = \left[\frac{c_o+w_o}{c_i+w_i}\frac{c_i}{c_o}\right]^2 \quad \textbf{(4.5)}$$

where; F is the theoretical strength ratio, c_o and w_o show the absolute volumes of cement and water for normal concrete and c_i and w_i show those of the fly ash concrete.

Based on the actual compressive strength test results, an experimental strength ratio of OPC concrete to fly ash concrete can also be calculated;

$$S_t = \frac{s_i}{s_o} \quad \textbf{(4.6)}$$

where, for a given curing time, S_t is the experimental strength ratio, s_i is the compressive strength of fly ash concrete and s_o is that of the normal concrete.

The ratio of the experimental strength ratio (S_t) to the theoretical strength ratio (F) is defined as the pozzolanic effectiveness ratio (PER) (Paya et al., 1997; Berry, 1980; Berry et al., 1989; Cheriaf et al., 1999).

$$PER = \frac{S_t}{F} \quad \textbf{(4.7)}$$

The PER values can be used for the assessment of pozzolanic activity of the fly ash. If PER value equals to 1, the theoretical and experimental strengths are the same. When it is less than 1, fly ash is inert. As the PER value increases gradually, the fly ash becomes more effective for the strength.

The PER values for concretes and mortars at different ages, are given in Tables 4.3 and 4.4. As seen in these tables, for a given fly ash content, PER values increase with increasing age, which is the result of the pozzolanic reaction of fly ash that takes place for a long time. The PER values also increase with increasing fly ash content. The fly ash was assumed to be inert for the calculation of theoretical strength ratio in Equation 4.3, and an increase of the PER value indicates the effect of fly ash on the cementing action and strength development. The PER values of mortars at 2 days decreases with increasing fly ash content which shows that fly ash has insufficient binding capacity. At later ages, however, even the compressive strength decreases with increasing fly ash content, PER values increase which shows the involvement of fly ash for strength development. Similar behavior was also recorded in other works (Paya et al., 1997; Berry, 1980; Berry et al., 1989; Ramyar et al., 1999)

Table 4.4: Pozzolanic Effectiveness Ratios of concretes

Mix Code	PER values of concrete			
	28 days	56 days	120 days	365 days
NC.00	1.00	1.00	1.00	1.00
FC.10	0.94	1.06	1.10	1.23
FC.20	0.92	1.25	1.27	1.37
FC.30	1.19	1.50	1.48	1.60
FC.40	1.44	1.66	1.67	1.79
FC.50	1.61	1.85	1.87	2.12
FC.60	1.65	2.20	2.24	2.56
FC.70	2.00	2.60	2.66	3.34

Table 4.5: Pozzolanic Effectiveness Ratios of mortars

Mix Code	PER values of mortar					
	2 days	7 days	28 days	56 days	120 days	365 days
NM.00	1.00	1.00	1.00	1.00	1.00	1.00
FM.10	1.00	1.04	1.12	1.14	1.12	1.17
FM.20	1.01	1.07	1.21	1.27	1.34	1.32
FM.30	1.03	1.08	1.42	1.48	1.59	1.64
FM.40	0.98	1.15	1.60	1.78	1.81	1.85
FM.50	0.86	1.21	1.73	2.02	2.05	1.99
FM.60	0.92	1.35	2.12	2.30	2.41	2.44
FM.70	0.75	1.34	2.71	2.71	2.89	3.46

4.5. Effect of Blast – Furnace Slag

4.5.1. Compressive Strength

The mixture compositions of concretes with different slag replacement ratios are given in Chapter 3.3.2.1. The compressive strengths of these concretes are given in Table 4.6 and illustrated in Figure 4.6.

Table 4.6: Compressive strength and modulus elasticity of the concretes with different slag amounts

Mixture	Cube Compressive Strengths, MPa						Modulus of elasticity at the age of 1 year (MPa)
	3 days	7 days	14 days	28 days	90 days	1 year	
100 % OPC	48.1	55.8	57.6	60.0	71.1	83.0	27700
40 % Slag	31.6	46.7	53.1	61.7	81.6	90.2	26400
60 % Slag	23.0	40.3	49.4	62.7	78.1	88.0	27000
80 % Slag	11.7	25.0	35.4	47.2	55.2	64.0	22500

During the early ages, the compressive strength of concretes with slag replacements are significantly lower than that of the portland cement concrete and the strength reduction increases with slag content. However, the rate of strength development in slag concretes are considerably rapid and at later ages (28 days and beyond) the compressive strength of concretes containing 40 % and 60 % slag replacement are higher than those of the portland cement concrete.

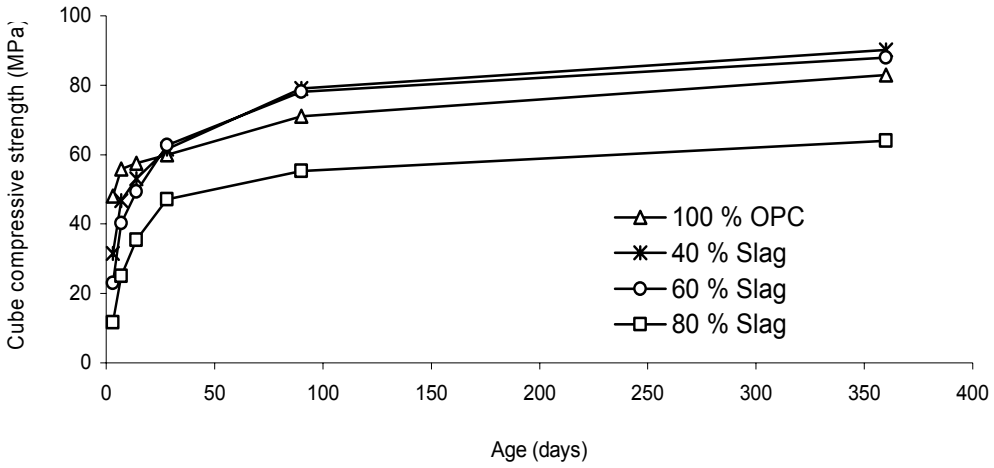

Figure 4.6: Compressive strength development of concretes with slag

Although the strength of concrete with 80 % slag has the lowest compressive strength at all ages, it is 47 MPa at 28 days and 64 MPa at 1 year. This concrete has the highest strength increase rate; i.e. between 3 days and 1 year, it has a strength increase of about 550 %, but this strength ratio between 1 year to 3 days, is only about 183 % for portland cement concrete, 285 % for the concrete with 40 % slag and 285 % for the one with 60 % slag.

It is known that the volume of capillary pores in a high volume of slag concretes is substantially lower than that of portland cement concrete (Bijen, 1996a). Coarse capillary pores are one of the factors affecting the strength of cement paste (Mehta and Monteiro, 1993) and the less coarse capillary pores in the slag concretes can be one of the causes for the higher compressive strength of these concretes at later ages. The strengthening of the aggregate – cement interface in concrete by the use of the fine slag can also be another important reason (Bijen, 1996b). It was reported that the thickness of the interface is also reduced by the use of pozzolanic materials (Larbi, 1991). The slag used in this study is relatively fine which may also has a beneficial effect on the densification of the aggregate – cement interfacial zone.

As seen in Table 4.6, when the compressive strength values are compared, it seems that 40 % to 60 % slag replacement is the optimum amount of slag to obtain a better strength performance. It was reported that, when highly active blast furnace slags have been tested, the greatest 28 – day strengths were found with blends of 40 to 50 percent (ACI Committee 233, 1995).

4.5.2. Modulus of Elasticity and Post – Peak Behaviour

The modulus of elasticity and the post – peak behaviour of the concretes were obtained at the age of 1 year. As presented in Table 4.6, the elastic moduli of the portland cement concrete and the concretes with 40% and 60% slag are almost the same. Modulus of elasticity of the concrete with 80% slag, however, is slightly lower.

The stress – strain curves of the slag concretes are presented in Figure 4.7. As seen in the figure, complete stress – strain curves could not be obtained. However, initial parts of the descending branches are presented. As seen in the figure, with the increase in the strength, the ascending branches became more linear up to peak point. The stress – strain curves were very similar for the portland cement concrete and the concretes with 40% and 60% slag. The strengths of these concretes were also very close. The strength of the concrete with 80% slag, however, was the lowest which can also be seen from the figure. When the peak strains are compared, it is clear that that the peak strain for the 80% slag concrete is less than those of the other concretes. The strains obtained for the portland cement concrete and the concretes with 40%

and 60% were similar as expected, because the strength of these concretes were also close to each other (Hsu and Hsu, 1994).

As seen in the figure, the initial part of the descending branch for the concrete with 60% slag seems steeper compared to the other concretes. The descending branches for the portland cement and 40% slag concretes were similar. A steep descending part of the stress – strain curve is an indication of the brittleness of the concrete and it can be concluded that the mixture containing 80% slag was the least brittle concrete.

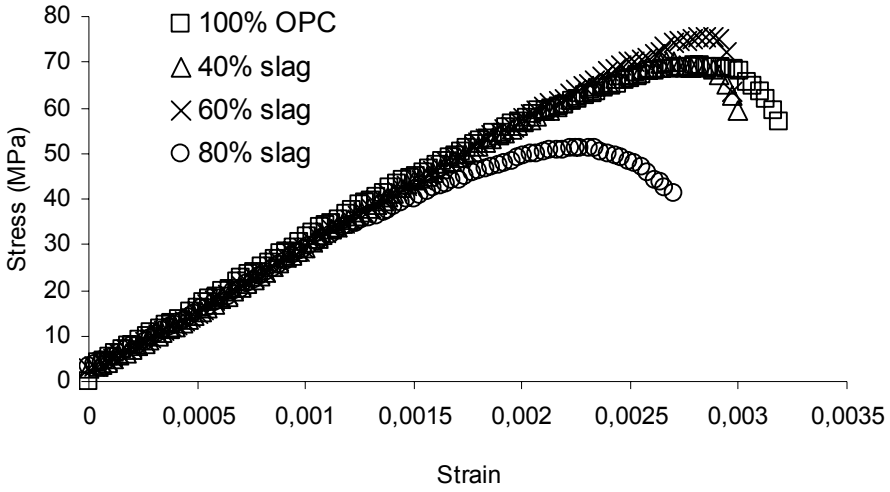

Figure 4.7: Stress – strain curves of the slag concretes

4.6. Effect of Silica Fume

4.6.1. Concretes Produced with OPC, Slag and Silica Fume

The mixture compositions of the concretes with ternary blends of portland cement, slag and silica fume are presented in Chapter 3.3.3.1 and their compressive strengths in Table 4.8 and Figure 4.7. The concretes with slag replacements presented in Chapter 4.5 were taken as a basis for these ternary blend concretes and in order to see the effect of the ternary blends more clearly, the compressive strengths of the portland cement concrete and concrete with 60 % slag presented in Chapter 4.5, were also included in Table 4.7.

As seen in Table 4.7, partial replacement of portland cement with the silica fume causes considerable strength increase at all ages and this strength increase is more significant when the silica fume content is changed from 5 % to 10 %; for example; at 28 days the strength of portland cement concrete increase from 60 MPa to 83 MPa

as result of 10% silica fume replacement. Unlike other pozzolans (such as slag or fly ash) which cause decreases in early strength, silica fume is effective in improving the strength also at the early ages. The strength of the concretes containing silica fume are substantially higher also at later ages. Besides being a highly reactive pozzolan, silica fume also has an extreme fineness which is very important for improving particle packing at the aggregate – cement interfacial zone, thus, for the strength development.

Table 4.7: Compressive strength of concretes with ternary blends of portland cement, slag and silica fume

Mixture	Cube Compressive Strengths, MPa						
	3 days	7 days	14 days	28 days	90 days	180 days	1 year
100 % OPC	48.1	55.8	57.6	60.0	71.1	–	83.0
5% SF + 95% OPC	52.8	61.3	72.5	75.1	84.1	87.8	89.5
10% SF + 90% OPC	54.9	66.7	77.7	83.0	89.9	96.2	98.3
60 % Slag	23.0	40.3	49.4	62.7	78.1	–	88.0
5% SF + 40% OPC + 55 % Slag	27.5	46.1	62.2	68.1	76.4	79.4	81.6
10% SF + 40% OPC + 50 % Slag	31.6	56.3	66.2	69.3	87.1	90.4	91.8

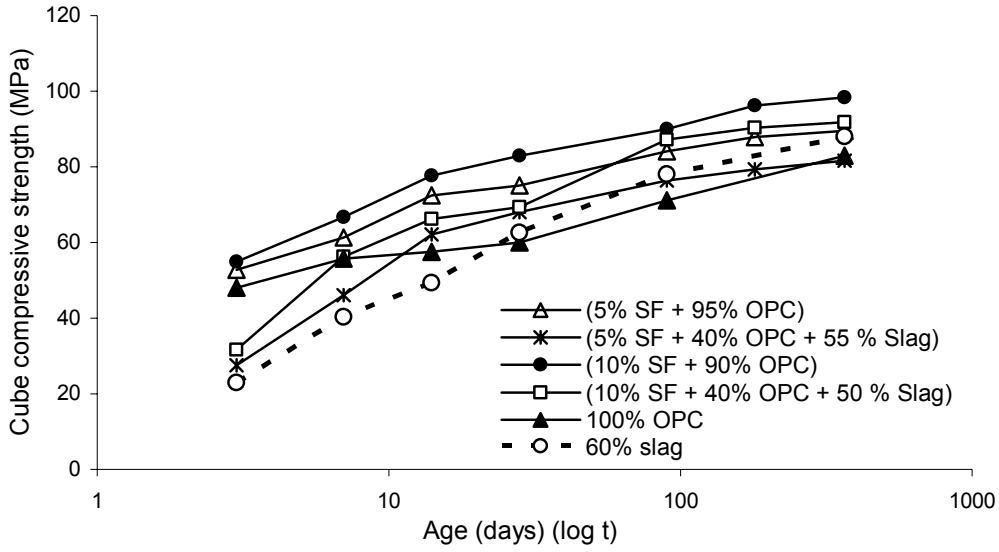

Figure 4.8: Development of compressive strength for the concretes containing ternary blends of portland cement, slag and silica fume

Partial replacement of slag by silica fume also increases the compressive strength of concrete, similar to the portland cement – silica fume blends. The lower early strength of the concrete containing 60 % slag was enhanced by replacing some of the slag by silica fume, i.e. at 3 days, the strength increased from 23 MPa to 27.5 MPa by the use of 5 % silica fume and to 31.6 MPa by using 10 %. When compared to concrete with 60 % slag, partial replacement of slag by the silica fume resulted in 37 % strength increase at 3 days. As seen in Table 4.7, the concrete containing ternary binder of 40 % portland cement, 10 % silica fume and 50 % slag, has a higher compressive strength than the reference portland cement as early as 7 days. Based on these test results, it can be concluded that the low early strength of high volume of slag concrete can be increased significantly by the incorporation of silica fume into mixture.

4.6.2. Concretes Produced with Fly Ash Cement, Slag and Silica Fume

Table 4.8 and Figure 4.9 presents the compressive strength of the ternary blends of fly ash cement, slag and silica fume. Because the fly ash cement consists of about 20 % fly ash and 80 % ordinary portland cement, these mixtures actually contain quaternary blends. For an easier comparison, the results of the concrete with 100 % ordinary portland cement given in Chapter 4.5, were also included in Table 4.8.

Table 4.8: Compressive strength of concretes with ternary blends of fly ash cement, slag and silica fume

Mixture	Cube Compressive Strengths, MPa						
	3 days	7 days	14 days	28 days	90 days	180 days	1 year
100 % OPC	48.1	55.8	57.6	60.0	78.3	–	83.0
100 % Fly Ash Cement (FAC)	45.3	52.6	59.6	68.6	86.0	92.7	97.2
5% SF + 95% FAC	46.5	56.3	65.1	79.7	83.3	94.2	98.0
10% SF + 90% FAC	50.2	64.8	76.0	89.0	92.8	100.5	106.1
5% SF + 40% FAC + 55 % Slag	22.3	44.8	57.1	65.0	73.2	77.5	79.3
10% SF + 40% FAC + 50 % Slag	25.6	48.0	58.6	67.0	78.6	89.0	91.8

As seen in Table 4.8, during the first 14 days the compressive strength of the concrete produced by the fly ash cement is slightly lower than that of the portland cement concrete, however, at 28 days and beyond, the strength of fly ash cement is significantly higher.

The fly ash cement used contains about 20 % fly ash and the composition and properties of this cement was optimized for a good performance. The fineness of the fly ash cement is higher in order to compensate for the strength loss at early ages, but as seen in Table 4.8, the strength was still slightly lower than portland cement concrete. At later ages (14 days and beyond), however, fly ash concrete has a better performance which can be due to the pozzolanic reaction of the fly ash.

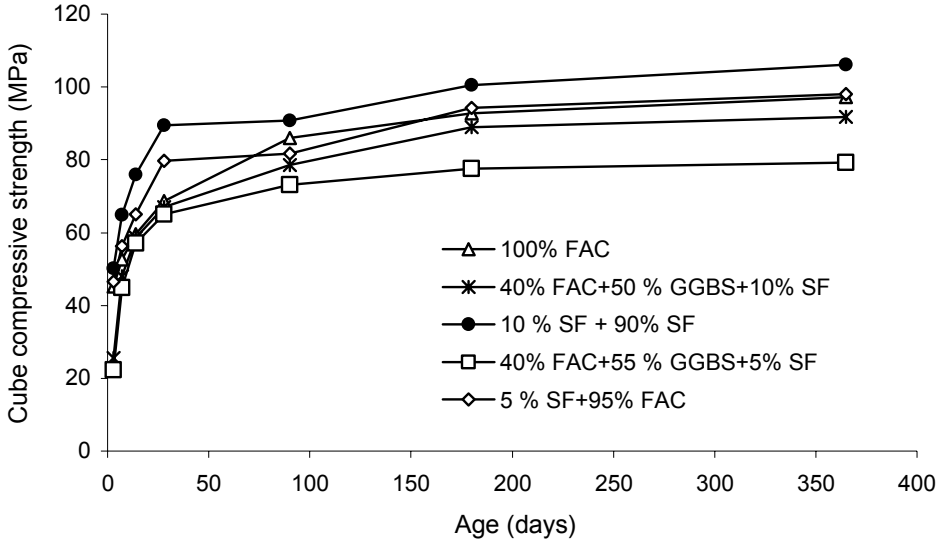

Figure 4.9: Development of the compressive strength of the concretes containing ternary blends of fly ash cement, slag and silica fume

Similar to the portland cement – silica fume binder systems presented in Chapter 4.6.1, the silica fume has an important impact on the strength development of the fly ash cement concretes. The compressive strengths of concretes containing fly ash cement and silica fume are higher than the strength of fly ash cement concrete at all ages and this improvement increases with the silica fume content. At later ages (28 days and beyond), for both silica fume replacement ratios (5 % and 10 %), the strength of the fly ash cement – silica fume blend also outperforms that of portland cement – silica fume blends.

The compressive strength of the concretes with the ternary blends of fly ash cement – slag – silica fume is significantly lower than of that the fly ash concrete at early ages but after 14 days the strength values are very similar. The ternary blend concretes perform better than the portland cement after 14 days. It should be noted that the compressive strength of the concrete with the ternary binder system increased almost 100 % between 3 and 7 days.

4.7. Effect of Ternary Blends of Portland Cement, Slag and Fly Ash

4.7.1. Compressive Strength

Mechanical properties of the concretes produced with ternary blend of ordinary portland cement, ground fly ash and slag are given in Table 4.9. The compositions of these concretes are presented in Chapter 3.3.4.2. For a clearer and easier evaluation of the strength development of the concretes, the strength results obtained for different replacement ratios are presented in different figures.

As seen in Figure 4.10 and Table 4.9, at the 20% replacement level and age of 7 and 28 days, there are slight decreases in the strengths of the concretes containing slag or fly ash. At the ages of 180 days and 1 year, however, the concretes produced with pozzolans perform better. For example at 180 days, these concretes have about 5% higher strength than that of the portland cement concrete. For this replacement level, the concrete containing 20% slag has the highest strength at the age of 1 year.

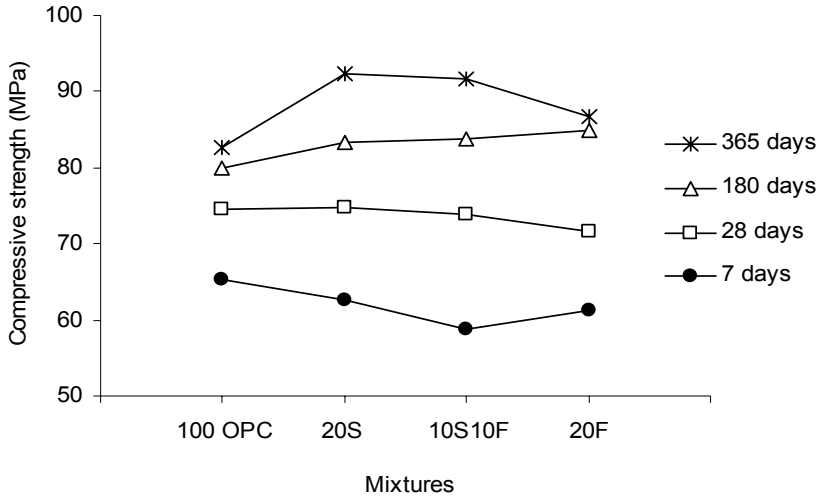

Figure 4.10: Compressive strength of the concretes produced with 20% fly ash and slag replacement

Table 4.9: Mechanical properties the concretes produced with ternary blend of ordinary portland cement, ground fly ash and slag

Mixture	Compressive strength (MPa)				Splitting strength at 28 days (MPa)	Modulus of elasticity at 28 days (MPa)	Brittleness index at 28 days
	7 days	28 days	180 days	365 days			
100 PC	65.3	74.5	80.0	82.7	8.9	40700	2.86
20S	62.5	74.8	83.3	96.7	8.6	42300	4.94
10S10F	58.8	73.8	83.8	91.6	9.7	40700	3.94
20F	61.3	71.7	84.8	86.8	9.5	41100	3.92
40S	54.5	71.6	87.9	88.7	8.8	39100	5.83
30S10F	53.8	70.3	83.1	93.8	8.8	40000	4.40
20S20F	50.2	73.6	81.2	90.0	9.1	38100	4.83
10S30F	50.8	71.8	74.6	85.8	8.9	37000	5.15
40F	48.9	64.5	71.7	92.8	9.4	38600	3.80
60S	53.2	66.1	83.1	83.1	9.2	37700	4.65
50S10F	50.3	65.7	80.8	84.9	8.5	36200	4.12
40S20F	48.5	68.1	80.2	85.6	8.3	35900	4.67
30S30F	46.3	61.4	79.4	80.0	8.2	35500	3.68
20S40F	45.2	59.9	75.1	80.9	8.0	35100	4.02
10S50F	37.8	56.2	69.8	75.3	7.5	35100	2.94
60F	29.4	53.9	70.3	79.1	7.4	34100	2.77

Figure 4.11 presents the strength development of the concretes produced with 40% pozzolan replacement. At the age of 7 days, concretes containing slag and fly ash have slightly lower strength compared to the portland cement concrete. At the age of 28 days, however, the portland cement concrete and the concretes with pozzolans have almost the same strength except the concrete containing 40% fly ash. Although this fly ash concrete reached the lowest strength at 28 days, the strength is only 13% lower than that of the portland cement concrete. As seen in Table 4.9 and Figure 4.10, beyond the age of 28 days, the concretes with pozzolans show significant strength development. At the age of 1 year and 40% replacement level, the concrete cast with 30% slag + 10% fly ash has the highest strength which is about 13% higher than the strength of portland cement concrete.

Compressive strengths of the concretes containing 60% pozzolanic materials are shown in Figure 4.12 together with those of portland cement concrete. At 7 days, concrete strength decreased with the increase in fly ash content. Compared to portland cement concrete, concrete cast with 60% have fly ash about 55% lower strength at the age of 7 days. Although this strength reduction is substantial, the strength is 29.4 MPa. Strength decreases with the increase in fly ash content was observed also for the 28 and 180 days. As seen in Figure 4.11, some of the strength results of 180 days and 1 year are close to each other but it can be concluded that the slag used is more effective than the fly ash in obtaining higher compressive strength.

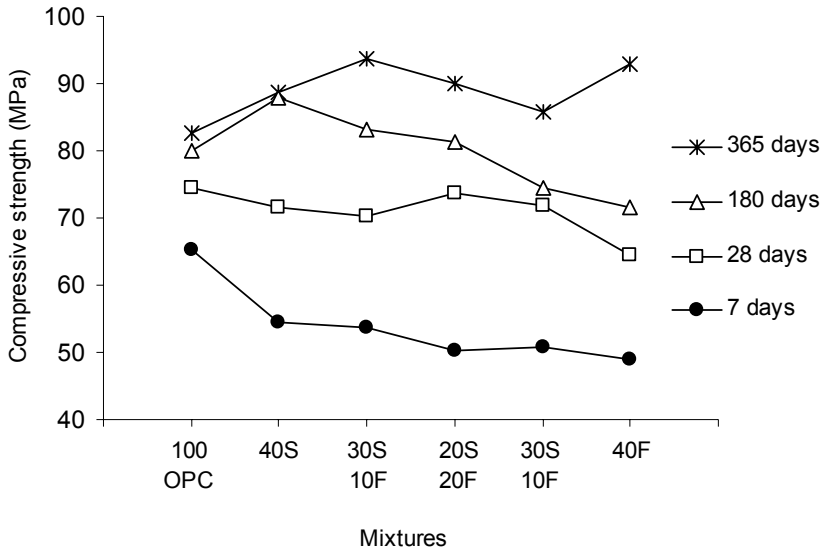

Figure 4.11: Strength of the concretes cast with 40% pozzolan replacement

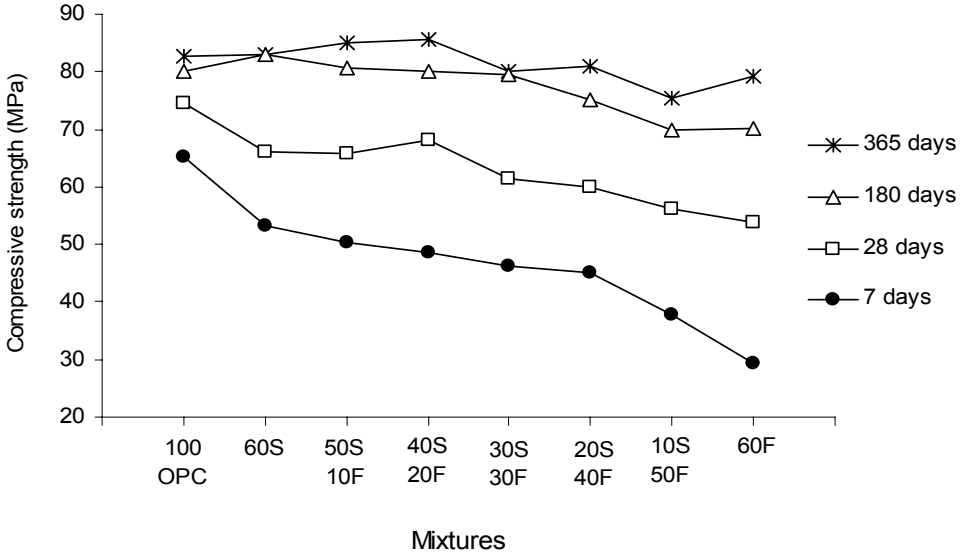

Figure 4.12: Strength development of the concretes containing 60% pozzolan

4.7.2. Splitting Strength

Splitting strength of the concretes produced with the ternary blend of ordinary portland cement, ground fly ash and slag are given in Table 4.9. When compared to portland cement concrete, no substantial differences in the splitting strengths were observed for the 20% and 40% replacement levels. At the 60% replacement level, splitting strength of the concretes decreased slightly with increasing fly ash content. Lowest splitting strength was obtained with the concrete cast with 60% fly ash and the strength is about 17% lower than that of the control concrete.

4.7.3. Modulus of Elasticity and Brittleness Index

As seen from Table 4.9, modulus of elasticity of the concrete is not affected significantly at the 20% and 40% replacement levels. For the 60% replacement level, however, the modulus elasticity decreased with increasing fly ash content. The lowest value was obtained for the 60% fly ash concrete which is about 16% lower than that of the portland cement concrete.

Figure 4.13 shows the relationship between brittleness index and compressive strength. As seen in the figure, although there is a big scatter in the values, the brittleness index increases with compressive strength. Similar results are also presented in the Chapter 4.3.2. Brittleness index is an indication of the strength of aggregate – cement interface and a higher brittleness index value represents stronger interface. As seen in Table 4.9, for all the replacement levels, the brittleness index of the concretes containing slag and fly ash are higher than that of the portland cement concrete. This result may be attributed to the modified interface in these concretes. For the concretes containing pozzolans, the brittleness index decreases with the increase in fly ash content. Compared to the slag, the slower pozzolanic reaction of the fly ash can be responsible for the slightly lower brittleness index.

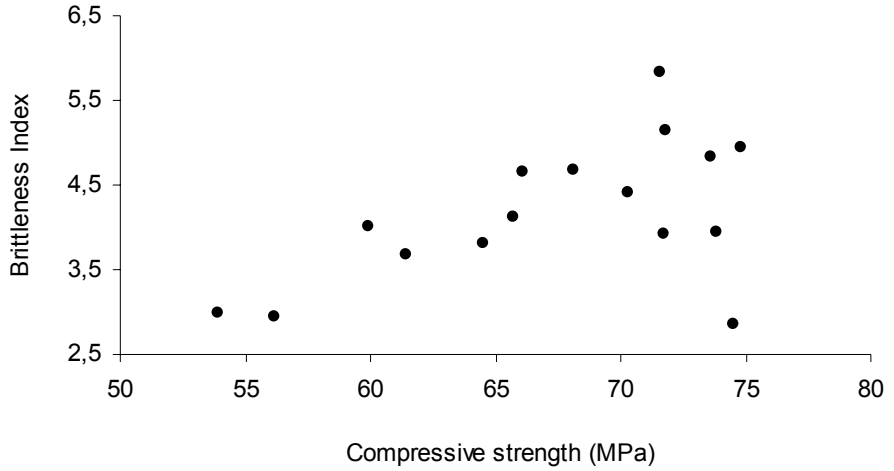

Figure 4.13: Brittleness index of the concretes produced with ternary blend of ordinary portland cement, ground fly ash and slag

4.8. Micro-indentation

Figure 4.14 illustrates results of the modulus of elasticity of pastes obtained by the indentation test. As seen in the figure, the modulus of elasticity of the portland cement paste and the paste containing silica fume are almost identical, no significant difference was observed. The change of the modulus of elasticity with the distance from the aggregate is also not significant. As seen in the figure, there is a big variation in the results even for the test locations away from the aggregate.

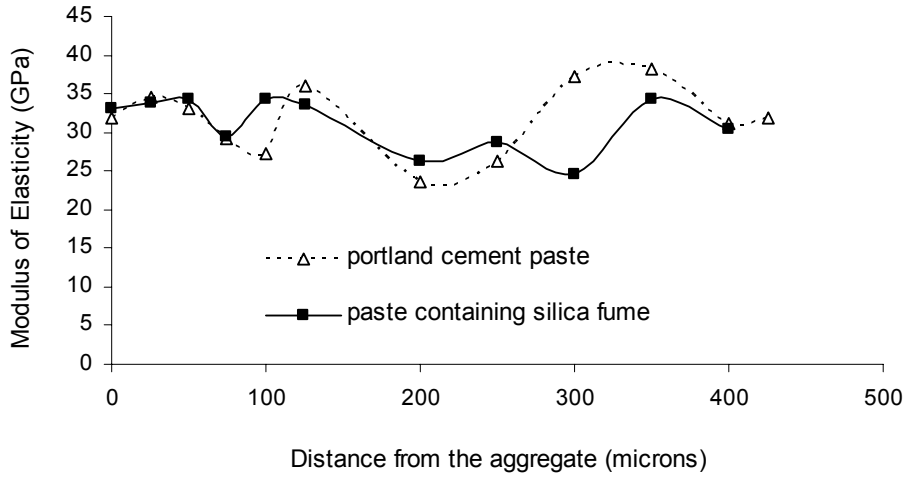

Figure 4.14: Modulus of elasticity of the pastes obtained by the indentation testing

The aggregate – cement paste transition zone is the weakest link in concrete, the interface is more porous, contains large crystals of CH and as a result, it is assumed that the mechanical properties at the interface are lower than that of the bulk paste. Lower modulus of elasticity and hardness values are expected at the interface, but as seen in the figure, there is no significant difference between the interface and the bulk paste. Several reasons may be responsible for obtaining such results.

A constant load of 100 mN (=10 grams) was used for the test and the resulting indent depth varied from 1.5 to 3.5 microns. The cement paste matrix is a heterogeneous material and has a high degree of porosity with a wide range of pore sizes. Because of using very low loads for nano-indentation tests, any pore near or under the indentation point will affect the contact area and lead to scatter of the results.

Because such low loads are used for testing and the average indent depth is about 2 ~ 2.5 microns, the surface preparation of the specimens is vital to obtain representative test results. As explained in detail in Chapter 3.5.8, the surfaces of the specimens were ground with silicon carbide paper up to No. 1200. However, one possible reason for the scatter of the indentation test results can be that the surface preparation process was not suitable and the surface characteristics obtained caused the scatter of the test results.

Igarashi et al. (1996) classified the microhardness profiles into four types and attributed the increase of the hardness near the aggregate to two main reasons: i) cement matrix - aggregate bonding is good and interface has the same properties of bulk matrix, ii) presence of massive CH at the interface. The microhardness at the interface is affected by the binder system and in mixtures which mineral admixtures such as GGBS are used, no difference in the microhardness of the interface and bulk paste can be observed (Kobayashi et al., 1998). It is well known that at lower water/cement ratios, aggregate-cement interface becomes more dense and homogeneous; bond strength increases and as a result the strength of concrete increases. The water/cement of the pastes produced in this work was 0.22 and this low water/cement ratio may be a reason for not obtaining lower results at the interface.

The model aggregate used in this work is limestone which may also be a cause for not obtaining lower elasticity at the interface. It is argued that a reaction occurs

between calcareous aggregates and cement paste which improves the properties of the interfacial zone (Monterio and Mehta, 1985; Zimbelman, 1985). Olliver et al. (1995) stated that Lyubimova and Pinus reported an increase in hardness at the interface for calcareous aggregates and a decrease for other aggregates.

Trtik and Bartos (1999) showed that creep values for the interface is about 35 % higher than that of the bulk paste. The loading rate chosen in this work is relatively slow. The loading and unloading were made in 60 steps with waiting for 1 second at each step. As a result of the loading rate used, the higher creep characteristic of the interface may be a factor for the high modulus of elasticity of the interface.

Table 9.10 presents the modulus of elasticity of the pastes obtained by testing on 100x200 mm cylinders. As seen in the table, the results for the portland cement paste and the paste with silica fume are almost the same. The values obtained are 31.5 GPa. As illustrated in Figure 4.14, the results obtained by the indentation test vary between 24 and 37 GPa. For the portland cement paste, the average of the modulus of elasticity values presented in Figure 4.14 is 31.7 GPa. The average for the silica fume is 31.2 GPa. When the results these two test methods are compared, it can be concluded that the modulus of elasticity of the cement paste can be obtained by the indentation test with a maximum of about 23 % deviation for the traditional testing on cylinder specimens. The differences between these methods are only about 1% if the averages of all the indentation tests are used for the comparison.

Table 9.10: Modulus of elasticity of pastes obtained by the stress – strain of the 100x200 mm cylinders

	Modulus of elasticity (MPa)
Portland cement paste	31500
Paste with 10% silica fume	31450

5. RESULTS AND DISCUSSION ON DURABILITY PROPERTIES

5.1. General

In this chapter all the durability test results are given and possible reasons behind these behaviours are discussed. Concrete characteristics like resistivity or chloride binding capacity are also included in this chapter.

5.2. Resistance to Chloride Ion Penetration

5.2.1. Effects of Water/Binder Ratio and High Volume Slag or Fly Ash

The mixture compositions of the slag and fly ash concretes are given in 3.3.4.1. The ASTM C 1202 rapid chloride ion penetration test (rcpt) results of the concretes are given in Table 5.1, and shown in Figure 5.1 and 5.2.

Table 5.1: Chloride permeability of slag and fly ash concretes

Water/binder ratio	Mixture Code	ASTM C1202 Chloride ion penetration test (Coulomb)	
		28 days	90 days
0.60	100PC-60	6813	5500
	50S-60	703	372
	50F-60	926	161
	25FS-60	660	376
0.38	100PC-38	1877	1780
	50S-38	395	206
	50F-38	531	144
	25FS-38	387	217

As shown in Figure 5.1, for the 0.60 water/binder ratio and age of 28 days, replacing 50 % of portland cement by the fine slag caused a decrease of about 90 % in the rapid chloride permeability of the concrete. Similarly, the decreases for the fly ash

concrete and for the concrete with the ternary binder are more than 86% and 90 %, respectively. For this water/binder ratio and 28 days age, the concrete with the ternary binder has the lowest rcpt value.

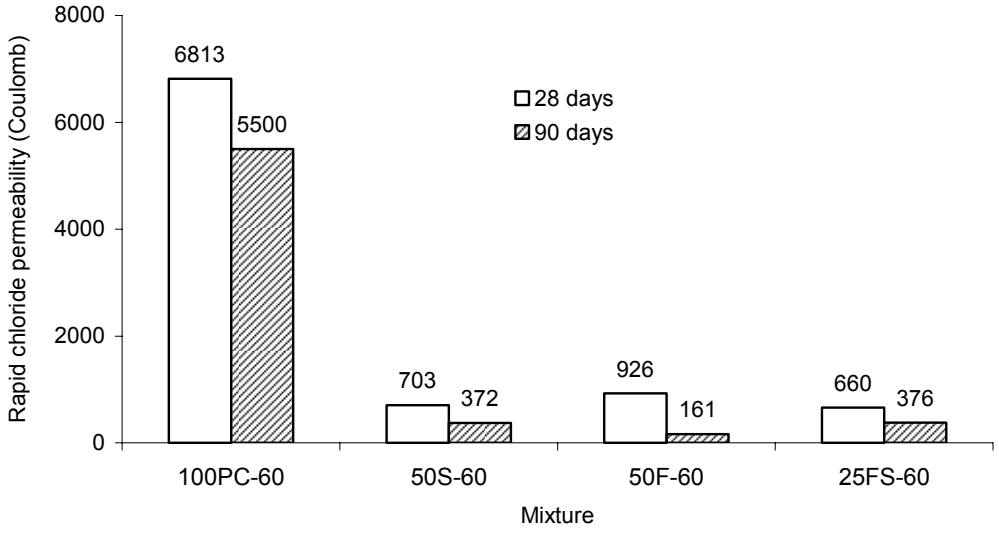

Figure 5.1: Rapid chloride permeability results of concretes with water/binder ratio of 0.60

As seen in the figures, the rapid chloride ion permeability decreases with age. For the water/binder ratio of 0.60, the total charge passing through the portland cement concrete decreases about 20 % between 28 and 90 days. This decrease, however, is more significant for the concretes containing high volume of pozzolans. For the 0.60 water/binder ratio, the reduction of the chloride permeability between 28 and 90 days is about 47 % for the slag concrete, 83 % for the fly ash concrete and 43 % for the concrete with ternary binder. At 90 days age and 0.60 water/binder ratio, the concrete with slag and with the ternary blend have rcpt values of about 7 % of the portland cement concrete and with a value of 161 coulombs the fly ash concrete has the lowest value which is less than 3 % of the normal concrete.

If Figure 5.1 and Figure 5.2 are compared, the effect of water/binder ratio on the rapid chloride ion permeability can be seen. For both 28 and 90 days, decreasing water/binder ratio from 0.60 to 0.38 caused a reduction of the rcpt value of about 70 % for the portland cement, 44 % for the slag concrete and 42 % for the concrete with the ternary binder. As a result of decreasing water/binder ratio, the total charge passing through the fly ash concrete reduced about 43% at 28 days, but only about

10% at 90 days. From these results, it can be concluded that the decrease in the water/binder ratio affects the rcpt value of the portland cement concrete more than those of the concretes with high amount of pozzolans.

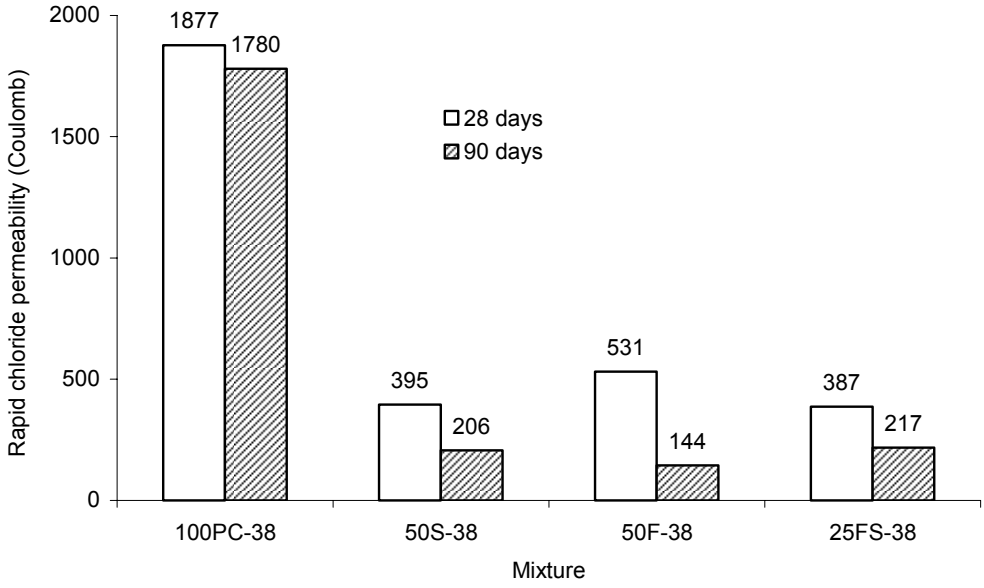

Figure 5.2: Rapid chloride permeability test results of concretes with water/binder ratio of 0.38

For the water/binder ratio of 0.38 and at 28 days, the concrete with the ternary binder and the slag concrete have the lowest rcpt values, which are about 20 % of the portland cement concrete. At 90 days, however, the fly ash concrete has the lowest rcpt value which is about 8 % of the portland cement concrete value.

At the low water/cement ratio, the chloride permeability of pozzolanic concretes also decreased substantially between 28 and 90 days For the 0.38 water/binder ratio, between 28 and 90 days the rcpt value of portland cement concrete decreased only about 6 %, however, decreases of 48 %, 73% and 44 % were obtained for the slag concrete, fly ash concrete and the ternary binder concrete, respectively.

All the specimens were cured in water until the testing day and for both water/binder ratios, the substantial decrease of the chloride ion permeability of pozzolanic concretes between 28 and 90 days indicates the high pozzolanic activity of the pozzolans taking place during this period.

The lower chloride permeability of the concretes with high volume pozzolans is a result of a denser microstructure. The pozzolanic reaction may cause lower amount

of capillary pores and clogging of the pores, which reduces chloride ion transport in concrete (Li and Roy, 1986). Reduced capillary pores and reduction in their connectivity due to the pozzolanic reaction and better particle packing may have caused the better performance of the concretes with high amount of pozzolans. Improvement of the aggregate – cement paste interface by the pozzolanic reaction may also play a role in decreasing the chloride ion permeability. Better chloride ion resistance of high volume fly ash concretes was also shown in other studies (Zhang et al., 1999). The ground fly ash used in this study has a high fineness which may have contributed to obtaining lower chloride ion permeability (Dhir and Jones, 1999).

Decreasing the water/cement ratio of a concrete reduces the amount of capillary pores which are mainly responsible for the permeability of the concrete. Even though the rcpt value of the portland cement concrete reduces about 70% by lowering the water/cement ratio, the values for the portland cement concrete at 0.38 water/cement ratio are still 2 times or even more higher than those of the concretes with pozzolans at 0.60 water/binder ratio. This result shows that for reducing the rcpt value, inclusion of pozzolans are much more effective than only reducing the water/cement ratio of the portland cement concrete.

As seen in Table 5, the decrease in the water/binder ratio was obtained by both reducing the water amount and increasing the binder content which may have also contributed to the better performance of the low water/binder ratio concretes. Studies show that, for a same water/binder ratio, increasing the binder content can also help to improve the permeability of the concretes (Buenfeld and Okundi, 1998; Dhir et al., 1996a).

5.2.2. Effect of Fly Ash

5.2.2.1. Concretes Produced with Ground Fly Ash and Ordinary Portland Cement

The rapid chloride permeability of the fly ash concretes are given in Table 5.2 and Figure 5.3.

Table 5.2: Rapid chloride permeability test results of the fly ash concretes

Mix Code	NC 00	FC 10	FC 20	FC 30	FC 40	FC 50	FC 60	FC 70
ASTM C1202 Chloride ion penetration at 1 year (Coulomb)	1536	447	345	135	140	148	159	116

The ASTM C 1202 rapid chloride ion penetration test is based on the electrical conductivity of concrete. The concrete sample was subjected to a potential difference of 60 V and the total charge passing through the sample at the end of 6 hours was measured and expressed in terms of Coulombs. A decrease in this total charge value indicates the better resistance to chloride ion penetration and lower permeability.

The total charge passing through the concrete without fly ash was 1536 Coulombs. As seen in Table 5.2, inclusion of fly ash greatly reduced the total charge which indicates better resistance to chloride ion penetration. The pozzolanic reaction of fly ash continued for a long time. The mechanical properties and permeability of the high volume fly ash concrete were lower than the OPC concrete at early ages; however, these properties improved significantly with time. The rapid chloride ion penetration tests were conducted on specimens of one year age which were cured in 20 ± 2^{0}C water until testing and significant pozzolanic reaction took place during this period. The test results showed the potential chloride resistance of high volume fly ash concrete. The lower chloride permeability of high volume fly ash concrete was due to the denser microstructure. The pozzolanic reaction of fly ash may cause clogging of pores, which reduces porosity and also chloride ion transport (Li and Roy, 1986). Better chloride ion resistance of high volume fly ash concretes was also shown in other studies (Sivasundaram, et al., 1991; Zhang, et al., 1999).

As seen in Figure 5.3, up to 30 % replacement, the total charge passing decreased significantly. The ASTM C 1202 suggests values for evaluating the test results and according to these values, the concretes in this study containing high volumes of fine fly ash can be considered as concretes of very low chloride permeability.

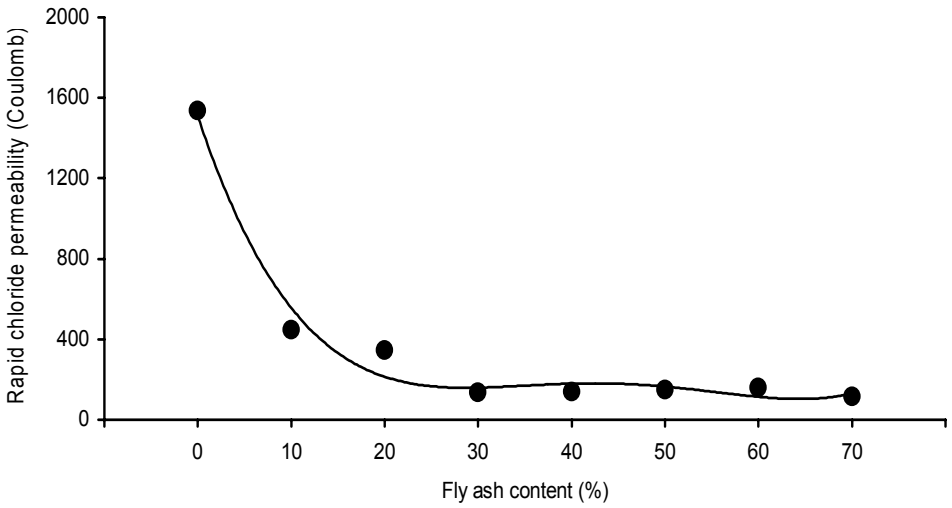

Figure 5.3: Rapid chloride permeability of concretes with different fly ash contents

5.2.2.2. Concretes Produced with Coarse Fly Ash, High Performance Portland Cement and Silica Fume

Table 5.3 shows the chloride diffusivity of the concretes produced with high performance portland cement, coarse fly ash and silica fume. Partially replacing high performance portland cement by fly ash reduced the chloride diffusivity of the concretes at 14 and 28 days.

Table 5.3: Effect of coarse fly ash on the concretes produced with high performance portland cement and silica fume

Mixture	Chloride Diffusivity, $m^2/s \times 10^{-12}$			
	14 days	28 days	60 days	90 days
00 F	8.9	5.2	5.4	–
20 F	19.5	9.9	–	–
40 F	17.6	9.3	–	–
60 F	32.4* *21 days	23.0	–	–
33 F	8.3	4.8	3.4	3.1

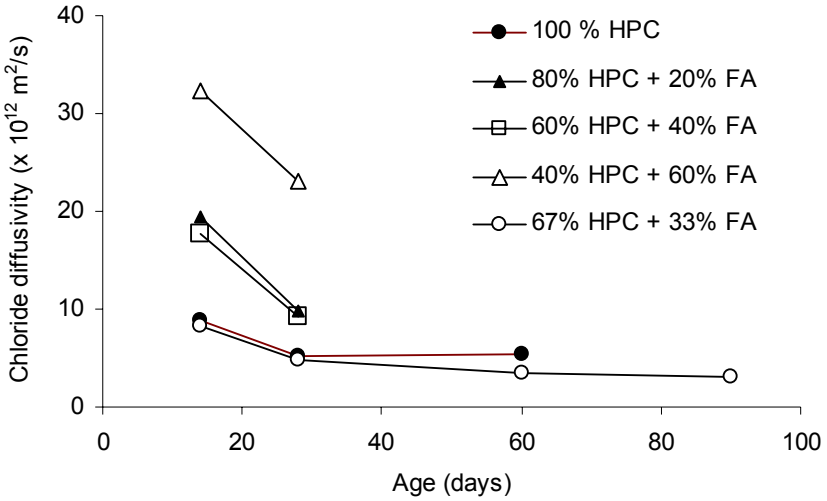

Figure 5.4: Effect of coarse fly ash on the chloride diffusivity of concretes produced with high performance portland cement and silica fume

5.2.3. Effect of Blast – Furnace Slag

5.2.3.1. Concretes Produced with Ordinary Portland Cement and Slag

The development of chloride diffusivity by time obtained by accelerated testing is presented in Table 5.4 and also in Figure 5.5.

Table 5.4: Chloride diffusivity of concretes with different slag replacement ratios

Mixture	Chloride Diffusivity, $m^2/s \times 10^{-12}$					
	3 days	7 days	14 days	28 days	90 days	1 year
100 % OPC	14.3	13.3	12.2	11.2	8.6	6.9
40 % Slag	23.4	11.9	7.5	4.9	4.0	2.9
60 % Slag	28.3	10.4	6.5	3.6	2.7	2.3
80 % Slag	18.1 (*)	9.2	3.9	2.3	1.9	1.3

As presented in the table, at the age of 3 days, the diffusivity of the concretes with slag replacements are significantly higher than that of portland cement and at this age the diffusivity increases with the slag content. An exception to this is the concrete with 80 % slag indicated by an asterisk which was tested at 4 days age instead of 3 days, which may be the cause of this lower diffusivity than expected. If the testing of this concrete was made at 3 days age, the result might be much higher.

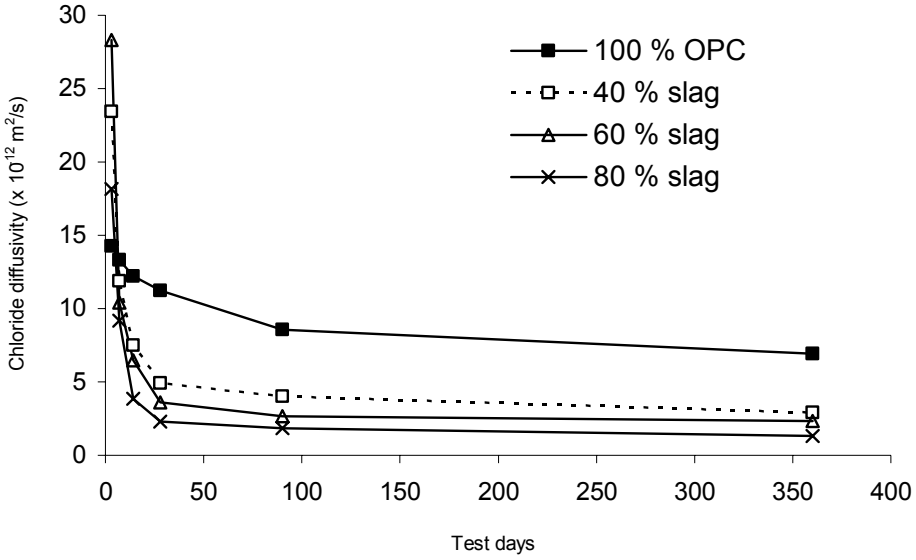

Figure 5.5: Development of chloride diffusivity with different slag contents

As illustrated in Figure 5.5, chloride diffusivity decreases with age, and especially at the early ages, the rate of diffusivity development of slag concretes are much more rapid when compared to portland cement. Although the diffusivities of slag concretes are higher at 3 days, they outperform the portland cement concrete at 7 days. After 7 days the chloride diffusivity decreases considerably with increasing slag content, for example; at 28 days, the ratios of diffusivity of slag concretes to that of portland cement concrete are 44 %, 32 % and 21 %, for the 40 %, 60 % and 80 % replacements, respectively.

Chloride ions are transported in the capillary pores of concrete and chloride diffusivity reflects the pore system of concrete. It was reported that the pore system of the slag concretes are significantly finer than the portland cement concrete (Bijen, 1996b). As a result of the lower capillary pores, the diffusivity of the slag concrete is substantially reduced. Clogging of pores and reduction in the connectivity of the pore system due to the pozzolanic reaction of slag was reported to be responsible for the better permeability characteristics of slag concrete.

Bulk diffusion test also confirms the beneficial effect of blast furnace slag on the chloride diffusivity of concrete. As seen in Figure 5.6, the diffusivity reduced substantially. Differences between the diffusivity of slag concretes, however, are small.

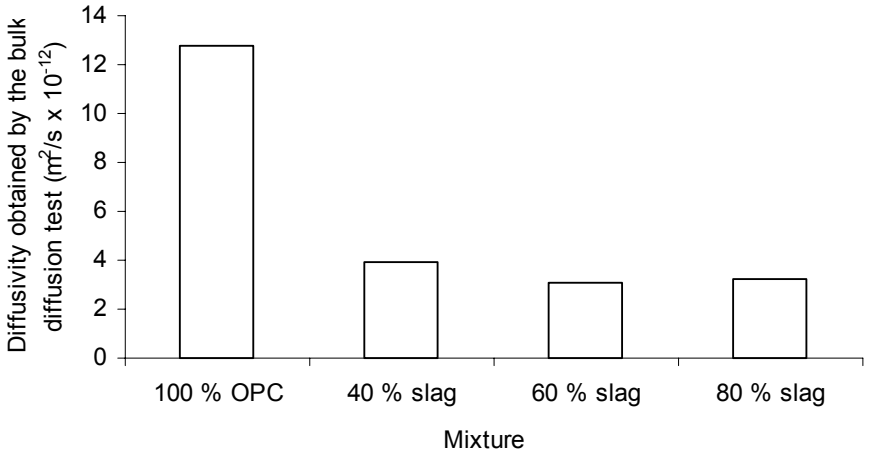

Figure 5.6: Effect of slag on the bulk diffusion

5.2.3.2. Concretes Produced with High Performance Portland Cement, Silica Fume and Slag

As seen from Table 5.5 and Figure 5.7, the diffusivity of the slag concretes reduced with the increase in slag content. The diffusivity of all the concretes improved with age, but this improvement was much more significant for the slag concretes, especially between 14 days to 60 days. The diffusivity of the concretes (coded as 4 and 5) produced with the slag cements were significantly lower than that of the portland cement at 60 days and beyond.

Table 5.5: Effect of slag on the chloride diffusivity of concretes produced by high performance portland cement and silica fume

Mixture	Chloride Diffusivity, $m^2/s \times 10^{-12}$						
	14 days	28 days	60 days	90 days	120 days	150 days	180 days
A	8,9	5,2	5,4				
2 A	20,0	9,7	6,0	4,7	3,3	3,4	5,3
4 A	17,8	8,0	4,1	3,9	3,1	3,2	4,1
6 A	13,1	6,4	3,8	2,6	2,6	2,1	1,5
4	6,1	4,6	2,9	2,0	1,7	2,7	2,1
5	9,0	5,7	2,9	2,9	2,9	4,1	

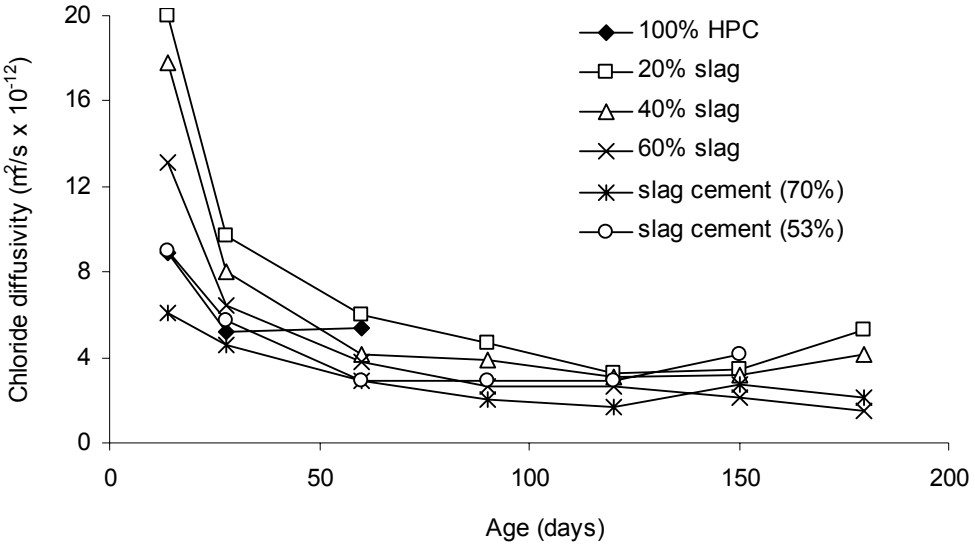

Figure 5.7: Effect of slag on the chloride diffusivity of concretes produced by high performance portland cement and silica fume

5.2.3.3. Concretes Produced with Fly Ash Cement, Silica Fume and Slag

Table 5.6 and Figure 5.8 present the effect of slag replacement on the chloride diffusivity of concretes produced with fly ash cement and silica fume. Combination of fly ash with slag performs better when compared to only fly ash cement mixtures. Replacement of fly ash by slag reduced the chloride diffusivity of the concretes at all ages and this reduction is more noticeable at later ages and higher replacement ratios. Microstructure of the concrete is modified by the addition of slag. A more refined pore system is responsible for the reduced diffusivity.

Table 5.6: Effect of slag replacement on the chloride diffusivity of concretes produced by fly ash cement and silica fume

Mixture	Chloride Diffusivity, $m^2/s \times 10^{-12}$					
	14 days	28 days	60 days	90 days	120 days	150 days
0 F	10.7	5.2	3.2	2.8	2.2	3.3
2 F	8.6	4.6	3.3	2.7	3.6	3.1
4 F	9.1	4.9	2.9	2.3	1.5	-
6 F	9.1	5.0	2.1	1.4	1.4	1.8

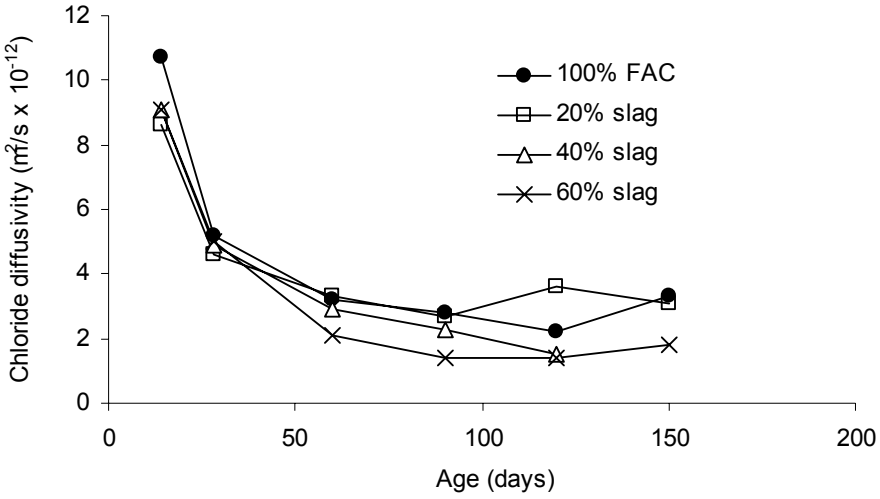

Figure 5.8: Effect of slag replacement on the chloride diffusivity of concretes produced by fly ash cement and silica fume

5.2.4. Effect of Silica Fume

5.2.4.1. Concretes Produced with Ordinary Portland Cement and Silica Fume

The partial replacement of portland cement by silica fume increased the diffusivity very slightly at the age of 3 days, but at 7 days and beyond, the diffusivity of the silica fume concretes are substantially lower and the reduction is more significant with the increase in the silica fume content. For example, at 28 days, the diffusivity for the concrete containing 5 % silica fume is about 32 % of the portland cement concrete and for the 10 % silica fume concrete this ratio is 13 %.

Table 5.7: Effect of silica fume on the diffusivity of concretes produced with OPC

Mixture	Chloride Diffusivity, $m^2/s \times 10^{-12}$						
	3 days	7 days	14 days	28 days	90 days	180 days	1 year
100 % PC	14.3	13.3	12.2	11.2	8.6	–	6.9
5% SF + 95% PC	14.9	7.5	3.9	3.3	3.0	3.1	3.0
10% SF + 90% PC	14.8	5.0	1.6	1.5	1.4	1.35	1.3

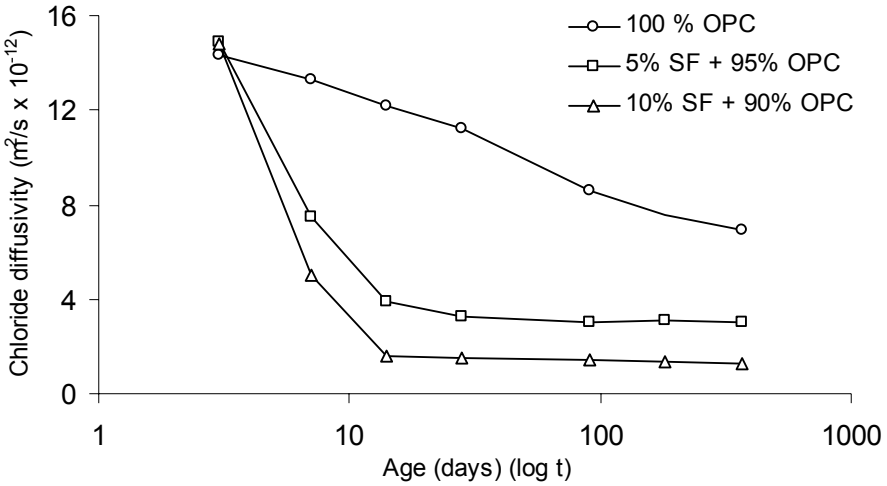

Figure 5.9: Effect of silica fume on the diffusivity of concretes produced with OPC

The important effect of silica fume on the resistance of concrete against chloride penetration is clearly demonstrated also by the bulk diffusion test. As seen in Figure 5.10, the diffusivity obtained by the bulk diffusion test reduced significantly by incorporating the silica fume. From these test results, however, it seems that increasing the silica fume content from 5 % to 10 % did not have a big impact on reducing the diffusivity.

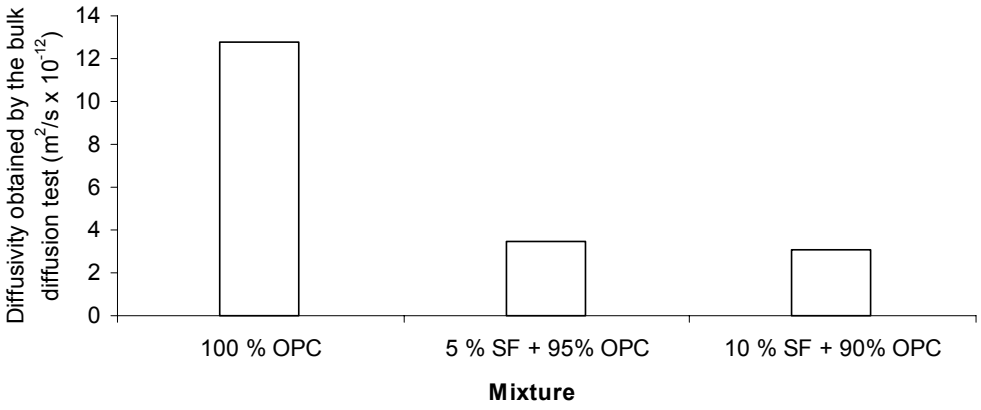

Figure 5.10: Effect of silica fume on the bulk diffusion of concretes cast with OPC

5.2.4.2. Concretes Produced with OPC, Slag and Silica Fume

The chloride diffusivity of concretes produced by the ternary blend of the portland cement, silica fume and slag are presented in Table 5.8 and Figure 5.11, together with those of portland cement and 60 % slag concrete.

Table 5.8: Chloride diffusivity of concretes with ternary blend of portland cement, slag and silica fume

Mixture	Chloride Diffusivity, $m^2/s \times 10^{-12}$						
	3 days	7 days	14 days	28 days	90 days	180 days	1 year
100 % PC	14.3	13.3	12.2	11.2	8.6	–	6.9
60 % Slag	28.3	10.4	6.5	3.6	2.7	–	2.3
5% SF + 40% PC + 55 % Slag	26.2	6.8	3.0	1.8	1.6	1.6	1.4
10% SF + 40% PC + 50 % Slag	22.5	4.6	1.4	1.1	0.64	0.60	0.52

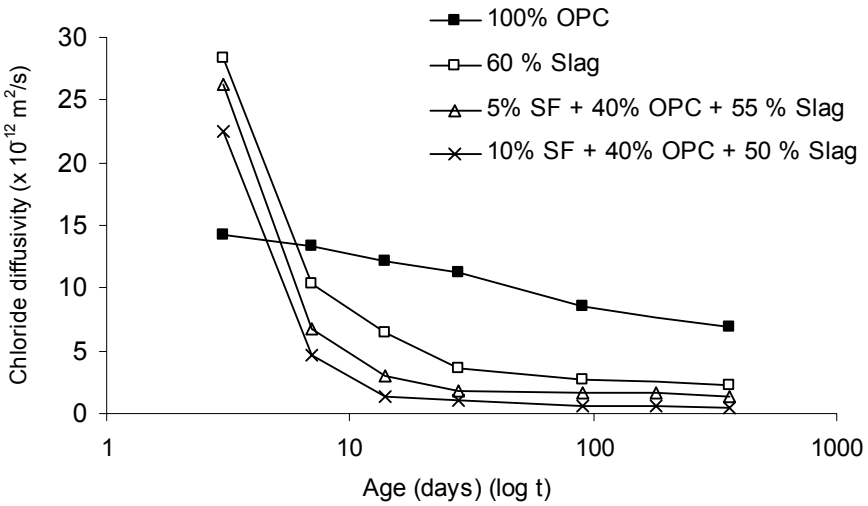

Figure 5.11: Chloride diffusivity of concretes produced by portland cement, silica fume and slag blends

Incorporation of silica fume is also very effective in decreasing the diffusivity of the slag concrete. This effect is little at 3 days but at 7 days and later on, the reduction in diffusivity is significant. As indicated in Table 5.8, the replacement amount of silica

fume is also important to achieve lower diffusivity. The change of silica fume replacement ratio from 5 % to 10 % decreased the diffusivity about 50 % at later ages. Because of its extreme fineness, silica fume has an important role for improving the porous aggregate – cement interface. In addition, silica fume is also efficient in reducing the coarse capillary pores in the cement paste, which as a result decreases the chloride diffusivity of the paste (Zhang and Gjørv, 1991).

As shown in Table 5.7 and 5.8, the use of slag and silica fume combination has produced the lowest chloride diffusivity values which are lower than those of the concretes containing only slag or silica fume. A better particle packing and refined pore system are the possible explanations for this result (Nagataki and Wu, 1995).

Figure 5.12 shows the results of bulk diffusion carried out on the concretes produced with portland cement, slag and silica fume. As seen in the figure, partially replacing slag by silica fume reduced the diffusivity at 10 % replacement level. However, a slight increase in the diffusivity level was observed for the concrete with 5 % silica fume.

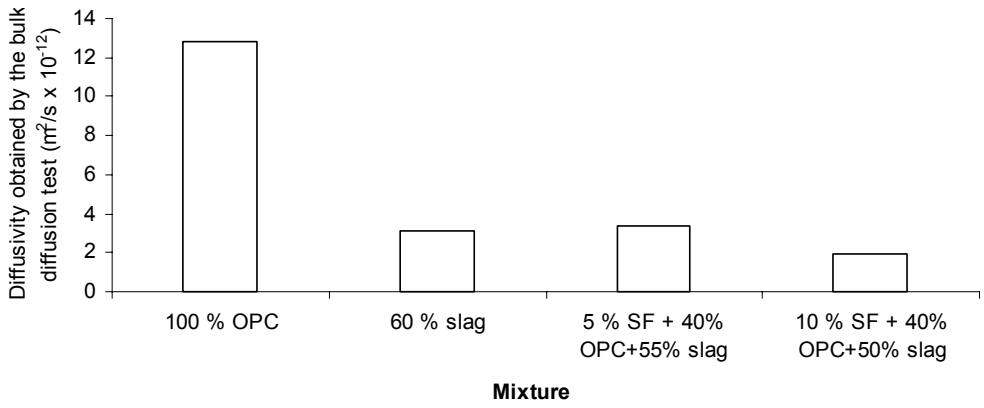

Figure 5.12: Effect of silica fume on the bulk diffusivity of concretes containing slag

5.2.4.3. Concretes Produced with Fly Ash Cement, Slag and Silica Fume

The chloride diffusivity of concretes produced by the fly ash cement, slag and silica fume blends, are given in Table 5.9. The results of the portland cement concrete are also included in this table.

Table 5.9: Chloride diffusivity of concretes produced using fly ash cement

Mixture	Chloride Diffusivity, $m^2/s \times 10^{-12}$						
	3 days	7 days	14 days	28 days	90 days	180 days	1 year
100 % PC	14.3	13.3	12.2	11.2	8.6	–	6.9
100 % Fly Ash Cement	19.5	13.9	8.6	6.2	3.0	2.4	1.9
5% SF + 95% FAC	17.5	7.3	4.0	2.7	1.4	1.36	1.1
10% SF + 90% FAC	16.0	5.2	2.3	1.5	1.5	0.9	0.64
5% SF + 40% FAC + 55 % Slag	39.3	7.1	3.2	2.0	1.2	1.2	1.0
10% SF + 40% FAC + 50 % Slag	37.3	5.8	2.8	1.1	0.65	0.57	0.52

At early ages, the diffusivity of the concrete with fly ash cement is higher than the portland cement concrete, but at 14 days and later ages, it is substantially lower than that of the portland cement concrete. Although the fly ash cement contains only about 20 % fly ash, it has a significant impact on the diffusivity at later ages, for example at 90 days; diffusivity of the concrete with fly ash cement is about 35 % of the concrete cast with portland cement. The better performance of the fly ash cement is a result of the change in the microstructure of the concrete. Previous studies show that inclusion of fly ash leads to a finer pore structure in concrete. Pozzolanic reaction of the fly ash is slow at early ages, which is responsible for the poor early age performance of fly ash concretes. However, after the fly ash is activated as a result of the increase in concrete alkalinity, the pozzolanic reaction between fly ash and CH improves concrete properties at later ages.

Incorporation of silica fume into the fly ash cement mixtures reduced the diffusivity further as presented in Figure 5.13. The effect of silica fume increases with the replacement amount, for example; at 28 days, the chloride diffusivity of the concretes produced by fly ash cement containing 5 % and 10 % silica fume, are about 44 % and 24 % of the concrete produced only by fly ash cement, respectively.

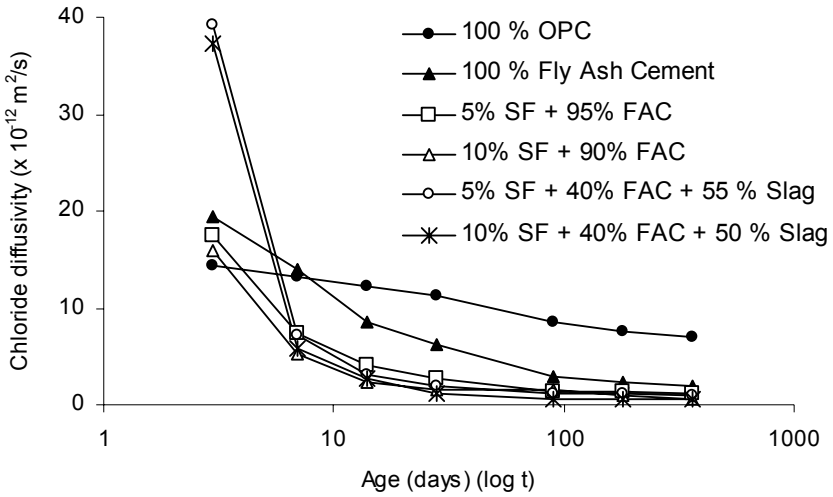

Figure 5.13: Chloride diffusivity of concretes produced by fly ash cement

As seen in Table 5.9, concretes produced by the fly ash cement – slag – silica fume blend have the highest diffusivity at 3 days, but these concretes also have the most rapid diffusivity development. For example at the age of 7 days, the diffusivity of the ternary blended concrete containing 10% silica fume decreased 84% compared to the diffusivity at the age of 3 days. Because fly ash cement consists of 20 % fly ash and 80 % portland cement, these concretes actually contain a quaternary blend of portland cement – fly ash – slag and silica fume. This multi – blended binder system has a wide range of particle sizes which is one of the reasons for their high performance after 7 days. Particle packing in these concretes are much higher as a result of the different particle sizes. Hydration characteristics of these cementitious materials also differ from each other and using them together can compensate some of their disadvantages.

The results of the bulk diffusion test are shown in Figure 5.14. Compared to the only portland cement concrete, fly ash cement caused a considerable reduction in the bulk diffusivity. However, not important differences were obtained for the concretes produced with the combinations of silica fume, slag and portland cement.

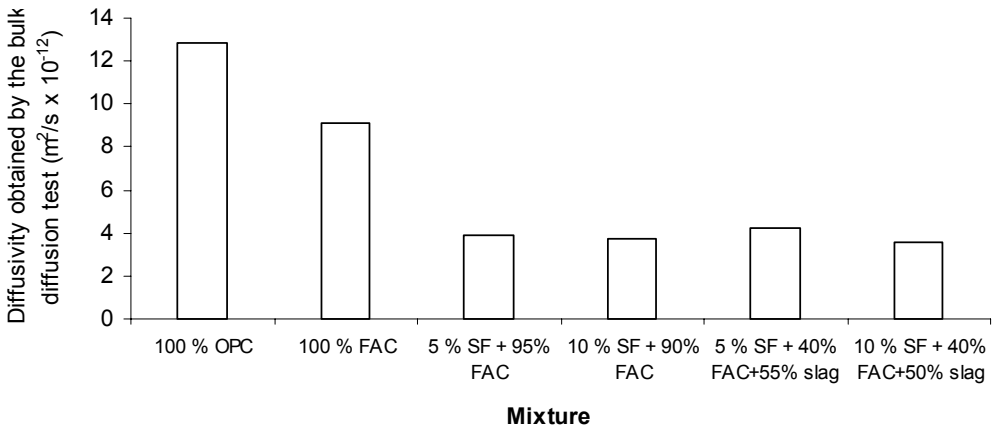

Figure 5.14: Bulk diffusion results of the concretes produced with fly ash cement, slag and silica fume

5.2.5. Relationship between Bulk Diffusion and Migration Testing

In this study, in order to investigate the effect of pozzolans on the resistance of concrete against chloride penetration, some of the concrete mixtures were tested according to two different methods; NT 443, the bulk diffusion test, and NT 492, the migration test. The test results are presented in previous chapters.

Bulk diffusion test is based on the immersion of concrete samples in a chloride solution for 35 days, which are then ground to obtain chloride profiles. This test is a non – steady state diffusion test method and chlorides penetrate into concrete as a result of diffusion. The migration test, however, uses an externally applied electrical field to force chloride ions into concrete.

Figure 5.15 compares the diffusivity of the concretes obtained by the bulk diffusion test and the migration test. All these concretes had the same water/binder ratio of 0.40, but contained different amounts of pozzolanic materials. Of the results obtained, concretes containing only portland cement and only fly ash cement had significantly higher diffusivity as presented in the figure.

By presenting the test results as in Figure 5.15, it seems that there is a linear relationship between these two methods. However, as seen in the figure, except for those of the portland cement and fly ash concretes, the results clearly form a group for the low diffusivity values. When the diffusivity of the portland cement concrete and fly ash cement concrete in Figure 5.15 were ignored; Figure 5.16 was obtained.

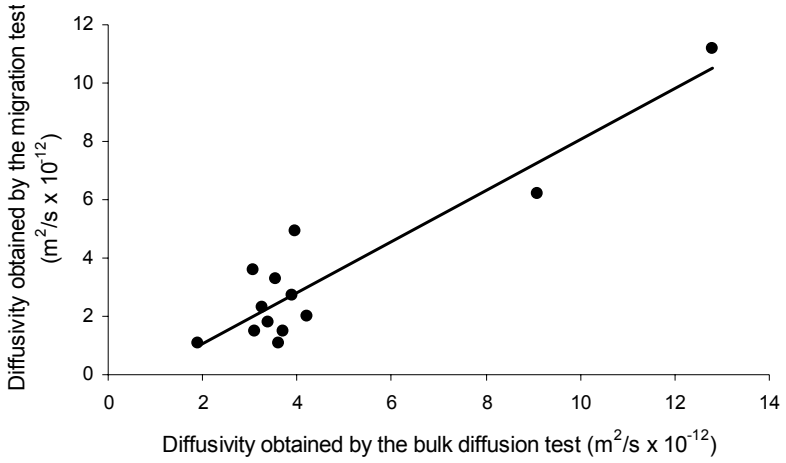

Figure 5.15: Relationship between the bulk diffusion test and the migration test

As shown in Figure 5.16, based on the high scatter of diffusivity values obtained by the two test methods, it can be concluded that the linear relationship presented in Figure 5.15 do not actually represent the bulk diffusion – migration test relation for the concretes with high resistance against chloride penetration. Different transportation mechanisms involved in these test methods may be the main reason behind this result. Other factors such as chloride binding can also be an additional cause.

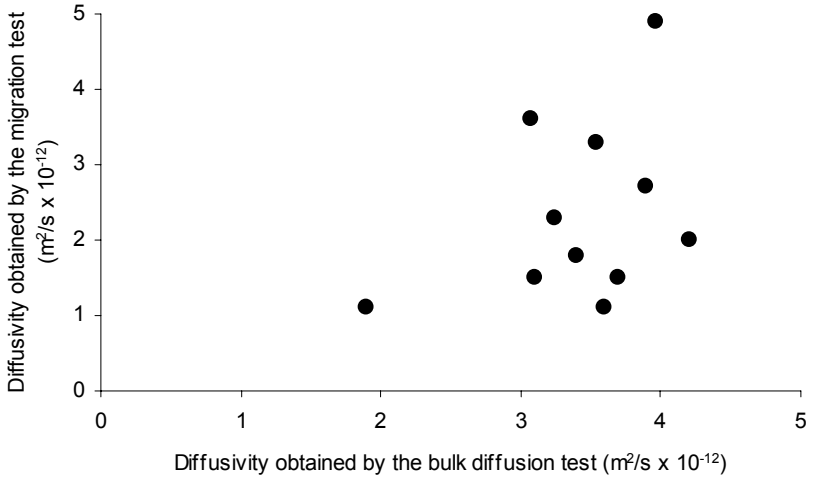

Figure 5.16: Relationship between the bulk diffusion test and the migration test when the results for the two lower quality concretes are ignored

5.3. Electrical Resistivity

5.3.1. Effect of Blast Furnace Slag on the Concretes Produced with OPC

5.3.1.1. Two Electrodes Method

For the the concretes containing different amounts of slag and ordinary portland cement, the development of electrical resistivities obtained by the two electrode method are presented in Figure 5.17. As expected, the resistivity of all the concretes increased with age. This increase, however, is significant for the concretes containing slag. At early ages (i.e. at 3 days), resistivity of the slag concretes were lower than that of the ordinary portland cement concrete and the decrease in resistivity became more important with the slag content. However, at 7 days and beyond, concretes with slag had substantially higher electrical resistivity; for example, at 28 days, concrete containing 60% slag has about 260 % higher resistivity than the portland cement concrete and this ratio is about 420 % at the age of one year.

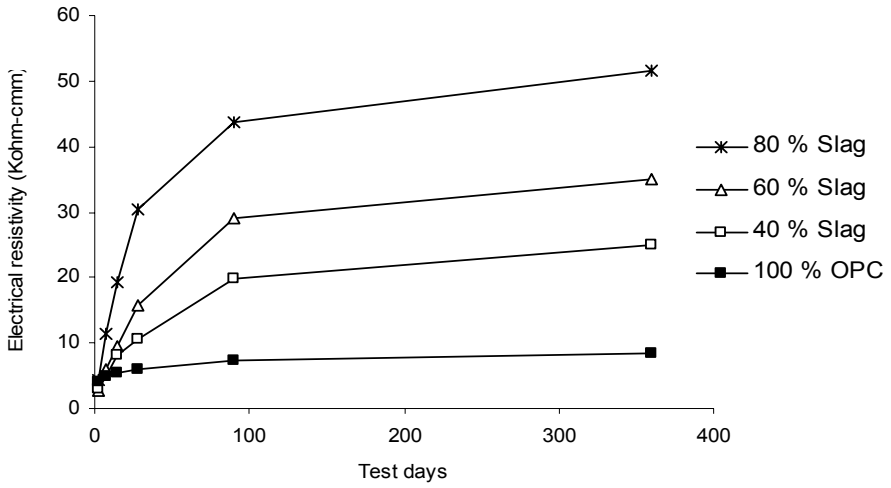

Figure 5.17: Effect of blast furnace slag on the electrical resistivity of concrete obtained by the two electrode method

5.3.1.2. Wenner Electrode Method

Results obtained by the wenner electrode method showed a similar development of the electrical resistivity when compared to the two electrode method. Figure 5.18 shows the wenner electrode test results obtained on ϕ100x200 mm cylinders for the probe spacing of 5 cm.

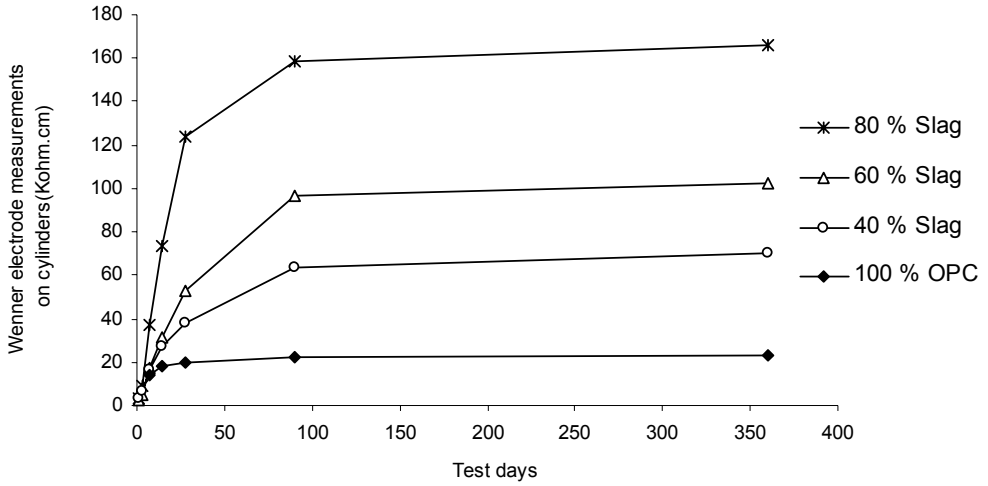

Figure 5.18: Effect of slag on electrical resistivity obtained on cylinders using the wenner electrode method

Wenner electrode measurements carried out on 100 mm cubes with 2.5 cm probe spacings are shown in Figure 5.19 and the results obtained on ϕ100x50mm discs in Figure 5.20.

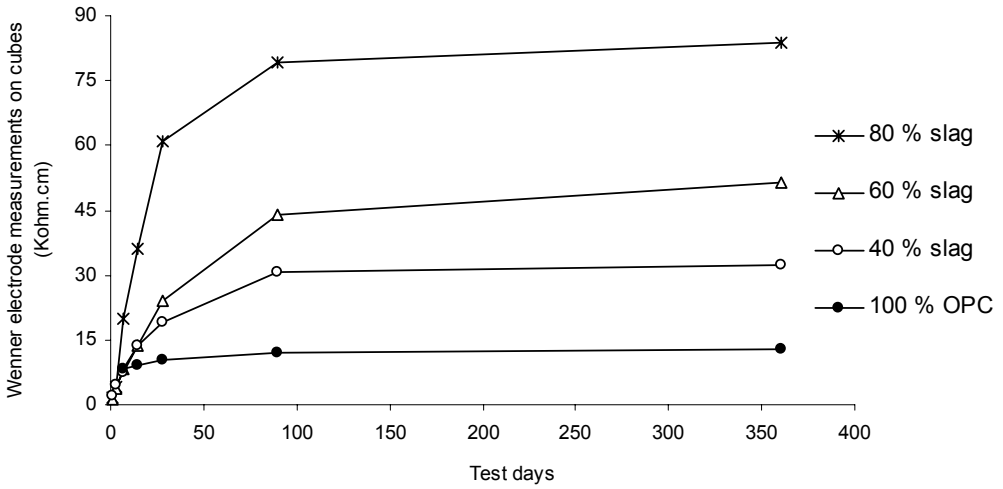

Figure 5.19: Effect of slag on electrical resistivity obtained on cubes using the wenner electrode method

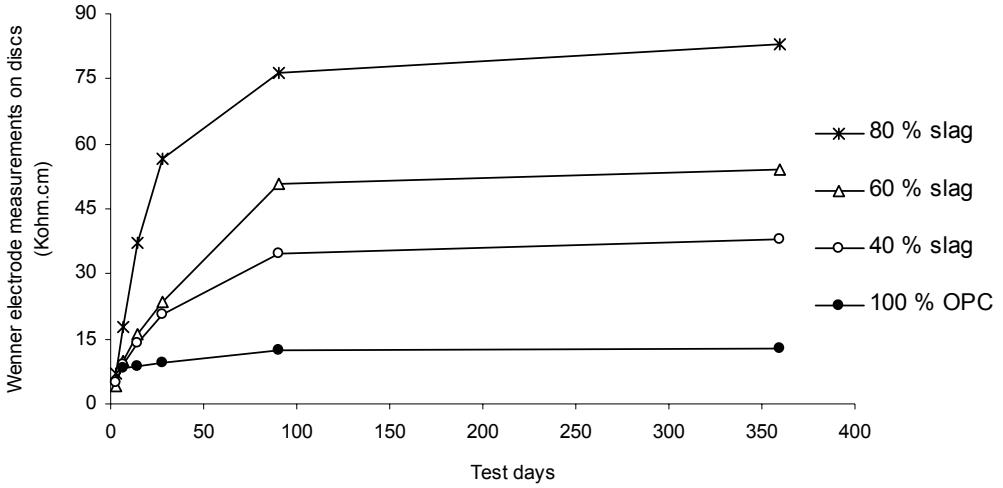

Figure 5.20: Effect of slag on electrical resistivity obtained on discs using the wenner electrode method

Although slag concretes had lower electrical resistivity at early ages, they had significantly higher strength at later ages and the resistivity increased with the slag replacement ratio. The better performance of these slag concretes were confirmed by the tests carried out on different specimen types.

5.3.2. Effect of SF on Concretes Produced with OPC and Slag

5.3.2.1. Two Electrodes Method

Partial replacement of ordinary portland cement by silica fume caused an important increase on the electrical resistivity of concrete as shown in Figure 5.21. Unlike the other pozzolans (fly ash or slag), silica fume didn't cause reduction in resistivity at early ages. At the age of 28 days, when compared to ordinary portland cement concrete, the resistivity of the concretes with silica fume were 470% and 950 % higher for 5% and 10% replacements, respectively.

The electrical resistivity of ternary blend of OPC, slag and silica fume are also shown in the figure. For a given silica fume content, resistivity of concrete containing ternary binder is higher than the binary blends of OPC-silica fume or OPC-slag. The higher resistivity is the indication of the better performance of these concretes against the corrosion of embedded steel. The modified microstructure of the concrete as a result of the different hydration characteristics of the OPC, slag and silica fume, is the main cause of the better results obtained.

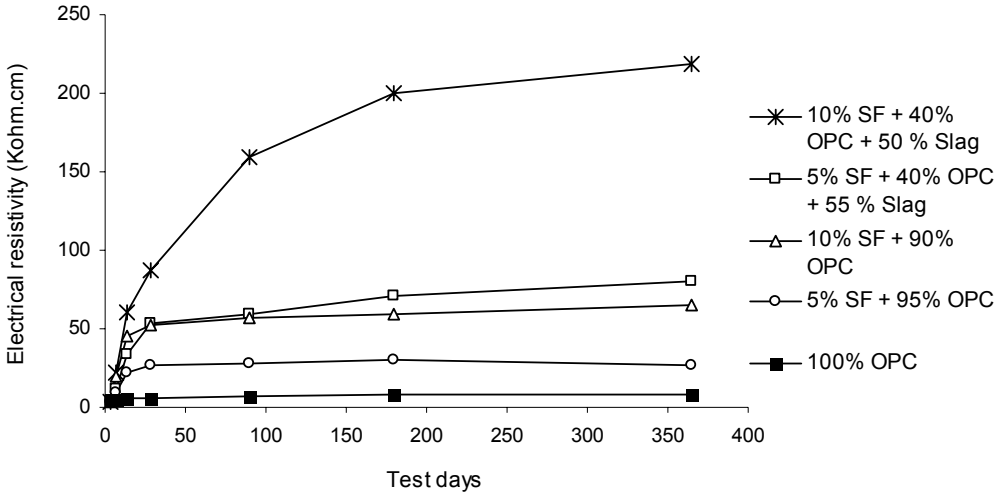

Figure 5.21: Effect of silica fume on the electrical resistivity obtained on disc specimens using the two electrode method

5.3.2.2. Wenner Electrode Method

Test results obtained by the Wenner Electrode Method give the same conclusion on the effect of silica fume on the electrical resistivity of concrete. Figure 5.22 illustrates the development of resistivity of cubes. As shown in the figure, the effect of silica fume increased with the replacement ratio.

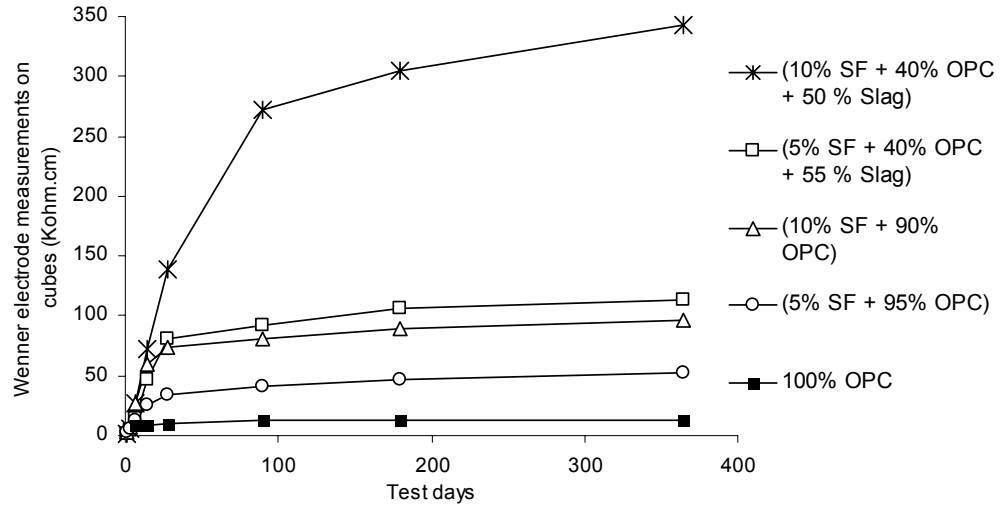

Figure 5.22: Effect of silica fume on the electrical resistivity obtained on cubes using the wenner electrode method

Similar to the results obtained by the two electrode method, values obtained by the wenner electrode method also proved that the ternary blends of OPC – slag – silica

fume are more effective on increasing the electrical resistivity than the binary blends. This increase in the resistivity is vital for obtaining a longer service life for the structure.

5.3.3. Effect of SF on concretes produced with FAC and Slag

5.3.3.1. Two Electrodes Method

Resistivities obtained on different mixtures containing fly ash cement are presented in Figure 5.23, together with the results of the concrete produced with ordinary portland cement. Compared to the ordinary portland cement concrete, at early ages, fly ash cement caused reductions on the resistivity, however, fly ash cement concrete had higher resistivity at later ages. Partial replacement of fly ash cement with silica fume increased the electrical resistivity further. As seen in the figure, replacement amount is also important for obtaining better performance from silica fume. For example; use of 10 % silica fume instead of 5% caused the resistivity of OPC – silica fume binary blend to increase 67 % at 28 days.

Silica fume is also effective on increasing the resistivity of concrete containing slag, and the concrete produced with ternary blend of 40% fly ash cement – 50% slag – 10% silica fume have the highest electrical resistivity. For example; at 28 days, the resistivity of this concrete is about 10 times higher than the only portland cement concrete and this difference is 18 times at the age of 90.

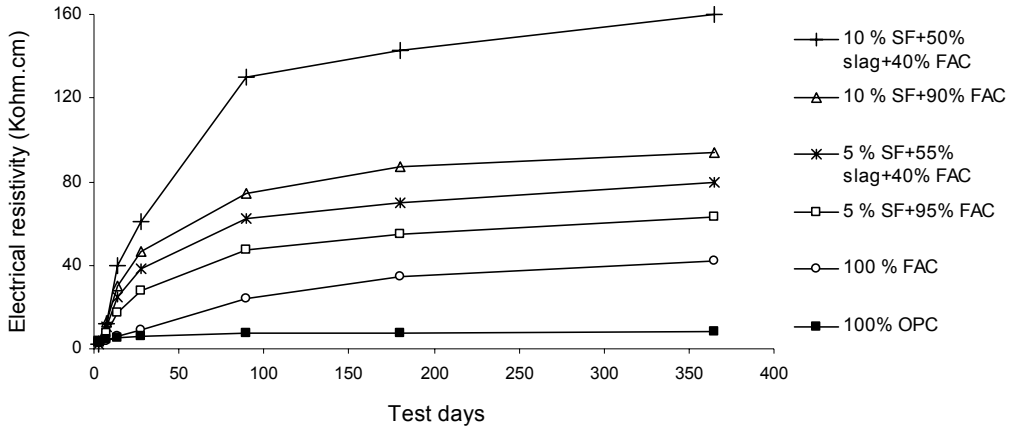

Figure 5.23: Effect of SF on the resistivity of concretes containing FAC and slag obtained by the two electrode method

5.3.3.2. Wenner Electrode Method

The wenner electrode method surface measurements carried out on different specimens confirmed the beneficial effect of silica fume on the resistivity of concretes produced with fly ash cement and slag. Addition of silica fume increased the electrical resistivity of concretes substantially. Figure 5.24 shows the results of wenner electrode measurements carried out on the cubes.

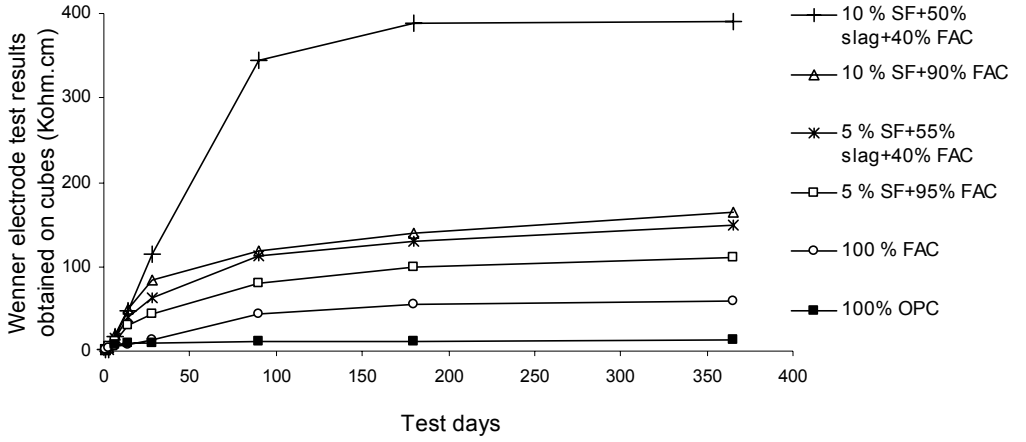

Figure 5.24: Effect of SF on the resistivity of cubes containing FAC and slag obtained by the wenner electrode method

5.3.4. Effect of Test Method

5.3.4.1. Resistivities Obtained on the Same Specimens

Electrical resistivity of the concrete discs of the 100 diameter and 50 mm height were obtained both by the two electrode method and the wenner electrode method and the test results are presented in previous chapters. Figure 5.25 shows the relation between these test methods obtained on the same specimens.

These results ain the figure are based on different concrete mixtures with the testing ages ranging from 3 days to 1 year. The figure demonstrates the strong relationship between the two test methods. The individual test results, however, may be different based on the test method. In the two electrode method, the electrical current passes through the whole volume of the specimen. In the wenner electrode method, however, the current passes through a depth related to the probe spacing

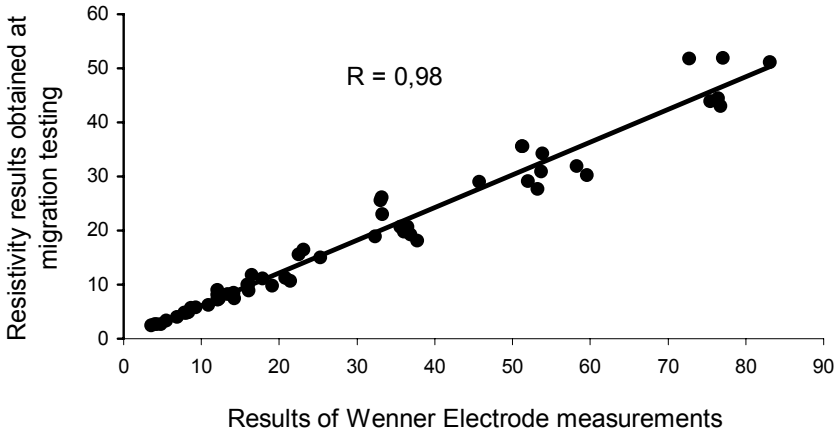

Figure 5.25: Effect of test method on the electrical resistivity ontained on the same specimens

If a relationship such as the one given in Figure 5.25 is established based on a particular concrete mixture, it is possible to obtain the resistivity with one of these methods and estimate the corresponding resistivity that can be obtained with the other method. Such an evaluation can be very important and useful for sites where different resistivity measurements are carried out.

5.3.4.2. Resistivities Obtained on Different Specimens

Figure 5.26 illustrates the relationship between the electrical resistivities otained on the disc and cube specimens using different methods. The 100x50 mm disc specimens were tested using the two electrode method and 100 mm cubes by the wenner electrode method. The figure is based on different concrete mixtures with the testing ages ranging from 3 days to 1 year.

Although different type of specimens and test methods were used for testing, there is a strong relationship (R=0.99) between these methods. Similar relationships between cubes and cylinders, or cubes and discs can be established, by which, one type specimen is tested with two electrode method and the other by wenner electrode method. Accurate evaluation of resistivities obtained from different specimens can be carried out by formulating relationships between different specimens tested with various methods.

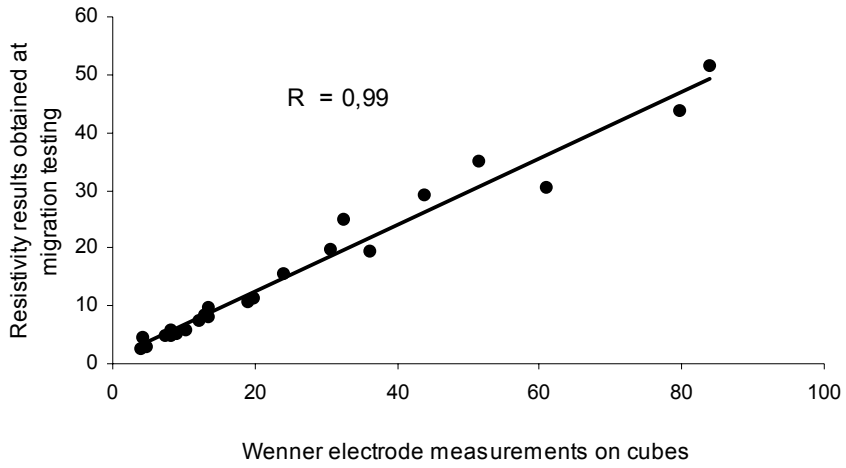

Figure 5.26: Effect of test method on the electrical resistivity ontained on different specimens

5.3.5. Effect of Specimen Type on the Resistivity Obtained by WEM

Electrical resistivity obtained by wenner electrode method is based on the measurements carried out on the surface. Electrical current generated on the concrete surface penetrates into the specimen and the depth of the current flow is related to the spacing between the probes. Specimen geometry is another important factor affecting the current flow. In order to study the effect of specimen type on the resistivity measured by the wenner electrode method; 100 mm cubes, 100x200 mm cylinders and 100x50 mm discs were tested. Probe spacing of 5 cm for the cylinders, and 2.5 cm for the cubes and discs were selected. Figure 5.27 illustrates relation between the test results obtained on the cubes and cylinders.

Although the probe spacings and as a result, electrical flow depth flow patterns in these specimens are different, as seen in the figure, the correlation between the results were significantly high (r=0.997). A similar relationship was also established between the cubes and the discs and Figure 5.28 shows the resistivity values obtained these specimens.

Figures 5.27 and 5.28 are based on different concrete mixtures with the testing ages ranging from 3 days to 1 year. These figures confirm the relation between different specimens when tested by wenner electrode method. As seen from the results, the resistivity obtained from a specimen type can be different from another specimen; however, it seems that these resistivity values are proportional to each other.

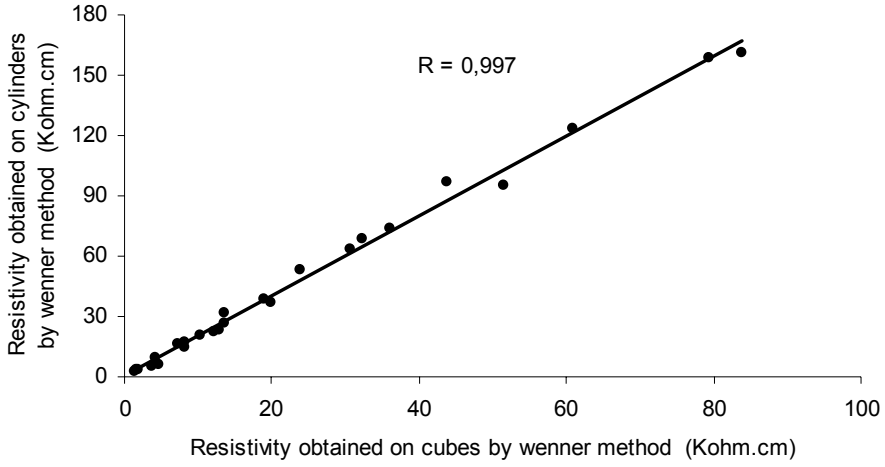

Figure 5.27: Relation between the resistivities obtained on the cubes and cylinders using wenner electrode method

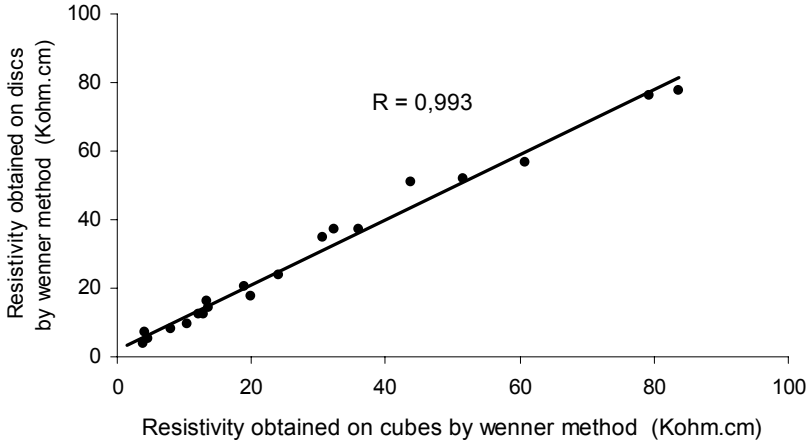

Figure 5.28: Relation between the resistivities obtained on the cubes and discs using wenner electrode method

Cubes are the most common specimen type used for the quality control of compressive strength of concrete. The specimens used used for the strength testing can also be used for the routine resistivity testing by wenner electrode method. By establishing relationships between different specimen types, it is possible to compare resistivities obtained from varios samples. For example, using such relationships, resistivity values obtained from the routine testing of the cubes can easily be compared to the values obtained from the cores taken from the structure.

5.4. Chloride Diffusivity – Electrical Resistivity Relationship

Figure 5.29 presents the relationship between electrical resistivity and chloride diffusivity. Although chloride diffusivity is a very important parameter for specification of the durability, a routine testing of this parameter may be too elaborate and time consuming for a regular quality control during concrete construction. For a given type of concrete and test conditions, the test results confirm that there is a strong linear relationship between chloride diffusivity and electrical resistivity. Monitoring of electrical resistivity may be a very appropriate way for monitoring the chloride diffusivity during concrete construction (Gjørv, 2002). As soon as the necessary reference curves are established, the regular in situ control of concrete quality can take place, mostly based on surface measurements of electrical resistivity, but partly also on concrete coring and accelerated testing of chloride diffusivity.

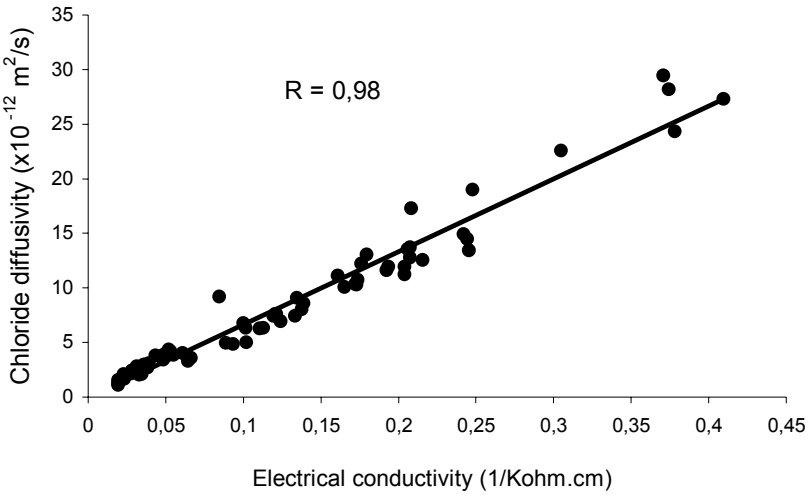

Figure 5.29: Relationship between electrical resistivity and chloride diffusivity

5.5. Effect of Slag on the Capillarity of Concrete

Capillarity number and capillarity resistance numbers of the concretes produced with slag are presented in Tables 5.10 and 5.11, respectively. In these tables, the values given in the brackets are the standard deviations for each average value.

Capillarity number is an indication of the rate of water absorption. Lower capillarity number shows less water suction which is beneficial for the resistance against the penetration of aggressive substances (Gjørv, 1994a). The effect of slag on reducing the capillary water absorption is clearly demonstrated in the tables. As seen in Table

5.10, it appears that capillarity decreases with slag replacement ratio. Substantial reductions were obtained for the 40% and 60% replacement ratios. For example, for a given age, the capillarity of the concrete containing 60 % slag has capillarity about half of the portland cement concrete. However, the values obtained for the 80% slag replacement were slightly higher than those for the concrete with 60% slag, which is an unexpected result.

Table 5.10: Effect of slag on the capillarity number of concrete

Mixture	Capillarity Number, $kg/m^2.s^{0.5} \times 10^{-2}$ (σ)			
	7 days	14 days	28 days	90 days
100 % OPC	1.94 (0.16)	1.94 (0.06)	1.92 (0.07)	1.72 (0.02)
40 % Slag	1.42 (0.05)	1.21 (0.03)	1.16 (0.05)	0.98 (0.04)
60 % Slag	1.03 (0.02)	0.91 (0.03)	0.83 (0.02)	0.77 (0.03)
80 % Slag	1.08 (0.01)	0.95 (0.03)	0.91 (0.02)	0.98 (0.03)

Table 5.11: Effect of slag on the capillarity resistance number of concrete

Mixture	Resistance Number, $s/m^2 \times 10^8$ (σ)			
	7 days	14 days	28 days	90 days
100 % OPC	4.68 (0.61)	4.40 (0.26)	4.50 (0.05)	4.33 (0.07)
40 % Slag	4.60 (0.14)	4.09 (0.18)	3.97 (0.11)	3.90 (0.09)
60 % Slag	3.80 (0.06)	4.10 (0.1)	3.80 (0.13)	3.83 (0.06)
80 % Slag	3.96 (0.15)	4.20 (0.99)	3.86 (0.10)	3.77 (0.06)

Capillary numbers and capillary resistance numbers reflect the size distribution and continuity of capillaries. Lower capillarity is a result of a refined pore system. Chloride diffusivity also depends on the pore system of concrete but unlike the results of the capillary water absorption, diffusivity of concrete with 80% slag was

the lowest compared to other mixtures. Electrical resistivity of the concrete with 80% slag is also the highest at 7 days and beyond. Although the capillarity test results for the 80 % slag concretes are unexpected, it appears that in general, the capillarity test confirms the results obtained from the migration testing and electrical resistivity testing.

5.6. Effect of Slag on the Porosity of Concrete

The total porosity, suction porosity and air porosity of the concretes produced with slag are presented in Tables 5.12, 5.13 and 5.14, respectively. The average values are presented together with the standard deviations values given in the brackets. Total porosity of the concretes decreases with age. As seen in Table 5.12, the total porosity of the concretes with 40 % and 60 % slag are lower than that of the portland cement concrete. It can be expected that the concrete produced with 80 % slag have the lowest total porosity but as presented in the table, the values are close to those of portland cement concrete.

Table 5.12: Effect of slag on the total porosity of concretes

Mixture	Total porosity, % (σ)			
	7 days	14 days	28 days	90 days
100 % OPC	14.28 (0.52)	13.24 (0.42)	13.41 (0.22)	12.6 (0.26)
40 % Slag	13.68 (0.54)	13.04 (0.33)	12.73 (0.25)	11.65 (0.43)
60 % Slag	11.73 (0.17)	12.43 (0.27)	11.83 (0.38)	11.52 (0.19)
80 % Slag	13.81 (0.35)	13.66 (0.16)	13.24 (0.35)	13.39 (0.25)

Suction porosity of the concretes also improved with age. Similar to the results of total porosity, suction porosity also decreased up to 60 % slag replacement but the suction porosity of 80 % slag concrete is even higher than those of the portland cement concrete.

Table 5.13: Effect of slag on the suction porosity of concretes

Mixture	Suction porosity, % (σ)			
	7 days	14 days	28 days	90 days
100 % OPC	12.44 (0.48)	11.84 (0.35)	11.88 (0.30)	11.31 (0.12)
40 % Slag	11.88 (0.46)	11.22 (0.24)	10.96 (0.21)	10.1 (0.41)
60 % Slag	10.78 (0.15)	10.69 (0.23)	10.19 (0.25)	9.81 (0.13)
80 % Slag	12.95 (0.24)	12.37 (0.28)	11.98 (0.25)	12.09 (0.34)

As seen in Table 5.14: no trend for the change of the air porosity was observed for the 60 % and 80 % slag concretes. For the concretes produced with portland cement and 40 % slag, however, in general, air porosity decreased with age which is the expected result.

Table 5.14: Effect of slag on the air porosity of concretes

Mixture	Air porosity, % (σ)			
	7 days	14 days	28 days	90 days
100 % OPC	1.70 (0.09)	1.47 (0.06)	1.64 (0.05)	1.36 (0.12)
40 % Slag	1.80 (0.17)	1.89 (0.14)	1.66 (0.12)	1.62 (0.16)
60 % Slag	0.94 (0.03)	1.75 (0.09)	1.61 (0.07)	1.70 (0.08)
80 % Slag	1.13 (0.12)	1.45 (0.06)	1.09 (0.27)	1.25 (0.02)

Frost protection coefficients of the concretes are presented in Table 5.15. Because there is an important scatter between the results of different ages and the values obtained do not reflect a trend, more data is needed to clarify the effect of slag on the frost protection coefficient of concrete.

Table 5.15: Effect of slag on the frost protection coefficient of concretes

Mixture	PF Coefficient, % (σ)			
	7 days	14 days	28 days	90 days
100 % OPC	12.05 (0.43)	11.01 (0.58)	12.15 (0.36)	10.73 (0.80)
40 % Slag	13.15 (1.01)	14.44 (1.01)	13.32 (0.52)	13.46 (0.26)
60 % Slag	8.77 (0.71)	14.47 (0.22)	13.87 (0.42)	14.40 (0.38)
80 % Slag	7.65 (0.32)	10.58 (0,22)	8.36 (0.5)	9.30 (0.11)

5.7. Temperature Development in Concrete

5.7.1. Effect of Blast Furnace Slag

Figure 5.30 shows the effect of slag replacement on the temperature development of concrete. Peak temperature in the reference portland cement concrete was 58.54^{o}C and it took 19.8 hours to reach this temperature. With the partial replacement of portland cement by slag, peak temperature generated in the concrete decreased substantially. In addition, the time to reach the peak temperatures increased significantly in the slag concretes. Table 5.16 summarizes the temperature measurements in the slag concretes.

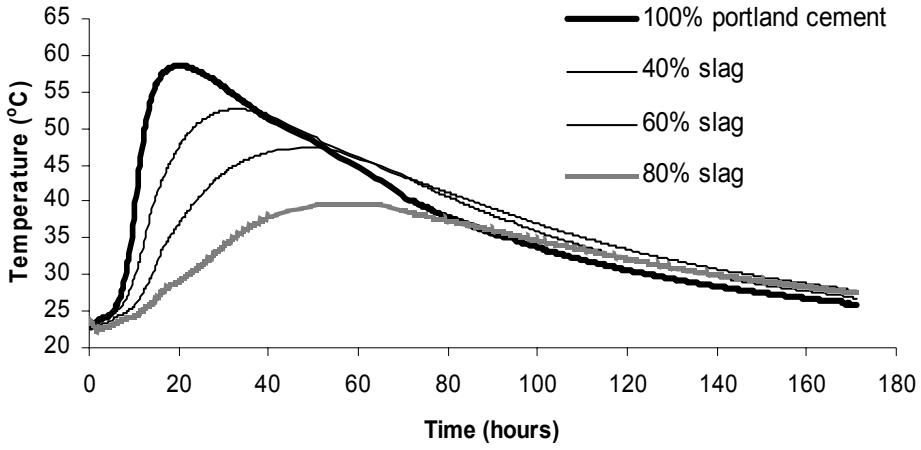

Figure 5.30: Effect of slag replacement on the temperature development of concrete

These results clearly demonstrate that, when compared to portland cement concretes, concretes containing high volumes of blast furnace slag can perform much better in mass concrete elements such as dams or foundations and also in concretes with high cement contents. The temperatures generated in the cores of such structures as a result of heat of hydration can be decreased significantly by using high volume blast furnace slag. The differences in temperature between the core and surface can be reduced, thus the risk of cracking can be minimized.

Table 5.16: Results of the temperature measurements in the slag concretes

Mixture	Peak temperature in concrete (^{o}C)	Time to reach the peak temperature (hours)
100 % OPC	58.54	19.8
60 % OPC + 40 % Slag	52.64	33.5
40 % OPC + 60 % Slag	47.35	44.8
20 % OPC + 80 % Slag	39.70	53.8

5.7.2. Effect of Silica Fume and Fly Ash Cement

As shown in Figure 5.31 and Table 5.17, replacing portland cement by fly ash cement did not have a beneficial effect in reducing the temperature rise. The fly ash cement used had a higher fineness (Blaine surface area=420 kg/m^2) than the fineness of the ordinary portland cement concrete. Although the fly ash cement contains 18% fly ash, the higher fineness of this cement can be a possible reason for the high temperature generated. Compared to portland cement concrete, the time to reach the peak temperature decreased for the fly ash cement concrete.

As a result of partially replacing portland cement by 5% and 10% silica fume, the peak temperature in concrete increased slightly. These rises can be attributed to the high reactivity of silica fume and the rapid pozzolanic reaction.

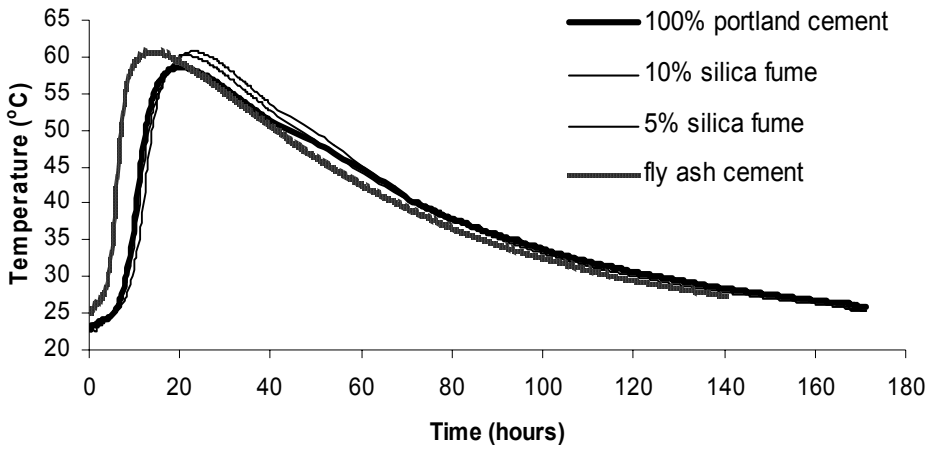

Figure 5.31: Effect of silica fume and fly ash cement on the temperature development of concrete

Table 5.17: Results of the temperature measurements in the silica fume and fly ash cement concretes

Mixture	Peak temperature in concrete (^{o}C)	Time to reach the peak temperature (hours)
100 % OPC	58.54	19.8
95%OPC + 5 % silica fume	60.75	23.0
90%OPC + 10 % silica fume	60.18	21.5
100 % Fly ash cement	60.61	14.0

5.8. Effect of Slag on Chloride Binding

The effect of slag replacement on the chloride binding of pastes is presented in Figure 5.32. As explained in detail in Chapter 3.6.7, a chloride solution with known concentration was mixed with powder cement paste, then filtered and the chloride concentration of the solution was determined. Thus a decrease in the chloride concentration represents the increased chloride binding.

As seen in the figure, chloride content decreases with age which shows the increased chloride binding property of the pastes. The results for the portland cement mixture and the mixtures with 40% and 60% slag are very close to each other and lowest chloride binding was obtained for the mixture with 40% slag. As seen in the figure, the paste containing 20% OPC + 80% slag had the highest chloride binding. Based

on the results shown in the figure, for the 40% and 60% slag replacements, it seems that the slag is not effective in binding the chlorides as expected. Previous studies (Dhir et al., 1996b; Luo et al., 2003), however, show that chloride binding of mixtures containing blast furnace slag is significantly higher when compared to portland cement and the binding increases with the slag amount.

Possible reason for these conflicting results between this study and literature, may be the procedure used. For all the mixtures and ages, powdered pastes dispersed in the NaCl solution were filtered after 20 hours. This 20 hour period may not be enough for different compositions for the equilibrium between the external solution (NaCl solution) and the pore solution of the sample. Most of the results given in the literature, however, are based on longer durations of paste – chloride solution mixing. More data is needed to clarify these results.

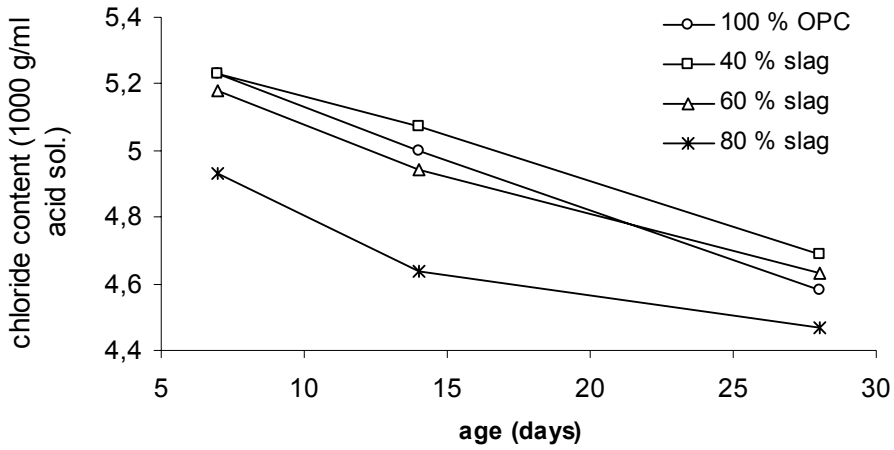

Figure 5.32: Effect of slag on the chloride binding

6. OPTIMIZATION OF CONCRETE

6.1. General

Concrete mixture optimizations carried out on two concrete series are presented in this chapter. Two different types of optimizations were performed. The first method is based on optimizing only one response. The second method of optimization, however, is based on optimizing several responses simultaneously.

6.2. Optimization Based on One Response

The optimization method which is based on only the compressive strength was carried out only on high volume fly ash concretes and mortars. The strength development of the fly ash concretes are given in Chapter 4.3.1 and those of fly ash mortars in Chapter 4.3.3.

In order to optimize the fly ash content, a mathematical model between the variables and the responses must be established. By the analysis of the mixture data and test results, a mathematical model can be fitted.

The variables for this optimization were taken as the fly ash replacement percentage and the age of the specimen. The response is the compressive strength. The optimization process was carried out to maximize the compressive strengths.

A mathematical model based on the fly ash replacement amount (ø) and curing time (t) for 3-28 days period has been proposed (Fisang et al. 1995). The model, however, was not appropriate for 3-365 days curing period and it was modified by using the logarithm of the curing time (log t) instead of curing time (t) (Paya et al. 1997). This modified model given in Equation 6.1 was used in this study;

$$R = \beta_1 + \beta_2\phi + \beta_3(\log_{10} t) + \beta_4\phi(\log_{10} t) + \beta_5\phi^2 + \beta_6(\log_{10} t)^2 + \beta_7\phi^2(\log_{10} t) + \beta_8\phi(\log_{10} t)^2 \quad \textbf{(6.1)}$$

where R is the compressive strengths of concretes and mortars obtained from the tests, ø is the fly ash replacement percentage ranging from 0 % to 70 % in steps of 10 % and t is the curing time. The curing times for concretes were between 28 to 365 days, and 2 to 365 days for the mortars.

The compressive strengths of the fly ash concretes are given in Table 4.2 and those of fly ash mortars in Table 4.3. For each curing age, the replacement amount and the resulting compressive strengths were placed in equation 6.1 and equations were obtained with unknown coefficients. These coefficients were then calculated by regression analysis.

Table 6.1: Coefficients of the mathematical model 6.1

Coefficient	Concrete	Mortar
β_1	57.2937	36.8649
β_2	-1.0585	-0.7662
β_3	1.0950	50.2605
β_4	0.7104	0.5324
β_5	0.0071	0.0021
β_6	8.6747	-6.9158
β_7	-0.0103	-0.0097
β_8	0.0008	0.0685
Standard Deviation, σ	6.21	4.39

The calculated coefficients of the Equation 6.1 are given in Table 6.1. By using these coefficients for the Equation 6.1, and maximizing the equation, optimum values of fly ash percentage were obtained for maximum compressive strength. The optimization results for concretes and mortars and for different curing times are given in Table 6.2 and 6.3.

As shown in Tables 6.2 and 6.3, the optimum fly ash content for obtaining the highest compressive strength increases with curing time. The effect of fly ash on the

early age strength development is not significant. The optimum fly ash content of concrete for the maximum compressive strength is 0 % for 28 days but it increases up to 20.1 % for 365 days. Similar results were also obtained for the mortar specimens. When Table 6.2 and Table 6.3 are compared, it appears that, after 28 days, for a given curing time, the optimum fly ash quantities for mortars are higher than for concretes. This result may be due to the higher binder content in mortars.

Table 6.2: Optimum replacement values of fly ash for concretes

Curing time, days	Optimum fly ash replacement percentage for concrete
28	0
56	8.6
120	14.9
365	20.1

Table 6.3: Optimum replacement values of fly ash for mortars

Curing time, days	Optimum fly ash replacement percentage for mortar
2	0
7	0
28	6.2
56	12.5
120	17.6
365	23.0

6.3. Multi-criteria Optimization Based on Several Responses

The method presented in Chapter 6.2 is based on only one response but optimization usually involves considering several responses simultaneously. For optimizing several responses, multi criteria optimization techniques can be carried out and different methods can be used (Brandt and Marks, 1993; 1996). A useful approach for the optimization of multiple responses simultaneously is to use desirability functions which reflect the levels of each response in terms of minimum and maximum desirability.

A desirability function (d_j) varies over the range of $0 \le d_j \le 1$ (Bayramov et al., 2004). In case of maximizing and minimizing the individual responses, d_i is defined by Equation 6.2 and Equation 6.3, respectively (Myers and Montgomery, 2002).

$$d_j = \begin{cases} 0 & Y_j \le \min f_i \\ \left[\dfrac{Y_j - \min f_j}{\max f_j - \min f_j}\right]^t & ve \quad 0 < d_j < 1 \;, \quad \min f_i < Y_j < maks\, f_i \\ 1 & Y_j \ge maks\, f_i \end{cases} \tag{6.2}$$

$$d_j = \begin{cases} 1 & Y_j \le \min f_i \\ \left[\dfrac{maks\, f_j - Y_j}{\max f_j - \min f_j}\right]^t & ve \quad 0 < d_j < 1 \;, \quad \min f_i < Y_j < maks\, f_i \\ 0 & Y_j \ge maks\, f_i \end{cases} \tag{6.3}$$

where; d_j, Y_j, min f_j and max f_j are the desirability function, the current, the lowest and the highest values of the *jth* response included in the optimization, respectively. The power value *t* is a weighting factor of the *jth* response.

By using an overall desirability function (D) given in Eq.(6.4), which is the geometric mean of the individual desirability functions (d_j), the multi-objective optimisation problem was solved. D takes values between 0 and 1. The maximum value of D gives the optimum solution (the most desirable mixture) (Cornell, 2002).

$$D = (d_1 \times d_2 \times d_3 \times \ldots \times d_m)^{\frac{1}{m}} \tag{6.4}$$

where m is the number of the responses.

For a durable concrete mixture, rapid chloride permeability must be minimized whereas concrete compressive strength should be maximized. For a cost effective project, the cost must be minimized to get an economical mixture.

6.3.1. Fly Ash Concretes

The mixture compositions of the fly ash concretes are given in Table 3.5, compressive strengths in Table 4.2 and the results of the rapid chloride ion permeability test in Table 5.2.

A very simple approach was used in order to compare the cost of concrete mixtures. Assuming that the aggregate, water and admixture amounts were the same for all the mixtures, only the cement and fly ash were taken into account in the calculation of the cost of concretes. Cost analysis showed that the ground fly ash costs nearly the half of the cement. Thus, the price of one kg cement was taken as a unit, where that of the ground fly ash was 0.5 unit. Based on these assumptions, the relative cost of the concrete mixtures according to the amounts of cement and fly ash are given in Table 6.4.

Table 6.4: Relative initial cost of the fly ash concretes

Mix Code	Relative cost of the fly ash concretes (unit)
NC 00	472.0
FC 10	447.5
FC 20	422.0
FC 30	400.5
FC 40	377.5
FC 50	355.5
FC 60	331.0
FC 70	307.0

For each mixture, the individual desirability functions for the compressive strength were calculated by Equation 6.2, and that of the rapid chloride permeability and the cost were calculated by using Equation 6.3. The responses in the optimization were considered to be of equal importance (t=1). The overall desirability function was calculated by using Equation 6.4 and given in Table 6.5.

As seen in Table 6.5 and Figure 6.1, the desirability functions were different for individual responses. The individual desirability function for compressive strength (d_1) had the highest value at the 10 % replacement level. At 30% fly ash replacement level, the individual desirability function for rapid chloride permeability (d_2) had the maximum value. The individual desirability function for cost (d_3) was 1.00 for 70 % replacement.

Based on the highest overall desirability function (D), it can be concluded that the optimum ground fly replacement level is 40 %, which maximizes the compressive strength and minimizes the rapid chloride permeability and the cost.

Table 6.5: Individual and overall desirability functions for fly ash concretes

Mix Code	Desirability function for compressive strength (d_1)	Desirability function for rapid chloride permeability (d_2)	Desirability function for cost (d_3)	Overall desirability function (D)
NC 00	0.76	0.00	0.00	0.000
FC 10	1.00	0.77	0.15	0.485
FC 20	0.95	0.84	0.30	0.622
FC 30	0.94	0.99	0.43	0.739
FC 40	0.74	0.98	0.57	**0.747**
FC 50	0.58	0.97	0.71	0.738
FC 60	0.31	0.97	0.85	0.633
FC 70	0.00	1.00	1.00	0.000

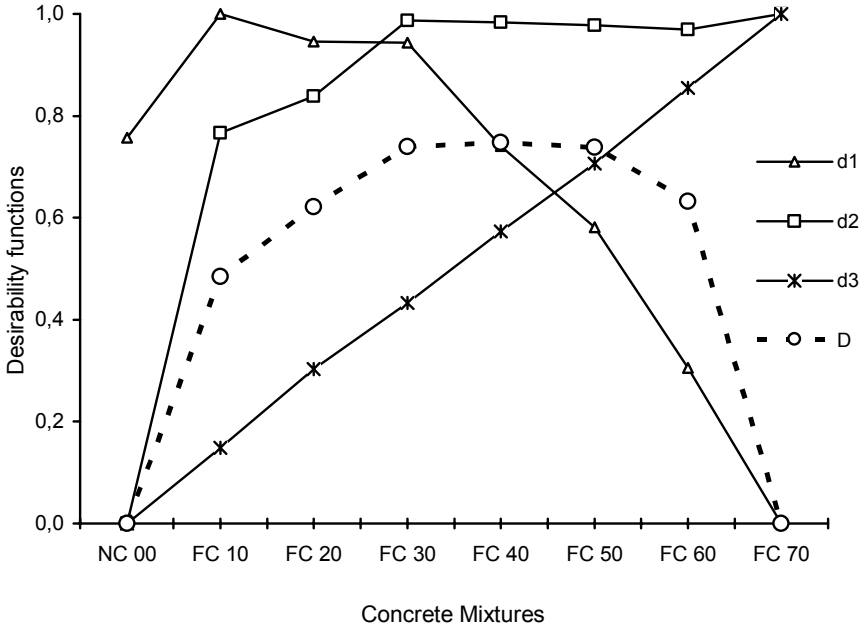

Figure 6.1: Individual and overall desirability functions for concretes

6.3.2. Slag and Fly Ash Concretes

The same simple approach used to compare the cost of the fly concretes in Chapter 6.3.1 was also used for the slag and fly ash concretes. Assuming that the aggregate, water and admixture amounts were the same for all the mixtures, only the cement, fly ash and slag were taken into account in the calculation of the cost of concretes. Cost analysis showed that the ground fly ash costs nearly the half of the cement and finely ground blast furnace slag has a cost of about 63 % of the cement cost. Thus, the price of one kg cement was taken as a unit, where that of the ground fly ash was 0.50 units and the finely ground blast furnace slag as 0.63 units. Based on these assumptions, the relative costs of the concrete mixtures calculated according to the amounts of cement, fly ash and slag are presented in Table 6.6.

Table 6.6: Relative cost of the fly ash and slag concretes

Water/binder	Mixture Code	Relative costs of concretes
0.60	100PC-60	348.0
	50S-60	285.3
	50F-60	264.0
	25FS-60	275.4
0.38	100PC-38	450.0
	50S-38	361.9
	50F-38	331.5
	25FS-38	347.4

The compressive strengths and chloride ion permeability at 28 and 90 days ages, and the costs were included in the optimization process. The individual desirability functions for compressive strengths at 28 and 90 days are d_1 and d_2, respectively. The d_3 and d_4 represents the 28 and 90 days desirability functions for chloride ion permeability and d_5 shows the function for the relative costs of the concretes. For each mixture, the individual desirability functions for the compressive strengths (d_1 and d_2) were calculated by Equation 6.2, and those of the rapid chloride permeability and the cost (d_3, d_4 and d_5) were calculated by using Equation. 6.3. The responses in the optimization were considered to be of equal importance (t=1). The overall desirability function was calculated by using Equation. 6.4 and given in Table 6.7.

As seen in Table 6.7, the highest overall desirability value (D) belongs to the slag concretes for both water/binder ratios. The overall desirability is obtained based on the individual desirability functions and lower individual desirability values results in a lower overall desirability value.

Table 6.7: Individual and overall desirability functions of fly ash and slag concretes

Mix Code	Desirability functions for compressive strength		Desirability functions for rapid chloride permeability		Desirability function for relative cost (d_5)	Overall desirability function (D)
	28 days (d_1)	90 days (d_2)	28 days (d_3)	90 days (d_4)		
100PC-60	1.000	1.000	0.000	0.000	0,000	0.000
50S-60	0.795	0.845	0.993	0.960	0,747	**0.759**
50F-60	0.000	0.000	0.957	1.000	1,000	0.000
25FS-60	0.405	0.556	1.000	0.960	0,864	0.683
100PC-38	0.772	1.000	0.000	0.000	0,000	0.000
50S-38	1.000	0.950	0.995	0.962	0,744	**0.827**
50F-38	0.000	0.000	0.903	1.000	1,000	0.000
25FS-38	0.602	0.600	1.000	0.955	0,866	0.754

As seen in Table 6.7, the desirability values for the chloride permeability of portland cement concretes are zero because of having the highest chloride permeability. For the fly ash concretes, the desirability values for the compressive strengths are also zero due to the lowest strengths in the test series. Because the overall desirability is based on the geometric mean of individual desirabilities, the zero values of the individual functions causes the overall value to become zero. The slag concretes have relatively high strength and low chloride permeability, and as a result, the overall desirability function is higher.

7. DURABILITY OF CONCRETE STRUCTURES IN CHLORIDE CONTAINING ENVIRONMENT

7.1. General

Durability of concrete can be defined as the concrete's ability to withstand deteriorating effects which may be physical, chemical, physico-chemical or biological. Most of these processes involve the ingress of aggressive substances, which may either cause degradation of the concrete itself or degradation of the embedded steel. In this chapter, the transport mechanisms in concrete are briefly summarized. Degradation processes and in particular chloride penetration and corrosion of the embedded steel in concrete, are presented. Different approaches for obtaining more durable concrete structures in chloride containing environments are discussed.

Poor durability of materials and uncontrolled and short service life of structures is one of the main problems designers, engineers and owners facing. As summarized in Chapter 7.3, there are numerous sources of deterioration processes and in many cases these processes interact with each other and increase the rate of deterioration. All these durability problems cause enormous economical losses.

The economic costs of inadequate and poor durability are those of repair or replacement and maintenance, including the costs of obtaining access to repair zone and the costs of interruption to the service. This interruption to service is especially critical in the case of transportation structures such as bridges and tunnels since the volume of traffic grows exponentially thorough the years (Gerwick, 1994).

In recent decades, the growing demands of road transport have meant a rapid expansion of the road networks in almost every country. Large numbers of bridges were built within a relatively short span of time. Many of these structures have since developed major problems within a few years of construction. In a study in UK, deterioration mainly due to the use of de-icing salts was identified in 144 put of 200 randomly sampled bridges (Baker, 1999). The increase in the maximum weight limit

for trucks from 32.5 tonnes to 40 tonnes is another reason for the deterioration of these bridges. In USA, it is estimated that 40% of the bridges are deficient and need repair or strengthening.

In UK, £2.2 billion is going to be spent until 2006 for repair and strengthening of highway bridges and also some other structures on the roads such as retaining walls (Baker, 1999). It has been estimated that in 1988 the value of building and civil engineering repairs and maintenance carried out in UK was about £15 billion (Mays, 1992). It is reported that this cost has increased to more than £26 billion for 2001 (Swamy, 2001). A recent report shows that the annual direct cost of corrosion repair or replacement for highway bridges in USA is about $8.3 billion (Yunowich et al., 2001). In the same study, the annual corrosion cost of ports and waterways in the country is estimated at $182 million (Yunowich and Mierzwa, 2001). The study concluded that the annual direct cost of corrosion in USA, for infrastructure including highway bridges, waterways, airports and railroads, is about $22.6 billion. It is estimated that the structural damage repair in Europe costs 1.4 billion Euros annually (Swamy, 2001).

Despite all these economic losses due to short service life, main concern of many structural engineers and designers is the structural strength of the structure. Design process is based on the achievement of durability through strength.

As discussed in Chapter 7.3, the degradation rates of structures are based on the quality of the concrete and the exposure conditions.

7.2. Transport Mechanisms in Concrete

7.2.1. Diffusion

Diffusion is the transport of ions due to a concentration difference when at least one face is continuously exposed to a solution (Boddy et al., 1999). Diffusion occurs in saturated concrete where there is no water movement inside. Transport of chloride ions into submerged concrete is an example of the diffusion process. Diffusion of ions in a solution in one dimension can be expressed by the Fick's first law of diffusion (Atkins, 1990; Crank, 1993) and given as;

$$F = -D\frac{\partial c}{\partial x} \tag{7.1}$$

where F: flow of ions [kg/(m^{2}s)]

D: diffusion coefficient (m^2/s)

c: concentration (g/m^3)

x: distance (m)

Fick's first law can be used for obtaining the steady – state diffusion coefficient. If the concentration gradient at any point of the diffusion medium is constant, the diffusion is referred as steady – state diffusion (Tiewei, 1997). Diffusion coefficient, D, is assumed to be constant in Equation 7.1. This expression, however, is a simplification and does not always reflect the actual situation. In most cases, the concentration of the diffusing substance at any point in the medium is time dependent; it increases with the diffusion process (Tiewei, 1997). Figure 7.1 shows the concentration profiles of the steady and non-steady diffusion in concrete (Andrade, 1993).

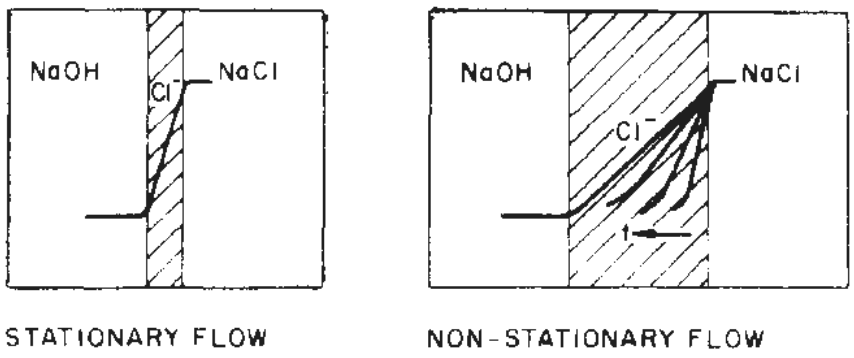

Figure 7.1: Steady and non-steady flow in function of the specimen thickness and time of testing

For the non-steady state diffusion where conditions change with time and chloride flow is not constant, Fick's second law of diffusion (Atkins, 1990; Crank, 1993) is applicable;

$$\frac{dc(x,t)}{dt} = D\frac{d^2c(x,t)}{dx^2} \tag{7.2}$$

The diffusion coefficient is a material characteristic describing the transfer ability of a given substance but the value obtained from steady – state diffusion is different from the one from non-steady state.

The diffusion coefficient of concrete partly depends on the physical permeability and partly on the chemistry of the pore water system. The degree of water saturation or the moisture conditions in the concrete is also very important, and so are the temperature conditions in the transport system.

7.2.2. Migration

Diffusion is a very slow process and diffusion tests need long testing periods. Therefore, different test methods have been developed based on the migration testing of chloride ions in concrete (Tiewei, 1997; Andrade, 1993). Migration is the transport of ions as a result of an externally applied electrical field. Such a transport of chloride ions by an electrical field is also used for removing chloride ions from concrete for repair and protection purposes. Figure 7.2 shows the processes occurring when an electrical field is applied in a migration test cell (Andrade, 1993).

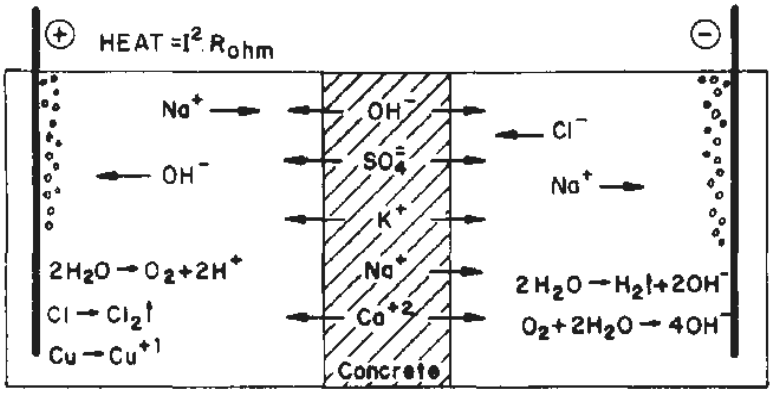

Figure 7.2: Processes occurring during migration testing

As a result of the electrical field, positive ions move towards negative electrode and negative ions towards positive electrode. The amount of the electrical potential applied and the concentration of the ions are important factors affecting the migration of ions into concrete. In a migration test, due to a concentration gradient, diffusion also takes place but this process can be ignored because of the high electrical fields generally used.

7.2.3. Permeation

Permeation is the liquid or gas flow under a pressure gradient. Water is the most common and important liquid penetrating into concrete. Ions can also be carried into the concrete with this flow which is more rapid when compared to diffusion.

The permeability coefficient is the material characteristic describing the permeation of fluids through a porous material due to a pressure head (Kropp et al., 1995). Darcy's law can be used for characterizing the permeability. Different tests are presented in the relevant standards for gas and water permeability.

7.2.4. Convection

Convection, also known as advection, is the movement of ions with a saturated water flow under a pressure gradient. In most applications diffusion and convection processes are combined in different ways (Hetek, 1996). The ingress of chloride ions into concrete at tidal, wave and splash zones are dominated by convection and diffusion.

7.2.5. Capillarity

Capillary suction is the transport of liquids into porous solids due to surface tension acting in capillaries. Capillary action is affected by the characteristics of both the liquid and the porous medium. Capillary suction occurs in non – saturated concretes.

Chloride ions are also sucked into concrete if it is exposed to a salt water solution. This is the fastest transport of chloride ions into concrete.

Capillarity can be characterized by the capillarity coefficient obtained from a sorptivity test. A surface of a dry concrete sample is placed in contact with water and the amount of water absorbed is measured at different intervals.

7.3. Degradation Processes of Concrete Structures

The degradation processes of concrete structures can be classified based on the cause of the deterioration; mechanical, physical, chemical, physico – chemical and biological (ACI Committee 201, 1992). A schematic representation of possible deterioration processes on a column in a marine environment is illustrated in Figure 7.3 (Mehta, 1991).

Mechanical deteriorations are a result of mechanical overloading or settlement. The loading conditions on the structure may be more than expected or the structure may be under-designed. If the structure was not designed for cyclic loading or impact loading, cracking can occur. Cracking due to mechanical loading can speed up the ingress of aggressive substances into concrete. The only solution for preventing

cracking due to loading is the realistic analyses of the loading conditions and design the structure accordingly.

Another mechanical deterioration cause of structures is abrasion. It is the loss of mass from concrete surface due to surface wear. The amount of the loss depends on the type of substances causing wear, surface conditions of the concrete and environmental conditions. Depending on the cause, there are different types of wear; i) abrasion, ii) erosion, iii) cavitation (Mehta and Monterio, 1993). Abrasion is the surface wear as a result of physical attrition of concrete. Pavements and industrial floors are exposed to abrasion caused by the traffic over them. Parts of the harbour structures and bridges exposed to wave action and drifting ice also deteriorates as a result of the abrasion. Erosion, the second type of surface wear, is the action of fluids containing solid particles in suspension (ACI Committee 210, 1998). Erosion takes place in hydraulic structures such as spillways of dams. Cavitation also occurs in hydraulic structures which is the formation and collapse of vapour bubbles in rapid flowing water. Surface conditions and the quality of the concrete are important parameters for obtaining high abrasion resistance (Sengul et al., 2003a).

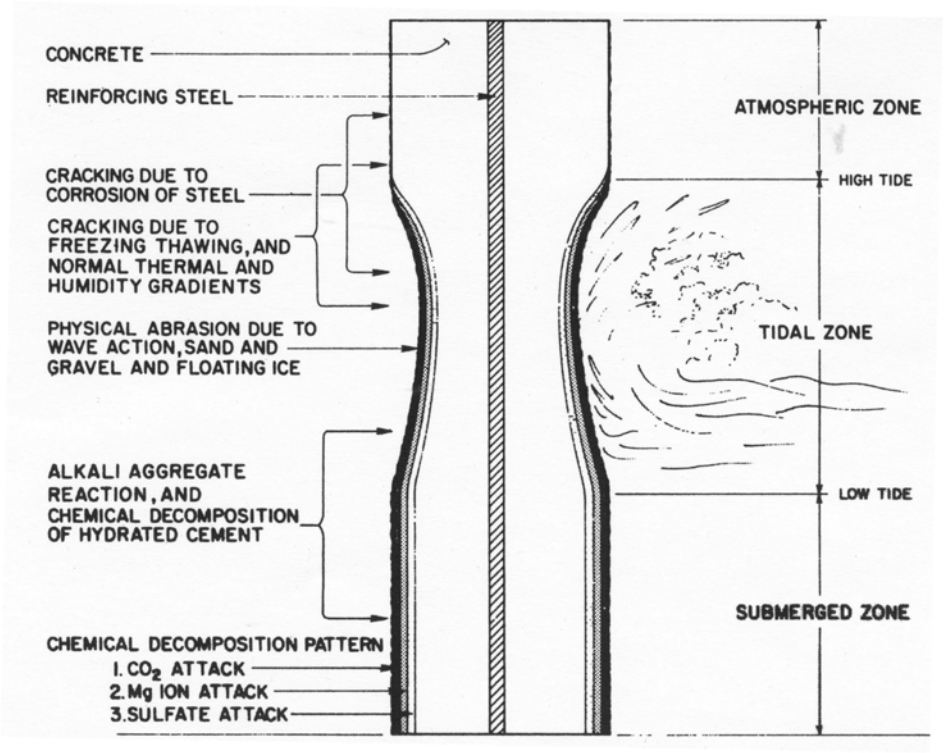

Figure 7.3: Representation of deterioration mechanisms on a column exposed to sea

Freeze – thaw cycles can cause physical deterioration in concrete. This process can result in severe deterioration especially at the early ages of concrete (ACI Committee 306, 1997). Volume of water increases about 9 % when freezing. When the water in the capillary pores freezes and there is not enough space in the pores where this excess volume can expand, internal pressure is exerted on the pore walls. Continuous freeze – thaw cycles cause cracking, spalling and surface scaling. Quality of the concrete, air – void system and saturation degree are important parameters affecting the frost resistance of concrete (Sengul et al., 2003b).

There are different forms of chemical deterioration processes which can cause cracking, volume expansion, loss of alkalinity or loss of strength.

Sulphate attack is one of these processes causing expansion in concrete which leads to cracking. Sulphate reacts with both $Ca(OH)_2$ and the hydrated C_3A which leads to formation gypsum and ettringite, respectively. The ettringite causes the volume instability of the concrete. Primary sources of the sulphate are natural sulphates of calcium, magnesium, sodium, and potassium present in soils or dissolved in ground water. Concrete quality and the environmental conditions are important against the sulphate attack in concrete (Skalny et al., 2001). Blast furnace slag cements or portland cements with low C_3A amounts or high amounts of pozzolans are effective in preventing the sulphate attack.

Alkali – aggregate reaction is another chemical degradation process causing cracking in concrete (Swamy, 1992). Alkali ions from portland cement can react with certain siliceous minerals in aggregate which can cause cracking. This reaction is not harmful for low moisture contents in the concrete. Alkali – reactivity of the aggregates, alkali content of the cement, availability of water and temperature are important parameters affecting the deterioration due to alkali – aggregate reaction (ACI Committee 221, 1998). The easiest way to prevent this reaction is to avoid using the reactive aggregates in concrete. If this is not possible or economically feasible, mineral admixtures such ash fly ash, slag or silica fume can be used to reduce the effective alkali content in concrete. Low alkali cements are also another option for solving the problem.

Acid attack can also cause degradation on concrete. Because concrete is an alkaline medium, hydration products can decompose and leach out or deteriorate as a result of

the acid attack. The source of acid may be acidic rains, acidic ground water or acidic solutions from industrial plants. Acidic rain consists of sulphuric acid and nitric acid and a pH value of 4 to 4.5 and pH value as low as 1.7 has been recorded (Mehta and Monterio, 1993). Blended cements with pozzolans reduce the ingress of aggressive substances into concrete. $Ca(OH)_2$ is the most vulnerable hydration product for the acid attack and pozzolanic reaction has a beneficial effect by reducing the $Ca(OH)_2$ amount in concrete (Neville, 2004).

Organic or mineral acids, such as nitric acid, formed by the biochemical process can also cause deterioration in concrete. The reason for these rare biological effects may be due to bacteria, fungi or insects. Keeping the concrete clean and using anti – bacterial admixtures can solve the problem (Mailvaganam, 1995).

Other mechanisms such as leaching, thermal effects or unexpected events such as fire are also important affecting the durability of structure.

7.4. Corrosion of Steel in Concrete

Concrete, with its high pH value, is a very good medium for protecting the embedded steel in concrete against corrosion. As a result of the hydration of portland cement, $Ca(OH)_2$ is produced, which in addition to smaller amounts of KOH and NaOH are responsible for the high alkalinity of the concrete. A thin passivation layer of iron oxide is formed around the steel that gives protection against corrosion. This protection continues as long as the high pH is maintained. However, carbonation or chlorides can penetrate the oxide film, both causing reduction in the alkalinity and the steel corrosion. The time period until start of corrosion is called the initiation phase is shown in Figure 7.4 (Tuutti, 1982).

7.4.1. Carbonation

The hydration product calcium hydroxide can react with carbon dioxide and form calcium carbonate. This reaction is called carbonation and shown in equation 7.3.

$$CO_2 + Ca(OH)_2 \rightarrow Ca(CO)_3 + H_2O \qquad (7.3)$$

Carbonation causes the alkalinity of concrete to reduce down to a pH value of about 9 (Neville, 2004). The passivation layer protecting the steel is destroyed when the carbonation front reaches the steel.

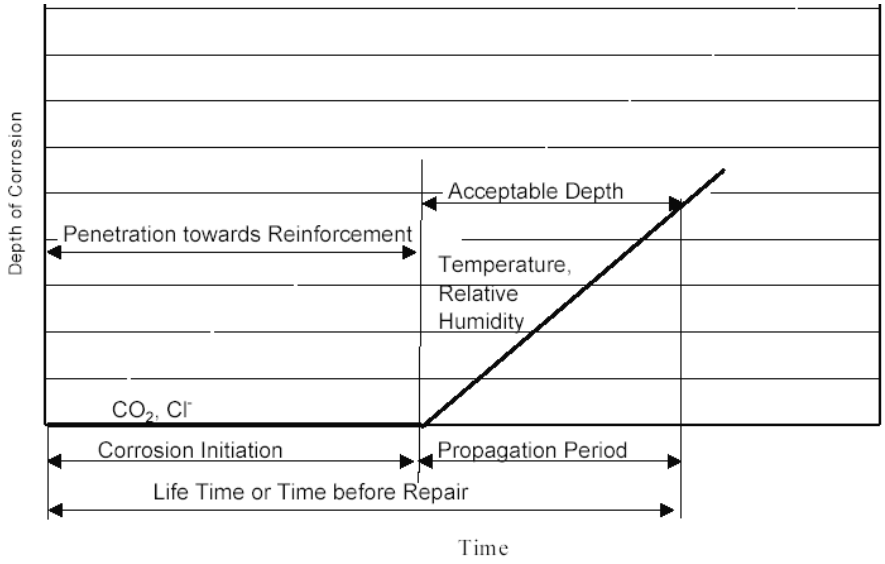

Figure 7.4: Initiation and propagation periods for corrosion in a structure

The ingress of carbon dioxide at normal atmospheric concentrations into concrete is a diffusion mechanism which is caused by the concentration difference. Water is essential for the carbonation process. Without water, carbon dioxide remains in gaseous form and does not react with the hydrated cement. On the other hand, the diffusion of carbon dioxide is slower if the pores of concrete are filled with water. The carbonated concrete layer has less permeability and higher hardness due to the calcium carbonate formed. As the carbonation proceeds, the carbon dioxide has to diffuse through this less permeable carbonated layer which slows down the process. The rate of carbonation is expressed as;

$$D = Kt^{0.5} \tag{7.4}$$

where: D: depth of carbonation (mm),

K: coefficient of carbonation (mm/year^2),

t: time (year).

Factors related to the concrete such as gas permeability, temperature and moisture content are important parameters controlling the carbonation rate of concrete.

Corrosion induced by carbonation can take place on the whole surface of the steel in contact with the carbonated concrete. This type of corrosion is described as general corrosion (Bertolini et al., 2004).

7.4.2. Chloride Penetration

Although carbonation induced corrosion is an important problem, it is the chloride induced corrosion which is threatening the durability of most concrete structures and in chloride containing environments. When the chloride ions reach the steel reinforcement, corrosion starts. Corrosion due to chlorides is localized, with penetrating attacks of limited area surrounded by non – corroded areas. This type of corrosion is called pitting corrosion.

7.4.2.1. Source of Chlorides

There are different sources for the chloride attack. The chlorides may be present in the concrete mix as part of the constituent materials or salt deposits on the reinforcements. The maximum permissible values of chloride concentrations of cements, aggregates, admixtures, mixing and curing waters are given in the related standards and specifications. Most of the sand used in Istanbul is obtained from the sea and after the 1999 Marmara earthquake in Turkey, there have been many discussions in the country about the use of fine aggregate dredged from the sea bottom.

Concrete in marine structures is exposed to sea water which is the main source of the chloride attack. The transport of the chlorides into concrete may vary depending on the location and different mechanism can act together. In submerged parts of the structure, diffusion is the main chloride transport mechanism. In the other parts of the structure, where wetting and drying takes place, capillary absorption will also contribute to the chloride ingress

Even the structures far away from the coast may be exposed to air – borne chlorides from the sea water. These air-borne droplets of sea water can be carried several kilometers by wind, depending on the wind conditions and topography.

Another source of the chlorides is de-icing salts. Bridges and roads may be exposed to calcium chloride once a day during the snow season. Chloride solution formed by such salt can also affect other structures nearby because the salt solution can be carried by splash caused by the traffic and wind.

7.4.2.2. Chloride Profiles in Concrete

The general method for determining the chloride penetration in an existing concrete structure is to take out cores, grinding out dust samples from the cores and to carry out chemical analyses on these dust samples. The results of such analyses provide a basis for the chloride profiles. A schematic representation of a theoretical chloride profile in concrete is shown in Figure 7.5.

The content of chlorides is largest at the exposed surface and the content decreases with increasing depth. As seen in figure 7.5, the slope of the profile is smaller and smaller at larger depths. At large depths, the concentration does not decrease down to zero because a certain amount of chlorides may be present. That is the initial chloride content in the concrete which was mixed into the concrete.

The chloride concentration at a certain depth depends on the concrete quality and exposure conditions. Chlorides in concrete are present as free chlorides or bound chlorides. Free chlorides are "free" in the pore solution while the bound chlorides are bound to the constituents and to the pore walls in the concrete. Normally, chloride profiles show the total amount of chlorides. The concentration of free chlorides in the pores of the concrete surface is usually assumed to be equal to the concentration of chlorides in the surrounding environment, i.e. the sea water (Hetek, 1996). The amount of bound chlorides is related to the concentration of free chlorides in the pore liquid.

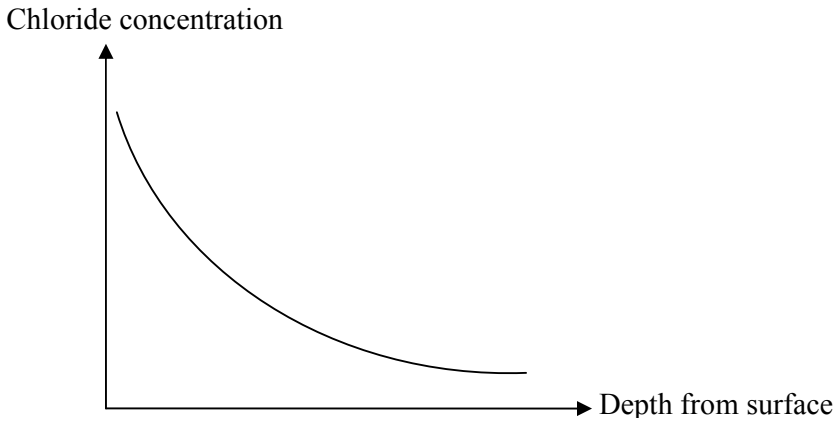

Figure 7.5: Schematic representation of a chloride profile in concrete

The binding of the chloride ions depends on the concrete composition and binder type. For example a concrete with high amounts of blast furnace slag has a higher

chloride binding capacity which affects the chloride profile. Figure 7.6 shows the chloride profiles for two concretes with different chloride binding properties at the same time of exposure.

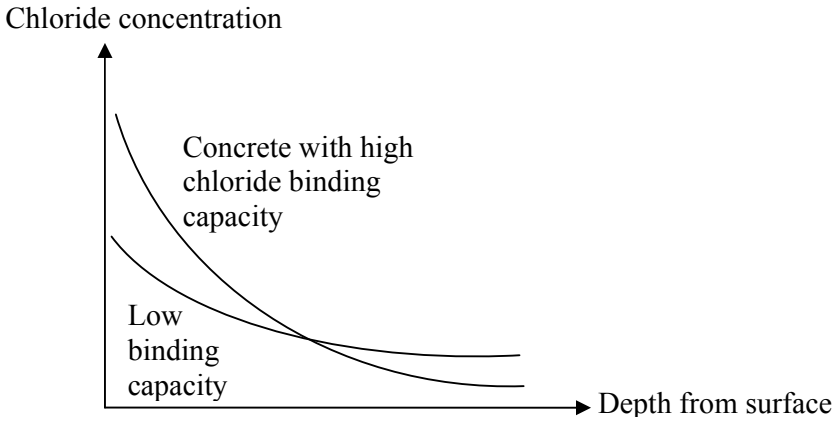

Figure 7.6: Representation of a chloride profiles for different binding capacities

The concrete with a higher binding capacity will have higher total chloride content at the concrete surface, since the amount of bound chlorides is larger. On the other hand, the penetration depth in that concrete will be smaller because more of the chlorides that penetrate are bound, which will delay the penetration.

The chloride profiles obtained from existing structures are different from the ideal curves shown in Figures 7.5 or 7.6. A typical chloride profile obtained from a structure exposed to sea water is shown in Figure 7.7.

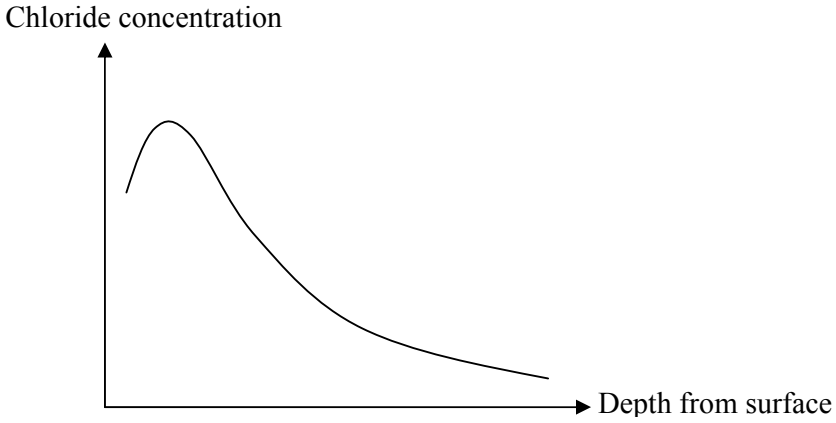

Figure 7.7: A typical chloride profile for an existing structure

There may be several reasons for the shape of the chloride profile in Figure 7.7. Washing out of the chlorides from the surface near region may be one of the reasons. Another explanation for this profile is carbonation since carbonated concrete has a lower binding capacity.

7.4.3. Mechanism of Corrosion

Corrosion is an electro – chemical process due to an electrical potential difference along the steel. An electro – chemical cell is set up with anodic and cathodic regions. This corrosion cell can be formed when two different metals are embedded in concrete. In most of the cases, however, only one metal is enough to form the cell due to concentration differences of chlorides, oxygen and alkalis, where one region of the steel becomes anodic and the other parts cathodic. These anodic and cathodic regions are connected by the electrolyte in the form of the pore solution in the hydrated cement paste. The positively charged ferrous ions (Fe^{2+}) at the anode pass into solution while the negatively charged free electrons (e-) pass along the steel to the cathode where they are absorbed by the constituents of the electrolyte and combine with water and oxygen to form hydroxyl ions $(OH)^-$. These ions then combine with the ferrous ions to form ferric hydroxide and this is converted by further oxidation to rust (Neville, 1995). A schematic representation of corrosion mechanism of embedded steel in concrete is shown in Figure 7.8 (Neville, 2004).

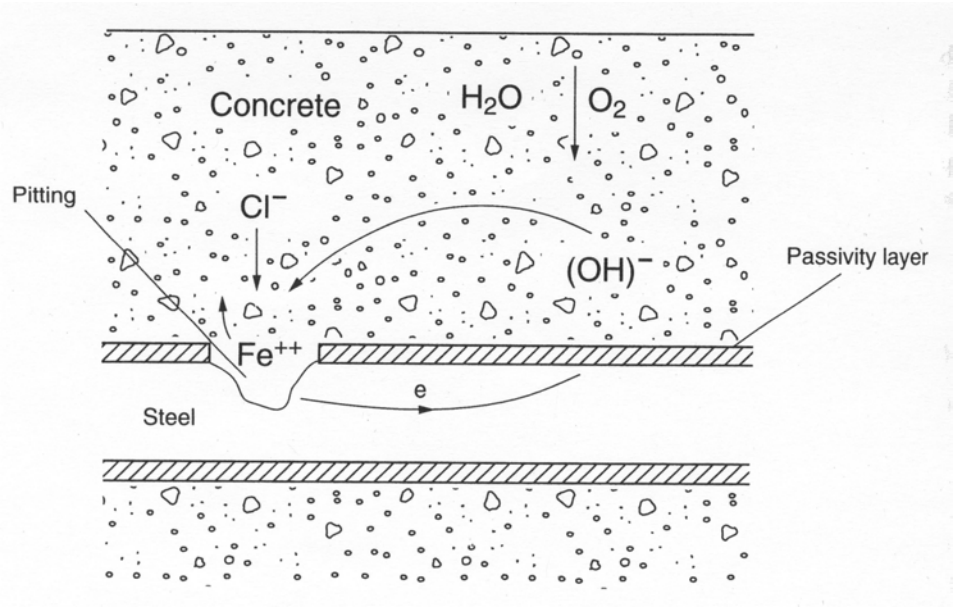

Figure 7.8: Corrosion mechanism of embedded steel in concrete

The corrosion products have a much greater volume than the original steel bar volume. The volume of these products may be up to 6 times more than that of iron. The consequence of this volume increase is the tensile stresses formed within the concrete which generates cracking and spalling of concrete. Cracks parallel to the reinforcement, spalling and delamination of concrete can be formed as shown in Figure 7.9 (Neville, 2004).

As a result of this cracking and spalling the bond strength between the steel and concrete is reduced. Because of these cracks, the ingress of water, oxygen and aggressive substances becomes much easier and faster, which further increases the rate of corrosion.

The corrosion process reduces the cross section area of the reinforcement and in some extreme cases where long exposure periods and low quality concretes are present, even the rupture of the reinforcement can occur. The reduction in cross section of the reinforcement causes decreases in the tensile and fatigue strength which reduces the load carrying capacity of the structural element.

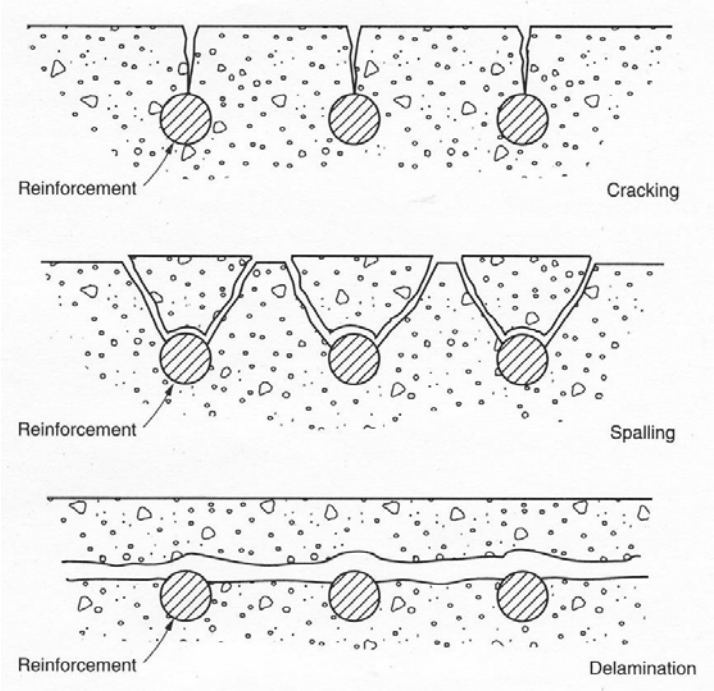

Figure 7.9: Damage caused in concrete cover due to corrosion

7.5. Current Codes and Practice on Concrete Durability

The EN 206 (2000) is in practice both in Europe in which six different exposure classes related to the degradation processes are defined; i) No risk of corrosion, ii) corrosion induced by carbonation, iii) corrosion induced by chlorides other than sea water, iv) corrosion induced by chlorides from sea water, v) freeze – thaw attack, vi) chemical attack. The exposure classes related to the corrosion of the reinforcement are given in Table 7.1.

Table 7.1: Exposure classes related to corrosion presented in EN 206

Class designation	Description of the environment	Informative examples where exposure classes may occur
1 No risk of corrosion or attack		
XS1	For concrete without reinforcement or embedded metal: All exposures except where there is freeze/thaw, abrasion or chemical attack For concrete with reinforcement or embedded metal: Very dry	
2 Corrosion induced by carbonation		
Where concrete containing reinforcement or other embedded metal is exposed to air and exposure, the exposure shall be classified as follows:		
XC1	Dry or permanently wet	Concrete inside buildings with low air humidity Concrete permanently submerged in water
XC2	Wet, rarely dry	Concrete surfaces subject to long-term water contact Many foundations
XC3	Moderate humidity	Concrete inside buildings with high air humidity External concrete sheltered from rain
XC4	Cyclic wet and dry	Concrete surfaces subject to water contact, not within exposure class XC2

Table 7.1 continued

3 Corrosion induced by chlorides other than sea water		
Where concrete containing reinforcement or other embedded metal subject to contact with water containing chlorides, including de-icing salts, from sources other than sea water, the exposure shall be classified as follows:		
XD1	Moderate humidity	Concrete surfaces exposed to airborne chlorides
XD2	Wet, rarely dry	Swimming pools Concrete exposed to industrial waters containing chlorides
XD3	Cyclic wet and dry	Parts of bridges exposed to spray containing chlorides Pavements Car park slabs
4 Corrosion induced by chlorides from sea water		
Where concrete containing reinforcement or other embedded metal subject to contact with chlorides from sea water or air carrying salt originating from sea water, the exposure shall be classified as follows:		
XS1	Exposed to airborne salt but not in direct contact with sea water	Surface near to or on the coast, but not subject to direct spray
XS2	Permanently submerged	Parts of marine structures
XS3	Tidal, splash and spray zones	Parts of marine structures

The exposure conditions given in EN 206 reflect the average conditions, not the microclimatic conditions. The microclimatic conditions which the structure is exposed to may differ significantly from these averages. Depending on the type of exposure and structure, aggressiveness conditions can get worse with increasing exposure time. For example, de-icing salts can accumulate with time on the beams of a bridge or the use of structure can change or the maintenance of the structure may be neglected. The structure can also be subject to different exposure conditions simultaneously or at the same and these exposure conditions may not cause

deterioration when considered individually but when acting together or simultaneously they can increase the deterioration rate dramatically.

The resistance of concrete to deterioration depends strongly on the quality of the concrete. The term "quality" represents the combination of different concrete properties such as water/binder ratio, binder content and type, strength and permeability characteristics. Based on the exposure conditions, maximum water/cement ratio, and minimum cement content are recommended in EN 206. The recommendations for chloride containing environments are shown in Table 7.2.

Table 7.2: Limit values of concrete composition in corrosive environments (EN 206)

Exposure class		Maximum water/cement	Minimum strength class	Minimum cement content (kg/m^3)
No risk of corrosion or attack	X0	–	C12/15	–
Carbonation induced corrosion	XC1	0.65	C20/25	260
	XC2	0.60	C25/30	280
	XC3	0.55	C30/37	280
	XC4	0.50	C30/37	300
Chloride induced corrosion – sea water	XS1	0.50	C30/37	300
	XS2	0.45	C35/45	320
	XS3	0.45	C35/45	340
Chloride induced corrosion – chloride other than sea water	XD1	0.55	C30/37	300
	XD2	0.55	C30/37	320
	XD3	0.45	C35/45	320

The values in Table 7.2 are based on the assumption of an intended working life of the structure is 50 years. The values in this table refer to the use of cement type CEM I conforming to EN 197-1 and aggregate with maximum nominal size in the range of 20 mm to 32 mm. The minimum strength classes were derived from the relationship

between water/cement ratio and the strength class of concrete made with cement of strength Class 32.5. The limiting values for the maximum water/cement ratio and the minimum cement content apply in all cases, while the requirements for concrete strength class may be additionally specified.

Besides concrete composition and exposure conditions, the thickness of concrete cover is also very important for the initiation period of the corrosion. Aggressive substances have to pass thorough this thickness in order to reach the steel. If this thickness is very small, the time for these substances to reach the steel will be short. Therefore, a certain cover thickness must be used in order ensure a certain level of durability. To use very high cover thickness, however, is not practical. In reality the concrete cover thickness cannot exceed certain limits because of mechanical and practical reasons. A thick un-reinforced layer of concrete cover can form cracks due to tensile forces exerted by drying shrinkage of the outer layer, while the wetter core does not shrink. In practice, cover thicknesses more than 70 mm are not considered realistic (Bertolini et al., 2004). EN 1992 (Eurocode 2) (2001) recommends concrete cover thicknesses based on the environmental exposure classes as shown in Table 7.3.

Table 7.3: Minimum cover thickness with regard to corrosion protection

Action	Exposure class	Minimum cover thickness for reinforcing steel for structure class 4 (mm)
No risk of corrosion or attack	X0	10
Carbonation induced corrosion	XC1	15
	XC2, XC3	25
	XC3	30
Chloride induced corrosion	XS1, XD1	35
	XS2, XD2	40
	XS3, XD3	45

The values given in Table 7.3 apply for ordinary carbon steel in normal weight concrete without special protection and a service life for the structure of 50 years. These are the minimum values for the transmission of bond forces, protection of the steel against corrosion and fire resistance. These minimum values should be increased 10 mm to obtain nominal values and to take construction variability into account.

The EN 206 standard or other present design codes and guidelines in practice are based on the assumption that sufficient durability will be obtained by specifying some limit values for concrete composition. The present design approach with respect to durability of concrete structures is mostly empirical. It is based on prescriptive rules such as maximum water/cement ratio, minimum cement content or nominal concrete cover thickness which are selected according to environmental factors. Additional rules (i.e. curing or air entrainment) are also specified for particular conditions. It is assumed that if these requirements are satisfied, the structure will achieve a long, but unspecified, service life.

Limit values for the structural dimensions and characteristics (i.e. minimum column or beam width, maximum crack width, minimum reinforcement diameter, minimum volume of reinforcement) are also given in these standards and specifications. After selecting the dimensions of structural elements based on experience and preliminary calculations, design engineer can change the dimensions based on structural loading and finalize the design. The limit state structural design processes are also given in these standards. Unlike the structural designing, after deciding the exposure class and some concrete properties, there is no method specified in these standards or specifications which can be used for the assessment of the durability performance of the structure. Current durability standards and guidelines have a common approach that differs significantly from the one for structural design. Durability design rules use prescriptive requirements, while the structural design methods are in principle based on performances and reliability. Although the prescriptive design approach would be unacceptable to a structural design engineer, this type of approach is accepted for durability problems (Gehlen and Schiessl, 1999).

In EN 206, it is assumed that the maximum water/cement ratio, minimum cement content and minimum cover thickness recommended for a particular environment will provide a service life of 50 years for the structure. Even if the concrete

composition and cover depth are selected according to the standard, there is no guarantee that the structure will have a long service life. As discussed in Chapter 8.2, field studies and experience have shown that in a marine environment corrosion of the embedded steel can start within 10 to 20 years of construction even for the concretes satisfying the EN 206 requirements.

The EN 206 code or other standards in practice recommend a maximum water/binder ratio, minimum binder content and strength but no limit values are given about the permeability characteristics, i.e. chloride ion permeability or water permeability. However, there are some test methods on permeability or chloride penetration which also classifies the quality of concrete based on the test result. The most common test method for evaluating the resistance of concrete to chloride ion penetration is the ASTM C 1202 (1997) test which is an indirect method based on the total charge passing through the concrete specimen at the end of 6 hours. The standard also gives a classification according to the test result as shown in Table 7.4.

Table 7.4: Chloride ion penetrability classification of concretes based on charge passed according to ASTM C 1202

Charge passed through the concrete specimen (Coulomb)	Chloride ion penetrability
> 4000	High
2000 – 4000	Moderate
1000 – 2000	Low
100 – 1000	Very Low
<100	Negligible

Some building contracts specify a maximum value of charge passed according to this method and assume that if the concrete has a lower value the structure will have a long service life. Even though the ASTM C – 1202 test is widely used, it is criticized that it does not reflect the actual behaviour of the concrete and the high voltage used in the test affect the results. A low or high test result does not give information about how long the service life of the structure will be. The test result, however, is a good indication of concrete quality and can be used for comparing different concretes.

7.6. Quality Control and Construction Quality

Realizing a construction project consists of different steps; after careful planning and design, comes the construction stage. In order to obtain a structure that can fulfill its requirements, it is vital that the structure is built according to its design. A very good design is meaningless if the structure is not built based on it. 1999 Marmara earthquake in Turkey proved once more that improper execution of the design (such as changed structural dimensions or low concrete strength) can lead to catastrophic consequences. Although some of the collapsed or severely damaged structures in Marmara region had proper design projects satisfying the national building codes, studies after the quake showed that most of these structures were not constructed according to their projects and the construction qualities were extremely poor.

Durability properties are more sensitive to the changes in the quality of the concrete than the mechanical properties, i.e. compressive strength. To achieve the long service life required from the structure, it is essential that a certain level of construction quality must be obtained at site. The design of a structure depends on the assumptions of obtained quality at site and also on laboratory data. However, the quality obtained on site are mostly lower than obtained in laboratory, and in addition, variations in the construction quality can also be very high as a result of concrete production, placing, curing conditions and workmanship at the site.

Quality assurance systems for the construction can be implemented to obtain the requirements for the structure (ACI Committee 121, 1998). Such a system consists of preliminary tests, production control, compliance testing and acceptance tests.

Although extensive guidelines and recommendations for quality control and quality assurance methods are available (ACI Committee 311, 1995), current practice is mostly based on prescriptive requirements which are not easy to verify and control. As a result, the new structures are handed over to the owners without any documentation of the obtained construction quality and after some time when the owner faces deterioration or damage at the structure, it is the owner's problem to find out the construction quality and in most of the cases it is late to take precautions to prevent the damage (Gjørv, 2003).

Documentation of the obtained construction quality is very important to monitor the in-situ properties for possible adjustments or corrective measures during the

construction stage (Gjørv, 2003). At the end of the construction when the final documentation of in-situ quality is obtained, an adjustment of both life cycle assessment and life cycle management can also be carried out. As a result of the durability based design, a concrete composition providing the required diffusivity and the concrete cover thickness are selected. Because the diffusivity and concrete cover are vital properties to ensure the long term performance of the structure, in-situ values of these properties are very important. Quality control of the chloride diffusivity can be carried out by concrete coring and non – destructively by the wenner electrode method (see Chapter 9).

Regular concrete coring on the structure may be difficult due to the reinforcement, and the need for the repair of these coring locations. In order to monitor the development of the chloride diffusivity, at an early stage of the construction, a reference element can be produced at the site which can represent the actual structural elements and regular coring and wenner electrode measurements can be carried on this element. Based on these measurements, reference curves relating chloride diffusivity to electrical resistivity can be established, which then can be used for monitoring the in – situ concrete quality in combination with coring and wenner electrode measurements on the structure.

Besides chloride diffusivity, the concrete cover is also important against the ingress of chlorides. For a given diffusivity, a higher cover thickness results in a longer time for chlorides to reach the embedded reinforcing steel. Cracking due to corrosion starts mostly at the location that has the lowest cover thickness. The reduction in the cover increases the risk of corrosion considerably. Studies show that cover thickness of existing structures are generally lower than their design specifications. On most of the construction sites, the control of concrete cover thickness is carried out only before the concrete casting, but in order to confirm the in – situ values of the cover thickness obtained after concreting has to be determined. This measured concrete cover and its variation is an essential input parameter for a reliable assessment of the service life of the structure.

7.7. Probability Based Durability Design

Although a concrete structure is a huge investment, as discussed in Chapter 7.5 and 8.2, current codes and practice do not give the long service life required for the

structure. Instead of prescriptive methods (like EN 206), performance based design processes have to be developed to ensure the long term durability and service life. Different aspects of the durability of structure must be covered with such a methodology. Realistic assessment of the exposure conditions and material properties and their scatter must be taken into account for the analysis. A model representing the actual deterioration mechanism has to be formulated for the service life design and prediction.

The need for reliable design processes which can provide a good long term performance has led to the development of probability based design methods. These design methods follow the same procedure of structural design in order to achieve the required performance throughout the predefined service life (Sarja and Veskari, 1996);

1. Specification of the target service life,
2. Analysis of environmental effects,
3. Identification of durability factors and degradation mechanisms,
4. Calculation of durability parameters,
5. Possible updating of the ordinary mechanical design (i.e. own weight of the structure),
6. Transfer of the durability parameters into the final design.

7.7.1. Service Life and Limit States

Service life of a structure can be defined as the period of time in which the structure is able to comply with the given requirements of safety, stability, serviceability and function, with or without periodic inspection and without extraordinary costs of repair and maintenance. There are different types of criteria for defining the end of the service life of a structure. Three different criteria were given by Sommerville (1992). For particular structures additional requirements can also be necessary, i.e. aesthetics or even the public opinion about the structure (Fidjestöl and Tuutti, 1995).

As shown in Table 7.5, the expected service life of a structure can be defined according to the type of the structure (ENV 1991-1, 1994).

For important concrete structures service life of 100 or more years is required. Table 7.6 gives some examples of the service life requirements for structures built or at the construction phase (Bertolini et al., 2004).

Table 7.5: Indicated values of required design working life

Class	Required design working life (years)	Example
1	1 – 5	Temporary structures
2	25	Replaceable structural parts, i.e. gantry girders, bearings
3	50	Building structures and other common structures
4	100	Monumental building structures, bridges and other civil engineering structures.

Table 7.6: Examples of service life requirements

Structure	Required service life (years)
Øresund Bridge (Sweden – Denmark)	100
Channel Tunnel (France – UK)	120
Alexandria Library (Egypt)	200
Eastern Scheldt Storm Barrier (Netherlands)	200
London National Library (UK)	250
Oslo Opera House (Norway)	300

A limit state defining the end of the service life must be selected for the durability analysis. Different limit states for structures are described in the relevant standards and specifications; Ultimate limit state, Serviceability limit state, Fatigue limit state, Limit state of progressive collapse. Serviceability limit state is related to the failure which leads to economic consequences such as the onset of corrosion or cracking. Ultimate limit state, however, is related to total failure (i.e. collapse or excessive material degradation) which leads to severe consequences such as loss of human lives or structural elements.

Based on Tuutti's model (1982), the stages of concrete deterioration as a result of the corrosion of the embedded steel are shown in Figure 7.10. The damage can be divided into two stages. First stage is the initiation as a result of chloride attack or

carbonation. The passivity layer is lost at the end of this stage and corrosion of the embedded steel starts. The second stage is the propagation in which corrosion takes place and as a result cracking and spalling starts in concrete. Although extensive research has been carried out in recent years for understanding and controlling the corrosion, only the depassivation stage of the embedded steel can be clearly defined (Gjørv, 2004a). Electrochemical potential mapping or the determination of the chloride ion penetration depth can easily identify this critical stage. After the depassivation the repair and protection of the structure against corrosion is more difficult and more expensive. Because of these reasons the onset of corrosion of the embedded steel can be used as the serviceability limit state for the analysis. Selection of the criterion as the maximum crack width is not possible because there are no reliable methods available to relate crack width due to corrosion of reinforcement to time (Cather and Marsh, 1997).

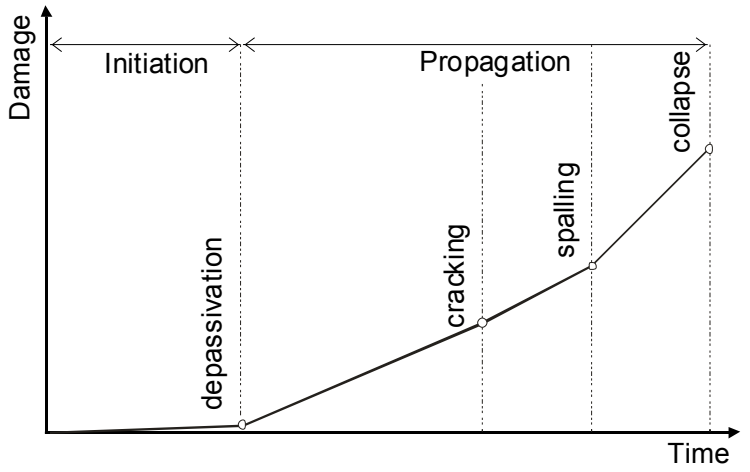

Figure 7.10: Deterioration of concrete due to corrosion reinforcement

7.7.2. Probability Analysis

The penetration of chloride ions into concrete can be modeled by Equation 7.5 (Collepardi et al., 1972).

$$C(x,t) = C_S\left[1 - erf\left(\frac{x}{2\sqrt{D_C t}}\right)\right] \tag{7.5}$$

where C(x, t) is the chloride concentration at depth x after time t, erf is the error function, C_s is the surface chloride concentration and D_c is the chloride diffusion coefficient of the concrete and it is given by 7.6,

$$D_C = D_0 \left(\frac{t}{t_0} \right)^{\alpha} \tag{7.6}$$

where D_o is the chloride diffusion coefficient after time to and α represents the time dependence of the diffusivity (Takewaka and Mastumoto, 1988).

Durability analysis for the chloride containing environments is based on the principles that; i) onset of the corrosion is the serviceability limit state, ii) the risk for this limit to be reached gives the probability of failure. For the depassivation of steel in a chloride containing environment, the chloride concentration at the depth of the steel must reach to a certain level. After the depassivation the corrosion starts within a short period or may take several years depending on several factors. For the analysis, however, it is accepted that the corrosion starts when the critical chloride content is reached which is also the serviceability limit.

The probability based durability analysis is similar to traditional structural design with one difference. In structural design, loads and resistances are independent of time. In durability analysis, however, the variables are time dependent. In structural design; the loads are actually acting on the structure such as traffic or wind and the resistances are the material parameters like the strength of concrete or steel. In durability design the loads are the environmental actions for example the penetration of chlorides or carbonation.

For traditional dimensioning of structural elements, the resistance of the element, R, has to higher than load, S. This principle can also be used for the durability analysis and can be formulated as follows;

$$R(t) > S(t) \quad \text{or} \quad g = R(t) - S(t) > 0 \tag{7.7}$$

where R(t) shows the resistance variable (i.e. resistance to chloride ion penetration), S(t) represents the load variable (i.e. chloride penetration) and g is the limit state function (or the design equation). Thus, the failure probability is given by (Haugen, 1980);

$$P_f = P[R - S < 0] \qquad or \qquad P_f(t) = P[R(t) < S(t)] \tag{7.8}$$

Both resistance R(t) and load effect ,S(t) are time dependent parameters and the changes with time both for their mean values and scatter is shown in Figure 7.11 (Melchers, 1987). Both S(t) and R(t) are stochastic and described by distributions around a mean value at every moment in time. The resistance of the structure R(t) decreases with time due to the deterioration effects. The load parameter S(t), however, can remain constant or increase with time as shown in the figure.

Because the resistance R(t) decreases and load effect S(t) increases with time, the failure of probability increases constantly with time. At the time t=0 the distributions of the resistance and load are far apart from each other and the probability of failure is small. With increasing time, the distributions approach to each other, forming an overlapping area of increasing size which represents the probability of failure. This overlapping distribution is also shown in Figure 7.12 (Melchers, 1987; Thoft-Christensen and Baker, 1982).

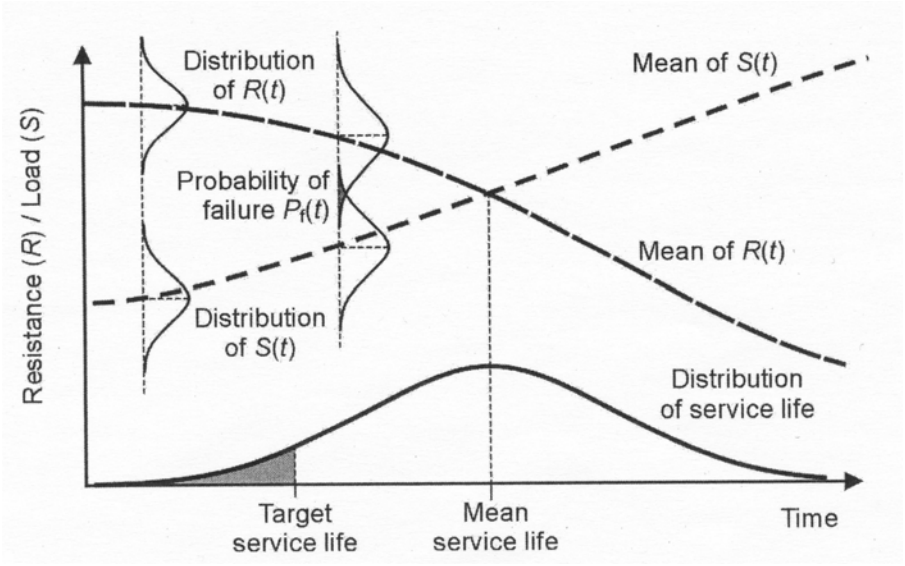

Figure 7.11: The change of resistance and load parameters with time.

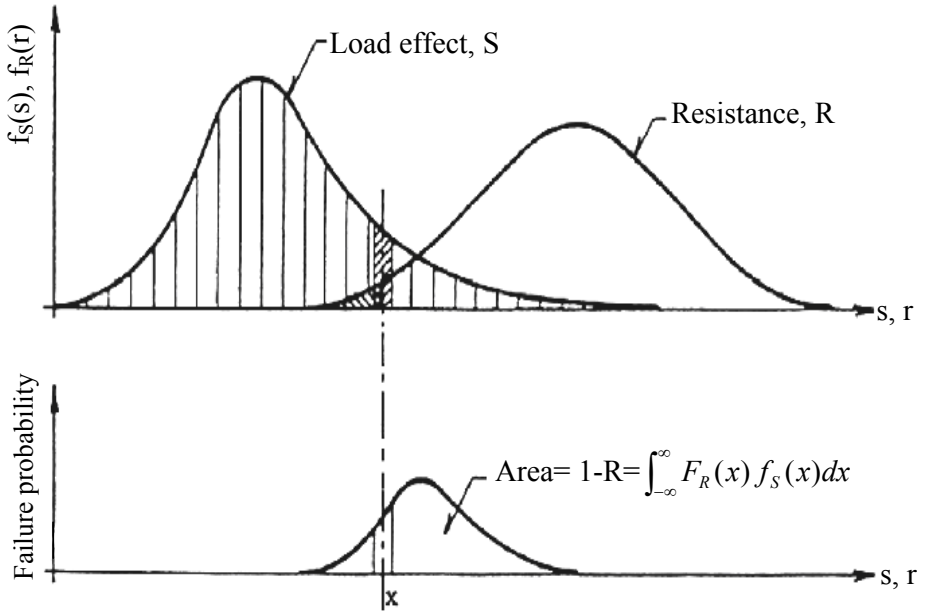

Figure 7.12: Representation of basic load – resistance problem

For a simple structural member selected at random from a population with a known distribution function F_R of strength R and a distribution function F_s of load effect S, the probability of failure under the action of the known load is given by Equation 7.9 under the condition that R and S are statistically independent. This equation is also represented in Figure 7.12.

$$P_f = P(R\text{-}S \leq 0) = \int_{-\infty}^{+\infty} F_R(x).fs(x)dx \tag{7.9}$$

Equation 7.9 gives the total probability of failure P_f as the product of probabilities of two independent events, summed over all occurrences. This means that the probability P_1 is that S lies in the range x, x+dx and the probability P_2 is that R is less than or equal to x. P_1 and P_2 is given by;

$$P_1 = f_S(x)dx \quad \text{and} \quad P_2 = F_R(x)dx \tag{7.10}$$

Under these conditions, the reliability is the probability that the structure will survive when the load is applied, and given as follows:

$$\text{Reliability} = 1 - P_f = 1 - \int_{-\infty}^{+\infty} F_R(x).fs(x)dx \tag{7.11}$$

This can also be expressed as;

$$\text{Reliability} = 1 - P_f = 1 - \int_{-\infty}^{+\infty} \left(1 - F_S(x)\right) f_R(x) dx \qquad (7.12)$$

Different methods are available for solving this reliability problem (Thoft-Christensen and Morutsu, 1986). In this study monte carlo simulation was used for the analysis. This method is based on the generation of random numbers which are then used for calculating the limit state probabilities as given in equation 7.9 (Hammersley and Hanscomb, 1975).

The probability of failure defines the end of the target service life. If this failure probability exceeds a certain limit, it is accepted that the service life has been reached. This limit can be defined by the codes or by the owner.

In most codes, an upper level of 10% for the probability of failure is normally accepted for the reliability of structures. In such a durability analysis, the input parameters have great importance in order to obtain realistic results. Concrete properties and environmental conditions affect the calculations extensively. These governing parameters are discussed below.

7.7.3. Input Parameters

7.7.3.1. Surface Chloride Concentration

This parameter is the representative chloride concentration at the concrete surface during the time of exposure. It is a time dependent parameter and affected by the salinity of the water, possibly the porosity of the surface layer (and thus the amount of saline pore water) and the length of wetting versus drying in the splash zone (Fluge, 2001). Figure 7.13 gives an example of the effect of microclimate on the surface chloride concentration (Fluge, 1997).

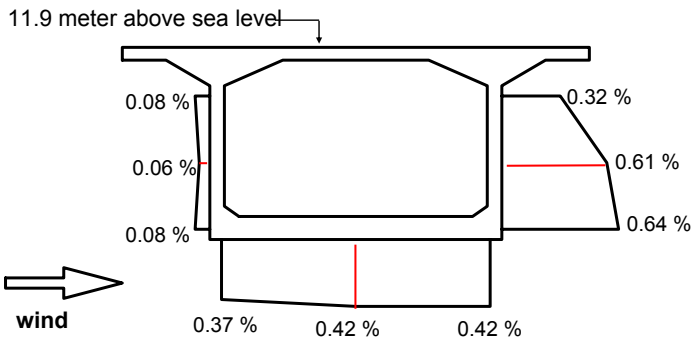

Figure 7.13: Average surface chloride concentrations on a bridge superstructure

Marine reinforced concrete structures at positions dominated by a strong wind from one direction, i.e. Norwegian coastal bridges, will receive chloride on all their surfaces during heavy wind and storm. During heavy rain showers, however, the concrete surfaces on the windward sides are rinsed and cleaned, and in this way these concrete surfaces are exposed to chlorides only for a short period of time. However, the concrete surfaces on the leeward sides are not rinsed by the rain showers in the same way. As a result, the chloride coatings established by strong wind to some extend remains at this concrete surface, and the chloride will penetrate into the concrete. The windward – leeward effect is the main reason for this result.

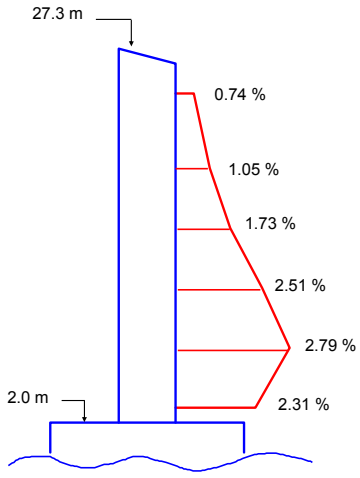

Figure 7.14: Average surface chloride concentrations on a column

Figure 7.14 shows the average values of surface chloride concentrations on a bridge column in a Norwegian marine environment (Fluge, 1997). As indicated in Figures 7.13 and 7.14, there are big differences in the surface chloride concentrations

depending on the concrete location. Extensive field studies at Norwegian harbor structures also confirm this high scatter (see Figure 7.15) (Hofsøy, 1999).

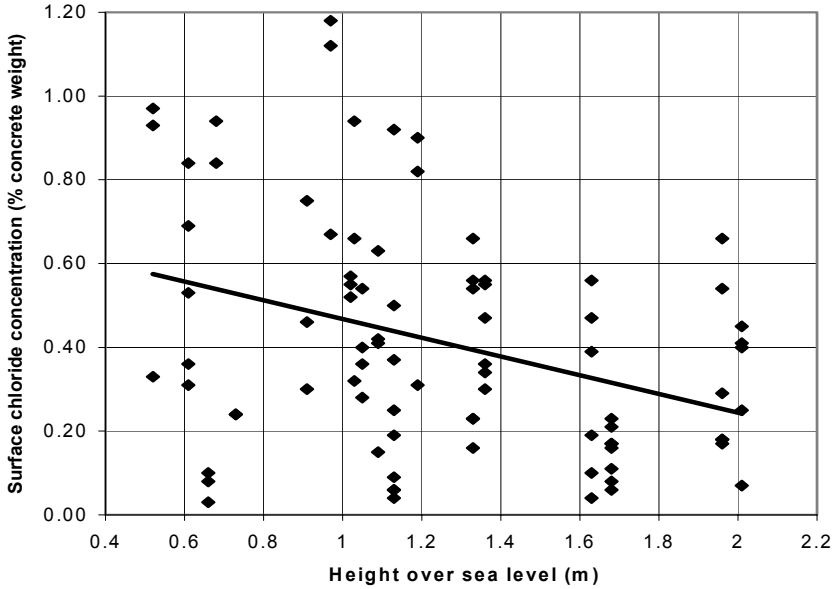

Figure 7.15: Surface chloride contents obtained from Norwegian harbor structures

The Figure 7.16 illustrates the change of the surface chloride concentration with the height of the measurement points which were obtained from the columns of 35 coastal bridges. The data include both windward and leeward effects. Different environmental zones are distinguishable in Figure 7.16 (Fluge, 2001). The results shown in Figure 7.15 and 7.16 represent the tidal, splash and atmospheric exposure zones for structures. The surface chloride concentrations increase as the distance from the sea level decreases which is due to the aggressiveness of chlorides. It is believed that the moisture content of the concrete close to the sea level did not affect the results significantly. As demonstrated in Figures 7.14 to 7.16, the splash zone of the structure is the most severe with regard to the accumulation of surface chlorides. This is due to the wetting and drying cycles which result in progressive build up of chlorides by a process of wetting with seawater, evaporation and salt crystallization (Bamforth and Price, 1993).

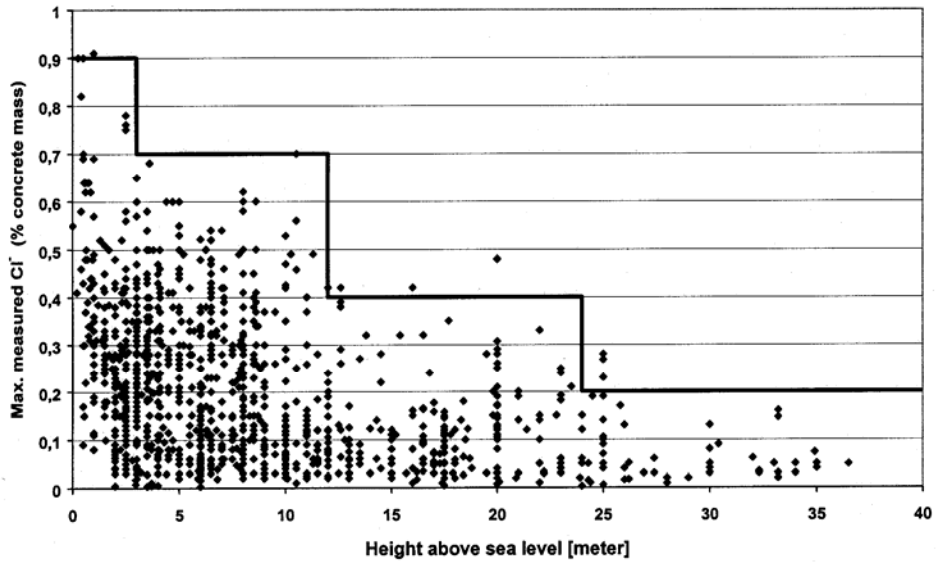

Figure 7.16: Change surface chloride concentration with the height from sea level

For an existing structure, surface chloride concentration can be obtained by the chemical analysis on samples obtained from the structure. At the design stage, in which even the construction of the structure hasn't started, representative values can be used. Data obtained from nearby structures or from similar environmental conditions can be used as an indication. The considerations have to be related to the worst exposed parts of the structure (i.e. splash zone).

7.7.3.2. Chloride Diffusion Coefficient

Concrete chloride diffusion coefficient is the most important material parameter governing the chloride ingress into concrete. The structure and distribution of pore system in concrete have a significant importance for permeability. The connectivity of both the pore system and the porous hydration products control the diffusion of aggressive substances into concrete (Garboczi and Bentz, 1998). Therefore, parameters affecting the restrictivity and tortuosity of the pore system also affect the diffusivity of the concrete. Water/binder ratio, degree of hydration, cement type, pozzolan types and amounts and curing are some of these important parameters.

The determination of chloride diffusion coefficients is a time-consuming and difficult procedure. Diffusivity of the concrete can be obtained by methods based on natural diffusion. In these methods concrete specimen is placed between diffusion cells where diffusion of chloride takes place. This kind of steady state tests can take

very long time. The thickness of the specimen has to be small which makes these tests impractical to use for concrete. In order to speed up the diffusion of chlorides an external electrical field can be applied (see Chapter 7.2.2). The steady state migration tests in which chloride ions are allowed to pass through the whole concrete specimen is also a time consuming process.

In practice, different transport mechanisms can act together and chloride penetration into concrete structures follows a non-steady state process. In order to simulate this process, conventional methods are to immerse the concrete specimens in chloride solutions with constant chloride concentration. This immersion period is usually between 35 to 90 days. After immersion, the chloride profile is measured by sampling the specimen successively from the exposed surface and by analysing the total chloride content in each sample. The chloride diffusion coefficient can be found from the Fick's law by curve fitting. These tests also require a long period before testing (i.e. concrete must have certain level of maturity, especially for concretes with pozzolanic materials).

The immersion methods mentioned above require at least about 60 days for obtaining any result. In the design period before the structural elements are constructed, the measured material performance (i.e. chloride diffusion coefficient) should be known as soon as possible. Similar to the compressive strength, routine quality control of the diffusivity of the produced concrete must also be carried out. Among different test methods, non steady – state chloride migration methods can be used to obtain the chloride diffusion coefficient of concrete. Although these types of tests are criticized that they don't actually represent the real behaviour, they can be used for the design and quality control purposes.

The diffusivity obtained from migration tests represents the permeability characteristics of concrete which also shows the concrete quality. Based on the chloride diffusivity, experience showed that the resistance against chloride ion penetration can be evaluated as shown in Table 7.7. (Gjørv, 2004b).

Table 7.7: Relationship between diffusivity and resistance to chloride penetration

Chloride diffusivity ($m^2/s \times 10^{-12}$)	Resistance against chloride ion penetration
> 15	Low
10 – 15	Moderate
5 – 10	High
2.5 – 5	Very high
< 2.5	Extremely high

7.7.3.3. Time Dependency of Chloride Diffusion Coefficient

As stated in Chapter 7.2.1, diffusion coefficients obtained from steady – state and non – steady conditions are different from each other. The first one is constant while the latter changes depending on various factors such as the time of exposure or exposure conditions. The value obtained from the non – steady state is called apparent, achieved or effective diffusion coefficient.

Diffusion coefficient of concrete is a time dependent parameter which decreases with time. Several reasons may be responsible for this. As the hydration continues, the microstructure of concrete changes constantly and porosity decreases, which as a result, reduces the chloride ingress into concrete. The improvement in pore system due to hydration is important mostly for the early ages and especially significant for the concretes with pozzolanic materials. Another explanation for the reduction in diffusivity may be the effect of chloride binding. The ion exchange between the sea water and the concrete may be another possible reason for this behavior. Magnesium and potassium blocking the pore system reduces the chloride penetration.

Not considering the time dependence of the diffusion coefficient or using unrealistic values can lead to overestimation of the chloride ingress or completely wrong and meaningless results (Markeset, 2004). Water/cement ratio, type of cement and the exposure conditions are important variables deciding the time dependency. Long term exposure tests or field studies are needed for obtaining the time dependency of diffusion coefficient of different types of concretes.

7.7.3.4. Critical Chloride Concentration

Critical chloride concentration can be described as the minimum chloride content needed for the onset of corrosion. This chloride threshold level depends on many parameters such as the water/cement ratio, cement type, pozzolanic materials, steel type and environmental conditions (Alonso, et al., 2000; Sandberg et al., 1995). Figure 7.17 shows a schematic representation of critical chloride concentration and moisture content relationship based on concrete quality (Gehlen, 1999).

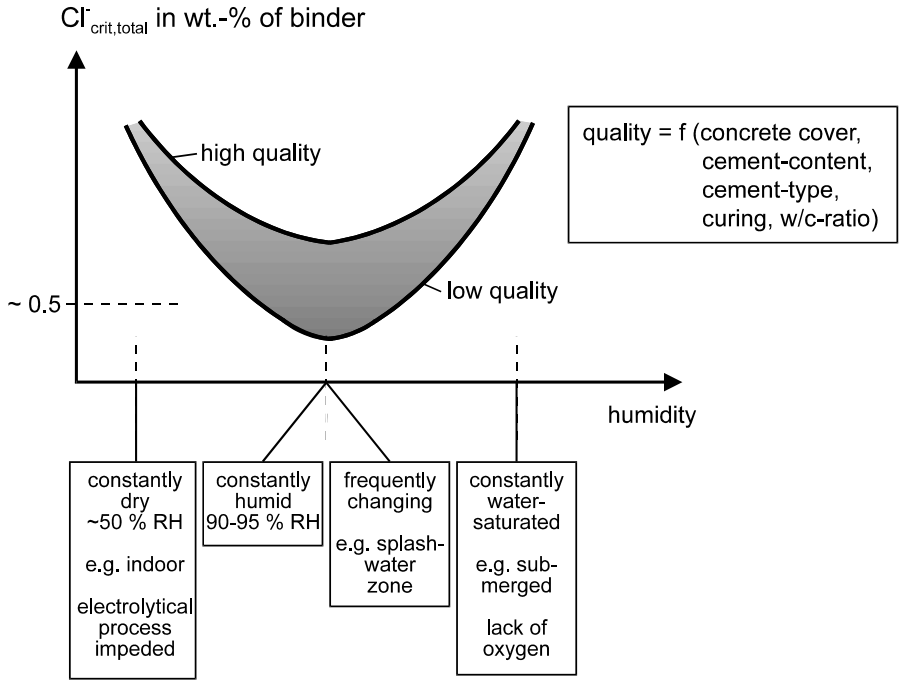

Figure 7.17: Critical chloride concentration and moisture content relationship

Water and oxygen are needed for the corrosion process and if one of them is not present in the environment corrosion doesn't take place. If the concrete is permanently dry or permanently water saturated much higher chloride contents are needed as illustrated in Figure 7.17.

Various methods have been used to determine the chloride threshold levels for different concretes. It is generally agreed that the threshold levels determined in solutions or obtained from concretes with mixed – in chlorides do not reflect the actual process in concrete (Arup, 1995). It is necessary to have specimens with chloride diffusing in from the surface, wait for the corrosion to initiate and then determine the chloride content at the level of the steel surface by analysis of a thin layer of concrete near the steel surface. The maximum allowable chloride

concentrations are given in the related standards. Typical chloride threshold levels for different concretes can also be obtained from literature (Alonso, 2000; Glass and Buenfeld, 1997; Thomas, 1996).

7.7.3.5. Thickness of the Concrete Cover

In a chloride containing environment chloride ions have to pass through the concrete cover to reach the steel reinforcement. As also presented in Chapter 7.5, relevant standards recommend minimum cover thicknesses (see Table 7.3). Although selecting a very thick concrete cover may seem like an easy way for obtaining a good long term performance, it is not practical due to possible cracking in this thick un-reinforced concrete. In very aggressive environments, one approach to obtain a high cover thickness is to place reinforcing steel in two rows instead of the classical method of one steel row and use stainless steel for the outer row. This approach, however, may be very costly due to the high prices of stainless steel.

The probability based design presented in this study is a method for calculating the risk of the onset of corrosion for a given cover thickness and finding the optimum solution in terms of concrete quality and cover thickness.

All the calculations for a durability design are based on the assumption that concrete cover is crack free. Cracking due to plastic or drying shrinkage, thermal gradients or overloading increase the permeability of the concrete which affect the ingress of aggressive substances. In addition, cold joints can also act similar to cracks.

Field studies show that there may big deviations of the cover thickness in a structure. At the end of the construction period the obtained cover thickness must also be documented.

2. LITERATURE REVIEW

2.1. General

The following literature review focuses on fly ash, blast furnace slag and silica fume which are the most widely used pozzolans. Brief information about the structure, formation and properties of these pozzolanic materials are presented in this chapter. The effects of these supplementary cementing materials on the microstructure, mechanical behaviour and resistance to chloride penetration of concretes are summarized based on previous studies.

2.2. Pozzolanic Materials

2.2.1. Fly Ash

Fly ash is a by-product of the combustion of coal in thermal power plants for electricity production. It is also known as pulverized fuel ash. It is removed by the dust collection system as a fine particulate residue from the combustion gases before discharging into atmosphere. Fly ash includes meta-stable alumino-silicates that react with calcium ions, in the presence of moisture to form silica hydrates.

Coal used in thermal power plants is pulverized before use. The fine coal particles are transported in an air stream to the boiler where they are burned, and the heat produced is used to generate steam in the steam-generating unit. During the combustion process, the volatile matter is vaporized and carbon is burned off. As the particles enter the burning zone, temperatures increase rapidly and typically reach values around 1000 – 1500° C. Mineral components present in the coal gangue, the inorganic part of the coal, such as clays and feldspars melt and form fused droplets that on rapid cooling solidify as spherical glassy particles that comprise the coal ash. Some mineral components also remain in the crystalline phase. The coarser ash collects at the bottom of the furnace, and is known as bottom ash. The finer ash is carried in the flue gases are collected by precipitators. It is this ash that is termed fly ash (Luke, 1999).

Fly ash is the most common artificial pozzolan worldwide. The use of fly ash in concrete technology dates back to late 1930s. It is estimated that about 450 million tons of fly ash is produced worldwide annually, but only about 6 percent of the total available fly ash is used as a pozzolan in blended cements or in concrete mixtures (Mehta, 2000). There are twelve active coal-burning power plants in Turkey (Bayat, 1998). The annual fly ash production in the country is about 15 million tons (Tokyay, 1998). Fly ash can be utilized as a blending component in blended cement or can be added separately during the concrete production.

According to ASTM C 618 (2000), fly ash can be divided into two categories: Class F and Class C. The Class F fly ash generally contains analytical CaO less than 10 %, whereas Class C fly ash typically contains it 15 % to 35 %. On the other hand, the Class F fly ash, produced from combustion of anthracite and bituminuous coals, is a low lime fly ash and mainly classified as a pozzolan. The Class C fly ash, however, is produced from combustion of either lignite or subbituminous coal. Due to the high calcium content Class C ashes possess substantial cementious properties besides pozzolanic properties (Naik et al., 1992). Fly ash particles, as shown in Figure 2.1, have mostly spherical, glassy particle shapes with different sizes varying from a few μm to 100μm (ACI Committee 232, 1996).

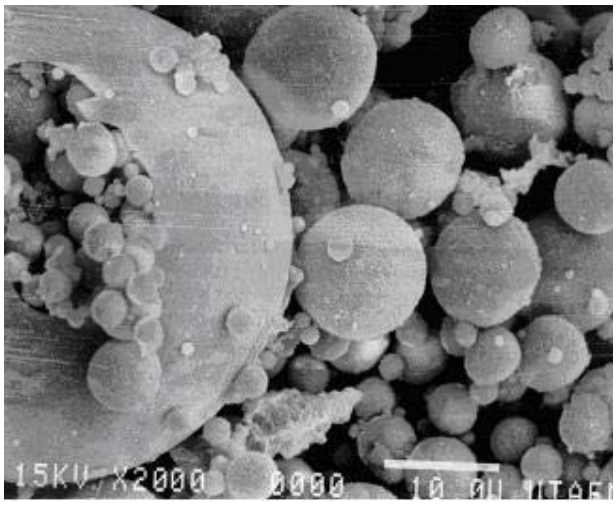

Figure 2.1: Fly ash particles

2.2.2. Ground Granulated Blast-Furnace Slag

Ground granulated blast-furnace slag is a by-product of iron production. The iron ore is a mixture of oxides of iron, silica and alumina, and the chemical reactions within

the blast-furnace reduce iron ore to iron. The iron ore is fed into the furnace with coke and limestone. The slag is formed at a temperature of 1300 – 1600^{o}C as a liquid layer floating on the top of liquid iron. It is then collected and cooled (Lee, 1974). The method of cooling affects the properties of the slag. When cooled rapidly, the slag has a non-crystalline, glassy structure. If water is used for cooling, sand sized particles of slag is obtained. An alternative treatment, pelletization, can also be used for granulation. The granular slag is then dried and finally ground to cement fineness or finer.

During the iron production process about 300 kg of slag is produced for each ton of pig iron (Neville, 2004). In production plants with older technology, however, the amount of slag obtained is usually higher. The use of blast furnace slag as a cementitious material dates back to the second half of 19th century. About 100 million tons of slag is produced annually worldwide but only a very small fraction is utilized. Today slag is widely used in Europe as a component in blended cements but the degree of usage varies significantly between different countries. Netherlands, for example, utilizes about 90 % of its slag production (Regourd, 2004) and slag cement has a market share of about 60 % in the country (Bijen, 1996a). According to the American Slag Cement Association, in US 3.1 million tons of slag cement was shipped for use in concrete and construction applications in 2003. Besides used as a blending component in cement, slag can also be added to concrete during production.

Although many pozzolanic by-products are being used as blending materials, blast furnace slag is the nearest to portland cement in chemical composition. The chemical composition of the slag depends on the materials used for iron production and the procedure for cooling. The CaO content of slags are mostly between 40% and 50%, and the SiO_2 is between 30% and 40%. ASTM C 989 (1999) classifies blast furnace slag into three grades; 80, 100 and 120 where this classification is based on the strength of the mortar containing 50 % slag by mass. Particle size of the blast furnace slag depends on its grinding process. Blast furnace slag particles have mostly rough, sharp edged shapes as shown in Figure 2.2.

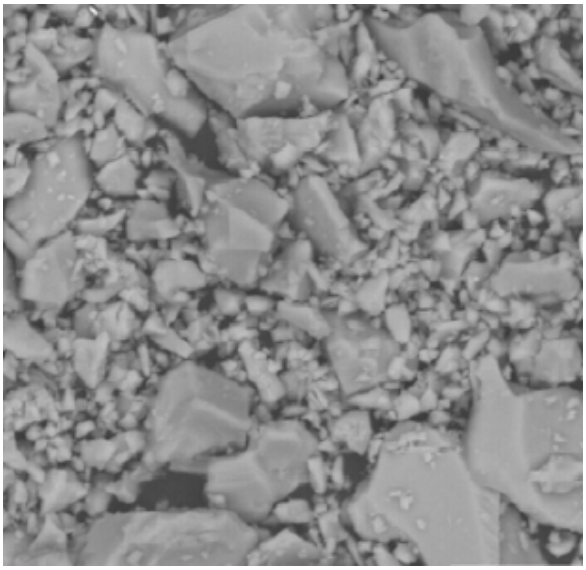

Figure 2.2: Ground granulated blast furnace slag particles

2.2.3. Silica Fume

Silica Fume is a by-product of silicon and ferrosilicon industries. It is also known as condensed silica fume or microsilica. Quartz is reduced to silicon in electric arc furnaces at temperatures up to 2000^{o}C. During this process, some SiO lost as gas oxidizes and condensates into spherical particles with very high amounts of amorphous SiO_2. It is filtered from the exhaust gases before discharging into atmosphere (Malhotra et.al, 1987). The raw materials used for producing silicon and also the type and design of the furnace affects the properties of the silica fume.

The usa of silica fume in concrete technology is relatively new when compared to fly ash or slag. The studies at the Norwegian Institute of Technology in Trondheim during the late 1970s and 1980s formed a basis for utilizing silica fume in concrete technology (Khayat and Aitcin, 1993; Fidjestøl and Lewis, 2004). Silica fume production is very low when compared to those of fly ash or slag. The annual production of silica fume is about half a million ton worldwide and Norway is the biggest producer of silica fume with about 140 thousand tons (Chandra and Berntsson, 1997). Silica fume is commercially available in various forms; undensified, densified (compacted), micro-pelletized and slurry form. Some synthetic forms of silica are also available on the market such as colloidal silica, silica gel, fumed and fused silica (Chandra and Berntsson, 1997).

Silica fume has spherical particles with average particle sizes of about 0.1 – 0.2 μm, which is more than 100 times smaller than the particle size of ordinary portland cement. Figure 2.3 illustrates the particle size of silica fume compared to those of cement (Aitcin, 1998). The SiO_2 content of silica fume is usually more than 85 % and in many national standards the minimum SiO_2 content of silica fume is also specified as 85 % (ASTM C 1240, 2000; NS 3045, 1992). Figure 2.4 gives a comparison of different pozzolans and cements based on their chemical compositions. Because of its extreme fineness and high silicon dioxide content, silica fume is very reactive when compared to fly ash or slag (Roy, 1989).

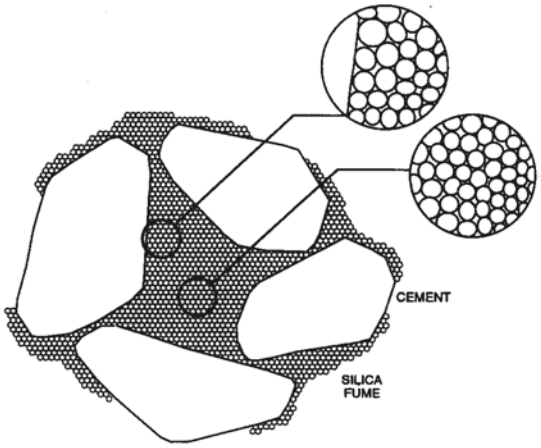

Figure 2.3: Comparison of silica fume and cement particles

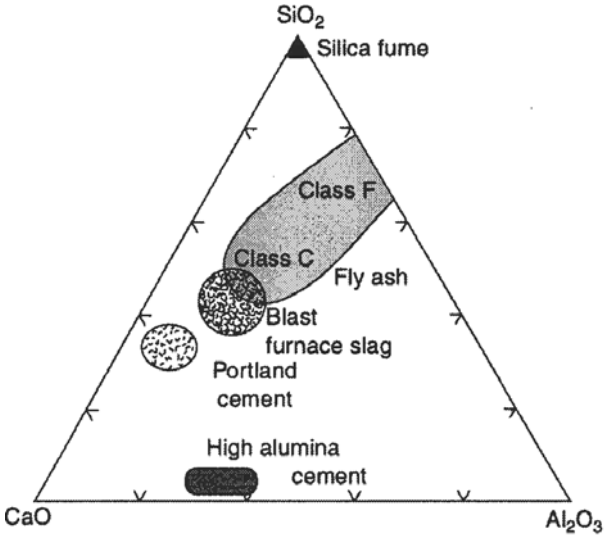

Figure 2.4: Compositions of cements and some pozzolanic materials; simplified representations of components as CaO-Al_2O_3-SiO_2

2.3. Hydration Mechanisms

2.3.1. Hydration of Portland Cement

Limestone and clay is burned up to 1450^{o}C for producing portland cement clinker. This material is then ground with gypsum and portland cement is obtained. The main constituents of portland cement are CaO, SiO_2, Al_2O_3 , which form the major phases; C_3S, C_2S, C_3A and C_4AF, where C: CaO, S: SiO_2, A: Al_2O_3 and F: Fe_2O_3. These phases have different characteristics and affect the properties of the cement.

The hydration of calcium silicates forms the calcium silicate hydrate (CSH) which is the main constituent of solids in cement paste. The reactions of the C_3S and C_2S may be expressed as:

$$2\ C_3S + 6\ H \longrightarrow C_3S_2H_3 + 3\ CH \qquad \textbf{(2.1)}$$

$$2\ C_2S + 4\ H \longrightarrow C_3S_2H_3 + \ CH \qquad \textbf{(2.2)}$$

where H and CH represents H_2O and $Ca(OH)_2$, respectively. The reaction of the aluminate phase is very fast and can cause rapid setting of cement. In order to control the rate of the reaction, about 5 % gypsum (calcium sulfate) is added to portland cement during grinding. The hydration reaction of C_3A with gypsum and water is given as:

$$C_3A + 3\ C\overline{S}\ H_2 + 26H \longrightarrow C_3A.3C\overline{S}\ .32H \qquad \textbf{(2.3)}$$

in which $\overline{S}$ represents SO_3. The product of this reaction, ettringite, is formed on the surfaces of C_3A as prismatic crystals. The ettringite then reacts with C_3A and transforms into calcium monosulfate that has lower sulfate content. The hydration of C_4AF is similar to C_3A but with a slower rate.

The studies on of these pure phases helps to understand the hydration process but the hydration of portland cement is more complex due to the interaction of the phases and minor constituents. (Taylor, 1992).

Many different techniques such as NMR, XRD, neutron activation analysis, atomic absorption spectroscopy, IR/UV spectroscopy, electron microscopy, surface area techniques, pore characterization, zeta potential, viscometry, differential thermal analysis (DTA), thermo-gravimetric analysis (TG), differential scanning calorimetry

(DSC), and conduction calorimetric methods have been used for investigating the hydration and microstructure of concrete.

The hydration reactions start right after mixing cement with water. The rates of the reactions are very fast during the first days. Calcium hydroxide content, chemically bound water and heat of development are the most commonly investigated properties during the hydration. As the hydration continues, the amount of CH and bound water increase as a result of the chemical reactions. The morphology of the CSH also changes with hydration. Figure 2.5 show the change of hydration products with the degree of hydration (Neville, 2004).

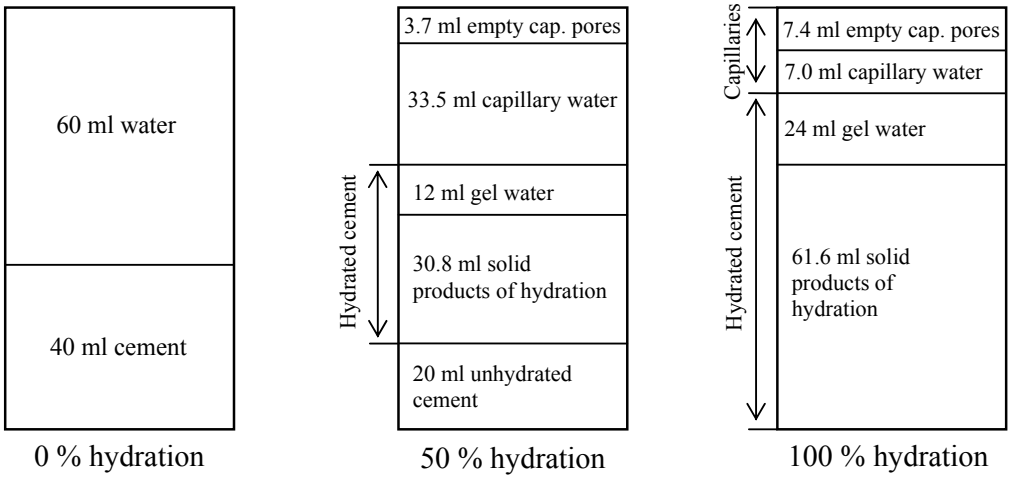

Figure 2.5: Diagrammatic representations of the volumetric proportions of cement paste at different stages of hydration

2.3.2. Hydration of Portland Cement with Fly Ash

The high calcium fly ashes have self hardening characteristics but low calcium fly ashes have very little or no cementing property. The pozzolanic reaction takes place between the CH and the fly ash. The CH, however, is produced from the hydration of cement. The CH reacts with the SiO_2 in the fly ash and CSH is formed as a result. These reactions are slower when compared to cement hydration and the rate of the reaction affects the characteristics of concrete.

The reaction of fly ash depends on the breakdown and dissolution of the glass phase which occurs when the pH of pore solution is higher than 13 (Fraay, 1989). The increase of the alkalinity of the pore water is because of the hydration of portland cement. The amount of CH formed during the first days is not enough for the

dissolution of the glass phase of fly ash and because of this, the fly ash is usually considered inert during the early days of hydration.

The amount of CH formed in the fly ash – cement system is initially lower than pure portland cement system. As a result of the pozzolanic reaction, the CH amount decreases and CH is consumed to form CSH. The change in the CH content is an indication of the pozzolanic activity. Figure 2.6 shows the change in CH content for different fly ash replacement levels (Taylor, 1992).

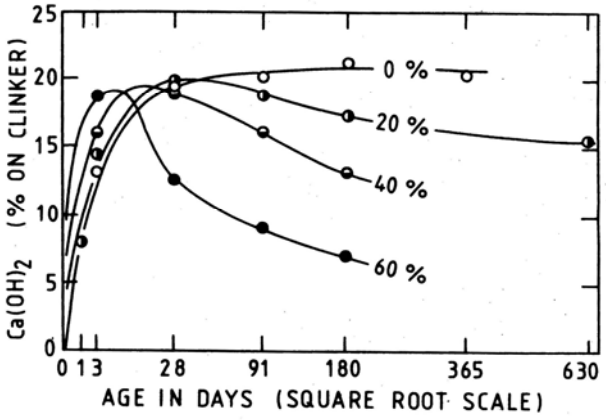

Figure 2.6: CH contents of pastes with different amounts of fly ash

2.3.3. Hydration of Portland Cement with Blast Furnace Slag

Granulated blast furnace slag reacts with the CH produced from the hydration of portland cement. CH serve as an activator for the dissolution of ions containing Si and Al by breaking the Si-O, Al-O, Al-O-Si covalent bonds (Roy and Malek, 1993). After slag cement is mixed with water, a pH level of about 12 is obtained in concrete within a short period, which is the reason the reaction of slag is more rapid when compared to fly ash.

Studies have shown that the principal hydration products of portland blast furnace slag cements are similar to those formed in pure portland cements (Taylor, 1992; Chandra, 2002). Some early slag hydration also takes place and the surface of slag is modified as soon as it contacts with water and a layer of CSH is formed on the surface of slag (Regourd et.al., 1983). A schematic representation of the blast furnace slag hydration products are shown in Figure 2.7 (Glasser, 1991). The gold coated surface in the figure shows the original slag surface before the hydration.

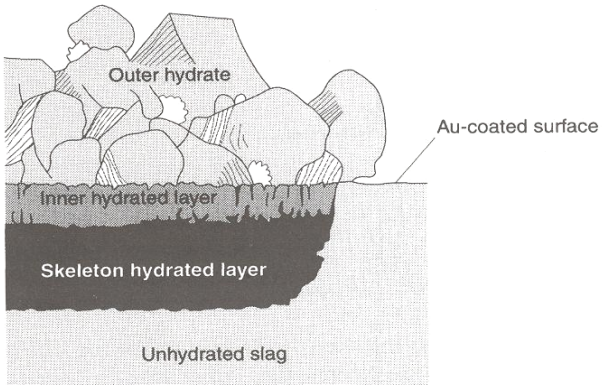

Figure 2.7: A schematic representation of the blast furnace slag products

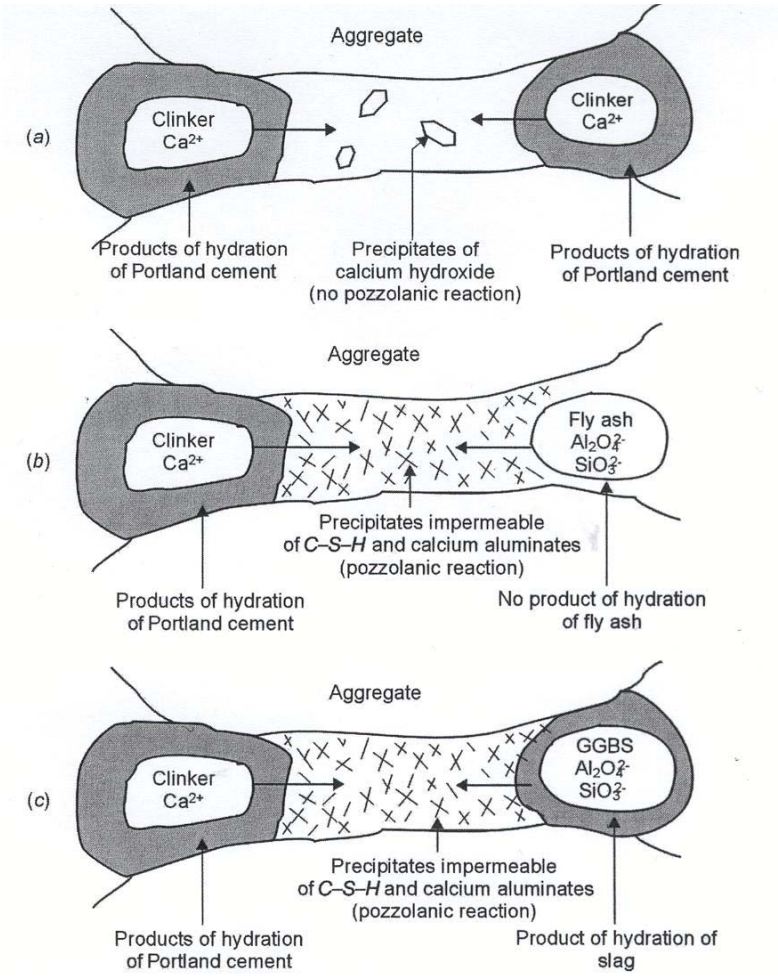

Figure 2.8: Hydration of (a) portland cement, (b) cement – fly ash blend, (c) cement – slag blend

Figure 2.8 shows the hydration of (a) portland cement, (b) cement – fly ash blend, (c) cement – slag blend (Bertolini et al., 2004). As seen in the figure, addition of fly ash

or slag leads to formation of very fine products of hydration that lead to refinement of pores.

2.3.4. Hydration of Portland Cement with Silica Fume

The hydration of a silica fume – portland cement is very rapid when compared to other pozzolans like fly ash or slag. Silica fume dissolves in a saturated CH solution within few minutes. When enough CH is produced as a result of cement hydration, CSH starts to form on the silica fume particles (Chandra, 2002). It was reported that half of silica fume can react in 1 day and two-thirds during the first 3 days (Neville, 2004). The characteristics of CSH, however, are different than those of produced by pure cement hydration. A schematic representation of CSH produced in silica fume pastes is shown in Figure 2.9 (Justnes, 2002).

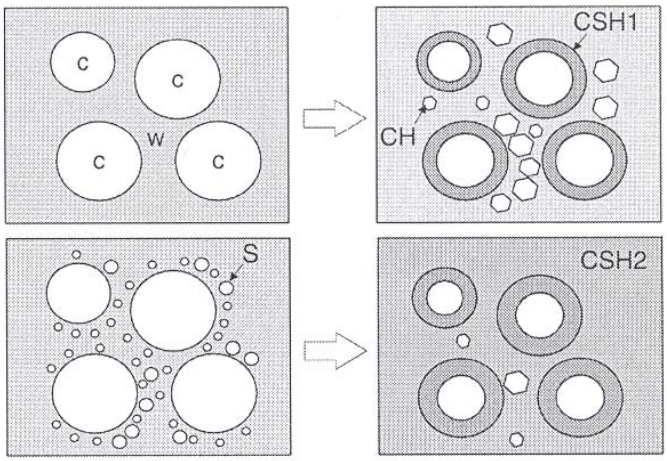

Figure 2.9: A schematic representation of the formation of two different CSH gels

In Figure 2.9; C, W, CH and S represent cement, water, calcium hydroxide, and silica fume, respectively. CSH-1 and CSH-2 are the CSHs by pure portland cement and silica fume, respectively. The general differences between these two gels are that CSH-2 produced in silica fume paste has longer linear polysilicate anions and has lower Ca/Si ratio. This ratio can be as low as 1 (Neville, 2004; Chandra, 2002). Ca/Si ratio decreases as the silica fume content increases (Taylor, 1992).

2.4. Microstructure

2.4.1. Microstructure of Portland Cement Concrete

Mechanical properties and durability of concrete is controlled by the microstructure (Mindess, 1985). On micro scale, concrete has a high degree of heterogeneity, consisting of different hydration products, aggregates, pores of different sizes and interfaces between these different phases. Figure 2.10 shows a schematic representation of the microstructure of a well hydrated portland cement paste (Mehta and Monteiro, 1996). In this figure A represents CSH particles, H shows hexagonal particles such as CH and C describes the capillary pores.

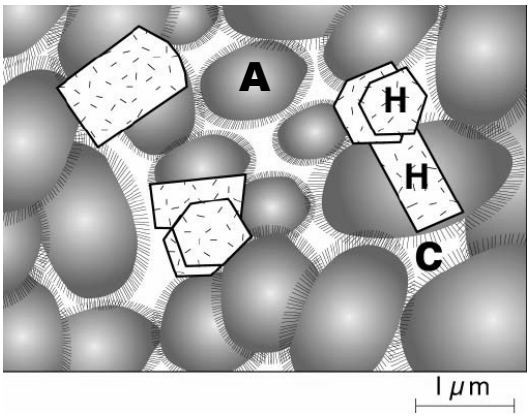

Figure 2.10: Model of a well hydrated portland cement paste

The amount of these different phases changes with the degree of hydration (see Figure 2.5); i.e. the volume of the CSH increases as the hydration proceeds but the amount of capillary pores decreases. The amount of gel pores in the cement paste also increases with the CSH amount. The CSH forms about 50 to 60 % of the volume of the solids in a completely hydrated cement paste and it is the main constituent responsible for the strength of the cement paste. Different types of CSHs are formed during the hydration process (Taylor, 1993). About 20 to 25 of the volume of solids in the cement paste is calcium hydroxide (CH) which are large hexagonal shaped crystals. Calcium sulfoaluminate hydrates form about 15 to 20 % of the volume of the solids. Besides these solid hydration products, the pores in the cement paste also have an important role on the properties of concrete.

A hardened cement paste is a porous material with an interconnected continuous pore system and depending on their sizes the pores can be divided as gel pores, capillary

pores and macro pores. Gel pores are interlayer spaces between the gel particles and have dimensions ranging from a few fractions of a nm to several nm (Neville, 2004). Because of their small sizes, gel pores do not affect the durability of concrete. Capillary pores, however, have much larger sizes ranging from 10 nm to several microns and interconnected capillary pores are one of the main factors affecting the permeability of cement paste. Macro pores such as entrained or entrapped air, are also present in the hardened cement paste with the dimensions sometimes up to a few mm.

Water/cement ratio is one of the main factors affecting the pore structure of hardened cement paste. Figure 2.11 shows the change of pore size distribution of cement paste due to change in water/cement ratio (Mehta and Monteiro, 1996).

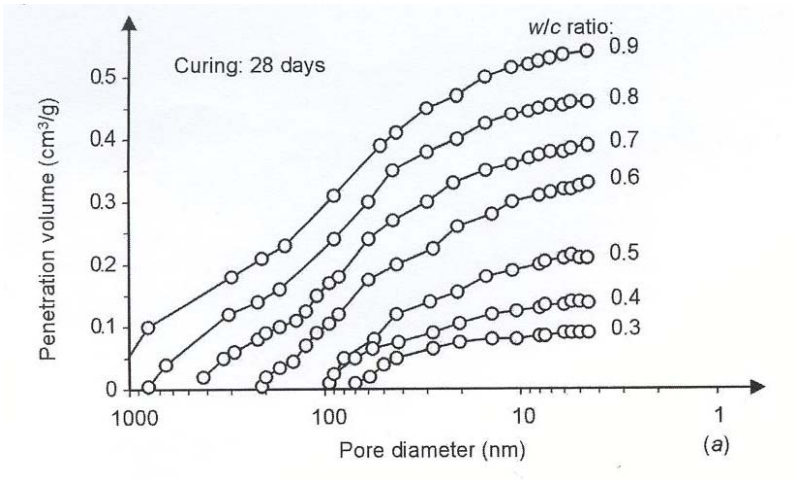

Figure 2.11: Effect of water/cement ratio on the pore size distribution of cement paste

The microstructure of cement paste at the immediate vicinity of the aggregate is different from that of the bulk paste. Figure 2.12 gives a schematic representation of this aggregate – cement paste interfacial zone (Mehta and Monteiro, 1996). Another representation of this zone is shown in Figure 2.13 (Chandra, 2002).

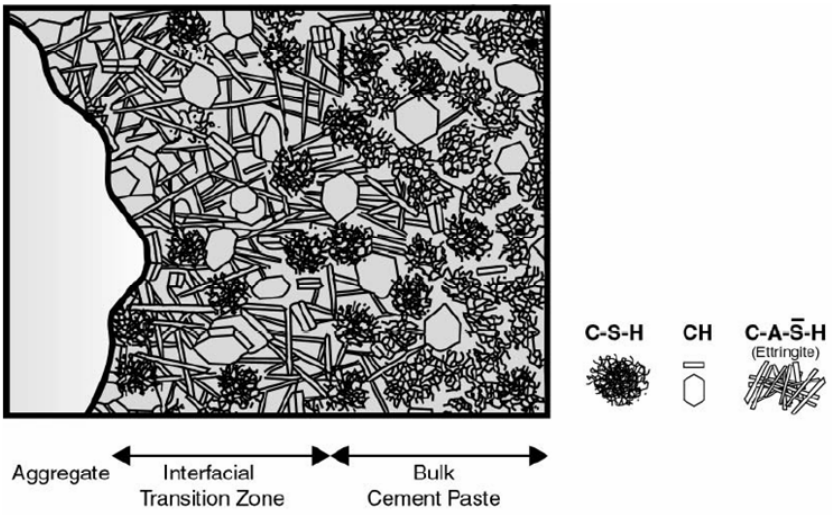

Figure 2.12: Aggregate – cement paste interfacial zone (Mehta and Monteiro, 1996)

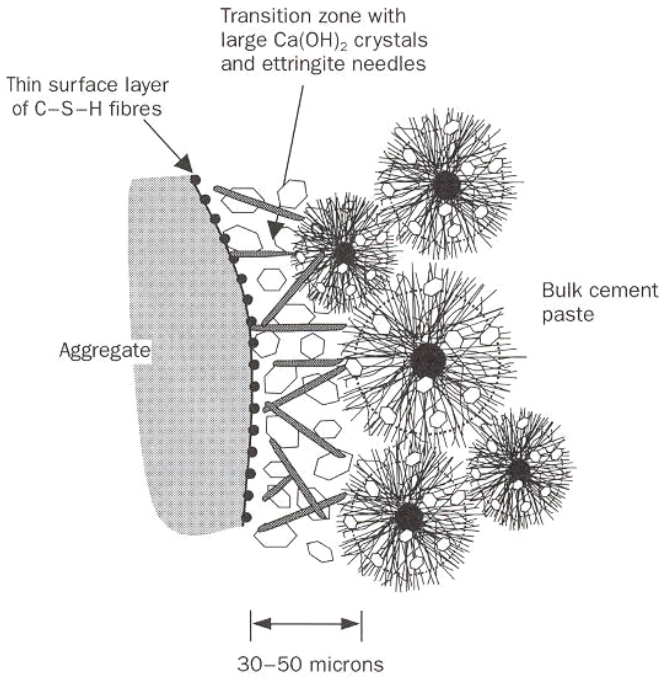

Figure 2.13: Aggregate – cement paste interface (Chandra, 2002)

Studies show that the amount of CH at the aggregate – cement paste interface is higher and the CH crystals are oriented perpendicular to the aggregate surface (Monteiro et al., 1985). A procedure for studying the orientation of CH crystals at the interface was developed in which the interface at the cement matrix side is successively removed by abrasion and X – ray diffraction analyses are carried out at each step. The diffraction intensities of CH crystals after the abrasions are then used for calculating an orientation index. The method is based on the fact that in the bulk

paste matrix the CH crystals are randomly oriented and the orientation index for random orientation equals to 1.0 (Monteiro et.al., 1985). Figure 2.14 shows the change of orientation index at the paste – aggregate interface (Massaza and Costa, 1986).

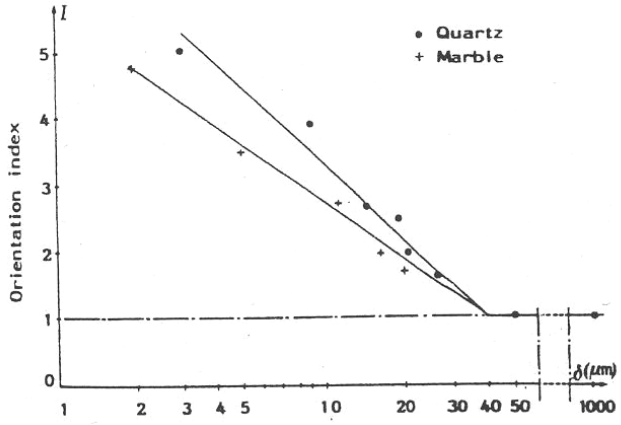

Figure 2.14: CH orientation index at the paste – aggregate interface

The porosity of the aggregate – cement interface is much higher and the strength is lower at this region. Figure 2.15 presents the variation in porosity of hydrated cement paste with distance from the surface of an aggregate particle (Neville, 2004).

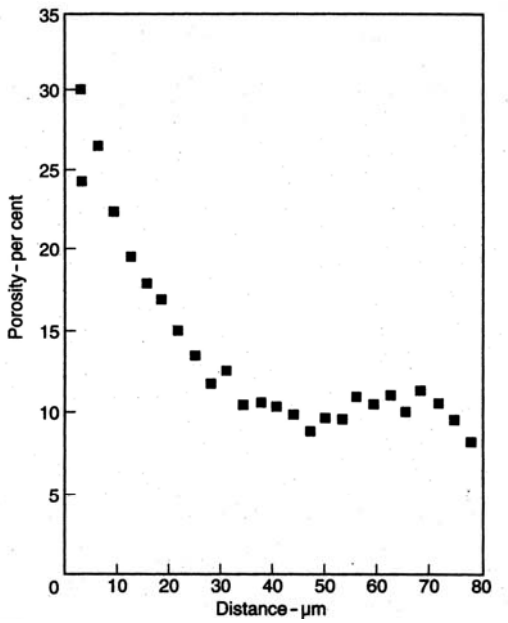

Figure 2.15: Porosity of the cement paste at the aggregate – cement interface

The formation of this interfacial zone with different properties may be due to combination different mechanisms. The cement grains pack poorly against a large

aggregate and as a result; there is less cement in this region to hydrate and to fill the voids. During the mixing of concrete, a water film forms around aggregate particles which causes a higher water/cement ratio at the aggregate surface. These effects may be the reasons behind the interface having different properties than the bulk paste.

The interface is the weakest link in concrete and has a big impact on the properties of concrete. Because of the higher porosity and lower strength, the interface can contain microcracks caused by shrinkage or thermal movements and these microcracks have an important effect on the stress – strain relationship of concrete. As a result of the higher porosity, the interface may also have an effect on the permeability of concrete.

2.4.2. Microstructure of Concrete Containing Fly Ash

Incorporation of fly ash into portland cement has an important influence on the microstructural properties of concrete such as refined pore size distribution or improved aggregate – cement paste interface.

Figure 2.16 shows the pore size distribution of a portland cement paste with and without fly ash (Fraay, 1989). As shown in the figure, the pore size distribution of cement paste with fly ash is initially coarser than the one without fly ash. At later ages, however, the pore size distribution of the paste containing fly ash is finer.

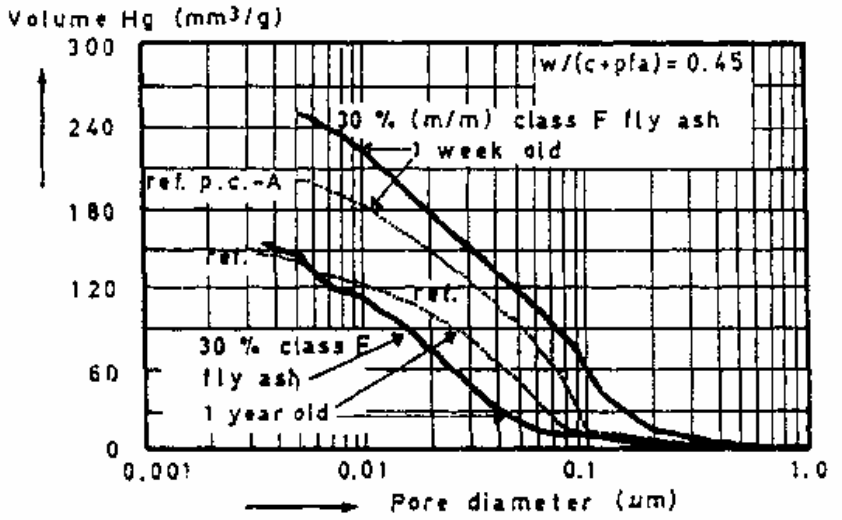

Figure 2.16: Pore size distribution of portland cement paste with and without fly ash

Fly ash has a significant effect on the aggregate – cement paste interface. Figure 2.17 shows the CH orientation index obtained for portland cement with and without fly ashes and quartz flour at 28 days age (Larbi, 1991). As seen in the figure, partially

replacing portland cement by fly ash reduced the orientation index in the immediate vicinity of the aggregate interface which indicates the decrease in the amount of CH at the interface. The thickness of the aggregate – cement paste interface can be defined as the region where properties are different than that of the bulk cement paste and as seen in Figure 2.17, the reduction in the CH orientation index indicates that the thickness of interface decreases with the use of fly ash. Since CH crystals have the planes of cleavage, the reduction of the orientation index values suggest that the resistance of the interface against the propagation of cracks increases with the use of fly ash (Saito and Kawamura, 1989). Pozzolanic reaction between the fly ash and CH is one of the reasons for the refinement of concrete microstructure. Better particle packing with the inclusion of fly ash also plays an important role for the improvement of the paste – aggregate interface.

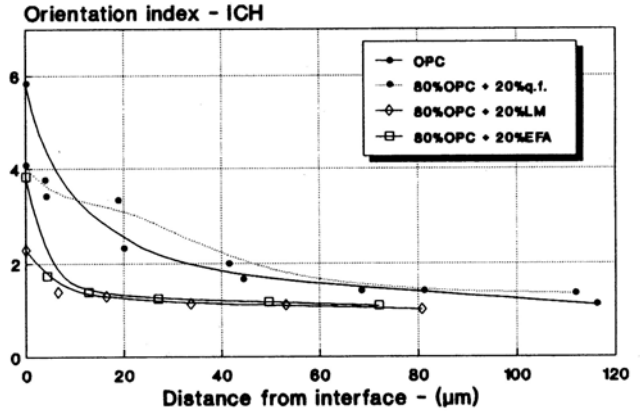

Figure 2.17: Effect of fly ash on the CH orientation index

2.4.3. Microstructure of Concrete Containing Blast Furnace Slag

Similar to the effects of fly ash, incorporation of granulated ground blast furnace slag also modifies the microstructure of concrete. CSH gel content of slag cement paste is significantly higher than that of portland cement as a result of less free lime generated (Bijen, 1996a). The CSH generated in concretes containing slag is compact, well crystallized and dense. Cement paste containing blast furnace slag has differences in total porosity and pore size distribution when compared to those of portland cement paste. At early ages slag, cement exhibits the same porosity as that of portland cement. However, at later ages, because the slag reaction continues for a long period, the volume of fine pores increases and the volume of capillary pores become lower. Although gel porosity increases and capillary porosity decreases by

the incorporation of slag, the total porosity is not affected significantly (Regourd, 2004). The amount used is also important for the effect of slag and Figure 2.18 schematically illustrates the change in the gel and capillary porosities based on the slag content (Lang, 2004). As seen in the figure, although the total porosity of the cement paste remains constant, capillary porosity decreases with slag amount.

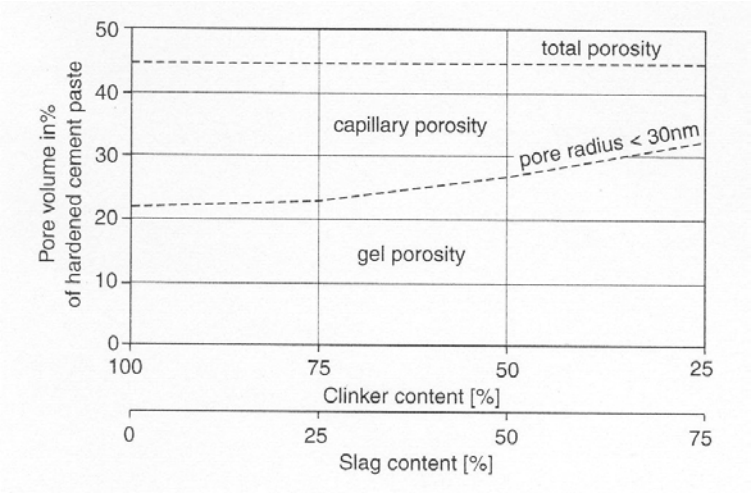

Figure 2.18: Pore size distributions of pastes based on the slag content

The additions of slag have a major effect on the transition zone between aggregate and cement paste. Figure 2.19 compares the degree of orientation of CH at the paste – aggregate interface in portland cement and blast furnace slag cement, for the age of 7 days (Larbi, 1991). As seen in the figure, the orientation index of slag paste is significantly lower even at 7 days.

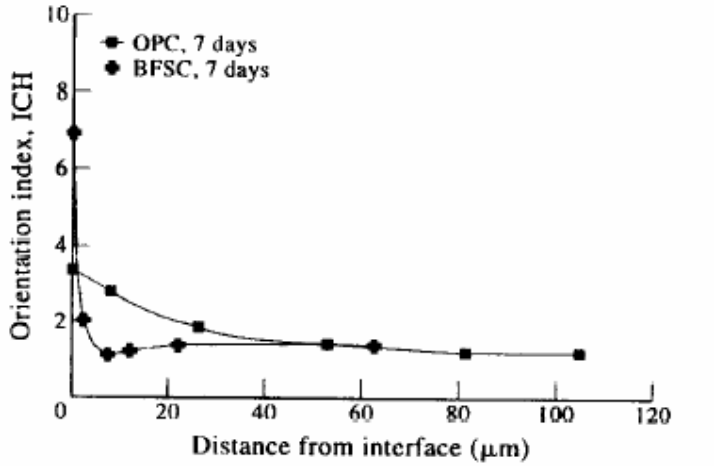

Fig. 2.19: Effect of slag on the orientation index at 7 days

2.4.4. Microstructure of Concrete Containing Silica Fume

Due to its high reactivity and extreme fineness, silica fume has a substantial effect on the concrete microstructure. Studies show that the pore structure of cement paste can be improved by the addition of silica fume. It was reported that refinement of pore size distribution of pastes takes place in a way that the content of larger pores reduces for decreasing water/cement ratios (Zhang and Gjørv, 1991). Figure 2.20 shows the effect of silica fume on the pore size distribution of low porosity cement pastes.

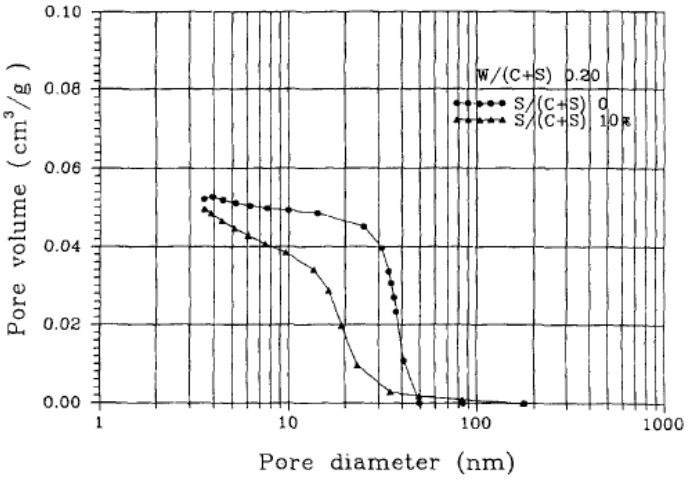

Figure 2.20: Effect of silica fume on the pore size distribution of paste

In addition to the refinement in pore size distribution of cement paste, silica fume also has an important effect in strengthening the aggregate – cement paste interfacial zone. This strengthening is attributed to the pozzolanic and the filler effects. For some researchers, however, the filler effect is more important than the pozzolanic effect. The filler effect depends on the fineness of the material which affects particle packing (Chengzhi et al., 1996).

In a previous study (Goldman and Bentur, 1994), strength of silica fume concrete was compared with that of a concrete containing an inert filler of similar fineness (carbon black). On the basis of microstructural studies and compressive strength tests, it was concluded that the primary effect of silica fume was generated by its physical (microfiller) properties, since the strengthening provided by reactive silica fume was similar to that obtained with nonreactive carbon black of similar size and shape. This effect was more significant from the point of view of the concrete strength enhancement than the chemical (pozzolanic) activity of the silica fume.

In the presence of silica fume or carbon black, densification of the transition zone occurred and significant refinement of pore structure was observed in both types of paste matrices (containing silica fume or carbon black). However, this refinement led to a relatively small influence on the paste strength. On the other hand, concretes containing reactive silica fume or an inert carbon black microfiller behaved as a composite material, unlike normal concrete. Figure 2.21 shows the results obtained in the study which indicates that microfiller effect has a higher importance than pozzolanic effect in strength enhancement of concrete (Goldman and Bentur, 1993).

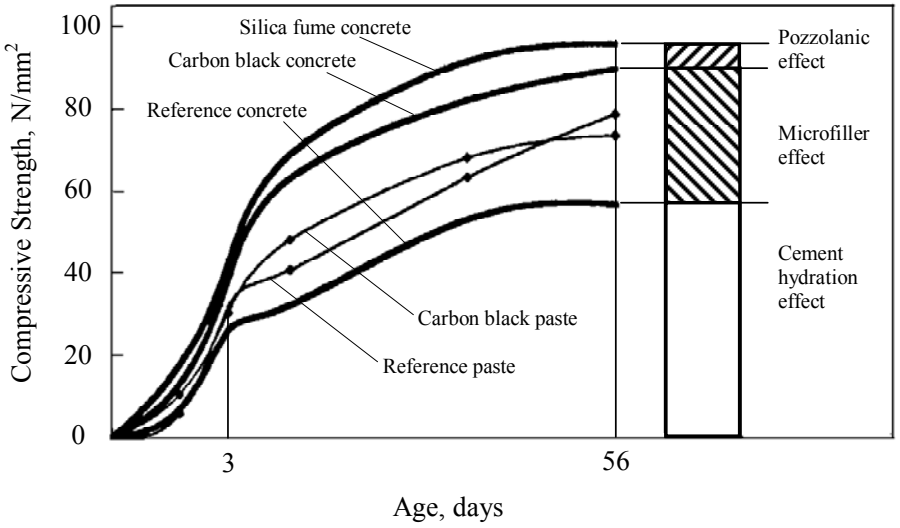

Figure 2.21: Strength of concretes containing silica fume and carbon black, and the contribution of pozzolanic and microfiller effects

It was also reported that, in the presence of silica fume, the orientation of CH crystals at the aggregate surface is affected during the first seven days of hydration, and at 28 days the CH is almost non-existent at the interface (Larbi and Bijen, 1990). Figure 2.22 schematically illustrates the aggregate – cement paste interface in the presence of silica fume (Larbi and Bijen, 1990).

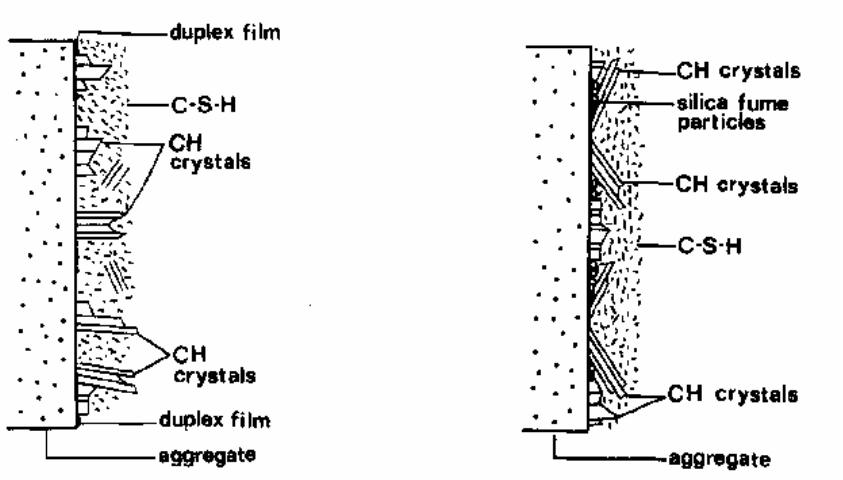

Figure 2.22: Schematic representation of the aggregate – cement paste interface (a) without silica fume, (b) with silica fume

2.5. Mechanical Properties of Concretes with Pozzolans

2.5.1. Concretes Containing Fly Ash

Due to the slow pozzolanic reaction of fly ash, fly ash concretes generally have a lower early strength. This strength reduction depends on the content and properties of the fly ash (Mehta, 1985). At later ages, however, with proper curing fly ash concretes can have a higher strength than the portland cement concrete. Figure 2.23 illustrates the effect of fly ash content on the strength of concrete (Neville, 2004).

Pozzolanic reaction takes place on the surface of the particles, thus, increasing the surface area of fly ash has an important effect on pozzolanic activity. The fineness of the fly ash is very important for the modification of cement paste-aggregate interfacial zone, which is the weakest link in concrete.

In a recent study (Demir et al., 2002), in order to study the influence of fly ash fineness on the strength development of concrete and the effect of grinding on the physical properties fly ash, a coarse F type fly ash with a Blaine surface area of 222 m^2/kg was ground to four different finenesses such as 337, 450, 538 and 604 m^2/kg. The corresponding retained values on a 45 μm sieve were 50%, 29.9%, 10.1%, 5.2%, and 3.7%, respectively. In grinding of the fly ash, a ball mill type of grinder has been used. Results showed that there is substantial effect of fly ash fineness on the strength development of concrete especially for long curing times; as the fineness of fly ash increases, the compressive strength of concrete increases significantly, and

more noticeable results are obtained for low cement/binder ratio. Results confirmed that the performance of concrete with fly ash depend not only on the mineralogical and chemical composition of fly ash, but also on its physical properties such as fineness and particle shape, and also on the water-binder ratio of the mix.

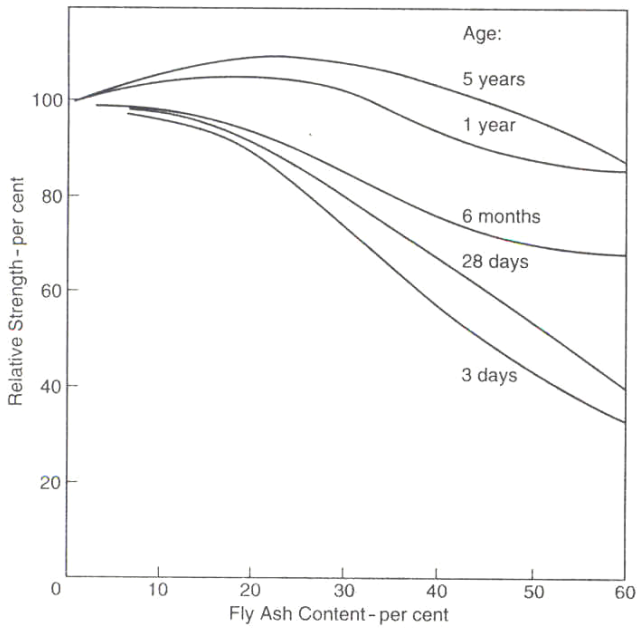

Figure 2.23: Effect of fly ash content on the strength development of concrete

The effect of fly ash fineness on the compressive strength is illustrated in Figure 2.24. In order to obtain higher strength with coarse fly ash, it was recommended to reduce water content or increase the binder content (McCarthy and Dhir, 1999).

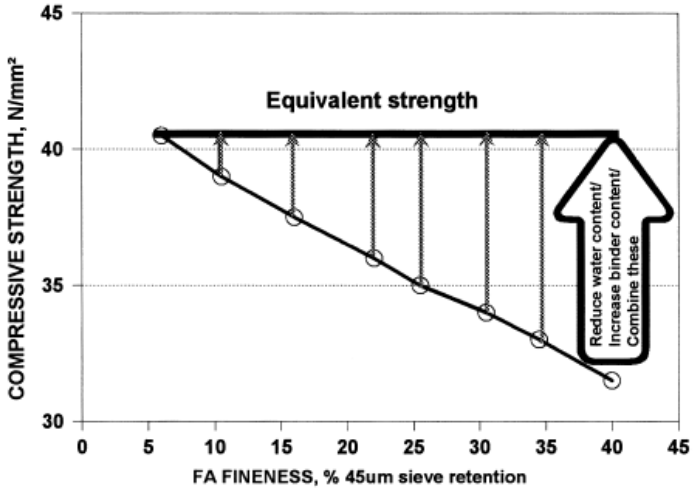

Figure 2.24: Effect of fly ash fineness on compressive strength

2.5.2. Concretes Containing Blast Furnace Slag

Strength of slag concretes are generally lower at early ages but slag concrete can outperform portland cement concrete at later ages. The replacement amount and properties of slag and curing conditions are important factors affecting the strength development of the slag concretes. The early age strengths of slag concretes are inversely proportional to the amount of slag (ACI Committee 233, 1995) and the replacement amount of slag is usually higher than fly ash (i.e. 50–70%). Separate grinding of slag and clinker, and blending them according to specific needs is a more optimized process (Oner, 2000). Figure 2.25 shows the effect of slag content on the strength development mortars (ACI Committee 233, 1995). As illustrated in the figure, at later ages the strength of mixtures containing slag are significantly higher than that of the portland cement mixture.

The particle size is also an important factor for the pozzolanic activity of the granulated blast furnace slag. Similar to the fly ash, the strength of slag concretes also increases with increasing slag fineness (Tasdemir et al. 1997). By using finely ground blast furnace slag, the aggregate – cement paste interface which is the weakest link in concrete can be improved and the thickness of this zone can be reduced. Better particle packing due to finer materials and the pozzolanic reaction of the slag are the reasons for this enhancement. By the densification of the aggregate – cement paste transition zone, concrete becomes more homogeneous and higher strengths can be obtained. This improvement may be more effective at lower water/binder ratios which can cause a better performance of the pozzolanic material. Figure 2.26 shows the effect of slag fineness on the compressive strength of mortars containing 75% slag (Hooton, 1987). As illustrated in the figure, the mortar strength increased about 30 % when the fineness of the slag was changed from 300 m^2/kg to 450 m^2/kg.

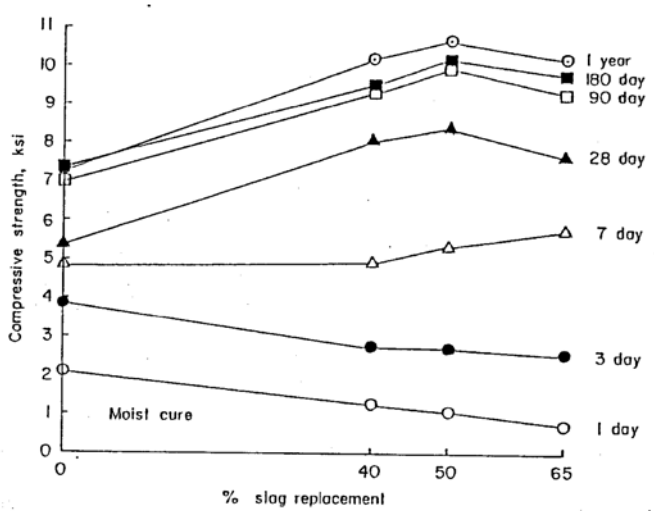

Figure 2.25: Effect of slag replacement amount on the strength development of mortars

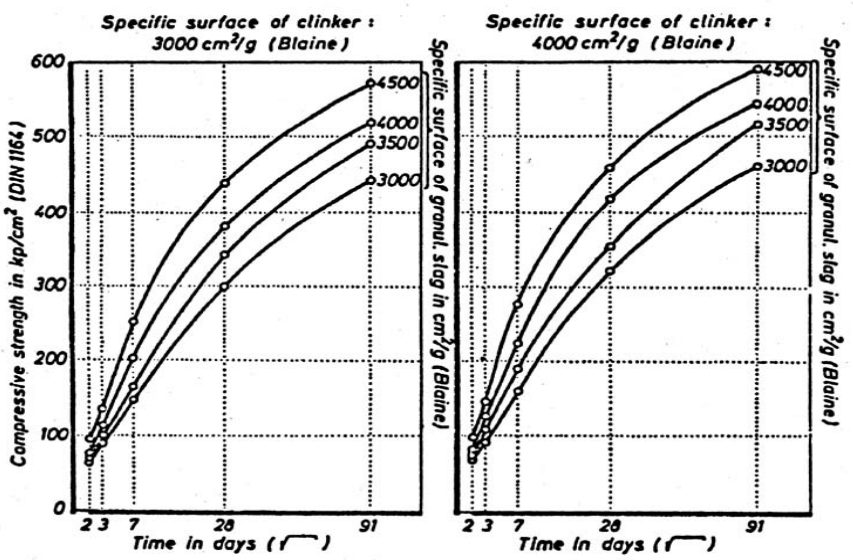

Figure 2.26: Effect of slag fineness on the strength development of mortars

2.5.3. Concretes Containing Silica Fume

Silica fume has an important impact on the aggregate – cement paste interface. The enhanced interfaces in silica fume concretes have been reported in numerous papers. As a result of strengthening the interfacial zone, mechanical properties of concrete is affected substantially. Unlike the other pozzolans (fly ash or slag), the silica fume takes effect at early ages and its contribution to the strength is important also in these ages. The effect of silica fume on the microstructure and strength of concrete was already discussed in previous chapters and strength development of silica fume

concrete was presented in Figure 2.21. Figure 2.27 illustrates the effect of silica fume replacement ratio on the compressive strength of concrete (ACI Committee 234, 1996). Although the figure shows the result for replacement up to 30%, the amounts used in practice are less than 15%.

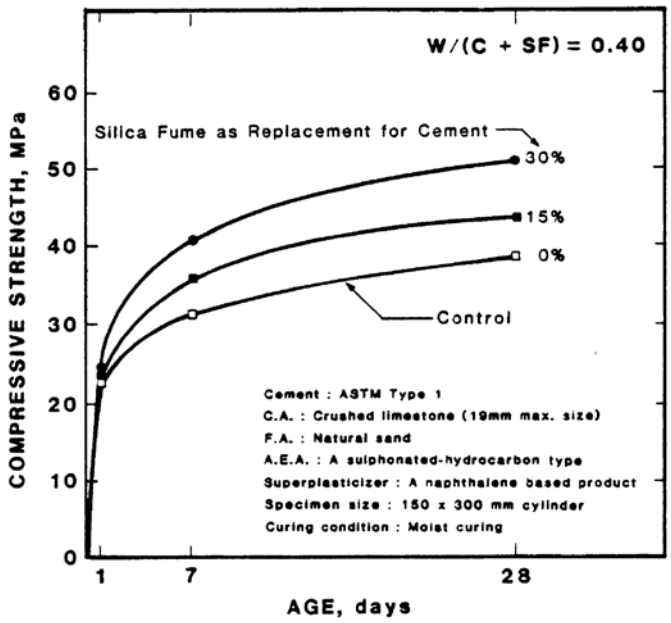

Figure 2.27: Effect of silica fume replacement ratio on the strength of concrete

Some of the disadvantages of using fly ash or slag concretes can be overcomed by the use of silica fume. Ternary (three part) and quaternary (four part) binders can be optimized with a synergistic effect in order to compensate for shortcomings of the component ingredients (Nehdi, 2001). By incorporating fly ash or slag with a highly reactive material such as silica fume, it is possible to obtain concretes with enhanced early age and also late age characteristics. For example, the low early age strength of high volume fly ash or slag concretes which can cause problems in winter concreting or in removal of formwork, can be improved with use of silica fume; or the heat development of silica fume concretes can be controlled by the use of fly ash or slag. Optimized particle packing and hydration characteristics are the main factors of the better performance of ternary and quaternary binder systems. The strength and density of interfacial zones in concrete are governed by the packing of materials at these zones. By using mineral admixtures of various sizes, the particle size distribution of the binder can be widened and a better particle packing can be obtained.

In addition to the filler effect, the synergic action in the multi blended binder systems continues for a long term. The early hydration of portland cement produces CH which is consumed by the early hydration of the highly reactive pozzolan (silica fume). The CH produced by the later hydration of the portland cement is consumed by the less reactive component in the blend such as fly ash or blast furnace slag, to provide further refinement of porosity and improvement of microstructure. This sequence of hydration reactions has a big impact in decreasing the permeability and a result in improving the durability of the concrete (Nehdi, 2001).

2.6. Chloride Resistance of Concretes Containing Pozzolans

2.6.1. Concretes Containing Fly Ash

Deterioration of concrete depends on the penetration of aggressive substances into concrete via microcracks and interconnected pore system. Permeability of fly ash concretes at early ages can be significantly higher when compared to that of portland cement concrete. At later ages, however, fly ash concretes can have much lower permeability depending on the replacement ratio and characteristics of the fly ash. Proper curing is especially important for fly ash concretes in order to achieve lower permeability (Tasdemir, 2003). As briefly discussed in previous chapters, the incorporation of fly ash modifies the microstructure of concrete and a much finer pore system can be obtained which affects the durability of concrete. Clogging of pores and increase in tortuosity of pore channel are responsible for the improved permeability properties (Li and Roy, 1986). The substantial effect of fly ash on the pore structure is not reflected so much in the permeability, but rather in the diffusivity of ions (Bijen, 1996b).

Figure 2.28 shows the effect of fly ash replacement ratio on the chloride diffusivity and chloride binding ratio, which were obtained on specimens 28 days old (Dhir et al., 1997). As seen in the figure, chloride diffusion coefficient is reduced with the fly ash replacement amount. The figure also shows that as the PFA content increases the chloride binding capacity increased up to a level of 50%. At 50% PFA content and a chloride exposure concentration of 5 mole/liter, the chloride binding capacity increases by a factor of 4 compared with the control. These results indicate that chloride binding would appear to be at least as important as improving the physical aspects of concrete and in the case of FA concrete may even be the dominant factor

in improving the resistance of concrete to chloride attack. The combined effect of improved permeability properties and chloride binding further improves the resistance of fly ash concrete against chloride penetration. Long – term sea water exposure tests confirm the better performance of fly ash concretes. Results obtained from reinforced concretes in a marine environment show that, concretes containing 30 % or more fly ash provides much improved protection to steel reinforcement compared with portland cement of equal strength grade, equal binder content or equal water/binder ratio (Thomas, 1991; Thomas and Matthews, 2004). A report on the resistance of the concrete to chloride ion penetration measured according to ASTM C 1202 on 10 year old concretes also indicate the long term performance of concretes with pozzolans (Malhotra, 2000). The charge passed through the concrete mixtures investigated in the study was less than 1000 coulombs at 10 years indicating very low chloride-ion penetrability. For the high-volume fly ash concrete, the charge passed was 0, giving a chloride-ion penetrability rating of this concrete as negligible. It is extremely rare to achieve values as low as this in portland cement concrete; one can obtain such a low value only for polymer or polymer impregnated concrete because of the extremely low porosity of the system (Malhotra, 2000).

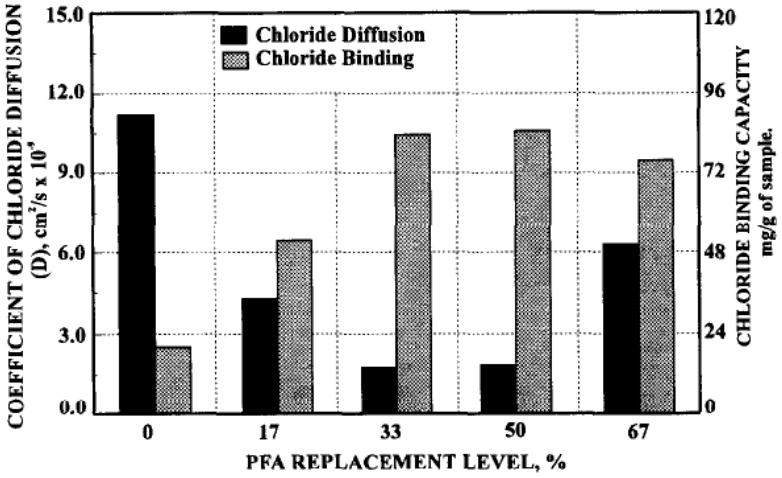

Figure 2.28: Effect of fly ash replacement ratio on the chloride diffusivity and chloride binding

Fineness of fly ash is one of the important factors influencing the chloride diffusivity of the fly ash concrete. Figure 2.29 compares the chloride diffusivity of a normal concrete with two fly ash concretes; one containing a normal (unprocessed) fly ash and the other with a ground fly ash (Dhir and Jones, 1999). In the study, a coarse fly

ash was processed until all particles were finer than 10 μm. This fine ash was used to directly replace portland cement by up to 30 % by weight to produce concrete samples with cube strength of 40 MPa. The accelerated chloride diffusion test was then used to determine the coefficient of chloride diffusion, as shown in the figure. As illustrated in Figure 2.29 the addition of unprocessed fly ash decreased the diffusivity more than 60 %. When the ground fly ash was used, the diffusivity was 88% lower than that of the portland cement concrete. If only the concretes containing fly ash are compared, the ones produced with ground fly ash had about 70 % lower diffusivity than the one produced with the unprocessed fly ash. The improved chloride resistance of concretes containing fine fly ash has been reported also in other studies (Dhir, et al., 1991; Schiessl and Wiens, 1995).

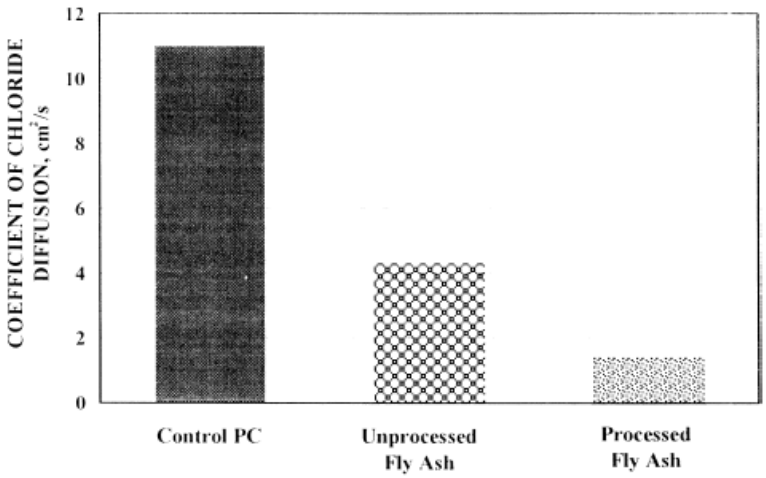

Figure 2.29: Effect of fly ash fineness on the chloride diffusivity of concrete

2.6.2. Concretes Containing Blast Furnace Slag

Studies have shown that concretes containing blast furnace slag provides significant protection against chloride induced corrosion of embedded steel. The rate of chloride is greatly reduced due to the improved pore structure of concrete. Depending on the amount and characteristics of the slag, the chloride diffusivity of concrete can be decreased by a factor 150 (Bijen, 1996). The resistance of concretes to chloride ion penetration increases with an increase in the slag content (Sivasundaram and Malhotra, 1992; Gjrøv and Vennesland, 1979; Pal, et al., 2002). Figure 2.30 illustrates the effect of slag replacement amount on the resistance of concrete against chloride penetration (Lang, 2004). Results given in the figure were obtained on concrete cubes stored in NaCl solution for one year. The chloride content had been

analyzed in a layer 20 – 40 mm under the concrete surface. As seen in the figure, the effect of slag is insignificant up to 20 % replacements, but beyond this ratio a substantial decrease in the chloride content was observed. Very similar results for the effect of slag content on the chloride diffusivity were also reported (Bijen, 1996a and 1996b). Field studies carried out on concrete structures along the sea coast confirm the better performance of slag concretes in marine environment (Bijen, 1996a; Osborne, 1999).

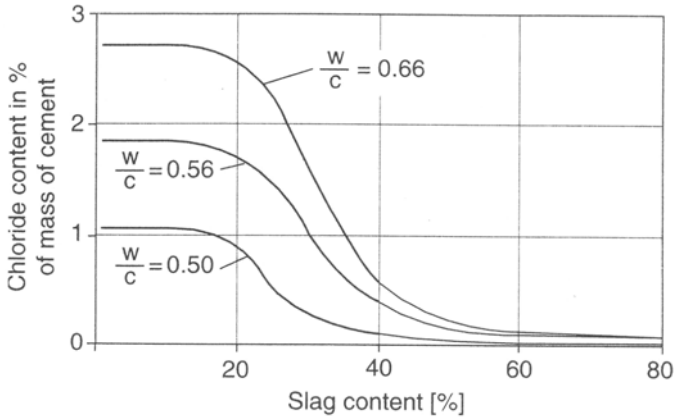

Figure 2.30: Effect of slag replacement amount on resistance of concrete against chloride penetration

The electrical resistivity of concrete is an important component of reinforcing steel corrosion cells, as high resistivity of the concrete reduce corrosion currents and slow the rate of corrosion (Whiting and Nagi, 2003). The electrical resistivities of concretes containing slag are significantly higher which extends the initiation and propagation period of corrosion of the embedded steel (Hou et al., 2004). As seen in Figure 2.31 the electrical resistivity of concrete increases with the slag amount (Geiseler et al., 1995).

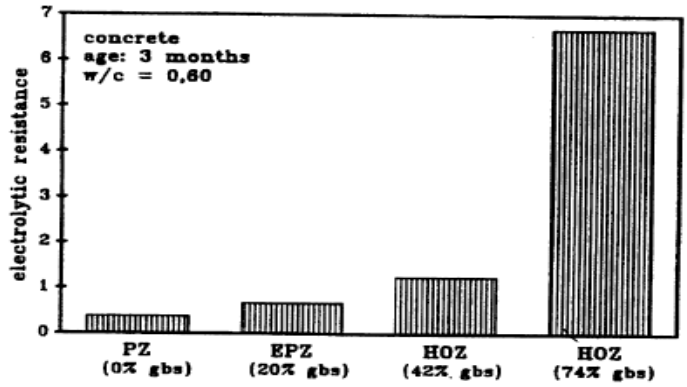

Figure 2.31: Effect of slag amount on the electrical resistivity of concrete

2.6.3. Concretes Containing Silica Fume

Silica fume is very effective in controlling chloride penetration into concrete and paste (Bentz et al., 2000). Improved cement paste pore system and densification of the porous aggregate – cement paste interface are the causes of better performance of the concretes containing silica fume. The replacement ratio has an important effect on the resistance against chloride penetration. It has been reported that inclusion of 7% silica fume can cause 80 % decrease in the diffusivity of portland cement concrete and this reduction can be about 90 % when 12 % silica fume is used (Hooton, et al, 1997). Silica fume is more efficient for reducing diffusivity of mixtures with lower water/cement ratios (Bentz, 2000).

In chloride containing environments, multi-blended binder systems containing silica fume perform better than the binary blends (Bleszynski et al., 2002) In a recent study, it was concluded that regardless of the type of fly ash, water/binder ratio or the fly ash and silica fume contents, the concrete made with the ternary blend of fly ash and silica fume outperforms the concrete made with portland cement alone as well as the concrete made with the binary system (Bouzoubaa et al., 2004).

The better durability characteristics of multi-blended binder systems are the results of decreased permeability properties. Porosity and microstructure are improved by the pozzolanic effects (of silica fume and fly ash or slag) and filler effect (of silica fume) that affect particle packing (Mangat et al., 1994). Interface porosity is reduced significantly by the incorporation of silica fume together with another pozzolan (Poon et al., 1999). The synergic action in the multi-blended binder systems continues for a long period and as a result very high resistance against the penetration of chlorides can be obtained (Hisada et al., 1999; Malhotra et al., 2000). Thus, substantial increase in the service life of the structures can be obtained.

2.7. Environmental and Economical Aspects of Concrete Production

2.7.1. Human Impacts on the Planet

During the last 100 years, world population has increased from 1.5 billion to more than 6 million. This increase was dramatic in the last 50 years in which the population has doubled. The increase from 5 billions to 6 billions has taken only 12

years (Swamy, 2001). It is estimated that the population will increase about 50 % in the next 50 years (US Census Bureau, 2004).

The lifestyle of people also changed noticeably in the last century; about 50 % of population now lives in and around cities rather than rural areas. As a result of the rapid growth in population and industrialization, the demand and consumption of natural resources of the planet is increasing and this consumption is unrestricted. Current economic models and technology choices are promoting wasteful consumption of materials. It is estimated that only 6 % of global flow of materials, some 500 million tons a year, actually ends up in the desired products while most of the virgin materials are returned to the environment as harmful solid, liquid and gaseous wastes (Mehta, 2001). The uncontrolled and wasteful consumption of resources is one of the main causes of the environmental damage.

The demand for energy is constantly increasing in today's world. During the past 100 years, the energy production from burning of the fossil fuels has increased 16 fold (Mehta, 2002) and fossil fuels are the primary source of energy today. Combustion of fossil fuels is a direct cause of the green house gas CO_2 release into the atmosphere. Thus, any approach to decrease fossil fuel consumption has a beneficial effect in reducing CO_2 emissions. In the past 100 years, the release of large volumes of CO_2 has increased atmospheric concentration of this gas from 260 to 370 ppm which is the highest level in 400000 years. The consequence of the emission of greenhouse gas is the global warming which causes serious disruptions to environment and also lives.

2.7.2. Ecological Impact of Concrete

Concrete is the world's most important and widely used construction material (Aitcin, 1995). According to CEMBUREAU, in 1998, the total world production of cement was about 1.6 billion tons and if it is assumed that about 250 kg of cement are used to produce 1 m^3 of concrete, about 6.5 billion m^3 of concrete was used in 1998. The cement production in the world is expected to exceed 2.5 billion tons in the year 2050. Being the largest user of natural resources, concrete production has a serious effect on environment (Mehta, 1999). Every year, concrete industry is consuming 10 billions tons of sand and rock, 1 billion tons of mixing water and even larger amounts for wash water and curing.

After aluminium and steel, the manufacture of portland cement is the most energy intensive material production process. Producing a ton of portland cement requires about 4 GJ energy and this manufacture releases about 1 ton of CO_2 greenhouse gas into the atmosphere. Minor amounts of other gases are also released. Cement production releases about 1.4 billion tons of CO_2 every year which is about 7 % of the CO_2 production worldwide (Malhotra, 2000). About half of the CO_2 emissions are due to the calcinations of limestone and the other half are due to the combustion of fossil fuels. The mining, processing and transport of the large quantities of aggregates also consume considerable amounts of energy and affect ecology.

Uncontrolled and short service life of concrete structures is another source of the environmental impact of concrete. Considerable amounts of concrete are being used for repair and strengthening of existing structures. In UK, for example, 50 % of the construction industry output is spent on repair, strengthening and maintenance. It is estimated that the structural damage repair in Europe costs 1.4 billion Euros annually (Swamy, 2001).

2.7.3. Environmental and Economical Effects of Using Pozzolans in Concrete

The long term approach to decrease environmental impact of any material is to reduce its rate of consumption, but reducing concrete consumption cannot be done in the next few decades. Increasing the effective use of the materials and portland cement, production of low energy intensive cements, increasing the service life of the structures and infrastructure, and recycling are some of the measures to reduce the environmental impact of concrete (Aïtcin, 2000).

First step in decreasing the energy consumption and greenhouse emissions caused by the concrete production can be reducing the portland cement use by incorporating pozzolanic materials in concrete (Malhotra, 1999). The pressure of ecological constraints and environmental regulations are bound to increase in the coming years which will lead to greater use of supplementary cementitious materials such as fly ash, blast furnace slag or silica fume (Bentur, 2002). As summarized in previous chapters, by replacing part of cement with the pozzolanic materials, it possible to obtain improved fresh and hardened concrete properties. Replacing more than 50% of cement by pozzolanic materials lead to the definition of “green concrete” (Glavind and Petersen, 2002). This term represents environmentally friendly concrete, which

contains high volumes of pozzolans, generally has low water/cement ratio and high durability properties.

Because most of the pozzolans are readily available for utilization and no need for production is needed, the cost of incorporating them into concrete includes mostly the transporting and storage costs. In some cases there can be a need for processing the pozzolan to obtain better performance. The cost of processing the pozzolan, however, is significantly lower than producing portland cement. Fly ash and silica fume normally do not need additional energy input before use, and with the use of fly ash for replacement of cement, energy saving in direct proportion to the amount of pozzolan can be obtained. Blast furnace slags, however, need to be dried and ground before use and it is estimated that the total energy requirement for this purpose is about 20% of that required for portland cement (Lohtia and Joshi, 1995).

Energy requirements for the production of pozzolan blended cements depend on the properties and the amounts of the pozzolan used in cement (Frigione, 1996). Figure 2.33 illustrates the effect of slag replacement amount on the energy consumption of cement (Lang, 2004). As seen in the figure, the energy consumption decreases with the slag replacement amount. For the 30 % slag replacement, the energy requirement decreased 24 %. The energy required for the production of cement with 75 % slag replacement is 38 % of the energy needed for portland cement.

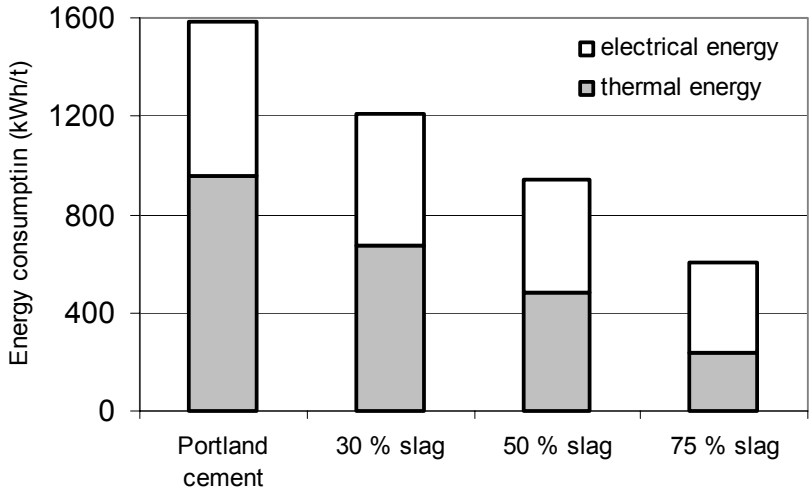

Figure 2.33: Effect of slag replacement on energy consumption

Among several methods, use of large amounts of pozzolanic materials in concrete appears to be the most effective method for reducing the emissions of CO_2 caused by the portland cement manufacture (Gartner, 2004). By incorporating pozzolans into cement, CO_2 emissions can be decreased substantially. For example, for the cement with 30%, 50% and 75% slag replacements, the emissions are 72%, 51% and 29.7% of the portland cement, respectively (Lang, 2004).

The most available pozzolan worldwide is fly ash. It is estimated that about 600 million tons of fly ash was available in 2000 but only 6% of it was used in cement or concrete industry. The annual slag production is about 100 million tons worldwide but again, only a very small fraction is utilized. These pozzolans are by-products and storage of these huge amounts is a major challenge. When they are stockpiled on land, they cause air pollution and during rainfall or snow melt season, the migration of ions from the dumped wastes can cause pollution of subsoil and ground water. In additon, toxic metals which are usually present as trace elements, can be released and pollute lakes or streams. By increased utilization in concrete and cement, some of the problems and costs associated with the environmentally safe storage or disposal of these materials can also be reduced. Besides using in concrete as supplementary cementing materials, pozzolans can be utilized in other applications in construction industry. Fly ash, for example, can be used in road construction for sub bases, in landfill applications or to produce aggregate for concrete (Sear, 2002).

2.8. Micro Indentation Testing of Cementitious Materials

2.8.1. Introduction

Concrete is an extremely complex system of solid phases, pores and water, with a high degree of heterogeneity. The properties of concrete are determined by the characteristics of constituent materials and the interfaces between cement paste and aggregate. Since about 75 percent of the concrete volume is occupied by aggregate, interfacial region between aggregate and cement paste matrix forms an important proportion of cement paste and this region greatly affect the durability and the structural performance of concrete. As described in Chapter 2.4, the microstructure of the hydrated cement paste in the immediate vicinity of coarse aggregate particles is different from that of the bulk cement paste. The thickness of the interfacial zone varies from 20 μm to 100 μm which depends on the materials used and the properties

of the concrete (Monterio et al., 1985; Zimbelman, 1985). The interfacial zone is porous and contains large crystals of $Ca(OH)_2$ perpendicular to the aggregate surface. There are two major reasons for the formation of this interfacial zone: i) wall effect: inefficient packing of the cement particles at the aggregate interface, ii) high water/cement ratio at the aggregate surface. It was well established that the paste-aggregate interface is the weakest link and therefore the mechanical properties of concrete are significantly affected by the properties of this interfacial zone. When the aggregate and cement paste are individually subjected to uni-axial compression, they exhibit an almost linear stress-strain relation. Concrete, however, shows inelastic behaviour due to the presence of interfaces between the cement paste and the aggregate (Neville, 1997). To determine the influence of the interfacial zone on the mechanical properties of concrete, the material can be considered as a three phase composite model consisting of mortar matrix (or cement paste), aggregate and interfacial zone between cement paste and aggregate (Tasdemir et al., 1998).

There are various techniques for determining the porosity, orientation of crystals or the chemical composition of the cement-paste aggregate interface, but measurement of the mechanical properties of such a small zone is difficult. Hardness measurements have been used successfully for many years and it is a useful technique for characterizing the properties of materials like metals, ceramics or rocks (Van Vlack, 1994). Hardness can be defined as the resistance of a material to penetration. An indenter is pushed into a smooth material surface under controlled load and the size of residual impression is measured to calculate the hardness (ASTM E 384a, 2005). The geometry of indenter tip may differ and hardness type is named after it (i.e. vickers, brinell, knopp hardness).

Hardness measurement is also used in characterizing the properties of cement-based materials and because of using very small loads; it is often termed as microhardness (Igarashi, et al., 1996). Microstructural properties of interfacial transition zone between cement paste and aggregate, and bulk paste can be evaluated by microhardness tests. It is a non-destructive technique by which the transition zone can be easily mapped.

In recent years there have been great developments in testing techniques. With the developments in “thin film” industry, measuring the mechanical properties at such a small scale became important and this need lead to a new testing method known as

depth sensing indentation. In this form of indentation testing; displacement of the indenter tip and load are recorded continuously under computer control and load – displacement curve is obtained during loading and unloading cycle. Elastic, plastic and time – dependent deformation properties of the material such as hardness, modulus of elasticity, fracture toughness or creep can be obtained with such loading (Trtik and Bartos, 1999). The interfacial zone between concrete and reinforcement and elastic modulus of cement phases can be studied by nano – indentation (Velez et al., 2001). Sub – micrometer indentations are possible and this technique is often referred as ultra – low load or nano – indentation. It is routinely used to characterize the properties of thin films, very soft coatings and materials like polymers, magnetic storage systems, micro-electromechanical system devices and in medical research (Li and Bhushan, 2002).

Nanotechnology based techniques like scanning and transmission electron microscopy, atomic force microscopy or mercury intrusion porosimetry have been used for characterizing cementitious materials, but up to recent years there were no nano – technology based mechanical testing methods. With the development in depth sensing nano – indentation testing techniques, it is now possible to evaluate the micromechanical properties of cement – based materials. There is very little information in the literature about mechanical testing of the aggregate – cement paste interface by nanotechnology based testing techniques.

Mechanical and physical properties of cementitious materials depend on the microstructure and the development of microstructure is a nanoscale process which is not fully understood. Establishing a realistic model of aggregate – cement paste is not possible without the mechanical properties of the interfacial zone.

2.8.2. Depth Sensing Nano Indentation Technique

In conventional indentation testing, a specified load is pressed onto a surface and hardness is obtained by;

$$H = \frac{P}{A} \tag{2.4}$$

where H is hardness of the material, P is the maximum load, and A is the projected area of permanent impression measured after the indentation.

A typical hysteresis curve, obtained during loading – unloading indentation cycle by a new – generation depth sensing microhardness tester, is given in Figure 2.34.

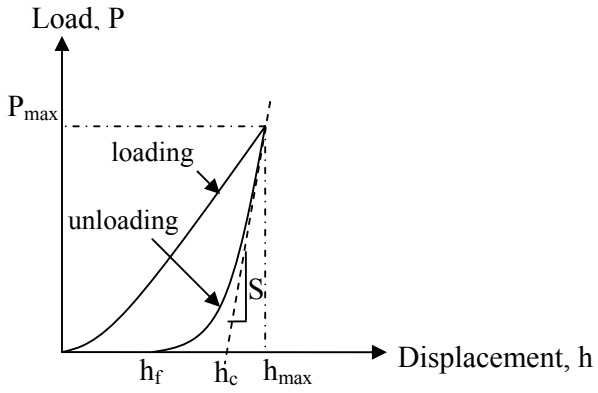

Figure 2.34: A typical load-deformation indentation curve

In Figure 2.34, h_{max} is the displacement at peak load P_{max}, h_f is the final displacement after complete unloading, hc is the plastic contact depth of indentation, and S is the initial unloading contact.

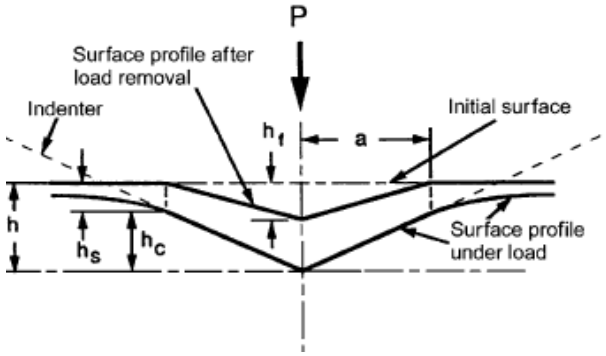

Figure 2.35: Deformations of a material during and after indentation

As seen in Figure 2.35, when indenter is pressed into the sample during loading both elastic and plastic deformations occur. During indenter withdrawal, however, only the elastic deformation is recovered and modulus of elasticity of the material can be obtained by analyzing this unloading curve. The load – displacement curves produced by depth sensing indentations may be analyzed based on Oliver – Pharr method (1992).

Initial unloading contact stiffness shown in Figure 2.34 is given as;

$$S = \frac{dP}{dh} \qquad \textbf{(2.5)}$$

which is equal to;

$$S = \frac{2\beta}{\sqrt{\pi}} E_r \sqrt{A} \tag{2.6}$$

where; A is the projected area of contact, β is a constant depending on indenter geometry, and E_r is the reduced modulus of elasticity which accounts for deformation of both sample and the indenter. E_r is given by

$$\frac{1}{E_r} = \frac{(1-\nu^2)}{E} + \frac{(1-\nu_i^2)}{E_i} \tag{2.7}$$

where E and ν are the elastic modulus and Poisson's ratio for the sample and E_i and ν_i are those of indenter. For diamond indenter E_i=1141 GPa and ν_i=0.07.

From Equations (2.6) and (2.7) the modulus of elasticity of the material can be calculated. The projected area of contact for an indenter with known geometry can be obtained as a function of depth. There is no need to measure the permanent impression using this type of new generation indentation testing machines as in conventional testing. The contact depth hc is given as

$$h_c = h_{\max} - \varepsilon \frac{P_{\max}}{S} \tag{2.8}$$

where ε depends on the geometry of indenter.

The deformation of the testing system must be calibrated and taken into account for the calculation of S, otherwise the measured displacement will be the displacement of the loading system and the obtained stiffness will be total system stiffness. The displacement of the load-frame is removed from the measured displacement and only the displacement of the indenter tip into the sample is obtained which is used to calculate the modulus of elasticity of the sample.

10. CONCLUSIONS

The effects of pozzolans on the mechanical and durability properties of concrete were investigated in this study. Fly ash, granulated blast furnace slag and silica fume were used in the experimental program, and of these pozzolanic materials mostly the ones with smaller particle sizes were preferred. Substitutions of commercially available cements by these pozzolans varied from low to high amounts and in addition to the binary blends of cements and pozzolans, ternary and quaternary blended mixtures were also prepared.

Some mechanical properties of concretes such as compressive strength and brittleness index were obtained at different ages. The main durability parameter investigated in this study was the resistance to chloride ion penetration. In addition, electrical resistivities of the mixtures were monitored with different methods and the relationship between the chloride diffusivity and electrical resistivity was presented.

An extensive study on the factors affecting the electrical resistivity obtained by the wenner electrode method was also investigated as a part of this study.

Based on the strength and resistance to chloride penetration of the concretes, two different optimization techniques were performed on some of the mixtures.

In addition to the mechanical and durability properties, tests such as chloride binding, temperature measurements and capillary water absorption were also carried out on some of the mixtures. In order to investigate the effects of the pozzolanic materials on the aggregate - cement paste interface, a new indentation technique was also included in the study.

Field studies also formed an important part of the experimental program. Results obtained from the chloride penetration tests and data obtained from the field studies were used as input in a probability based durability design of a typical structure in a marine environment.

The conclusions obtained from this study can be summarized as follows;

10.1. Effect of Pozzolans on the Mechanical Properties

i) In general, depending on the replacement ratio, mechanical properties of the concretes containing pozzolans have lower early strength when compared to portland cement concretes.

ii) Partially replacing portland cement by slag or fly ash is more effective in low water/binder ratios for obtaining better concrete strength properties.

iii) When portland cement was partially replaced with ground fly ash, the compressive strengths were in excess of 34 MPa at 28 days even at 70 % replacement level; and such a fly ash concrete can be considered as a structural concrete. At the age of 1 year, the compressive strength of concretes containing 40% fly ash was almost the same with that of the no fly ash concrete. At this age, the compressive strength of the concrete with 70% ground fly ash was 80 MPa. Mortar specimens confirmed the beneficial effect of the fly ash on the strength development.

iv) At the age of 28 days and beyond, the compressive strength of the concretes containing 40% or 60% finely ground blast furnace slag were higher than those of the portland cement concrete.

v) Silica fume enhanced the strength of the concretes even for the early ages such as 3 days.

vi) Strength of the ternary blends of portland cement – slag – silica fume concrete outperform the portland cement concrete at later ages.

vii) Pozzolanic effectiveness ratio can be used for the assessment of pozzolanic activity of the fly ash. The PER values increased with the age of concrete and also with the fly ash replacement ratio.

viii) A force of 10 gr was used for the micro - indentation test and the resulting depth of the indent was between 1.5 – 3.5 microns. Modulus of elasticity of cement paste obtained by the micro-indentation testing was close to the ones obtained from the stress – strain diagram of the cylinder specimens.

ix) Brittleness index of the concretes increased with compressive strength.

10.2. Effect of Pozzolans on the Durability Properties

10.2.1. Resistance to Chloride Ion Penetration

i) Partially replacing portland cement by pozzolanic materials caused significant improvements in the resistance of concrete against chloride penetration, especially at later ages.

ii) Decrease in the water/binder ratio from 0.60 to 0.38 affected the rapid chloride permeability of the portland cement concrete more than those of the concretes with high amount of slag or fly ash. However, the chloride permeability of the fly ash or slag concretes at 0.60 water/binder ratio were lower than that of the portland cement concrete at the water/cement ratio of 0.38.

iii) Replacing portland cement by ground fly ash up to 30% reduced the chloride permeability significantly. Beyond this level, the chloride permeabilities were almost constant.

iv) Incorporation of the blast furnace slag resulted in important decreases in the chloride diffusivity of concrete. Lower diffusivities were obtained with increasing slag content. This effect was more significant for the concretes containing ordinary portland cement.

v) The use of silica fume reduced the chloride diffusivity of the concretes also at the early ages.

vi) Ternary (three-part) or quaternary (four-part) blended concretes performed better than the binary blended concretes.

10.2.2. Electrical Resistivity

i) Blast furnace slag increased the electrical resistivity of the concrete significantly and the increase was more noticeable with the amount of slag.

ii) Addition of silica fume increased the resistivity of concrete.

iii) Ternary (three-part) or quaternary (four-part) blended concretes had higher resistivity than the binary blended concretes.

iv) The relationship between the two electrode method and the wenner electrode method were confirmed with the test results.

v) Specimen type affected the resistivity obtained by the wenner electrode method. However, strong relationships were obtained between different types of specimens and probe spacings.

vi) Test results confirmed the strong relationship between electrical resistivity and chloride diffusivity. Using such a relationship the diffusivity can be estimated by testing the resistivity.

10.2.3. Capillarity Characteristics

Capillary water absorption tests were carried out on the concrete series containing blast furnace slag. Capillarity water absorptions of concretes were reduced with the replacement of portland cement by slag and the reduction became more noticeable with the increase in the slag ratio. The porosities of these concretes were also reduced compared to portland cement concrete.

10.2.4. Temperature Development

With the partial replacement of portland cement by slag, maximum temperature generated in the concrete decreased substantially. Compared to portland cement concrete, the time to reach the peak temperatures increased in the slag concretes.

Silica fume did not have beneficial effects on the temperature development in concrete and slight increases in the peak temperatures were recorded. Using fly ash cement instead of portland cement also resulted in a higher peak temperature. Compared to portland cement concrete, the time to reach the maximum temperature decreased for the fly ash cement concrete.

10.2.5. Chloride Binding

The tests were carried out on paste samples. The results indicate that the chloride binding increases with the age. The chloride binding for the portland cement mixture and the mixtures with 40% and 60% slag are very close to each other which was an unexpected result. The paste containing 20% OPC and 80% slag had the highest chloride binding.

10.3. Optimization of Concrete

Two different types of optimizations were performed. The first method was based on optimizing only one response. The second method of optimization, however, was based on optimizing several responses simultaneously and desirability functions were used for this purpose. Some of the responses can be maximized, and some can be minimized with the desirability function method. The compressive strengths were maximized whereas the rapid chloride permeabilities and the costs were minimized in the study. As a result, for the concrete series containing different amounts of ground fly ash, the one with 40% fly ash was obtained as the optimum mixture. Among the concretes containing fly ash, slag or both, the ones with the slag were the optimum for both low and high water/binder ratios.

10.4. Durability of Concrete Structures in a Chloride Containing Environment

As outlined in Chapter 7, current codes and practice on obtaining durable structures are based on prescriptive requirements. However, probability based durability design methods are being developed which takes the scatter of the variables into account.

10.4.1. Field Experience

Five different structures exposed to sea water were investigated in the study. Results show that even for the same structure, chloride penetration into concrete can vary considerably depending on the testing location and micro-climate. Except one, the structures investigated in this study were built using portland cement. Although the structures were relatively new and satisfy the EN 206 criteria, test results show that sufficient amount of chlorides to initiate corrosion had reached the embedded steel within the 10 to 20 years of exposure. These results prove that obtaining a long service life is very difficult with the use of prescriptive requirements and traditional binder systems; therefore another approach must be established to obtain a durable structure with a long service life.

10.4.2. Effect of Diffusivity and Binder System on the Durability of a Concrete Structure

A durability analysis was carried out based on a probability based design method and chloride diffusivities obtained from the testing of different concrete mixtures were

used as input. The results showed that the concrete produced only with ordinary portland cement had the highest chloride diffusivity, and as a result; reinforcing steel embedded in a structural member produced with ordinary portland cement could start corroding in within 10 to 20 years. However, the risk for corrosion reduced substantially for the concretes containing pozzolanic materials.

10.5. Quality Control of Concrete by Electrical Resistivity using Wenner Electrode Method

Test results showed that the electrical resistivity of concrete obtained by the wenner electrode method can be quite different from the one obtained by wenner method. The differences between these methods depend on the specimen type used and testing locations. In general, for a given specimen type, the electrical resistivity increased with the increase in the distance between the probes. For different specimen types, probe spacings or test locations, relationships between the resistivities obtained by wenner electrode and two electrode method were established in the study.

Tests conducted on the specimens with embedded steel proved that the resistivity can be affected by the presence of steel. Distance to the embedded steel, measurement direction relative to the steel and cover depth were some of the factors investigated. Wenner electrode testing longitudinal to the embedded steel resulted in about 40% decrease in resistivity when tested over the steel. Results indicated that for a given probe spacing, the resistivity obtained by the wenner electrode method was affected less more for a higher cover depth.

REFERENCES

ACI Committee 121, 1998. Quality Management System for Concrete Construction, American Concrete Institute, ACI 121.R – 98, Detroit, MI, USA.

ACI Committee 201, 1992. Guide to Durable Concrete, American Concrete Institute, ACI 201.2R – 92, Detroit, MI, USA.

ACI Committee 210, 1993, Reaaproved 1998. Erosion of Concrete in Hydraulic Structures, American Concrete Institute, ACI 210.R – 93, Detroit, MI, USA.

ACI Committee 221, 1998. State of the Art Report on Alkali – Aggregate Reactivity, American Concrete Institute, ACI 221.1R – 98, Detroit, MI, USA.

ACI Committee 232, 1996. Use of Fly Ash in Concrete, American Concrete Institute, ACI 232.2R – 96, Detroit, MI, USA

ACI Committee 233, 1995. Ground Granulated Blast-Furnace Slag as a Cementitious Constituent in Concrete, American Concrete Institute, ACI 233R – 95, Detroit, MI, USA.

ACI Committee 234, 1996. Guide for the Use of Silica Fume in Concrete, American Concrete Institute, ACI 234R – 96, Detroit, MI, USA.

ACI Committee 306, 1988. Reaaproved 1997. Cold Weather Concreting, American Concrete Institute, ACI 306.R – 88, Detroit, MI, USA.

ACI Committee 311, 1995. Guide for Concrete Inspection, American Concrete Institute, ACI 311.4R – 95, Detroit, MI, USA.

Aïtcin, P.C., 1995. Concrete the Most Widely Used Construction Material, in *Adam Neville Symposium on Concrete Technology*, June, pp. 257-266.

Aitcin, P.C., 1998. High Performance Concrete, E & FN Spon, London.

Aïtcin, P.C., 2000. Cement and Concrete Development from an Environmental Perspective, in *Concrete Technology for a Sustainable Development in the 21st Century*, pp. 206-217, Eds. Gjørv, O.E. and Sakai, K., E&FN Spon, London.

Alonso, C., Andrade, C., Castellote, M. and Castro, P., 2000. Chloride Threshold Values to Depassivate Reinforcing Bars Embedded in a Standardized OPC Mortar, *Cement and Concrete Research*, **30**, 1047 – 1055.

Andrade, C., 1993. Calculation of Chloride Diffusion Coefficients in Concrete From Ionic Migration Measurements, *Cement and Concrete Research*, **23**, 724 – 742.

Arskog, A., Ferreira, M. and Gjørv, O.E., 2004a. Durability and Performance of Norwegian Concrete Harbour Structures, *Fourth International Conference on Concrete under Severe Conditions*, ed. B.H. Oh, Korea Concrete Institute, Korea, June, 133-140.

Arskog, A., Ferreira, M. and Gjørv, O.E., 2004b. Durability Analysis and Performance of Concrete Barges, *Fourth International Conference on Concrete under Severe Conditions*, ed. B.H. Oh, Korea Concrete Institute, Korea, June, 1604-1611.

Arskog, A., Gjørv, O.E., Sengul, O., and Dahl, R., 2005. Chloride Penetration into Silica Fume Concrete after 10 Years of Exposure in Aursundet Bridge, *XIX Symposium on Nordic Concrete Research*, 13-15 June, Sandefjord, Norway, 97-99.

Arup, H., 1995. The Chloride Threshold of Steel in Conrete – Is it a Function of Potential?, *Proceedings of the Nordic Seminar in Lund on Corrosion of Reinforcement*, University of Lund, 1 – 2 February, 251 – 255.

ASTM C 311, 1985. Standard Methods of Sampling and Testing Fly Ash or Natural Pozzolans for Use as a Mineral Admixture in Portland Cement Concrete, *The American Society for Testing and Materials*, Pennsylvania.

ASTM C 618, 2000. Standard Specifications for Coal Fly Ash and Raw or Calcined Natural Pozzolan for Use as Mineral Admixture in Portland Cement Concrete, *The American Society for Testing and Materials*, Pennsylvania.

ASTM C 989, 1999. Standard Specifications for Ground Granulated Blast – Furnace Slag for Use in Concrete and Mortars, *The American Society for Testing and Materials*, Pennsylvania.

ASTM C 1202, 1997. Standard Test Method for Electrical Indication of Concrete's Ability to Resist Chloride Ion Penetration, *The American Society for Testing and Materials*, Pennsylvania.

ASTM C 1240, 2000. Standard Specification for Use of Silica Fume as a Mineral Admixture in Hydraulic Cement Concrete, Mortar and Grout, *The American Society for Testing and Materials*, Pennsylvania.

ASTM E 384a, 2005. Standard Test Method for Microindentation Hardness of Materials, *The American Society for Testing and Materials*, Pennsylvania.

Atkins, P.W., 1990. Physical Chemistry, Oxford University Press, Oxford.

Baker, D., 1999. The Maintenance of the Highways Agency's Structures, in *Management of Highway Structures*, pp. 7-13, Ed. Das, P.C., Thomas Telford, London.

Bamforth, P.B. and Price, W.F., 1993. Factors Influencing Chloride Ingress into Marine Structures, *Concrete 2000*, Scotland, UK, 7-9 September, 1105 – 1118.

Bayat, O., 1998. Characterization of Turkish Fly Ashes, *Fuel*, **77**, 1059 – 1066.

Bayramov, F., Taşdemir, C., and Taşdemir, M.A., 2004. Optimization of Fibre Reinforced Concretes by Means of Statistical Responce Surface Method, *Cement and Concrete Composites*, **26**, 665-675.

Bertolini, L., Elsener, B., Pedeferri, P. and Polder, R., 2004. Corrosion of Steel in Concrete, Wiley – VCH, Weinheim.

Bentur, A., 2002. Cementitious Materials – Nine Millennia and a New Century: Past, Present, and Future, *Journal of Materials in Civil Engineering*, **14**, 2 – 22.

Bentz, D.P., 2000. Influence of Silica Fume on Diffusivity in Cement Based Materials II – Multi-scale Modeling of Concrete Diffusivity, *Cement and Concrete Research*, **30**, 1121 – 1129.

Bentz, D.P., Jensen, O.M., Coats, A.M. and Glasser, F.P., 2000. Influence of Silica Fume on Diffusivity in Cement Based Materials II – Experimental and Computer Modeling studies on Cement Pastes, *Cement and Concrete Research*, **30**, 953 – 962.

Berry, E.E., 1980. Strength Development of Some Blended-Cement Mortars, *Cement and Concrete Research*, **10**, 1-11.

Berry, E.E., Hemmings, R.T., Langley, W.S., and Carette, G.G., 1989. Beneficiated Fly Ash: Hydration, Microstructure, and Strength Development in Portland Cement Systems, *Third International Conference on Fly Ash, Silica Fume, Slag and Natural Pozzolans in Concrete*, Trondheim, Norway, ACI SP 114, Vol.1, 241-273.

Bijen, J., 1996a. Blast Furnace Slag Cement, Association of Netherlands Cement Industry, The Netherlands.

Bijen, J., 1996b. Benefits of Slag and Fly Ash, *Construction and Building Materials*, **10**, 309 – 314.

Bleszybski, R., Hooton, R.D., Thomas, M.D.A. and Rogers, C.A., 2002. Durability of Ternary Blend Concrete with Silica Fume and Blast Furnace Slag: Laboratory and Outdoor Exposure Site Studies, *ACI Materials Journal*, **99**, 5, 499 – 508.

Boddy, A., Bentz, E., Thomas, M.D.A. and Hooton, R.D., 1999. An Overview and Sensivity Study of a Multimechanistic Chloride Transport Model, *Cement and Concrete Research*, **29**, 827 – 837.

Bouzoubaa, N., Bilodeau, A., Sivasundaram, V., Fournier, B. and Golden, D.M., 2004. Development of Ternary Blends for High Performance Concrete, *ACI Materials Journal*, **101**, 1, 19 – 29.

Brandt, A.M. and Marks, M., 1993. Examples of the Multicriteria Optimization of Cement – Based Composites, *Composite Structures*, **25**, 51 – 60.

Brandt, A.M., 1995. Cement – Based Composites, E&FN Spon, London.

Brandt, A.M. and Marks, M., 1996. Optimization of the Material Structure and Composition of Cement – Based Composites, *Cement and Concrete Composites*, **18**, 271-279.

Buenfeld, N.R. and Okundi, E., 1998. Effect of Cement Content on Transport in Concrete, Magazine of Concrete Research, **50**, 4, 339-351.

Cather, B. and Marsh, B., 1997. Service Life of Concrete Structures – Current and Emerging Approaches, *International Seminar on the Management of Concrete Structures for Long Term Serviceability*, University of Sheffield, 13 November, 21-32.

Chandra, S. and Berntsson, L., 1997. Use of Silica Fume in Concrete, in *Waste Materials Used in Concrete Manufacturing*, pp.554-623, Ed. Chandra, S., Noyes Publications, New Jersey.

Chandra, S., 2002. Properties of Concrete with Chemical and Mineral Admixtures in *Structure and Performance of Cements*, pp. 140-185, Eds. Bensted, J. and Barnes, P., E & FN Spon, London.

Chengzhi, Z., Aiqin, W., Mingshu, T. and Xiaoyu, L., 1996. The Filling Role of Pozzolanic Material, *Cement and Concrete Research*, **26**, 943 – 947.

Cheriaf, M., Rocha, J.C., and Pera, J., 1999. Pozzolanic Properties of Pulverized Coal Combustion Bottom Ash, *Cement and Concrete Research*, **29**, 1387-1391.

Collepardi, M., Marcialis, A. and Turriziani, R., 1972. Penetration of Chloride Ions into Cement Pastes and Concretes, *Journal of American Ceramic Society*, **55**, 10, 534-535.

Cornell, J., 2002. Experiments with Mixtures, John Wiley & Sons Inc., New York.

Crank, J., 1993. The Mathematics of Diffusion, Oxford University Press, London.

Demir, M., Erenoglu, T., Ekim, H. and Tasdemir, M.A., 2002. Effects of Fineness and Amount of Fly Ash on Strength Development of Concrete, *Fifth International Congress on Advances in Civil Engineering,* 25-27 September, Istanbul, 1349-1358.

Dhir, R.K., Jones, M.R., and Seneviratne, A.M.G., 1991. Diffusion of Chlorides into Concrete – Influence of PFA Quality, *Cement and Concrete Research*, **21**, 1092 – 1102.

Dhir, R.K., Jones, M.R., and McCarthy, M.J., 1996a. Binder Content Influences on Chloride Ingress in Concrete, *Cement and Concrete Research*, **26**, 12, 1761-1766

Dhir, R.K., El-Mohr, M.A.K., and Dyer, T.D., 1996b. Chloride Binding in GGBS concrete, *Cement and Concrete Research*, **26**, 12, 1767-1773.

Dhir, R.K., El-Mokr, M.A.K., and Dyer, T.D., 1997. Developing Chloride Resisting Concrete Using PFA, *Cement and Concrete Research*, **27**, 1633 – 1639.

Dhir, R.K. and Jones, M.R., 1999. Development of Chloride Resisting Concrete Using Fly Ash, *Fuel*, **78**, 137 – 147.

EN 206, 2000**.** Concrete - Part 1: Specification, Performance, Production and Conformity, *European Committee for Standardization, CEN*, Brussels.

ENV 1991-1, 1994. Eurocode 1: Basis of Design and Actions on Structures – Part 1: Basis of Design, European Prestandard, *European Committee for Standardization, CEN*, Brussels.

EN 1992, 2001**.** Eurocode 2: Design of Concrete Structures – Part 1: General Rules and Rules for Buildings, *European Committee for Standardization, CEN*, Brussels.

Ferreira, M., Årskog, V., Jalali, S. and Gjørv, O.E., 2004. Software for Probability-Based Durability Analysis of Concrete Structures, *Fourth International Conference on Concrete under Severe Conditions*, Seoul, Korea Concrete Institute, 1015-1024.

Fidjestöl, P. and Tuutti, K., 1995. The Importance of Chloride Diffusion, *International RILEM Workshop on Chloride Penetration into Concrete*, 15 – 18 October, St-Remy-les-Chevreuse, 470 – 480.

Fidjestöl, P. and Lewis, R., 2004. Microsilica as an Addition, in *Lea's Chemistry of Cement and Concrete*, pp. 679-712, Ed. Hewlett, P.C., Elsevier Ltd, Oxford.

Fisang, L.J., Djuric, M., Neducin, R.M., Ranogajec, J., and Mihajlov, A., 1995. An Optimization of Fly Ash Quantity in Cement Blending, *Cement and Concrete Research*, 25, 1480-1490.

Fluge, F., 1997. Environmental Loads on Coastal Bridges, *International Conference on repair of Concrete Structures*, Svolvær, Norway, 28 – 30 May, 89 – 98.

Fluge, F., 1998. Aursundet Bru, *Betongindustrien*, **3**, 16-17.

Fluge, F., 2001. Marine chlorides – A Probabilistic Approach to Derive Provisions to EN 206-1, *Workshop on the Service Life Design of Concrete Structures,* 10-12 June, Tromsø, Norway, 48 - 68.

Fluge, F., 2001. Bakgrunnen for de Nye Kravene for Kloridutsatte Konstruksjoner, *Norsk Betongdag 2001*, Kompendium, Norsk Betongforening, Trondheim, Norway, 1 – 3 November, 11 p.

Fraay, A.L.A., Bijen, J.M. and Haan, Y.M.D., 1989. The Reaction of Fly Ash in Concrete; A Critical Examination, *Cement and Concrete Research*, **19**, 235 – 246.

Frigione, G. and Frigione, M., 1996. Role of Blended Cements in Optimization of Energy in cement Manufacture, in *Energy Conservation and Environmental Control in Cement Industry*, pp. 183-223, Ed. Ghosh, S.N., Akademia Books International, New Delhi, India.

Garboczi, E.J. and Bentz, D.P., 1998. Diffusivity – Porosity Relation for Cement Paste, *Seminar on Sulfate Attack Mechanisms*, Quebec City, Canada October 5-6, 259 – 264.

Gartner, E., 2004. Industrially Interesting Approaches to low CO_2 Cements, *Cement and Concrete Research*, **34**, 1489 – 1498.

Gehlen, C. and Schiessl, P., 1999. Probability – Based Durability Design for the Western Scheldt Tunnel, *Structural Concrete*, **1**, No. 2, 1-7.

Geiseler, J., Kollo, H., and Lang, E., 1995. Influence of Blast Furnace Cements on Durability of Concrete Structures, *ACI Materials Journal*, **92**, 3, 252 – 257.

Gerwick, B.C., 1994. The Economic Aspects of Durability – How Much added Expense Can be Justified?, *P.K. Mehta Symposium on Durability of Concrete*, Nice, France, May 1994, 1-19.

Gjørv. O.E., Vennesland, Ø. and El-Busaidy, A.H.S., 1977. Electrical Resistivity of Concrete in the Oceans, *9th Annual Offshore Technology Conference,* Houston, May 2-5, 581 – 588.

Gjørv. O.E., and Vennesland, Ø., 1979. Diffusion of Chloride Ions from Seawater into Concrete, *Cement and Concrete Research*, **9**, 229 – 238.

Gjørv O.E, 1994a. Important Test Methods for Evaluation of Reinforced Concrete Durability, Concrete Technology Past, Present, and Future, Ed. P.K. Mehta, ACI SP – 144, Detroit, 545-574.

Gjørv, O.E., Tan, K. and Zhang, M.H., 1994b. Diffusivity of Chlorides from Seawater into High – Strength Lightweight Concrete, *ACI Materials Journal*, **91**, 5, 447 – 452.

Gjørv O.E., 2002. Durability and Service Life of Concrete Structures, *Proceedings, The First fib Congress 2002*, Japan Prestressed Concrete Engineering Association, Tokyo, 2002, Vol. 6., 1-16.

Gjørv, O.E., 2003. Durability of Concrete Structures and Performance-Based Quality Control, *International Conference on Performance of Construction Materials in The New Millenium*, ed. by A.S. El-Dieb, M.M.R. Taha and S.L. Lissel, Shams University, Cairo, 10 pp.

Gjørv, O.E., 2004a. Durability Design and Construction Quality of Concrete Structures, *Fourth International Conference on Concrete Under Severe Conditions – Environment and Loading*, Seoul, Korea, June, 44-55.

Gjørv, O.E., 2004b. Bestandige Betongkaier, Norsk Havneingeniørforening, Oslo, Norway.

Glass, G.K. and Buenfeld, N.R., 1997. The Presentation of the Chloride Threshold Level for Corrosion of the Steel in Concrete. *Corrosion Science*, **39**, 5, 1001 – 1013.

Glasser, F.P., 1991. Chemical, Mineralogical, and Microstructural Changes Occurring in Hydrated Slag – Cement Blends, in *Material Science of Concrete II*, pp. 41-81, Eds. Skalny, J. and Mindess, S., The American Ceramic Society, Westerville.

Glavind, M., and Petersen, C.M., 2002. Green Concrete – A Life Cycle Approach, in *Sustainable Concrete Construction*, International Conference held at the University of Dundee, Eds. Dhir, R.D., Dyer, T.D. and Halliday, J.E., 9-11 September, 771-786.

Goldman, A. and Bentur, A., 1993. The Influence of Microfillers on Enhancement of Concrete Strength, *Cement and Concrete Research*, **23**, 962 – 972.

Goldman, A. and Bentur, A., 1994. Properties of Cementitious Systems Containing Silica Fume or Nonreactive Microfillers, *Advanced Cement Based Materials,* **1**, 209 – 215.

Govers, K.R. and Millard, S.G., 1991. The Effect of Steel Reinforcement Bars on the Measurement of Concrete Resistivity, *British Journal of Non-Destructive Testing*, **33**, 11, 551 – 556.

Govers, K.R. and Millard, S.G., 1999. Measurement of Concrete Resistivity for Assessment of Corrosion Severity of Steel Using Wenner Technique, *ACI Materials Journal*, **96**, 5, 536 – 541.

Hammersley, J.M. and Handscomb, D.C., 1975. Monte Carlo Methods, Methuen & Co ltd, London.

Haugen, E.B., 1980. Probabilistic Mechanical Design, John Wiley & Sons, Inc., New York.

Hetek, 1996. Chloride Penetration into Concrete, Report No: 53, Danish Road Directorate, Denmark.

Hisada, M., Nagataki, S. and Otsoki, N., 1999. Evaluation of Mineral Admixtures on the Viewpoint of Chloride Ion Migration through Mortar, *Cement and Concrete Composites*, **21**, 443 – 448.

Hofsøy, A., Sørensen, S.I. and Markeset, G., 1999. Erfaringer fra Kaier, NFR-Prosjektet Bestandige Betongkonstruksjoner Vegdirektoratet, Raport No. 2.2, Oslo.

Hooton, R.D., 1987. The Reactivity and Hydration of Blast Furnace Slag, in *Supplementary Cementing Materials for Concrete*, pp. 245-288, Ed. Malhotra, V.M., CANMET, Canada.

Hooton, R.D., Pun, P., Kojundic, T. and Fidjestol, P. 1997. Influence of Silica Fume on Chloride Resistance of Concrete, *PCI/FHWA International Symposium on HPC*, October, New Orleans, 245 – 256.

Hou, W.M., Chang, P.K., and Hwang, C.L., 2004. A Study on Anticorrosion Effect in High performance Concrete by the pozzolanic Reaction of Slag, *Cement and Concrete Research*, **34**, 615 – 622.

Hsu, L.S. and Hsu, C.T.T., 1994. Complete Stress – Strain Behaviour of High Strength Concrete under Compression, *Magazine of Concrete Research*, **46**, 169, 301 – 312.

Hunkeler, F., 1997. Monitoring of Repaired Concrete Structures by Means of Resistiviy Measurements, *International Conference on repair of Concrete Structures*, Svolvær, Norway, 28 – 30 May, 223 – 232.

Igarashi, S., Bentur, A. and Mindess, S. 1996, Microhardness Testing of Cementitious Materials, *Advanced Cement Based Materials*, **4**, 48-57.

Justnes, H., 1998. A Review of Chloride Binding in Cementitious Systems, *Nordic Concrete Research*, **21**, 48-63.

Justnes, H., 2002. Condensed Silica Fume as a Cement Extender, in *Structure and Performance of Cements*, pp. 399-408, Eds. Bensted, J. and Barnes, P., E & FN Spon, London.

Keru, W. and Jianhua, Z., 1988. The Influence of the Matrix – Aggregate Bond on the Strength and Brittleness of Concrete, in *Materials Research Society Symposium*. pp. 29 – 34, Proceedings Vol. 114, Materials Research Society.

Khayat, K.H. and Aitcin P.C., 1993. Silica Fume – A Unique Supplementary Cementitious Material, in *Mineral Admixtures in Cement and Concrete*, pp. 226-265, Eds. Sarkar, S.L. and Ghosh, S.N., ABI Books Ltd., New Delhi, India.

Kobayashi, K., Hattori, A. and Miyagawa, T., 1998. Characteristics of Interfacial Transition Zone in Cement Paste with Admixtures, in *The Interfacial Transition Zone in Cementitious Composites*, pp. 311-318, Eds. Katz, A., Bentur, A., Alexander, A. and Arligguie, G., E & FN Spon, London

Kropp, J., Hilsdorf, H.K., Grube, H., Andrade, C. and Nilsson, L.O., 1995. Transport Mechanisms and Definitions, in *Performance Criteria for Durability*, pp. 4-13, Eds. Kropp, J. and Hilsdorf, H.K., E & FN Spon, London.

Lam, L., Wong, Y.L. and Poon, C.S., 2000. Degree of Hydration and Gel/Space Ratio of High-Volume Fly Ash/Cement Systems, *Cement and Concrete Research*, **30**, 5, 747-756.

Lang, E., 2004. Blast-furnace Cements, in *Structure and Performance of Cements*, pp. 310-325, Ed. Hewlett, P.C., Elsevier Ltd, Oxford.

Larbi, J.A. and Bijen, M.J.M., 1990. Orientation of Calcium Hydroxide at the Portland Cement Paste – Aggregate Interface in Mortars in the presence of Silica Fume: A Contribution, *Cement and Concrete Research*, **20**, 461 – 470.

Larbi, J.A., 1991. The Cement Paste - Aggregate Interfacial Zone in Concrete, *PhD Thesis,* Technical University of Delft, Netherlands.

Lea, F.M., 1970. The Chemistry of Cement and Concrete, Third edition, Edward Arnold Ltd, London, UK.

Lee, A.R., 1974. Blast furnace and Steel Slag: Production, Properties and Uses, Edward Arnold Ltd., London.

Li, X. and Bhushan, B., 2002. A Review of Nanoindentation Continuous Stiffness Measurement Technique and Its Applications, *Materials Characterization*, **48**, 11 – 36.

Li, S. and Roy, D.M., 1986. Investigation of Relations Between Porosity, Pore Structure, and Chloride Diffusion of Fly Ash and Blended Cements, *Cement and Concrete Research*, **16**, 749 – 759.

Lohtia, R.P. and Joshi R.C., 1995. Mineral Admixtures, in *Concrete Admixtures Handbook*, pp. 657-739, Ramachandran, V.S., Noyes Publications, New Jersey.

Luke, K., 2002. Pulverized Fuel Ash as a Cement Extender, in *Structure and Performance of Cements*, pp. 353-371, Eds. Bensted, J. and Barnes, P., E & FN Spon, London.

Luo, R., Cai, Y., Wang, C. and Huang, X., 2003. Study of Chloride Binding and Diffusion in GGBS concrete, *Cement and Concrete Research*, **33**, 1-7.

Mailvaganam, N.P., 1995. Miscellaneous admixtures, in *Concrete Admixtures in Concrete*, Ed. Ramachandran, V.S., Noyes Publications, New Jersey. 939-1025.

Malhotra, V.M., Ramachandran, V.S., Feldman, R.F. and Aitcin, P.C., 1987. Condensed Silica Fume in Concrete, CRC Press, Florida.

Malhotra, V.M, 1999. Making Concrete Greener with Fly Ash, *Concrete International*, **13**, 61 – 66.

Malhotra, V.M., 2000. Role of Supplementary Cementing Materials in Reducing Greenhouse Gas Emissions, in *Concrete Technology for a Sustainable Development in the 21st Century*, pp. 226 – 235, Eds Gjørv, O.E. and Sakai, K., E&FN Spon, London.

Malhotra, V.M., Zhang, M.H., Read, P.H. and Ryell, J., 2000. Long-Term Mechanical Properties and Durability Characteristics of High-Strength/High-Performance Concrete Incorporating Supplementary Cementing Materials under Outdoor Exposure Conditions, *ACI Materials Journal*, **97**, 5, 518 – 525.

Mangat, P.S., Khatib, J.M. and Molloy, B.T., 1997. Microstructure, Chloride Diffusion and Reinforcement Corrosion in Blended Cement Paste and Concrete, *Cement and Concrete Composites*, **16**, 73 – 81.

Markeset, G., 2004. Levetidsprosjektering Sett fra en Byggherres Side, Levetidsprosjektering av Betong Konstruksjoner, Kompendium, Norsk Betongforening, Oslo, 30 p.

Massaza, F and Costa, U., 1986. Bond: Paste – Aggregate, Paste – Reinforcement and Paste – Fibers, *The 8th International Symposium on Chemistry of Cement*, Rio de Janeiro, 158-180.

Mays, G., 1992. Durability of Concrete Structures, E & FN Spon, London.

McCarthy, M.J. and Dhir, R.K., 1999. Towards Maximizing the Use of Fly Ash as a Binder, *Fuel*, **78**, 121 – 132.

Mehta, P.K., 1985. Influence of Fly Ash Characteristics on the Strength of Portland – Fly Ash Mixtures, *Cement and Concrete Research*, **15**, 669 – 674.

Mehta, P.K., 1991**.** Concrete in the Marine Environment, Elsevier Applied Science, Essex.

Mehta, P.K. and Monteiro, P.J.M., 1996**.** Concrete, Prentice Hall, New Jersey.

Mehta, P.K., 1999. Concrete Technology for Sustainable Development, *Concrete International*, **13**, 47-53.

Mehta, P.K., 2000. Reflections on Recent Advancements in Concrete Technology, *Second International Symposium on Cement and Concrete Technology in the 2000s*, 6-10 September, Istanbul, Vol.1, 43-57.

Mehta, P.K., 2001. Reducing the Environmental Impact of Concrete, *Concrete International*, **15**, 61 – 66.

Mehta, P.K., 2002. Durable Concrete Structures: Modern Materials and Construction Practice, Short Course, Middle East Technical University, 23-27 September.

Melchers, R.E., 1987. Structural Reliability – Analysis and Prediction, Ellis Horwood Limited, West Sussex, England.

Mindess, S., 1985. Relationships between Strength and Microstructure for Cement Based Materials, *Very High Strength Cement Based Materials*, MRS Proceedings, Ed. J.F. Young, Vol. 2, 53-68.

Monteiro, P.J.M., Maso, J.C. and Ollivier, J.P., 1985. The Aggregate – Mortar Interface, *Cement and Concrete Research*, **15**, 953 – 958.

Monteiro, P.J.M. and Mehta, P.J.M., 1986. Interaction between Carbonate Rock and Cement Paste, *Cement and Concrete Research*, **16**, 127 – 134.

Morris, W., Moreno, E.I. and Sagaues, A.A., 1996. Practical Evaluation of Resistivity of Concrete in Test Cylinders Using a Wenner Array Probe, *Cement and Concrete Research*, **26**, 1779 – 1787.

Myers, R.H. and Montgomery, D.C., 2002. Response Surface Methodology, John Wiley & Sons Inc., New York.

Naik, T.R., Singh, S.S., and Hu, W.Y., 1992. High Volume Fly Ash Concrete Technology, **Research Project No. 3176-1**, The University of Wisconsin-Milwaukee, Center for By-Products Utilization.

Nehdi, M., 2001. Ternary and Quaternary cements for Sustainable Development, *Concrete International*, **23**, 35-42.

Neville, A.M., 1995. Chloride Attack of Reinforced Concrete: An Overview, *Materials and Structures*, **28**, 63-70.

Neville, A.M., 1997. Aggregate Bond and Modulus of Elasticity of Concrete, *ACI Materials Journal*, **94**, 71-74.

Neville, A.M., 2004. Properties of Concrete, Pearson Prentice Hall, Essex.

Nilsson, L., Ngo, M.H. and Gjorv, O.E., 1998. High-Performance Repair Materials for Concrete Structures in the Port of Gothenburg, *Second International Conference on Concrete Under Severe Conditions – Environment and Loading,* ed. by O.E.Gjorv, K. Sakai and N. Banthia, E & FN Spon, London, V. 2, 1193-1198.

NS 3045, 1992. Silica Fume for Concrete – Definitions and Requirements, *Standard Norge*, Lysaker.

NS 3420, 1986. Specifications for Buildings and Construction, *Standard Norge,* Oslo.

NT 368, 1991. Concrete, Repair Materials: Capillary Absorption, *Nordtest*, Espoo, Finland.

NT 443, 1995. Concrete, Hardened: Accelerated Chloride Penetration, Espoo, Finland.

NT 492, 1999. Concrete, Mortar and Cement Based Repair Materials: Chloride Migration Coefficient from Non-Steady State Migration Experiments, *Nordtest,* Espoo, Finland.

Oliver, W.C. and Pharr, G.M., 1992. An Improved Technique for Determining Hardness and Elastic Modulus Using Load and Displacement Sensing Indentation Experiments, *Journal of Materials Research*, **7**, 6, 1564 – 1583.

Olliver, J.P., Maso, J.C. and Bourdette, B., 1995. Interfacial Transition Zone in Concrete, *Advanced Cement Based Materials*, **2**, 30 – 38.

Oner, M., 2000. A Study of Intergrinding and Separate Grinding of Blast Furnace Slag Cement, *Cement and Concrete Research*, **30**, 473 – 480.

Osborne, G.J., 1999. Durability of Portland – Blast Furnace Slag Cement Concrete, *Cement and Concrete Composites*, **21**, 11 – 21.

Pal, S.C., Mukherjee, A. and Pathak, S.R., 2002. Corrosion Behavior of Reinforcement in Slag Concrete, *ACI Materials Journal*, **99**, 6, 521-532.

Paya, J., Monzo, J., Borrachero, M.V., Peris, E. and Gonzalez-Lopez, E., 1997. Mechanical Treatments of Fly Ashes – Part III: Studies on Strength Development of Ground Fly Ashes-Cement Mortars, *Cement and Concrete Research*, **27**, 9, 1365-1377.

Polder, R., 2000. Electrochemical Techniques for Measuring Metallic Corrosion, *Materials and Structures*, **33**, 603 – 611.

Polder, R., 2001. Test Methods on Site Measurement of Resistivity of Concrete – a RILEM TC – 154 Technical Recommendation, *Construction and Building Materials*, **15**, 125 – 131.

Poon, C.S., Lam, L., and Wong, Y.L., 1999. Effects of Fly Ash and Silica Fume on Interfacial Porosity of Concrete, *Journal of Materials in Civil Engineering*, August, 197-205.

Poon, C.S., Lam, L., and Wong, Y.L., 2000. A Study of High Strength Concrete Prepared with Large Volumes of Low Calcium Fly Ash, *Cement and Concrete Research*, **30**, 3, 447-455.

Pruckner, F., 2001. Corrosion and Protection of Reinforcement in Concrete – Measurements and Interpretation, *PhD thesis*, University of Vienna.

Ramyar, K., Erdogan, T.Y., 1995. Pozzolanic Effectiveness Ratio Of Fly Ashes and Their Contribution to the Strength of Portland Cement-Fly Ash Mortars and Concretes, in *Supplementary Papers of the Fifth CANMET/ ACI International Conference on Fly Ash, Silica Fume, Slag and Natural Pozzolans in Concrete*, Milwaukee, USA, 433-441.

Regourd, M., Thomassin, J.H., Bailiff, P. and Touray, T.C., 1983. Blast Furnace Slag Hydration – Surface Analysis, *Cement and Concrete Research*, **13**, 549 – 556.

Regourd, M.M., 2004. Cements Made from Blast-furnace Slag, in *Lea's Chemistry of Cement and Concrete*, pp. 637-678, Ed. Hewlett, P.C., Elsevier Ltd, Oxford.

Roy, D.M., 1989. Fly Ash and Silica Fume Chemistry and Hydration, *3rd International Conference on Fly Ash, Silica Fume, Slag and Natural Pozzolans in Concrete,* ACI SP-114, Trondheim, 117 – 138.

Roy, D.M. and Malek, R.I.A., 1993. Hydration of Slag Cement, in *Mineral Admixtures in Cement and Concrete*, pp. 84-117, Eds. Sarkar, S.L. and Ghosh, S.N., ABI Books Ltd., New Delhi, India.

Saito, M. and Kawamura, M., 1989. Effect of Fly Ash and Slag on the Interfacial Zone Between Cement and Aggregate, *3rd International Conference on Fly Ash, Silica Fume, Slag and Natural Pozzolans in Concrete,* ACI SP-114, Trondheim, 669 – 688.

Saleem, M., Shamemm, M., Hussain, S.E. and Maslehuddin, M., 1996. Effect of Moisture, Chloride and Sulphate Contamination on the Electrical Resistivity of Portland Cement Concrete, *Construction and Building Materials*, **10**, 3, 209 – 214.

Sandberg, P., Pettersen, K., Sorensen , H.E. and Arup, H., 1995. Critical Chloride Concentrations for the Onset of Active Reinforcement Corrosion, *Proceedings of the International RILEM Workshop Chloride Penetration into Concrete,* 15-18 October, St-Remy-les-Chevreuse, France, 453-459.

Sarja, A. and Vesikari, E., 1996. Durability Design of Concrete Structures, E & FN Spon, London.

Schiessl, P. and Wiens, U., 1995. Rapid Determination of Chloride Diffusivity in Concretes with Blending Agents, *Proceedings of the International RILEM Workshop Chloride Penetration into Concrete,* 15-18 October, St-Remy-les-Chevreuse, France, 115-125.

Sear, L.K.A., 2002. The Environmental Benefits of Using PFA in cementitious Systems, in *Sustainable Concrete Construction*, International

Conference held at the University of Dundee, Eds. Dhir, R.D., Dyer, T.D. and Halliday, J.E., 9-11 September, 313-322.

Sellevold, E.J., 1997. Resistivity and Humidity Measurements of Repaired and Non-repaired Areas in Gimsøystraumen Bridge, *International Conference on Repair of Concrete Structures*, Svolvær, Norway, 28 – 30 May, 283 – 295.

Sengul, O., Tasdemir, C. and Tasdemir, M.A., 2002. Influence of Aggregate Type on the Mechanical Behavior of Normal and High Strength Concretes, *ACI Materials Journal*, **99**, 6, 528-533.

Sengul, O., **Tasdemir, C., Koruç, S. and Yuceer, Z**., 2003a. Effects of Aggregate Type on Abrasion Resistance of Normal and High Strength Concrete, *5th National Congress on Concrete*, The Chamber of Turkish Civil Engineers Istanbul Branch, Istanbul, 1-3 October, pp.525-534.

Sengul, O., **Tasdemir, C., Koruc, S. and Sonmez, R**., 2003b. Effect of Aggregate on the Freezing - Thawing Resistance of Concrete, *3rd National Symposium on Crushed Stone*, The Chamber of Turkish Mining Engineers Istanbul Branch, Istanbul, 3-4 December, pp. 43-50.

Sengul, O., Tasdemir, C. and Tasdemir, M.A., 2005. Mechanical Properties and Rapid Chloride Permeability of Concretes with Ground Fly Ash, *ACI Materials Journal*, **102**, 6, 414-421.

Sivasundaram, V., Carette, G.G. and Malhotra, V.M., 1991. Mechanical Properties, Creep, and Resistance to Diffusion of Chloride Ions of Concretes Incorporating High Volumes of ASTM Class F Fly ashes from seven Different Sources, *ACI Materials Journal*, **88**, 4, 407-416.

Sivasundaram, V. and Malhotra, V.M., 1992. Properties of Concretes Incorporating Low Quantity of Cement and High Volumes of Ground Granulated Slag, *ACI Materials Journal*, **89**, 6, 554-563.

Skalny, J., Marchand, J. and Odler, I., 2002. Sulfate Attack on Concrete, Spon Press, London.

Sommerville, G., 1992. Service Life Prediction – An Overview, *Concrete International*, **14**, 45-49.

Swamy, R.N., 1992. The Alkali – Silica Reaction in Concrete, Blackie Ltd, London.

Swamy, R.N., 2001. Holistic Design: Key to Sustainability in Concrete Construction, *Structures & Buildings*, **146**, 4, 371-379.

Takewaka, K. and Mastumoto, S., 1998. Quality and Cover Thickness of Concrete based on the Estimation of Chloride Penetration in Marine Environments, *Second International Conference on Concrete in Marine Environment,* St. Andrews by-the-Sea, Canada, ACI SP 109-17, American Concrete Institute, 381-400.

Tasdemir, C., 1995. Effects of Aggregate-Cement Paste Interface Microstructure on Fracture Parameters of HSCs, *PhD Thesis*, Istanbul Technical University.

Tasdemir, C., Sarkar, S.L., Tasdemir, M.A., Akyüz, S. and Koca, C., 1995. Effect of Silica Fume on the Brittleness of HSCs under Compression, *Proceedings of ERMCO 95*, 444-452

Tasdemir, M.A., Tasdemir, C., Ozbek, E. and Altay, B., 1997. Fineness Effect of GGBS on the Properties and Microstructure of Concrete, in *First International Symposium on Mineral Admixtures in Cement*, Istanbul, 198-215.

Tasdemir,M.A., Tasdemir,C., Akyuz,S., Jefferson,A.D., Lydon,F.D. and Barr, B.I.G., 1998. Evaluation of Strains at Peak Stresses in Concrete: A Three Phase Composite Model Approach, *Cement and Concrete Composites*, **20**, 301-308.

Tasdemir, C., 2003. Combined effects of mineral admixtures and curing conditions on the sorptivity coefficient of concrete, *Cement and Concrete Research*, **33**, 1637 – 1642.

Taylor. H.F.W., 1992. Cement Chemistry, Academic Press, London.

Taylor. H.F.W., 1993. Nanostructure of C-S-H: Current Status, *Advanced Cement Based Materials*, **1**, 38 – 46.

Telford, W.M., Geldard, L.P. and Sheriff, R.E., 1990. Applied Geophysics, Cambridge University Press, Cambridge.

Thoft-Christensen, P. and Baker, M.J.. 1982. Structural Reliability Theory and Its Applications, Springer Verlag, Berlin.

Thoft-Christensen, P. and Morutsu, Y.. 1986. Applications of Structural Systems Reliability Theory, Springer Verlag, Berlin.

Thomas, M., 1997. Chloride Thresholds in Marine Concrete. *Cement and Concrete Research*, **26**, 4, 513 – 519.

Thomas, M.D.A., 1991. Marine Performance of PFA Concrete, *Magazine of Concrete Research*, **43**, 171 – 185.

Thomas, M.D.A. and Matthews, J.D., 2004. Performance of PFA Concrete in a Marine Environment – 10 year results, *Cement and Concrete Composites*, **26**, 5 – 20.

Tiewei, Z., 1997. Chloride diffusivity in concrete and its measurement from steady state migration testing, *Dr. ing. Dissertation*, NTNU, Trondheim, Norway.

Tokyay, M., 1998. Characterization of Turkish Fly Ashes, Turkish Cement Manufacturers Association, Ankara, 70 pp.

Tong, L. and Gjørv O.E., 1997. Brent Concrete Testing, Norwegian University of Science and Technology, Department of Building Materials, Internal Report, Trondheim, Norway.

Trtik, P. and Bartos, P.J.M., 1999. Micromechanical Properties of Cementitious Composites, *Materials and Structures*, **32**, June, 388 – 293.

Tuutti, K., 1982. Corrosion of Steel in Concrete, Swedish Cement and Concrete Research Institute, Stockholm.

US Census Bureau, 2004. Global Population at a Glance: 2002 and Beyond, WP/02/1, U.S. Department of Commerce, Economics and Statistics Administration, Washington.

Van Vlack, L.H., 1994. Elements of Materials Science and Engineering, Literatür Ltd., Istanbul.

Velez, K., Maximilien, S., Domidot, D., Fantezzi, G., and Sorrentiano, F., 2001. Determination by Nanoindentation of Elastic Modulus and Hardness of Pure Constituents of Portland Cement Clinker, *Cement and Concrete Research*, **31**, 555 – 561.

Yunovich, M. and Mierzwa, A.J., 2001. Corrosion Cost and Preventive Strategies in the United States – Appendix F – Waterways and Ports, FHWA-RD-01-156, Office of Infrastructure Research and Development, Federal Highway Administration, VA.

Yunovich, M., Thompson, N.G., Balvanyos, T. and Lave, L., 2001. Corrosion Cost and Preventive Strategies in the United States – Appendix D – Highway Bridges, **FHWA-RD-01-156**, Office of Infrastructure Research and Development, Federal Highway Administration, VA.

Whiting, D.A. and Nagi, M.A., 2003. Electrical Resistivity of Concrete, R&D No**. 2457**, Portland Cement Association, Illinois.

Wilkins, N.J.M., 1982. Resistivity of Concrete, AERE Harwell – Materials Development Division, **AERE – M 3232, HL 82/231**, Didcot, Oxon, OTD, United Kingdom.

Zhang, M.H. and Gjorv, O.E., 1991. Effect of Silica Fume on Pore Structure and Chloride Diffusivity of Low Porosity Cement Pastes, *Cement and Concrete Research*, **21**, 1006 – 1014.

Zhang M.H., Bilodeau, A., Malholtra, V.M., Kim, K.S. and Kim, J.C., 1999. Concrete Incorporating Supplementary Cementing Materials: Effect on Compressive Strength and Resistance to Chloride Ion Penetration, *ACI Materials Journal*, 96, 181-189.

Zimbelman, R., 1985. A contribution to the Problem of Cement – Aggregate Bond, *Cement and Concrete Research*, **15**, 801 – 808.